**Międzyuczelniany Wydział Biotechnologii**
Uniwersytetu Gdańskiego i Gdańskiego Uniwersytetu Medycznego

*mgr Marta Matuszewska*

# Badanie wpływu glukozy i glicerolu oraz jonów żelaza na syntezę związków przeciwdrobnoustrojowych i formowanie biofilmu przez *Pseudomonas donghuensis* P482

Investigation of the influence of glucose, glycerol and iron ions on the synthesis of antimicrobials and formation of biofilm by *Pseudomonas donghuensis* P482

Praca przedstawiona
Radzie Dyscypliny Nauki Biologiczne Uniwersytetu Gdańskiego
celem uzyskania stopnia doktora
w dziedzinie nauk ścisłych i przyrodniczych
w dyscyplinie nauki biologiczne

Promotor: dr hab. Sylwia Jafra, prof. UG
Jednostka organizacyjna: Zakład Mikrobiologii Roślin

GDAŃSK 2022

PhD thesis

# Investigation of the influence of glucose, glycerol and iron ions on the synthesis of antimicrobials and formation of biofilm by *Pseudomonas donghuensis* P482

**Marta Matuszewska, MSc**

University of Gdańsk

2022

# Table of Contents

# 1. Abbreviations

**2,4-DAPG** – 2,4-diacetylphloroglucinol

**7-HT** – 7-hydroxytropolone

**aa** – amino acid

**AcN** – acetonitrile

**bp** – base pairs

**$C_q$** – quantitation cycle (threshold cycle)

**c-di-GMP** – cyclic diguanylate monophosphate

**cDNA** – complementary DNA

**cfu** – colony forming units

**COG** – Clusters of Orthologous Genes

**dd$H_2O$** – double distilled water

**DNA** – deoxyribonucleic acid

**dNTPs** – deoxyribonucleoside triphosphates

***e.g.*** – for example (Latin: *exempli gratia*)

**ESI** – electrospray ionisation

**EtOAc** – ethyl acetate

**EtOH** – ethanol

**FA** – formic acid

**FC** – fold change (statistics)

**gDNA** – genomic DNA

**HPLC** – high-throughput liquid chromatography

***i.a.*** – among others (Latin: *inter alia*)

**LPM** – Laboratory of Plant Microbiology

**MCS** – multiple cloning site

**MeOH** – methanol

**mRNA** – messenger RNA, the transcribed DNA

**MS** – mass spectrometry

**m/z** – ion mass to charge ratio (mass spectrometry)

**NRPS** – non-ribosomal peptide synthetase

**$OD_{600}$** – optical density measured at $\lambda$ = 600 nm (spectrophotometry)

**ORF** – open reading frame

**PCA** – principal component analysis (statistics)

**PCR** – polymerase chain reaction

**PGPR** – plant growth-promoting rhizobacteria

**PKS** – polyketide synthetase

**PVD** - pyoverdine

**qPCR** – quantitative (Real Time) PCR

**Q-TOF** – quadrupole – time-of-flight (mass spectrometry detection type)

**rcf** – relative centrifugal force

**RNA** – ribonucleic acid

**rpm** – rotations per minute

**RT** – reverse transcription

**TB** – transformation buffer

**TBE** – Tris/borate/EDTA, an electrophoresis buffer

**TSB** – Tryptic Soy Broth, a growth medium

**UV-Vis** – ultraviolet-visible light spectrum (spectrophotometry)

**VOCs** – volatile organic compounds

**wt** – wild type strain

## 2. Abstract (EN)

*Pseudomonas donghuensis* P482 is a tomato rhizosphere isolate. It has been investigated due to its abilities to inhibit growth of bacterial and fungal plant pathogens and to colonise plants' roots. The literature data suggest that biosynthesis of antimicrobials and biofilm formation (necessary for the efficient plant colonisation) in bacteria are significantly influenced by the metabolised nutrients that take part in crucial biochemical pathways and regulate gene expression. Carbon and iron sources were shown to be highly important for these processes in *Pseudomonas* spp. In this study two carbon sources (glucose and glycerol) as well as iron(II) and iron(III) were used to examine their influence on *P. donghuensis* P482 antimicrobial activity, biosynthesis of antimicrobials and expression of the genes responsible for these processes. Additionally, the influence of the given nutrients on biofilm formation by P482 on abiotic surface was analysed.

The research involved previously constructed P482 mutants with inactivated genes in three regions selected for their involvement in antimicrobial activity: 7 hydroxytropolone (7-HT) biosynthesis cluster, two genes responsible for pyoverdine (PVD) biosynthesis, and "cluster 17", responsible for the biosynthesis of an unknown antimicrobial; and two regulatory genes: *fur,* responsible for iron metabolism and *gacA*, a transcription regulator of the global regulatory system Gac-Rsm. The tests of direct antagonism of these mutants towards three plant pathogenic bacteria (*Dickeya solani* IFB0102, *Pectobacterium brasiliense* Pcb LMG21371 and *Pseudomonas syringae* pv. *syringae* Pss762) on minimal media with the given carbon and iron sources were performed. These tests indicate no significant involvement of the 7-HT biosynthesis cluster in P482 antagonistic activity in the minimal medium with glycerol as a sole carbon source. However, "cluster 17" genes were shown to play an important role for the P482 antibacterial activity in glycerol. Additionally, the PVD biosynthesis genes are significantly involved in P482 antimicrobial activity regardless of the carbon source. The supplementation with iron(II) ions causes the reduction of P482 antimicrobial activity dependent on these genes.

Furthermore, the extracts containing secondary metabolites obtained from the postculture filtrates of P482 wild type (wt) and mutants cultured in rich and minimal media with different carbon sources were analysed using HPLC MS. The differences in the metabolome of P482 wt and mutants under given nutritional conditions were identified. No 7-HT was detected to be produced by all tested strains under minimal media conditions.

The expression of the genes of the aforementioned regions of P482 genome was tested in minimal medium with glucose/glycerol and with or without the iron(II)/iron(III) supplementation using RT-qPCR method. The analyses were preceded with a detailed selection and validation of reference genes. Three genes, namely *gyrB, rpoD* and *mrdA*, were found to be the most stably

expressed. The expression of P482 7-HT biosynthesis genes was observed to be significantly downregulated in glycerol medium in comparison to glucose medium. Moreover, iron(II) supplementation was shown to downregulate the expression of 7-HT and PVD biosynthesis genes. These results confirm that glycerol and iron(II) negatively impact the biosynthesis of the known P482 antimicrobials.

The analysis of the dependence of P482 biofilm formation ability on carbon and iron sources in the medium showed that the supplementation with iron(II) ions has a mild stimulatory effect on biofilm formation when glycerol is a sole carbon source, and a moderately negative effect in the glucose medium.

The study presents an overall dependence of the P482 antimicrobial activity, secondary metabolism and selected genes' expression on the tested carbon and iron sources. The results obtained in the study contribute to the understanding of the influence of nutrients on the biocontrol mechanisms of P482.

## 3. Abstrakt (PL)

*Pseudomonas donghuensis* P482 jest izolatem bakteryjnym pochodzącym z ryzosfery pomidora wykazującym aktywność przeciwdrobnoustrojową względem bakteryjnych i grzybowych patogenów roślin. Szczep ten wykazuje zdolność do kolonizacji korzeni roślin (pomidora, kukurydzy, ziemniaka, sałaty). *P. donghuensis* P482 jest jednym z kilku opisanych do tej pory szczepów należących do tego gatunku. Wszystkie opisane do tej pory szczepy wykazują aktywność biobójczą, obserwowane są jednak różnice względem aktywności przeciwbakteryjnej i przeciwgrzybowej badanych szczepów. Dane literaturowe wskazują, że istotnymi czynnikami wpływającymi na bakteryjną syntezę biobójczych metabolitów wtórnych oraz tworzenie biofilmu (niezbędnego do wydajnej kolonizacji roślin) są m. in. składniki odżywcze metabolizowane przez bakterie i wchodzące w szereg ścieżek biochemicznych oraz regulujące ekspresję genów. W przypadku bakterii z rodzaju *Pseudomonas* istotną rolę odgrywają źródła węgla oraz żelaza. Aby zbadać zależności w modulacji aktywności bakteriobójczej P482 oraz syntezy biobójczych metabolitów i ekspresji genów za nie odpowiedzialnych, a także tworzenia biofilmu w warunkach abiotycznych, zastosowałam dwa źródła węgla, glukozę i glicerol, a także jony żelaza(II) i żelaza(III).

W pracy wykorzystałam mutanty insercyjne P482, w których inaktywowane zostały wybrane geny w trzech regionach zaangażowanych w aktywność przeciwdrobnoustrojową P482: klaster biosyntezy 7 hydroksytropolonu (7-HT), dwa geny odpowiedzialne za biosyntezę piowerdyny oraz „klaster 17.", odpowiedzialny za syntezę nieznanego czynnika przeciwdrobnoustrojowego; a także geny zaangażowane w regulację: metabolizmu żelaza (gen *fur*) i transkrypcji przez system Gac-Rsm (gen *gacA*). Analiza bezpośredniej antybiozy mutantów P482 wobec trzech bakteryjnych patogenów roślin (*Dickeya solani* IFB0102, *Pectobacterium brasiliense* Pcb LMG21371 i *Pseudomonas syringae* pv. *syringae* Pss762) na podłożach minimalnych z odpowiednim źródłem węgla i żelaza wykazała brak udziału klastra biosyntezy 7-HT w aktywności bakteriobójczej P482, gdy jedynym źródłem węgla jest glicerol. Zaobserwowałam natomiast, że ważną rolę dla aktywności przeciwbakteryjnej P482 w podłożu z glicerolem pełni „klaster 17.". Z kolei geny biosyntezy piowerdyny są wysoce istotne dla aktywności przeciwdrobnoustrojowej P482 niezależnie od źródła węgla, a suplementacja żelazem(II) powoduje osłabienie aktywności od nich zależnej.

W ramach dalszych badań, ekstrakty zawierające metabolity wtórne (w tym bakteriobójcze) pochodzące z filtratów pohodowlanych P482 lub pochodnych mutantów w podłożach pełnych oraz minimalnych z różnym źródłem węgla poddane zostały analizom z użyciem techniki HPLC-MS. Dzięki tym badaniom zidentyfikowałam różnice pomiędzy

metabolomem P482 i poszczególnych mutantów w danych warunkach hodowli. W warunkach podłoża minimalnego nie wykryto produkcji 7-HT u żadnego z badanych szczepów.

Ekspresja wybranych do analiz genów P482 w podłożach minimalnych z glukozą/glicerolem bez żelaza lub z suplementacją jonami żelaza(II)/żelaza(III) została zbadana metodą RT-qPCR. Badania poprzedziłam szczegółową selekcją i walidacją genów referencyjnych, z których najwyższą stabilność ekspresji wykazały *gyrB, rpoD* oraz *mrdA*. Wykazałam, że ekspresja genów związanych z produkcją 7 HT jest znacznie obniżona w komórkach *P. donghuensis* P482 hodowanych z glicerolem jako jedynym źródłem węgla w porównaniu do hodowli z glukozą, a suplementacja żelazem (II) obniża ekspresję genów biosyntezy 7-HT oraz piowerdyny. Wyniki te potwierdzają poprzednie wnioski, że glycerol i żelazo (II) wpływają negatywnie na produkcję 7-HT i PVD.

W ramach prowadzonych badań analizowałam także zależności formowania biofilmu abiotycznego przez P482 od źródeł węgla i żelaza obecnych w podłożu hodowlanym. Wyniki sugerują, że suplementacja jonami żelaza(II) ma stymulujący wpływ na formowanie biofilmu przez P482 w podłożu z glicerolem, jednakże wpływ ten jest negatywny w podłożu z glukozą.

Przeprowadzone analizy wskazują na wysoką zależność metabolizmu wtórnego i aktywności bakteriobójczej P482 od badanych źródeł węgla i żelaza. Wyniki przeprowadzonych badań podstawowych przyczyniają się do zrozumienia wpływu powyższych substancji odżywczych na mechanizmy działania szczepu P482 o potencjalnym zastosowaniu w biologicznej ochronie roślin uprawnych.

## 4. Popular science abstract

Bacterial plant pathogens cause huge losses in crop production. One of the emerging methods to fight them is using natural agents, such as plant-beneficial microbes. By inhabiting the plant and producing antimicrobial compounds, they can protect crops from diseases. One of the bacterial strains explored in the context of these useful traits is *Pseudomonas donghuensis* P482, an isolate from a tomato plant root.

P482 produces compounds known as pyoverdine (PVD) and 7-hydroxytropolone (7-HT). They show antimicrobial activity and help P482 acquire one of the fundamental nutrients, iron. Additionally, P482 colonises roots of many crop plants. However, we still have a lot to learn about how these mechanisms work. In my study I explored how external conditions may affect the basic beneficial traits of P482. This is an important topic because the conditions of the environment may affect every little process inside the bacterial cell, changing its profile of activity. The external conditions I tested were the nutrients present in the environment: carbon sources (glucose and glycerol) and iron ions. The crucial P482 traits tested for whether they're affected by the mentioned nutrients were: P482 antagonistic activity against bacterial plant pathogens, its secondary metabolism, gene expression (activation of specific genes), and biofilm formation (which is necessary to colonise the plants).

My study found that P482 uses different mechanisms of its antimicrobial activity depending on whether it uses glucose or glycerol as the carbon source. Additionally, I described the identification of "cluster 17", one of the genetic components in part responsible for this activity. Inactivation of a gene (BV82_4240) from this cluster caused the lack of antibacterial activity of P482 when it consumed glycerol as a carbon source. Additionally, several molecular biology tools got developed during this study: I introduced several gene-inactivating mutations to P482 to produce mutant strains I could use in the study, I also found the 3 very stably expressed genes in P482 to use them as a reference in gene expression studies.

Further in this work, the differences caused in P482 by the carbon and iron sources were characterised on the level of certain genes, their expression and metabolic profile. I found that glucose stimulates the production of 7-HT by P482, while glycerol represses it. In case of PVD, it was iron presence in the environment that disrupted its production by P482. PVD is a compound necessary for bacteria to obtain poorly available iron so its lower production was expected when iron is easily accessible. Furthermore, P482 biofilm was found to be only slightly affected by the changes in the genetic background of P482 and environment combined.

This study adds new knowledge to our understanding of the carbon source regulation of biocontrol traits in bacteria, strengthens our current theories about iron ions regulation of PVD production and its importance, and suggest further research directions.

# 5. Introduction

## 5.1. *Pseudomonas donghuensis* P482 – a plant-associated pseudomonad with antibacterial capabilities

### 5.1.1. Plant-associated *Pseudomonas* spp.

Gram-negative, rod-shaped γ-proteobacteria of the genus *Pseudomonas* are ubiquitous in the environment. They can be found in soil, water (sea or fresh), and colonising plants and animals. Moreover, the physiological and genetic diversity among pseudomonads is remarkable (Loper *et al.*, 2012, Spiers *et al.*, 2000). Therefore, the existence of *Pseudomonas* species that are pathogenic to plants, such as *Pseudomonas syringae*, or even to humans, such as *Pseudomonas aeruginosa*, is not surprising. However, this genus consists also of many other plant-associated species. Many of them are studied for their potential in plant protection against phytopathogens (Haas and Défago, 2005, Höfte, 2021).

Rhizosphere, a soil layer around plant roots, is actively influenced by the presence of plant root exudates. The primary contribution of plants is secreting up to 40% of the carbon they assimilate and turn into organic compounds like carbohydrates, organic acids or amino acids (Badri and Vivanco, 2009). This provides a suitable environment for heterotrophic microorganisms. For this reason, the number of bacterial cells inhabiting the rhizosphere is 10 to 1000 times higher than that observed for bulk soil (Lugtenberg and Kamilova, 2009). Furthermore, the plant-associated-bacteria often actively colonise plant roots, protecting crops from pathogens and/or secreting plant-beneficial compounds. These features gave them the common name of **P**lant **G**rowth-**P**romoting **R**hizobacteria [PGPR] (Kloepper and Schroth, 1978).

PGPRs are often considered as the biological agents in an agricultural strategy of sustainable defence of crops against pests and pathogens, called "biological plant protection" (biological control or biocontrol). This approach involves using the so-called "natural enemies" (antagonists and the compounds they produce) of all types of organisms harmful to plants to stop their spread and contain the disease or other damage they inflict to the crops. Several mechanisms by which the potential microbial biocontrol agents combat the pathogenic microorganisms have been characterised. The most often described in the literature is a direct antagonism based on the secretion of antibacterial or antifungal compounds by the potential biocontrol bacteria (Fravel, 2003, Köhl *et al.*, 2019). Another common bacterial plant protection mechanism is competition, in which plant-beneficial microbes compete with potential pathogens for niches or nutrients (Lugtenberg and Kamilova, 2009). A particular case of this mechanism is the competition for iron ions involving the secretion of siderophores. These compounds chelate ferric iron ions ($Fe^{3+}$), usually unavailable for the direct uptake by microorganisms, and transport them to the cells of

the siderophore producers using specific receptors. This way PGPR can limit iron availability for other microorganisms, what protects plants in case of the emergence of plant pathogenic bacteria and fungi (Bloemberg and Lugtenberg, 2001, Leong, 2003).

*Pseudomonas* spp. possess many favourable traits that make them one of the most interesting genera in microbiological research, especially in the field of plant protection (Haas and Défago, 2005). The most extensively researched plant-associated pseudomonads are the fluorescent strains, particularly those belonging to *P. fluorescens*, *P. putida, P. chlororaphis* or *P. protegens* species (Budzikiewicz, 1993, 1997, Mavrodi *et al.*, 2013, Raaijmakers *et al.*, 1995). Among many potentially valuable metabolites, they secrete fluorescent compounds – the **pyoverdines** [PVDs] acting as siderophores that bind ferric iron ions and make it available for the bacteria to utilise (Visca *et al.*, 2007). Data show that PVDs can limit the growth of plant pathogens in controlled iron-depleted environments (Liu *et al.*, 2021a), however, the ability to synthesise PVDs and scavenge iron ions is not enough to suppress the disease development *in planta* (Loper and Buyer, 1991). Therefore, biocontrol *Pseudomonas* spp. must also be characterised by plant protection and growth promotion mechanisms other than the iron competition.

A different mechanism of plant protection developed by *Pseudomonas* spp. is based on **direct antibiosis**. The literature describes a wide selection of bioactive compounds produced by pseudomonads and inhibiting the growth of plant pathogens. Among them, the best-studied compounds are those inhibiting the growth of plant pathogenic fungi, e.g., phenazines (Thomashow and Weller, 1988, Tupe *et al.*, 2015), 2,4-diacetylphloroglucinol [2,4-DAPG] (Biessy and Filion, 2021, Keel *et al.*, 1992, Nowak-Thompson *et al.*, 1994) and pyrrolnitrin (Howell and Stipanovic, 1979, Tripathi and Gottlieb, 1969). The activity of phenazines was shown, among others, against *Fusarium oxysporum,* which causes wilting of a range of different crop plants in agricultural settings (Mazurier *et al.*, 2009). 2,4-DAPG is one of the most prominent microbial antifungals, inhibiting the growth of many versatile fungal and oomycete root pathogens belonging to genera *Pythium, Rhizoctonia* and *Fusarium* (Keel *et al.*, 1992, Rezzonico *et al.*, 2007). Moreover, the *in vitro* and *in vivo* activity of 2,4-DAPG against a take-all wheat disease-causing agent, *Gaeumannomyces graminis* var. *tritici,* is well documented in the literature (Kwak *et al.*, 2009, Raaijmakers and Weller, 1998, Weller, 2007). Pyrrolnitrin biocontrol activity was confirmed against such fungi as *Rhizoctonia solani* (the causal agent of cotton seedling disease, potato black scurf, sheath blight of rice and many more) and *Fusarium graminearum*, the pathogen responsible for fusarium head blight of wheat (Howell and Stipanovic, 1979, Park *et al.*, 2011). Another group of antifungals produced by *Pseudomonas* spp. are the volatile organic compounds [VOCs]. Hydrogen cyanide is a VOC produced by multiple species of fluorescent pseudomonads and it highly contributes to the broad antifungal potential of these bacteria (Blumer and Haas, 2000,

Voisard *et al.*, 1989). Other antifungal VOCs identified in various species of *Pseudomonas* include nonanal, 2-ethyl-1-hexanol, n-decanal, benzothiazole, cyclohexanol and dimethyl trisulphide, which inhibit the growth of *Sclerotinia sclerotiorum* (Fernando *et al.*, 2005). Among other natural fungicides produced by *Pseudomonas* spp. are cyclic lipopeptides, proven to act against plant and human fungal pathogens (Nybroe and Sørensen, 2004). These compounds, being biosurfactants, serve not only as antimicrobials but also play a role in *Pseudomonas* spp. plant colonisation and motility (Raaijmakers *et al.*, 2006).

The direct **antibacterial** activity of fluorescent *Pseudomonas* spp. is not documented as meticulously as their antifungal activity, it is, however, also a vital biocontrol trait. For example, 2,4-DAPG, in addition to its antifungal activity, was reported to inhibit symptoms of several plant diseases caused by bacterial pathogens such as *Pectobacterium carotovorum* (Cronin *et al.*, 1997) or *Clavibacter michiganensis* (Lanteigne *et al.*, 2012). Bacteriocins are another class of compounds, tested as potential antibacterial agents for biocontrol. Since they act only against the closely related species, they can be used to contain diseases caused by pathogenic *Pseudomonas* spp., which several studies up to date have confirmed (Lavermicocca *et al.*, 2002, Parret *et al.*, 2005, Vidaver, 1976).

A trait that allows certain species from genus *Pseudomonas* to be considered as biocontrol agents is their ability to form biofilms and efficiently colonise the plant surface and interior. Most research on this topic focuses on plant root system colonisation. This microbial feature is defined with the term **rhizocompetence** and it is already relatively well understood for plant-associated pseudomonads (Zboralski and Filion, 2020). Bacteria are drawn to certain plants with chemotaxis, flagella-driven motility towards the plant exudates. As a result, they attach to the root surface and form a biofilm, which is more advantageous for both bacteria and plants than the planktonic bacterial presence in the rhizosphere (Santoyo *et al.*, 2021). Biofilm formation, which provides the bacteria with higher antibiotic resistance, was also described to increase the production of specific PGPR metabolites (e.g., plant growth hormones, siderophores and antimicrobials) by the root colonisers (Backer *et al.*, 2018).

### 5.1.2. P482 as a strain of *Pseudomonas donghuensis*

*Pseudomonas donghuensis* is one of the newly established species belonging to the genus *Pseudomonas* that recently caught the attention of researchers as potential antimicrobial agents (Gao *et al.*, 2015). One of the first strains identified as belonging to this species is *P. donghuensis* P482, isolated and researched at the Laboratory of Plant Microbiology [LPM], Intercollegiate Faculty of Biotechnology, University of Gdańsk. Thanks to its exceptional characteristics, the P482 strain is the main subject of this study.

The strain P482 was isolated from a tomato rhizosphere in Gdynia (Poland). It was first described by Krzyżanowska *et al.* (2012a) and Golanowska *et al.* (2012) as one of the plant-associated isolates that inhibit the growth of potato soft-rot causing agents (bacteria from genera *Dickeya* and *Pectobacterium*) and stone fruit trees pathogens (two pathovars of *Pseudomonas syringae*). At the same time, research was conducted in China on a local strain of *Pseudomonas*, named HYS$^T$, isolated from the Donghu lake and characterised by a high yield of siderophores (Gao *et al.*, 2012, Yu *et al.*, 2014). Studies on HYS$^T$ and P482 have yielded the sequences of their genomes (Gao *et al.*, 2012, Krzyzanowska et al., 2014, 2021) and the results obtained reveal a very high identity between these two strains. However, both HYS$^T$ and P482 were found to be significantly different to other known *Pseudomonas* strains. Therefore, the Chinese research team established a novel species named *Pseudomonas donghuensis*. The name was derived from the isolation place of the HYS$^T$ strain (Gao et al., 2015). Since then, in the last few years, several other strains of *P. donghuensis* coming from different settings have been described, i.e.: SVBP6 in bulk soil of a soybean field in Argentina (Agaras et al., 2018), 22G5 in the cotton rhizosphere in China (Tao *et al.*, 2020), JS1 in compost soil in Brazil (Villamizar et al., 2020) and P17 in cherry tree rhizosphere in Canada (Marin-Bruzos et al., 2021).

Phylogenetic analyses showed that *P. donghuensis* belongs to the *Pseudomonas putida* group and is most closely related to *Pseudomonas vranovensis* (Gao *et al.*, 2015, Krzyżanowska *et al.*, 2016) (**FIGURE 1**). Furthermore, the recent advances in accessibility to genome sequencing have let researchers discover several new isolates very closely related to *P. donghuensis* and novel species were established in the phylogenetic studies (Frasson *et al.*, 2017, Oh *et al.*, 2019). In general, the *P. putida* group strains are characterised by environmental versatility typical for the genus *Pseudomonas*: they inhabit waters, soil, sewage, as well as plants and animals. This diversity is visible not only in the habitat variety, but also in the genomes and phenotypes of strains belonging to *P. putida* group (Gomila *et al.*, 2015, Guo *et al.*, 2016). Recently, a study by Girard *et al.* (2021) proposed partitioning of the *P. putida* group into sixteen suggested subgroups due to the abundance of highly pronounced differences in their genomes, especially the genomic regions responsible for the biosynthesis of cyclic lipopeptides. Following these novel rules, *P. donghuensis* got classified into the *P. vranovensis* subgroup of the *P. putida* group.

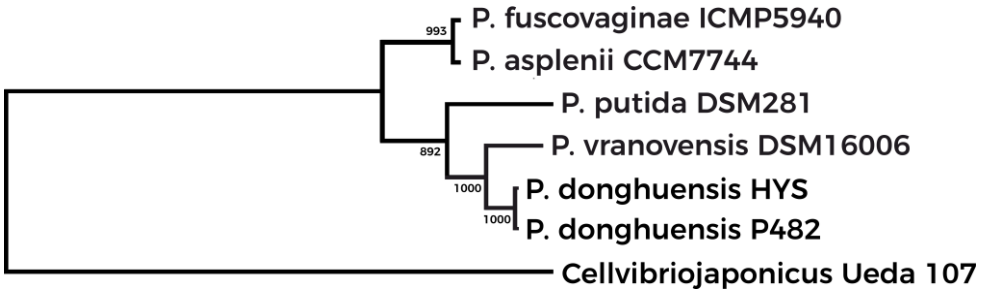


**FIGURE 1. Phylogenetic tree representing relationship between *P. donghuensis* and selected species from the *P. putida* group** (figure adapted from Krzyżanowska *et al.* (2016), see the referenced study for details).

Overall, the multitude of *P. putida* group representatives, their extraordinary genomic diversity and the 21st-century molecular biology and bioinformatics techniques, like genome mining (Paterson *et al.*, 2017), allow for research on finding novel functional traits to utilise in medicine, industry, and biocontrol. The studies on *P. donghuensis* confirm that this approach can unveil many valuable features.

### 5.1.3. P482 as an antagonist of phytopathogens

The research on *P. donghuensis* P482 in the LPM concentrates mainly on its potential as a bacterial phytopathogen antagonist and a plant protection agent (Golanowska *et al.*, 2012, Krzyżanowska *et al.*, 2012a, 2016). P482 is characterised by a considerable antibacterial activity tested primarily against bacterial plant pathogens (Krzyżanowska *et al.*, 2016). Among these plant pathogens are bacteria from the *Pectobacteriaceae* family of high economic importance, such as *Dickeya solani* and *Pectobacterium brasiliense* (Van Gijsegem *et al.*, 2021). Moreover, P482 inhibits the growth of pathogens from its own genus *Pseudomonas,* among them various pathovars of phytopathogenic *Pseudomonas syringae* (Golanowska *et al.*, 2012, Matuszewska *et al.*, 2021) and *Pseudomonas aeruginosa*, pathogenic to humans and animals (Maciąg, MSc thesis, Gdańsk, 2015). *P. syringae* is a versatile plant pathogen whose pathovars have been described by Mansfield *et al.* (2012) as the most impactful for the general understanding of bacterial pathogenicity and causing economically significant crop diseases on *e.g.*, tomatoes, stone fruit trees and numerous other cultivated plants.

Excluding the LPM studies on P482, the other *P. donghuensis* strains mainly described in the literature are HYS$^T$ and SVBP6. *P. donghuensis* HYS$^T$, isolated in China, was first introduced in a genome announcement of a strain of unknown *Pseudomonas* species, producing high amounts of iron chelators (Gao *et al.*, 2012). The following phylogenetic analysis allowed HYS$^T$ to be classified as a novel species, *P. donghuensis* (Gao *et al.*, 2015), establishing HYS$^T$ as the type strain for this species. Subsequently, Jiang *et al.* (2016) proposed that a non-fluorescent compound, namely 7-hydroxytropolone [7-HT], plays the iron-scavenger role in HYS$^T$. Additionally, a complex regulatory mechanism of 7-HT production was unveiled for *P. donghuensis* HYS$^T$ (Chen M. *et al.*, 2018, Yu *et al.*, 2014). Briefly, the mechanism involves a positive regulation by GacA and GacS proteins, a part of the global regulatory Gac/Rsm system, which in turn controls certain transcriptional regulators from LysR and TetR/AcrR families. These regulators activate the expression of 7-HT biosynthesis genes. Furthermore, HYS$^T$ was found to be pathogenic to a developmental biology model organism, the nematode *Caenorhabditis elegans,* and 7-HT was reported to be responsible for this activity of the examined pseudomonad (Gui *et al.*, 2020).

The importance of 7-HT was also recognised in SVBP6, the other well-documented strain of *P. donghuensis*. Isolated in Argentina, SVBP6 was recognised as a plant-beneficial microbe primarily due to its broad antifungal activity against phytopathogens (Agaras *et al.*, 2018). Furthermore, the functional Gac/Rsm pathway proved essential for *P. donghuensis* potentially plant-probiotic activity. A subsequent study on the SVBP6 strain showed that 7-HT is the main contributor to its antifungal activity (Muzio *et al.*, 2020). Finally, it is worth noting that the P482 strain also inhibits growth of numerous phytopathogenic fungi (from highly virulent species such as *Fusarium oxysporum* or *Rhizoctonia solani*); however, the mechanism of this activity is based upon the production of VOCs by P482 (Ossowicki *et al.*, 2017).

The two strains (HYS$^T$ and SVBP6) were described, albeit briefly, to inhibit growth of bacteria such as *Xanthomonas campestris* pv. *badri* and *Bacillus subtilis* (Agaras et al., 2018, Gao et al., 2015). However, the topic of the broad antibacterial activity of *P. donghuensis* was expanded in the P482 strain. Primarily, Krzyżanowska *et al.* 2016 showed that this feature could not be attributed to the common antimicrobial substances produced by other fluorescent pseudomonads. Genome mining analyses showed that P482 lacks the biosynthetic gene clusters required to produce 2,4-DAPG, pyochelin, pyrrolnitrin, phenazines and other typical antimicrobials of *Pseudomonas* spp. (Krzyżanowska *et al.*, 2016). The same study on P482 revealed that the biosynthetic cluster necessary to produce 7-HT is involved in the antibacterial activity of *P. donghuensis* (Krzyżanowska *et al.*, 2016). *P. donghuensis* also produces pyoverdine [PVD], a highly potent siderophore that can be responsible for the antimicrobial activity of its producer (Liu et al., 2021a). However, the ability to synthesise PVD was not shown to be a significant contributor to the antibacterial activity of P482 under the tested conditions (LB-agar – a rich growth medium) (Krzyżanowska et al., 2016). On the other hand, the study of Maciąg (MSc thesis, Gdańsk, 2015) unveiled another gene cluster possibly responsible for P482 antimicrobial activity – "cluster 17". This analysis utilised antiSMASH 2.0 (Blin et al., 2013), a tool for genome mining of the secondary metabolites' biosynthetic clusters. The *in silico* research suggested a vague link of "cluster 17" with polyketide synthesis. Polyketides comprise a group of metabolites with a broad spectrum of biological activities. Among them, we can find a variety of antibiotics, antifungal agents and other drugs (Staunton and Weissman, 2001), and this wide array of valuable compounds belonging to the polyketide group prompted the more detailed inspection of "cluster 17". Overall, the study presented here further explores the involvement of all three mentioned genomic regions (7-HT biosynthetic cluster, PVD biosynthetic genes and "cluster 17") in the P482 antibacterial activity towards plant pathogens. The analyses included in this dissertation are also partially covered in the primary research article published in the course of this study (Matuszewska et al., 2021).

Another crucial trait of P482 making it a promising strain in biocontrol research is its ability to colonise crop plants. The process of plant root colonisation by bacteria is highly dependent on external factors, such as environmental and nutritional conditions, and internal factors, including bacterial ability to move and form biofilms (Molina *et al.*, 2003, Zboralski and Filion, 2020). *P. donghuensis* P482 is a flagellated strain able to perform swimming and swarming motility. Moreover, P482 forms biofilm efficiently on both abiotic, namely glass and polystyrene, as well as biotic surfaces, such as plant roots (Krzyzanowska *et al.*, 2012b, Rajewska *et al.*, 2020). Although it was isolated from the rhizosphere of tomato, it also colonises potato (Krzyzanowska *et al.*, 2012b) and maize (Rajewska *et al.*, 2020).

Nevertheless, whether P482 or any other organism exhibits these crucial abilities: antibiosis and plant colonisation, depends not only on the internal factors (encoded in the genome) but also the environmental regulation that impacts gene expression. For example, in the author's previous study (Matuszewska, MSc thesis, Gdańsk, 2016), culturing temperature ≥ 34 °C caused lower antimicrobial activity of P482 culture extracts, whereas the change of the pH of the culture in the range from 6 to 9 did not affect this activity. The mentioned study also suggested that nutrients provided in the environment can entirely rearrange microbial secondary metabolism. Thus, the study presented in this thesis focuses on the impact of specific nutrients on the antimicrobial ability, selected genes' expression and the abiotic biofilm formation by P482.

## 5.2. Carbon and iron metabolism

Carbon is the fundamental element of all life on Earth. Since the beginnings of organic life more than 3 billion years ago, different organisms have evolved different ways of carbon metabolism. In prokaryotes, the form in which they uptake and process carbon from the environment substantially and inherently affects their entire functioning.

### 5.2.1. Carbon metabolism in *Pseudomonaceae*

Basic carbohydrate catabolism in *Pseudomonas* spp. is unique. Bacteria from the genus *Pseudomonas*, including *P. donghuensis* P482, are aerobic chemoorganotrophs characterised by a vast range of utilised carbon sources (Lessie and Phibbs, Jr., 1984, Palleroni, 2005). Unlike most bacteria and archaea, but also higher organisms, many *Pseudomonas* spp. do not utilise the Embden-Meyerhoff-Parnas [EMP] pathway in glycolysis (Temple *et al.*, 1998). This alteration is caused by the lack of one enzyme needed for employing the EMP pathway – 6-phosphofructokinase. Instead, the majority of pseudomonads seems to metabolise six- and three-carbon carbohydrates, such as **glucose** ($C_6$) and **glycerol** ($C_3$), through a cycle involving the Entner-Doudoroff pathway [EDP] (Lessie and Phibbs, Jr., 1984) or through a recently discovered hybrid pathway including reactions from EMP, EDP and pentose pathway (Dolan *et al.*, 2020, Nikel *et al.*, 2015).

Another important trait of these bacteria is the profound carbon catabolite repression [CCR] and its regulation. CCR is a process occurring when bacteria have access to more than one carbon source and it regulates which one of them is assimilated preferentially (Rojo, 2010). In pseudomonads, unlike in i.e., *Escherichia coli*, glucose is not the primarily preferred carbon source and glycerol is also not readily degraded by these bacteria. Instead, they favour certain organic acids and amino acids and due to this unique order of preferred carbon sources their CCR has been recently named the reverse CCR (Park *et al.*, 2020). To optimise the metabolism, *Pseudomonas* spp., thriving in various environments and utilising numerous compounds, possess an elaborate regulatory system for CCR (Collier *et al.*, 1996, Rojo, 2010). It is mainly based on the Crc protein, a global regulator. Its mode of action relies on posttranscriptional regulation of gene expression – Crc can bind to the different mRNAs which encode proteins facilitating catabolism of given carbon sources. However, the recent findings have provided an even more unclear picture of this complex system, suggesting CCR regulation is highly species-dependent, involves many other mechanisms and regulators such as the Hfq protein, and remains not entirely explored (Park *et al.*, 2020, Sonnleitner and Bläsi, 2014, Wang *et al.*, 2021).

The complexity of pseudomonad catabolism is also manifested in the considerable number of secondary metabolites they can synthesise and the nuanced regulation of their biosynthesis (Gross and Loper, 2009). The pathways leading to the biosynthesis of many of these compounds

comprise diverse reactions, a variety of them facilitated by non-ribosomal peptide synthetases [NRPSs] or polyketide synthetases [PKSs], or both. NRPSs take part in peptide synthesis independently of mRNAs, which further complicates understanding *Pseudomonas* biology. All described biochemical intricacies provided the basis for numerous studies on primary and secondary metabolic pathways, their regulation and significance.

### 5.2.2. Carbon sources influence secondary metabolism

The regulatory role of nutrients on secondary metabolism in *Pseudomonas* spp. has been researched mainly to provide data on enhancing the production of the most valuable metabolites – antibiotics. Carbon sources have been studied most extensively of all the nutrients (Sánchez *et al.*, 2010). The earliest research on nutritional regulation in *Pseudomonas* spp. was conducted to establish the media composition for the production of fluorescent compounds (Georgia and Poe, 1931, King *et al.*, 1954). One of the early contemporary studies on single carbon source regulation of antibiotics production by PGPR pseudomonads was published by James and Gutterson (1986). They describe the modulatory effect of glucose on the production of yet unknown antifungals by *P. fluorescens* HV37a, some of which are produced only in the presence of glucose, whereas others are synthesised only in the absence of this sugar.

The subsequent research showed that the way carbon source influences the secondary metabolism of pseudomonads is complex, compound-dependent, and strain-dependent. For example, in *Pseudomonas* sp. F113 (now classified as *Pseudomonas kilonensis*) the production level of 2,4-DAPG was raised by sucrose and fructose, while glucose reduced it (Shanahan *et al.*, 1992). However, a Duffy and Défago (1999) study on various strains of *P. fluorescens* (currently some of them classified as *P. protegens*) revealed that this relationship is strain-dependent, as some of the strains included in their study exhibited a glucose-stimulated increase in 2,4-DAPG yield. Thus, more studies are being conducted to investigate the inconsistent regulatory nature of different carbon sources in various secondary metabolites' production by *Pseudomonas* spp. (Li *et al.*, 2008, Park *et al.*, 2011, van Rij *et al.*, 2004, Vindeirinho *et al.*, 2020).

Among the most studied carbon sources in the context of *Pseudomonas* spp. secondary metabolism are **glucose and glycerol**. Glucose serves as a primary energy source for most living organisms and is the most ubiquitous carbohydrate on Earth. *Pseudomonas* spp. metabolise glucose efficiently, however, when the environment is abundant also in organic acids or amino acids, they will be metabolised by pseudomonads in the first place instead of glucose due to the CCR (Rojo, 2010). The second mentioned carbon source is **glycerol**. It is a common organic compound, a simple polyol mostly found in nature as a component of glyceride lipids. It can be assimilated as a carbon source by the majority of Gram-negative bacteria, including *Pseudomonas* spp. The primary metabolism of glycerol in pseudomonads has been researched

mainly utilising *P. putida* KT2440 as a model organism (Nikel *et al.*, 2015, 2014, Poblete-Castro *et al.*, 2020).

Prior to the studies included in this thesis, no data were published regarding the glucose/glycerol influence on the phenotype of *P. donghuensis*. However, the preliminary data (some of which were obtained as a part of the author's Master's project; Matuszewska, MSc thesis, Gdańsk 2016, **FIGURE 2**) revealed the significant relationship between these two carbon sources and *P. donghuensis* P482 secondary metabolism and antimicrobial activity. In that study, P482 was cultured on minimal medium with either glucose or glycerol as a sole carbon source and the post-culture filtrates were extracted with ethyl acetate [EtOAc]. The extracts were tested for their antimicrobial activity in a range of different concentrations against several plant pathogens. The results showed that none of the extracts from P482 cultured in minimal medium inhibited the growth of *Dickeya solani* and *Pectobacterium brasiliense*. However, the extract obtained from P482 cultured in glycerol, to some extent inhibited the growth of a plant pathogenic *Pseudomonas* strain, *P. syringae* pv. *syringae* Pss762. Interestingly, the extract from P482 cultures in glucose did not possess this activity, which suggested the carbon source-dependent differences in regulation of P482 antimicrobials biosynthesis and, in effect, prompted this study.

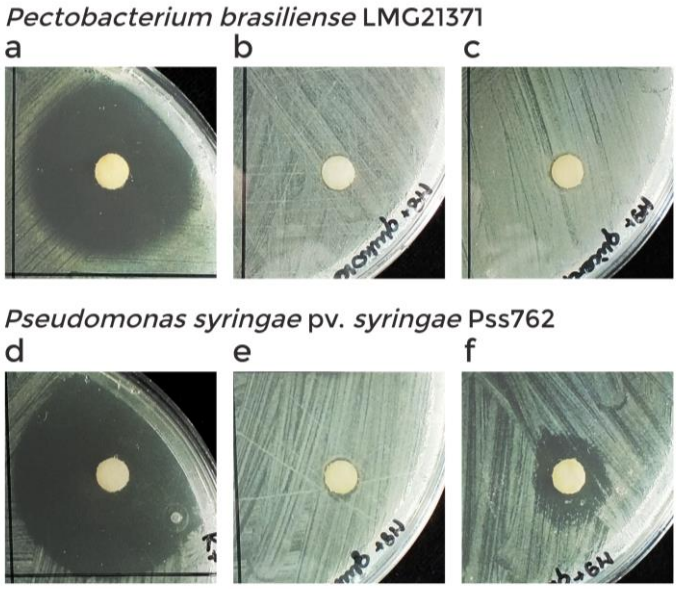


**FIGURE 4. Photographs of pathogen growth inhibition zones obtained in a disk-diffusion test of EtOAc extracts from P482 post-culture filtrates.**
The extracts were obtained from P482 cultures in:
**a, d –** 0.1 TSB medium (control),
**b,e –** M9 medium with glucose,
**c,f –** M9 medium with glycerol.
(see growth media in section **8.1.3**).
Figure adapted from Matuszewska, MSc thesis, Gdańsk, 2016.

### 5.2.3. Iron metabolism in bacteria

In small, organism-specific amounts, iron is essential to almost all known life. It is often described as one of the microelements, the basic life-building blocks. Iron metabolism in bacteria has been studied extensively since the mid-twentieth century. The descriptions of these first efforts in the field of microbial iron metabolism were meticulously gathered together in a book by J. B. Neilands (1974), one of the most prominent researchers in this discipline. In the course of

the described studies, multiple important bacterial enzymes were found to be dependent on iron ions as their cofactors. These metalloproteins, such as cytochromes, catalases, hydrogenases and ferredoxins, are primarily involved in oxidation and general electron transport. Considering how crucial these processes are, it is not surprising that iron uptake and transport in bacterial cells is a fundamental issue. Iron uptake in prokaryotes can be achieved through several strategies. The soluble ferrous iron ($Fe^{2+}$), often present in the environment in anaerobic conditions, can be imported to bacterial cells using Feo transporters, whereas animal pathogens are often able to scavenge haem from their hosts (Andrews *et al.*, 2003, Cornelis, 2010). However, iron is not often readily available in the oxygenated environment due to its oxidised and insoluble state, the ferric ions ($Fe^{3+}$). As a result, many bacterial species developed an efficient and well-regulated system of iron acquisition. At the core of this system are siderophores, compounds of varied structures but similar in their ability for ferric iron chelation and its import into bacterial cells (Neilands, 1995).

#### 5.2.3.1. General iron metabolism regulation in Gram-negative bacteria

While being a crucial nutrient, iron becomes toxic in excessive concentrations and under aerobic conditions. This toxicity results from the Fenton reaction, which utilises ferrous iron and hydrogen peroxide to produce highly reactive oxygen species. Therefore, to protect bacteria from oxidative stress, all cell processes involving iron, especially its uptake and storage, have to be strictly controlled (Cornelis *et al.*, 2011). *Pseudomonas* spp. and other Gram-negative bacteria have developed a particular system of regulation of iron homeostasis.

The iron management system in pseudomonads is supervised by a ferric uptake regulator [Fur] protein (Escolar *et al.*, 1999). It is a representative of the bacterial protein family known as FUR, which consists of various metal uptake regulators, such as zinc uptake regulator [Zur] or nickel uptake regulator [Nur] (Ahn *et al.*, 2006, Patzer and Hantke, 1998). The *fur* gene product can regulate many vital processes in *Pseudomonas* spp., including biofilm formation and *quorum sensing* (Cha *et al.*, 2008, Pasqua *et al.*, 2017). However, Fur is most notably known for its transcriptional regulation of iron uptake by modulating siderophore biosynthesis (Cornelis *et al.*, 2011). When bacteria remain under conditions of good availability of ferrous ions ($Fe^{2+}$), Fur protein dimer binds to these ions. Subsequently, this metalloregulator binds to the specific operators in bacterial DNA (*Fur-box*, consensus sequence: GATAATGATAATCATTATC), which causes the repression of gene clusters involved in siderophore biosynthesis and transport (**FIGURE 3a**). However, if the ferrous ion availability falls below a certain threshold, iron ions dissociate from Fur, which causes its incapability of binding to DNA. One of the consequences is that it leads to the expression of genes responsible for siderophore biosynthesis and other genes the products of which lead to facilitated iron acquisition (**FIGURE 3b**). In addition to Fur, several

$\sigma^{70}$-like transcription factors have been found to have regulatory effects on particular siderophores biosynthesis in *Pseudomonas* spp. (Venturi *et al.*, 1995).

**Siderophores**, the iron scavengers, are ubiquitously produced among bacteria, but their production has also been described in fungi and plants (Haas, 2003, Schaaf *et al.*, 2004). The microbial siderophores are small molecules with a high affinity to ferric iron, and they have been divided into three main categories based on their molecular structure: catecholate siderophores i.e., enterobactin and salmochelin; dihydroxyamate siderophores i.e., exochelin and desferrioxamine B, and mixed siderophores such as pyoverdines and pyochelin (Hider and Kong, 2010). The biosynthesis of siderophores, similarly to many other secondary metabolites, relies on a myriad of enzymes working together. PVD, a fluorescent iron scavenger of various pseudomonads, is an assembly of an oligopeptide chain (with a strain-dependent sequence) and a fluorescent chromophore core (constituted by the (1S)-5-amino-2,3-dihydro-8,9-dihydroxy-1H-pyrimido[1,2-a]quinoline-1-carboxylic acid). As many as fourteen genes encoding various

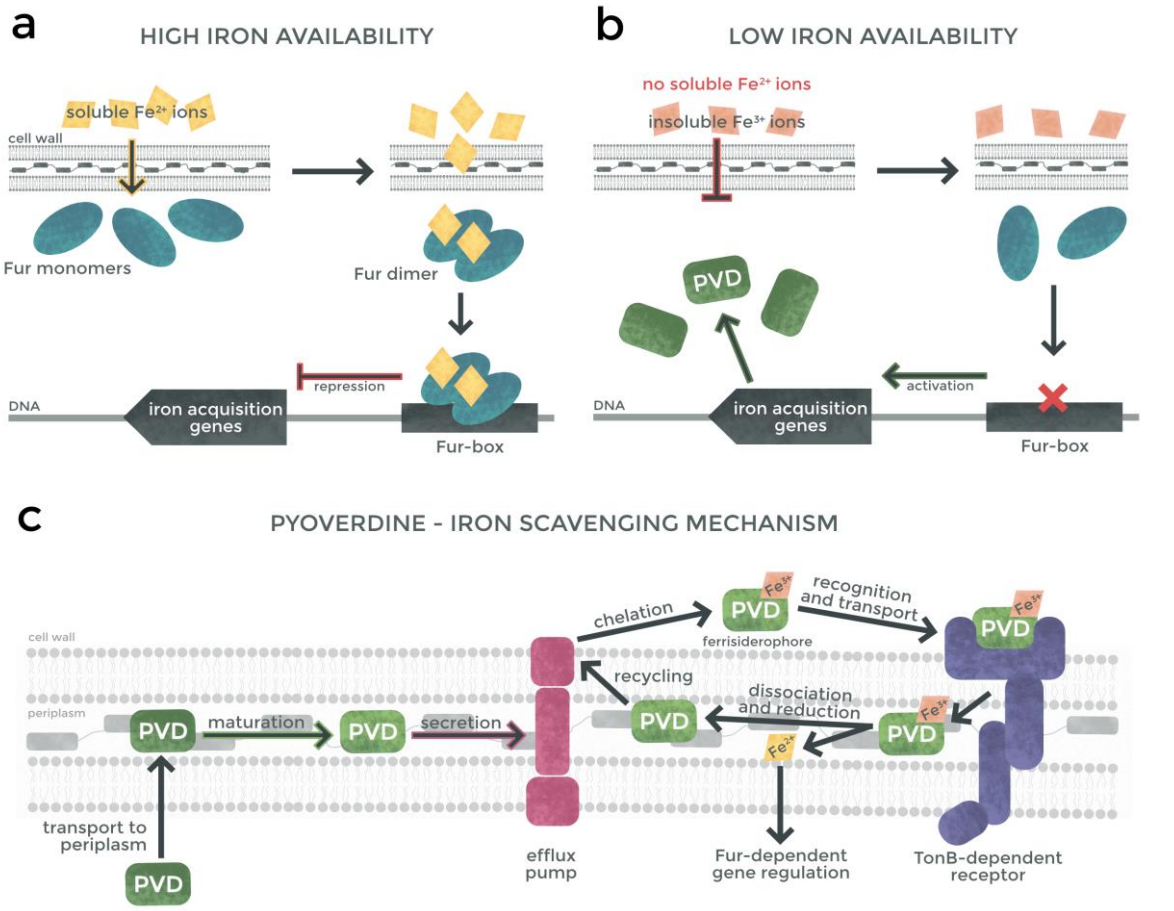


**FIGURE 5. Simplified representation of the iron uptake management in *Pseudomonas* spp.**
Diagram **a** shows the situation when environment is abundant in easily accessible $Fe^{2+}$ ions. Fur protein employs $Fe^{2+}$ as cofactor and represses the expression genes, among others, involved in iron acquisition. Diagram **b** shows the opposite situation which leads to the expression of genes facilitating acquisition of the otherwise inaccessible $Fe^{3+}$ ions. Diagram **c** depicts the iron scavenging mechanism using pyoverdine [PVD] as an example of *Pseudomonas* spp. siderophore.

proteins, such as NRPSs and sigma factors, were identified to be involved in the PVD biosynthesis pathway in *P. aeruginosa* (Lamont and Martin, 2003).

Once synthesised in the cytoplasm, siderophores are transported outside the cell and act as the iron scavengers (**FIGURE 3c**). In most cases, the siderophore secretion seems to be facilitated by various efflux pumps however the siderophore maturation and export process is not yet fully understood (Chen *et al.*, 2016, Cornelis, 2010, Henríquez *et al.*, 2019). In the extracellular space, siderophores scavenge and chelate ferric ($Fe^{3+}$) ions which cannot enter the cell otherwise. The iron chelation causes the formation of ferrisiderophores which are then recognised by specific, TonB-dependent receptors and imported into the cell (Cornelis, 2010). $Fe^{3+}$ ions are reduced to $Fe^{2+}$ ions in the periplasm (the case of pyoverdine as seen in **FIGURE 3c**, Bonneau *et al.*, 2020) or the cytoplasm of the recipient bacterial cell (Cornelis, 2010). These ions are then available for the organism to employ in cellular processes and are mainly used as enzyme cofactors, such as the ubiquitous iron-sulphur clusters (Beinert *et al.*, 1997, Neilands, 1995).

#### 5.2.3.2. Siderophores and carbon source nutritional dependence

Similarly to the production of any secondary metabolite biosynthesised by bacteria, siderophore production is susceptible to the nutritional conditions of a given environment. The previously described regulation of this system by iron ions is already well-established knowledge. However, the more indirect nutritional aspects of the siderophore biosynthesis management remain only partially explored.

A recent study by Mendonca *et al.* (2020) revealed that the probable carbon source regulation of pyoverdine biosynthesis is directly related to the pathway of substrate utilisation by *P. putida* and *P. protegens*. Briefly, the carbon sources that are metabolised using gluconeogenic pathways (such as succinate or malate) promote pyoverdine production. In contrast, the metabolism of glycolytic substrates (namely, glucose and fructose) results in relatively reduced yields of this siderophore. This explanation finds confirmation in several other studies. In one of them, glucose being a sole carbon source for *P. putida* substantially reduced pyoverdine levels compared to benzyl alcohol (Joshi *et al.*, 2014).

The process of siderophore biosynthesis being affected by carbon source is a result of regulation of the expression of genes encoding proteins involved in the siderophore production. However, it is also true for other genes involved in siderophore-mediated iron acquisition, such as those encoding siderophore receptors. A notable example of this case was found in *P. aeruginosa*, where the expression of genes encoding two different ferripyoverdine receptors is contrastingly regulated by glycerol being a carbon source (Ghysels *et al.*, 2004).

#### 5.2.3.3. Iron impact on secondary metabolism and biofilm formation

Iron is an element of high importance in *Pseudomonas* biochemistry and molecular biology research, primarily in the studies concerning siderophores. However, the abundance or lack of available iron can also affect other processes and biochemical pathways of pseudomonads, leading to varied outcomes. For example, a comprehensive transcriptomic and proteomic study by Lim *et al.* (2012) on *P. protegens* Pf-5 revealed that iron depletion significantly upregulates the expression of specific genes involved in the biosynthesis of antimicrobial secondary metabolites, 2,4-DAPG and pyrrolnitrin. On the other hand, the expression of the HCN and flagella biosynthesis genes was downregulated in Pf-5 cultured in an iron-depleted medium. Iron deficiency also has a profound effect on *Pseudomonas* primary metabolism. An analysis of glucose metabolism in *P. putida* KT2440 explained how the iron limitation causes rerouting the metabolic pathways from biomass growth promotion to enhanced secretion of gluconate and siderophore biosynthesis (Sasnow *et al.*, 2016). In another study using the KT2440 strain as a model organism, Molina *et al.* (2005, 2006) revealed the importance of iron acquisition in the colonisation of plant roots and seeds. These studies showed that not only is the iron in a maize seed acting as a signal for *P. putida* to start colonisation, but also that the genes involved in iron acquisition are necessary for efficient rhizosphere colonisation by KT2440.

Taken together, all the studies considering the carbon/iron source influence on the biosynthesis of antimicrobials (direct, such as 2,4-DAPG, or indirect, such as siderophores) by *Pseudomonas* spp. acknowledge the remarkable importance of environmental conditions on this process. The study presented in this thesis focuses on augmenting this knowledge with insight into another pseudomonad species, its potential in biocontrol and the nutritional impact on its capabilities.

## 5.3. Gene expression

Gene expression is defined as the process by which information encoded in nucleic acids is utilised to synthesise a functional product, mainly proteins and RNA molecules. It is a manifestation of a gene in a phenotypic form. The intensity of expression of genes in any living organism is regulated at the cellular level with various molecular mechanisms and their adaptation to environmental/external conditions. This regulation can occur at any stage of gene expression, including transcription and translation, but also during all the intermediate phases before and after these crucial steps. Gene expression levels are often measured to visualise the relationship between the applied conditions/treatment, the organism's genetic makeup and its phenotypic display.

### 5.3.1. RT-qPCR as a method of gene expression analysis

One of the most ubiquitous approaches in gene expression analysis is measuring the relative amount of a given gene transcript, which is an indicator of the transcriptional up- or downregulation of expression. There are two leading methods of the transcript levels' analyses, both of which utilise RNA extracted from a given organism as a studied material. The first one utilises RNA sequencing [RNAseq] to reveal the differences in global transcription regulation for the entire genome. It is widely applied in screening research where no specific genes are targeted regarding their expression levels. The second method employs a quantitative (Real-Time) polymerase chain reaction performed on reverse transcribed RNA. Similarly to other PCR-based approaches, this assay targets only selected DNA regions, amplified during the assay using specific primers. Therefore, this type of analysis is relevant when the study aims to determine the levels of expression of pre-established genes and requires information about their sequence.

Reverse transcription-quantitative polymerase chain reaction [RT-qPCR] is one of the most popular methods for the analysis of gene expression, a so-called "golden standard" in this field (Rocha *et al.*, 2020). The method relies on quantifying target cDNA fragments obtained after reverse transcription from the mRNA isolated under certain experimental conditions (Bustin [Ed.], 2009). The quantification of the amplified target cDNA is possible due to the light-emitting probes or nucleic acid dyes (usually the SYBR Green dye). The intensity of the light emitted is proportionate to the quantity of the amplicon and it is detected after every qPCR cycle. The light detection limit allows for establishing a „threshold cycle" [$C_q$] value for every given reaction. These are the values that indicate the amounts of the target transcript in the samples. The following calculation of gene expression is based on the notion that the abundance of target mRNA in samples can be normalised with respect to the reference genes [RGs] transcript abundance. The RGs are established from the range of housekeeping genes (i.e., genes involved in DNA replication and other tasks crucial for cell functioning) and to select valid RGs their

expression levels should be assessed as remarkably stable regardless of the experimental conditions.

The selection of suitable reference genes for bacterial RT-qPCR is an essential step towards the validity of the obtained gene expression data. The stability of the RGs expression should be tested experimentally. It is recommended that 7-10 potential RGs genes have their expression levels measured under all conditions used in subsequent gene expression analyses (Taylor *et al.*, 2019). The most stable RGs are usually determined with the use of one or more algorithms designed for this purpose, namely geNorm (Vandesompele *et al.*, 2002), NormFinder (Andersen *et al.*, 2004), BestKeeper (Pfaffl *et al.*, 2004), to mention the most prominent ones.

The workflow of RT-qPCR, though considered cheaper and easier to carry out than the RNAseq, is a complex multiple-step procedure with each stage of it, from planning to data analysis, being prone to theoretical and experimental errors (Bustin and Nolan, 2017). This complexity of an RT-qPCR assay became an issue of irreproducibility and inconsistency of published studies. Thus, in 2009, a group of researchers published a guide known as MIQE [***M**inimum **I**nformation for publication of **Q**uantitative real-time PCR **E**xperiments*]. These guidelines highlight the problematic points of this routinely used procedure and suggest the measures that should be undertaken during RT-qPCR studies to accomplish transparency and coherence of the published results (Bustin *et al.*, 2009). Among the practices that found their way into the MIQE guidelines are, e.g., the use of proper control samples, primer pair validation and meticulous selection of RGs.

### 5.3.2. Gene expression in *Pseudomonas* spp.

The twentieth-century molecular biology studies revealed that gene expression regulation differs fundamentally between eukaryotes and prokaryotes. Unlike the eukaryotic genes, bacterial genes are grouped in operons. The genes of one operon often represent proteins belonging to one metabolic pathway or by other means functionally related to each other. Additionally, the genes of the operons are co-expressed and their transcription is co-regulated (a single promoter region precedes an operon). This fact, however, does not mean that the regulation of bacterial transcription is a straightforward process. Instead, transcription factors (activators or repressors of transcription) may be controlled by a unique regulatory mechanism for the given operon as well as the global regulation of transcription (Gottesman, 1984).

#### 5.3.2.1. Gac/Rsm global regulatory mechanism

The principal global regulatory mechanism in *Pseudomonas* spp. is a Gac/Rsm signal transduction system that controls the expression of ca. 10% of genes in strains of *P. protegens, P. chlororaphis*, *P. fluorescens* and possibly other species (Ferreiro and Gallegos, 2021, Heeb and

Haas, 2001). In this system, GacS is a sensor kinase that undergoes autophosphorylation after encountering an unknown signal (Latour, 2020). This activates the response regulator protein, GacA, which subsequently propels an entire regulatory cascade consisting of Rsm proteins, the RNA-binding expression regulators (Ferreiro and Gallegos, 2021). This system was shown to control major phenotype traits of plant-associated pseudomonads such as biofilm formation and motility (Zboralski and Filion, 2020), and the production of secondary metabolites crucial in biocontrol: siderophores, 2,4-DAPG, phenazines, hydrogen cyanide and cyclic lipopeptides (Blumer and Haas, 2000, Heeb and Haas, 2001, Mavrodi *et al.*, 2006, Raaijmakers *et al.*, 2006, Yu *et al.*, 2014). Moreover, the Gac/Rsm pathway controls the production of toxins and virulence factors of plant and human pathogens among the *Pseudomonas* spp. (Ferreiro and Gallegos, 2021, Francis *et al.*, 2017).

The Gac/Rsm system was also acknowledged in the studies on *P. donghuensis* strains P482, HYS$^T$ and SVBP6. The previously mentioned 7-HT biosynthetic gene cluster was demonstrated to be positively regulated through the Gac/Rsm signal transduction pathway (Chen M. *et al.*, 2018, Yu *et al.*, 2014). This was confirmed by the study of Muzio *et al.* (2020), which additionally showed no effect of the Gac/Rsm system on PVD biosynthesis in SVPB6. Moreover, this system's inactivation by a mutation in the *gacA* gene showed the involvement of Gac/Rsm regulation in the antagonistic activity of P482 towards fungal plant pathogens by VOCs production (Ossowicki *et al.*, 2017). The conclusions drawn from these studies and preliminary research prompted the inclusion of the Gac/Rsm system in this study to explore the carbon and iron source effect on P482 antibacterial activity and biofilm formation.

#### 5.3.2.2. Environmental influences on gene expression in pseudomonads

By measuring gene expression in bacteria, we can reveal how the slightest environmental changes can affect the microorganism's phenotype. Understanding the mechanisms of gene expression regulation can lead to the development of environmental conditions modulation strategies to increase the efficiency of the biocontrol agents (Narayanasamy, 2013). The majority of the published research on gene expression in PGPR *Pseudomonas* spp. focuses on how it is affected by biotic factors. In a comprehensive study on *P. protegens* CHA0 strain, Notz *et al.* (2007) observed a host plant-dependent expression of the *phl* gene cluster, responsible for 2,4-DAPG production. The expression of *phl* cluster genes was observed to be much higher when CHA0 colonised monocot plants (maize and wheat) compared to the dicot plants (cucumber and bean). The *phl* region expression upregulation was also detected when the plants were infected with *Pythium ultimum.* Other studies investigated the expression of genes involved in the biosynthesis of such compounds as phenazines or hydrogen cyanide (Arseneault *et al.*, 2016, Jamali *et al.*, 2009).

Although these analyses provide valuable insight into the *in vivo* modulation of *Pseudomonas* spp. biocontrol traits, they do not reveal how the individual abiotic (chemical) factors produced by the given biotic agents influence the gene expression. Thus, research exploring the impact of particular compounds on gene expression in plant-associated pseudomonads has also been published in the last decades. These studies concern, *inter alia*, the impact of benzyl alcohol utilisation on the expression of siderophore biosynthetic genes in *P. putida* (Joshi *et al.*, 2014) or the contrasting regulation of phenazine and pyrrolnitrin biosynthetic genes' expression by glucose in *P. chlororaphis* (Park *et al.*, 2011).

Due to the relatively recent discovery of *P. donghuensis* as a species, the data about its gene expression is lacking. Thus, studies are still needed to uncover how this species regulates its phenotype (especially the biocontrol traits) in response to external factors. The presented study explores the influence of the selected nutritional factors on the expression of P482's genes involved in its antagonistic activity. Part of the research presented in this thesis was published as the first study of gene expression in *P. donghuensis* P482 (Matuszewska *et al.*, 2021). It is also the first account of a comprehensive selection of RGs for RT-qPCR in *P. donghuensis* species.

## 6. General research hypothesis

*Pseudomonas donghuensis* P482 is a biofilm-forming antagonist of phytopathogens, a potentially valuable plant-associated bacterium. However, its beneficial phenotype is dependent on environmental conditions, such as carbon and iron source. Glucose and glycerol are ubiquitous carbon sources, which affect the P482 phenotype by unknown molecular mechanisms. In addition, iron cations abundance and charge are other important factors regulating the biocontrol phenotype of P482. Exploring these issues, their mechanisms and consequences can lead to a better understanding of the P482 strain as well as the *P. donghuensis* species and its application potential.

## 7. Aims of the study

The main goal of the study was to verify the influence of glucose, glycerol and iron ions on antimicrobial activity and biofilm formation of *Pseudomonas donghuensis* P482.

The specific objectives and steps towards their realisation have involved:

1. characterisation of the antibacterial activity of P482 on minimal media supplemented with glucose/glycerol and iron ions by:
    - obtaining and characterisation of P482 mutants with insertions inactivating selected genes involved in iron metabolism and characterisation of "cluster 17" mutants
    - determination of how these particular nutrients affect the antimicrobial activity of P482 mutants with inactivation of selected P482 genes (involved in the antagonism towards plant pathogens and the obtained iron metabolism mutants)
    - analysis of the P482 metabolome changes in relation to the tested nutrients
2. verification of whether the changes in antimicrobial activity of P482 caused by the tested nutrients occur on the transcriptional level of gene expression by:
    - selection and validation of reference genes for RT-qPCR in *P. donghuensis* P482
    - analysis of the expression of selected P482 genes under given nutritional conditions
3. investigation of how the tested nutrients affect abiotic biofilm formation by P482 by:
    - analysis of biofilm formation by P482 and selected mutants on polystyrene surface under selected nutritional conditions

# 8. Materials and methods

## 8.1. Strains and growth conditions

### 8.1.1. Strains and mutants

The bacterial strains used in the study are listed in **TABLE 1**. The P482 strain mutants used and obtained in the study are listed in **TABLE 2**.

**TABLE 1**. Bacterial strains used in the study and their features.

| strain | origin | features | references |
|---|---|---|---|
| *Pseudomonas donghuensis* P482 | tomato rhizosphere, Poland | wild type | (Krzyżanowska *et al.*, 2012a) |
| *Pseudomonas donghuensis* HYS$^T$ | Donghu lake, China | *P. donghuensis* type strain | (Gao *et al.*, 2012) |
| *Pseudomonas vranovensis* DSM16006$^T$ | soil sample, Czechia | control strain, no antibiotic properties | (Tvrzová *et al.*, 2006) |
| *Pseudomonas syringae* pv. *syringae* Pss762 | apricot, Poland | plant pathogen, wild type | (Kałużna *et al.*, 2009) |
| *Pseudomonas aeruginosa* PA01 | an infected wound, Australia | human pathogen, wild type, control strain: significant biofilm forming properties | (Holloway, 1955) |
| *Dickeya solani* IFB0102 | a potato plant, Poland | plant pathogen, wild type | (Sławiak *et al.*, 2009) |
| *Pectobacterium brasiliense* LMG 21371$^T$ | a potato plant, Brasil | plant pathogen, wild type | (Nabhan *et al.*, 2012) |
| *Escherichia coli* ST18 | - | donor strain for a biparental mating: *pro thi hsdR*+ Tpr$^R$ Smr$^R$; chromosome:RP4-2 Tc::Mu-Kan::Tn7/λpir *ΔhemA* | (Thoma and Schobert, 2009) |
| *Staphylococcus epidermidis* ATCC 12228 | - | control strain, no biofilm-forming properties | (Zhang *et al.*, 2003) |

**TABLE 2** *Pseudomonas donghuensis* P482 mutants used in the study. The comprehensive list of the study's loci of interest and their annotations can be found in **SUPPLEMENTARY TABLE 1**

| mutant name | mutation locus | mutation type | References |
|---|---|---|---|
| | | **"cluster 17" mutants** | |
| KN4240 | BV82_4240 | pKNOCK[a] | this study (Matuszewska *et al.*, 2021) |
| KN4243 | BV82_4243; *emrA* gene | pKNOCK[a] | this study (Matuszewska *et al.*, 2021) |
| | | **7-HT biosynthesis cluster mutants** | |
| KN4705 | BV82_4705 | pKNOCK[a] | (Krzyżanowska *et al.*, 2016) |
| KN4706 | BV82_4706; *citE* gene | pKNOCK[a] | (Krzyżanowska *et al.*, 2016) |
| KN4709 | BV82_4709 | pKNOCK[a] | (Krzyżanowska *et al.*, 2016) |
| | | **pyoverdine biosynthesis cluster mutants** | |
| KN1009 | BV82_1009; *psvA/pvdL* gene | pKNOCK[a] | (Krzyżanowska *et al.*, 2016) |
| KN3755 | BV82_3755 putative *pvdD* gene | pKNOCK[a] | (Krzyżanowska *et al.*, 2016) |
| | | **iron metabolism genes mutants** | |
| KN0255 | BV82_0255, *iscA* gene | pKNOCK[a] | this study |
| KN0562 | BV82_0562 | pKNOCK[a] | this study |
| KN2408 | BV82_2408 | pKNOCK[a] | this study |
| KN4870 | BV82_4870, *fur* gene | pKNOCK[a] | this study |
| KN4879 | BV82_4879 | pKNOCK[a] | this study |
| | | **Gac/Rsm pathway mutant** | |
| KN3318 | BV82_3318, *gacA* gene | pKNOCK[a] | (Ossowicki *et al.*, 2017) |

[a] pKNOCK insertion mutagenesis description can be found in sections **8.4.4** and **8.4.5**

### 8.1.2. Standard growth conditions

All bacterial strains were typically maintained as liquid cultures in LB medium or agar plate cultures on LB-agar medium with or without supplementation (**8.1.3.1**). All the strains were cultured in stationary or shaker incubators at 28 °C, except *Escherichia coli* ST18 cultivated at 37 °C. For the long-term storage 50% glycerol stocks of all bacterial strains were deep-frozen at -80 °C.

### 8.1.3. Growth media and buffers

All microbiological growth media used in the study and their ingredients were purchased at BTL (Poland), Sigma-Aldrich (Merck, USA) or POCH (Avantor, Poland) unless stated otherwise. The media and the stock ingredients used for their preparation were routinely sterilised by autoclaving unless stated otherwise.

#### 8.1.3.1. Lysogeny broth [LB, LB-agar] and modifications

Lysogeny broth [LB] granulate in Miller formulation (Miller, 1972) was used as a standard culture medium. LB contained 10 g peptone, 5 g yeast extract and 10 g NaCl dissolved in 1 litre of double-distilled water [dd$H_2O$]. LB-agar medium contained all basic LB ingredients and bacteriological agar (15 g/l).

#### 8.1.3.2. M9 minimal medium [M9, M9-agar] and modifications

Minimal medium M9 (Sambrook and Russell, 2001) was used for most of the experiments performed to examine the influence of carbon and iron sources on P482 traits. The composition of the medium is listed in **TABLE 3.**

The **5x concentrated M9 salts** consisted of $Na_2HPO_4 \cdot 7H_2O$ 64 g/l, $KH_2PO_4$ 15 g/l, NaCl 2.5 g/l, $NH_4Cl$ 5 g/l. The individual salts were mixed, dissolved in dd$H_2O$, autoclaved for 30 minutes at 121 °C and cooled down prior to full medium preparation. The full medium was prepared by mixing the sterile ingredients: water, salts, a preferred carbon source and the optional supplementation (all ingredients were sterilised by autoclaving, except for 20% glucose and root exudates which were sterilised by filtration).

One litre of the solid version of the medium was prepared by autoclaving 15 g of bacteriological agar in 700 ml of dd$H_2O$, cooling it down to 50-60 °C, adding all the sterile ingredients, filling up with sterile water to 1 l and thorough mixing.

The version of the M9-glucose medium containing tomato/maize root exudates was prepared by supplementing the medium with 10% (v/v) root exudates solutions obtained by M. Jabłońska, PhD and D. Krzyżanowska, PhD from LPM. Briefly, the sprouts of tomato

(var. St. Pierre) and maize (var. Bejm) plants obtained from the sterilised seeds were transferred into sterile containers with aquatic gravel and medium. The medium used was Hoagland's No. 2 Basal Salt Mixture (Sigma-Aldrich) with the producer's suggested concentrations adjusted to ½ Hoagland's for the tomato cultures and ¼ Hoagland's for the maize cultures. Following 18 days of culture, the remaining growth medium with root exudates was aspired from the containers and filtered through a sterile 0.22 µl filter. The exudates were stored for less than a year at -20 °C.

The versions of M9-glucose and M9-glycerol media with *D. solani* filtrate [DsFIL] were obtained by supplementing the medium with 20% (v/v) of DsFIL obtained after filter sterilising the 48 h cultures of *D. solani* IFB0102 in M9 medium The M9 medium used for the IFB0102 culture utilised the same carbon source as the M9 medium to which the DsFIL were added.

**TABLE 3.** M9 minimal medium composition.

| Ingredients | volume per 1 l | final concentration |
|---|---|---|
| **basic salts** | | |
| **5x M9 salts** | 200 ml | - |
| **1 M $MgSO_4$** | 2 ml | 2 mM |
| **0.05 M $CaCl_2$** | 2 ml | 0.1 mM |
| **carbon source selection (one per medium)** | | |
| **20% glucose** | 20 ml | 0.4% |
| **or** | | |
| **80% glycerol** | 5 ml | 0.4% |
| **iron source (optional)** | | |
| **100 mM $FeSO_4$** | 0.3 ml | 30 µM |
| **100 mM $FeCl_3$** | 0.3 ml | 30 µM |
| **other supplementation (optional)** | | |
| **tomato root exudates** | 100 ml | 10% |
| **maize root exudates** | 100 ml | 10% |
| ***D. solani* filtrate [DsFIL]** | 200 ml | 20% |

#### 8.1.3.3. Tryptic soy broth [TSB, 0.1 TSB, TSB-agar]

Tryptic soy broth [TSB] granulate was purchased from Oxoid (Thermo Fisher Scientific, USA). 0.1 TSB stands for tenfold diluted TSB medium, and it was used as an optimal liquid medium for the production of antimicrobials by P482 in metabolomic analyses (Matuszewska, MSc thesis, Gdańsk, 2016). Complete TSB medium contains 17 g/l pancreatic digest of casein, 3 g/l papaic digest of soybean meal, 2.5 g/l NaCl 5 g/l, $K_2HPO_4$, 2.5 g/l glucose. The solid version of the medium was prepared by adding the bacteriological agar (15 g/l) before autoclaving.

#### 8.1.3.4. MSgg medium.

MSgg medium is a biofilm formation promoting formulation finding use in colony morphology assays. MSgg plates were prepared according to Townsley *et al.*, (2018) and contained 5 mM $KPO_4$ (pH 7), 100 mM MOPS (pH 7), 2 mM $MgCl_2$, 700 µM $CaCl_2$, 50 µM $MnCl_2$, 50 µM $FeCl_3$, 1 µM $ZnCl_2$, 2 µM thiamine, 0.5% glycerol, 0.5% glutamate. Bacteriological agar in concentration 1.5% was used as a solidifying agent. To prepare an agar medium, the agar water solution was autoclaved and cooled down to 50-60 ℃. The MSgg ingredients (filter-sterilised) were added from the stock solutions to obtain the final concentrations.

#### 8.1.3.5. Antibiotic and other supplementation

The standard LB medium and other media used were supplemented with antibiotic kanamycin (30 mg/l) and 5-aminolevulonic acid (5-ALA, 50 mg/l) if necessary.

#### 8.1.3.6. Buffers

All buffers were prepared according to standard recipes found in the literature. All the names, compositions and references can be found in **TABLE 4**.

**TABLE 4.** Buffers used in the study

| buffer | composition | purpose | references |
|---|---|---|---|
| TE<br>(Tris/EDTA) | 10 mM Tris-Cl (pH 7.5)<br>1 mM EDTA (pH 8.0) | DNA storage | Cold Spring Harbor Protocols:<br>10.1101/pdb.rec092338 |
| TBE<br>(TRIS/Borate/EDTA) | 5x concentrated TBE:<br>54 g of Tris base<br>27.5 g of boric acid<br>20 mL of 0.5 M EDTA (pH 8.0) | electrophoresis (working solution: 0.5 x TBE) | Cold Spring Harbor Protocols:<br>10.1101/pdb.rec8458 |

| buffer | composition | purpose | references |
|---|---|---|---|
| PBS<br>(Phosphate Buffered Saline) | 137 mM NaCl<br>2.7 KCl<br>10 mM Na2HPO4<br>1.8 mM KH2PO4<br>adjusted to pH 7.2 with HCl | bacterial cells washing (e.g., in biofilm testing) | Cold Spring Harbor Protocols:<br>10.1101/pdb.rec8247 |
| TB<br>(Transformation Buffer) | 55 mM MnCl2<br>15 mM CaCl2<br>250 mM KCl<br>10 mM PIPES (0.5 M, pH 6.7) | bacterial transformation | Cold Spring Harbor Protocols:<br>10.1101/pdb.rec102855 |

### 8.1.1. Growth curves

Growth curve assays were performed to assess the growth rate of the tested strains and mutants under different nutritional conditions. The assay was started with inoculation of the precultures of the tested strains in the same type of medium that was later used for the growth curve assay. First, the precultures were incubated at 28 °C for 24 hours. Their turbidity was then measured with the DEN-1 densitometer (BioSan, Latvia) and adjusted to 1.0 on the McFarland scale [McF]. Ten microlitres of the given preculture were then used to inoculate 200 µl of the fresh medium, which was placed into a well of the sterile, flat-bottomed 96-well plate. The plate was sealed with a transparent film and placed in the chamber of Epoch Microplate Spectrophotometer (BioTek, USA) or EnVision Microplate Reader (PerkinElmer, USA).

The assay protocol comprised a minimum of 44 h of incubation (with shaking) at a chosen temperature with 600 nm absorbance measurements [$OD_{600}$] every 20 minutes; 4 biological replicates of each sample were measured. Mean values from the replicates' readouts were used to calculate the growth curves of each strain under given conditions.

## 8.2. Direct antibacterial activity tests

Direct antimicrobial activity of P482 and its mutants was tested against pathogens in a plate assay. *Pseudomonas vranovensis* DSM16006$^T$ was used as a negative control based on its lack of antimicrobial activity against the pathogens used in the study. To inoculate the plates for the test, the precultures of all strains used in 5 ml of a liquid medium were prepared. The nutritional conditions of the liquid precultures were always equivalent to those of the agar medium used in the assay. The precultures were incubated in a shaker-incubator at 28 °C overnight.

After the incubation, the turbidity of the precultures was measured using DEN-1 densitometer (BioSan, Latvia) and adjusted to 4 McF for the pathogens and 12 McF for P482, its mutants, and the control strains. One hundred microlitres of the pathogen suspension was spread on the appropriate agar medium with a sterile swab and left to dry for ca. 10 minutes. Subsequently, 2 µl drops of suspensions containing P482, its mutants or control strains were placed on the plates inoculated with pathogens. The plates were incubated at 28 °C from 24 to 44 hours (depending on the bacteria growth rate under given nutritional conditions).

The resulting pathogen growth inhibition zones around the macrocolonies of the test strains were measured. For higher reliability of the assay, the macrocolony diameter was subtracted from the growth inhibition zone diameter, which was interpreted as a primary representation of antibacterial activity. For P482 mutants, the results were then converted to a percentage of a growth inhibition zone caused by P482 wt (which served as a positive control). Basic statistical analysis was carried out by calculating standard deviations of the biological replicates (three replicates per experimental setup).

## 8.3. Analyses of secondary metabolites

### 8.3.1. Extraction of secondary metabolites

Bacteria (P482 strain or its mutants) were cultured in 250 ml or 500 ml of a given liquid medium at 28 °C with shaking. To keep the environment well oxygenated for the entire culturing time, culture flasks with baffled bottom and vented caps with filters were used. The cultures were stopped after 96 hours, long after entering the stationary growth phase, regardless of the nutritional conditions. Subsequently, they were centrifuged for 30 min in 10000 x g and the supernatant was collected and subjected to the extraction of secondary metabolites with ethyl acetate [EtOAc].

Two different methods of liquid-liquid extraction were applied to extract secondary metabolites produced by P482 and its mutants.

In the first method (further referred to as the “stirring method”), EtOAc volume equal to half of the extracted supernatant volume was gently poured onto the supernatant earlier put into a conical flask (sized four times the supernatant volume). Next, a stirring bar was placed into the two-phased mixture (bottom water phase: supernatant; top organic phase: EtOAc) and the flask was then placed onto a magnetic stirrer with the lowest possible mixing intensity. The gentle stirring continued overnight to extract as many metabolites as possible, but simultaneously avoid forming the emulsion at the EtOAc/supernatant interface. The next day the EtOAc phase was collected and the solvent was evaporated using a vacuum rotary evaporator and a vacuum

centrifuge. The dry extract was then dissolved in HPLC-grade methanol [MeOH] (100 µl MeOH per 500 ml of the initial culture).

In the second extraction method (further referred to as the "separatory funnel method"), the supernatant:EtOAc volume ratio was the same as in the "stirring method". The extraction was performed by combining the two phases in a separatory funnel. The thorough phase mixing by separatory funnel shaking was performed at least three times with a minimum of 15-minute breaks in between for phase separation. The phases were then fully separated and the organic phase was collected. If the organic phase contained traces of emulsion, it was salted out with anhydrous sodium sulphate and then filtered through a Whatman No 1 cellulose filter. Subsequently, the organic phase containing the extracted metabolites was submitted to solvent evaporation and the crude extract was dissolved in MeOH as in the "stirring method".

The extracts dissolved in methanol were stored at -20 °C for as long as two years with no observable loss of antimicrobial activity.

### 8.3.2. Thin-layer chromatography

Thin-layer chromatography [TLC] was performed to visualise the complexity and differences between the extracts prior to HPLC-MS analyses. It was carried out either in normal- [NP] or reverse-phase [RP] setup. The NP assay utilised TLC Silica Gel 60 $F_{254}$ plates and the mobile phase consisting of dichloromethane:MeOH mixture in ratio 9:1 or 19:1. The RP assay utilised TLC Silica Gel 60 RP-18 $F_{254}$s plates and the mobile phase consisting of MeOH:$H_2O$ mixture in ratio 1:1. Two to three microlitres of each sample were put on the TLC base line as single spots and plates were put into the respective eluent mixtures. The chromatography was stopped when the eluent front reached about 2 cm from the top of the plate. The compound separation on the plates was then visualised with UV light in two wavelengths: 254 nm (detection of absorbing compounds) and 365 nm (detection of fluorescence).

### 8.3.3. HPLC-MS analyses (metabolomics)

The selected extracts of P482 secondary metabolites obtained in the study were subjected to **high-performance liquid chromatography coupled with mass spectrometry** [HPLC-MS]. This part of the study was carried out during the internship at the Institute of Sustainable Plant Protection (IPSP-CNR, Portici, NA, Italy) under the supervision and kind help of prof. Francesco Vinale, PhD and Alessia Staropoli, MSc.

The extract samples were prepared by evaporating the solvent, weighing the crude extract and dissolving it in 40 µl of EtOAc:MeOH mixture (1:1) per 1 mg of the extract (all used solvents were of HPLC-grade purity). All the samples were filtered with a 0.22 µm regenerated cellulose syringe filter and diluted tenfold prior to chromatography.

HPLC-MS was carried out using the Agilent 1260 Infinity Series chromatograph coupled with Ultra High Definition [UHD] quadrupole-time of flight [Q-TOF] mass spectrometer (model G6540B) with a dual electrospray ionisation (Dual ESI) source (Agilent Technologies, USA). Agilent Mass Hunter software (Agilent Technologies, USA) was used for instrument control and data acquisition. The sample injection volume was 5 µl. The reverse-phase [RP] HPLC separation utilised a Zorbax Eclipse Plus C-18 column (4.6 × 100 mm, with 3.5 µm particles, Agilent Technologies) and the linear gradient elution program with $H_2O$ and acetonitrile [AcN] (both acidified with 0.1% formic acid [FA]) as the solvents (**TABLE 5**). The flow was set at 0.6 ml/min. The UV detection on the diode array detector [DAD] was set for 254 nm, 300 nm and 420 nm wavelengths.

The MS equipment operated in the positive mode. Mass spectra were recorded as centroid spectra in the m/z range 100-1700. The spectra were analysed using MassHunter Qualitative Analysis Software and subjected to MassHunter Profinder (Agilent Technologies, USA) batch feature analysis using the bacterial compound database created at IPSP-CNR (courtesy of prof. Francesco Vinale and prof. Roberta Marra).

Further data analyses were carried out also with the use of OpenChrom software version 1.4.x (Lablicate GmbH, Germany) and using publicly available online databases: ChemSpider (www.chemspider.com, Royal Society of Chemistry), MetaCyc (www.metacyc.org, Caspi *et al.*, 2018) PubChem (https://pubchem.ncbi.nlm.nih.gov, Kim *et al.*, 2021) and KEGG COMPOUND (www.kegg.jp/kegg/compound/, Kanehisa and Goto, 2000).

**TABLE 6.** HPLC elution program for the extract samples.

| time (min) | solvent volume (%) | |
|---|---|---|
| | A ($H_2O$, 0.1% FA) | B (AcN, 0,1% FA) |
| **0** | 95 | 5 |
| **12** | 0 | 100 |
| **15** | 0 | 100 |
| **17** | 95 | 5 |
| **20** | 95 | 5 |

### 8.3.4. HPLC-MS analysis (7-HT detection)

The extracts obtained from the P482 wt cultures in M9 media containing *D. solani* IFB0102 filtrate were subjected to HPLC-MS analysis to determine whether these conditions promote 7-HT biosynthesis by P482. These analyses were performed by Michał Puchalski, MSc from the Laboratory of Biopolymers Structure (Intercollegiate Faculty of Biotechnology UG & MUG, Gdańsk, Poland) using the equipment of Mass Spectrometry Laboratory (Core Facility Laboratories, Intercollegiate Faculty of Biotechnology UG & MUG, Gdańsk, Poland).

The crude extracts (obtained from initial 200 ml of culture each) were dissolved in 50 µl of HPLC grade MeOH (Merck, USA) per sample. HPLC-MS was carried out using the micro-HPLC LC200 (Eksigent, Dublin, CA, USA) system with autosampler CTC PAL (CTC Analytics AG, Zwinger, Switzerland). The chromatograph was coupled with QTRAP 6500 mass spectrometer (AB Sciex LLC, Framingham, MA, USA) paired with Sciex Analyst software (version 1.6.2) for data acquisition and analysis. The sample injection volume was 1 µl. The RP-HPLC separation utilised a ChromXP C18 CL column (0.3 × 150 mm, 3 µm particles, 120 Å, AB Sciex LLC). The elution program was a linear gradient (A: 2% ⟶ 98%; 10 minutes) of buffers A: $H_2O$ + 0.1% FA and B: AcN + 0.1% FA. The MS equipment operated in the positive mode with the scan type Q1. Mass spectra were recorded as centroid spectra in the m/z range 30-500.

### 8.3.5. UV-Vis absorption spectra

The selected culture supernatants of P482 and mutants were tested for the presence of pyoverdine and 7-hydroxytropolone using UV and visible light [UV-Vis] spectrophotometry (Gao *et al.*, 2015). The bacteria were cultured in liquid M9 media with different carbon and iron sources. The samples of the cultures were collected after 1, 2 and 4 days of incubation. The sample bacterial suspensions were centrifuged, the supernatant was collected and subsequently subjected to filtration to exclude the presence of cells that may interfere with the absorption read. The supernatant samples were then placed in a 96-well plate with a transparent bottom and their absorption spectra in the wavelength range from 200 to 900 nm were measured using Epoch Microplate Spectrophotometer (BioTek, USA).

## 8.4. Molecular biology and genetic engineering

### 8.4.1. Genomic DNA isolation

Genomic DNA [gDNA] was routinely isolated from bacterial cells using Wizard Genomic DNA Purification Kit (Promega, USA) as described in the manufacturer's protocol. Briefly, bacteria were cultured overnight in LB medium and 1 ml of the culture (ca. 3 × $10^8$ cfu) was

centrifuged to collect the cells. First, using the provided buffer, the cells were lysed. Subsequently, the lysate was treated with RNase A and proteins were precipitated with the kit-provided solution. The sample was then centrifuged, the supernatant was treated with isopropanol and mixed gently until the formation of thin, thread-like strands (DNA precipitation). After centrifugation, the DNA pellet was washed with 70% ethanol and the dry DNA pellet was dissolved in 50 µl of nuclease-free water. Finally, the quality and concentration of DNA in the sample were assessed using NanoDrop 2000 spectrophotometer (Thermo Fisher Scientific, USA) and by separation on an agarose gel electrophoresis (0.7% agarose in 0.5 x TBE buffer). The gDNA samples were stored at -20 °C.

### 8.4.2. Plasmid DNA isolation

Bacterial plasmid DNA was routinely isolated according to manufacturer's protocol with GeneJET Plasmid MiniPrep Kit (Thermo Scientific, USA). The principle of this commercial procedure is the combination of alkaline lysis with the use of a silica column that selectively binds DNA to concentrate it before the elution with water. If the yield of plasmid DNA obtained with the GeneJET kit was not satisfactory (<50 ng/µl), plasmid DNA was extracted with the use of a standard alkaline lysis protocol (Sambrook and Russell, 2001). Briefly, 1 ml of the overnight culture of the given strain in LB was centrifuged and the pellet was resuspended in 100 µl SOL I buffer (pH = 8.0). Subsequently, 200 µl of SOL II buffer were added and the contents of the tube were mixed by inverting it several times. After this step, 150 µl of SOL III buffer were added to the tube and again its contents were mixed by inverting. The tube was incubated on ice for 5-10 minutes and centrifuged at 16000 x g for 5 minutes. The supernatant (ca. 400 µl) containing plasmid DNA was transferred to a fresh tube and extracted with an equal volume of phenol:chloroform:isoamyl alcohol (25:24:1). The aqueous phase was then transferred to a fresh tube and 800 µl od 96% ethanol were added to denature the extracted plasmid DNA. After vortexing and 2-5 minute incubation in room temperature, the tube was centrifuged for 5 minutes at 16000 x g. The pellet was then washed with 1 ml of 70% ethanol and centrifuged again under the same conditions. The supernatant was discarded, the plasmid DNA pellet was dried and finally, it was resuspended in 50 µl of dd$H_2O$.

Alkaline lysis solutions (SOL I, SOL II and SOL III) were prepared as described in the mentioned protocol (Sambrook and Russell, 2001) with the reagents purchased at Sigma-Aldrich (Merck, USA) or POCH (Avantor Performance Materials, Poland). The quality and quantity of purified plasmid in the samples were established with the use of NanoDrop 2000 spectrophotometer (Thermo Fisher Scientific, USA) as well as an agarose gel electrophoresis (1% agarose in 0.5 x TBE buffer).

### 8.4.3. Polymerase chain reaction [PCR]

Depending on the purpose of the PCR, the reaction was conducted under different conditions and using various reagents. Therefore, the reaction mixtures (**MIX**) and conditions (**COND**) are labelled with the mentioned tags and numbers and referred to as such in the text. Primers (listed in **SUPPLEMENTARY TABLE 2**) were synthesised by Sigma Aldrich (Merck, USA); polymerases, buffers and other reagents were purchased from Thermo Fisher Scientific (USA). All the variables of the reactions are indicated in the tables below (**TABLE 6, 7, 8**).

**TABLE 6** PCR reaction mixtures (*Phusion* polymerase – **MIX PX**)

| reagent | MIX P1 (25 µl) | MIX P2 (25 µl) |
|---|---|---|
| **Phusion GC Buffer (5x)** | 5 | 5 |
| **dNTPs (10 mM)** | 0.5 | 0.5 |
| **forward primer [#F] (10 µM)** | 0.75 | 0.75 |
| **reverse primer [#R] (10 µM)** | 0.75 | 0.75 |
| **DMSO** | 0.75 | 0.75 |
| **$H_2O$, nuclease-free** | 16.65 | 15.05 |
| **Phusion HSII polymerase (2U/µl)** | 0.1 | 0.2 |
| **template DNA (10-100 ng/µl)** | 1 | 2 |
| **final reaction volume** | 25 | 25 |

**TABLE 7** PCR reaction mixtures (*DreamTaq* polymerase – **MIX TX**)

| reagent | MIX T1 (volume in µl) | MIX T2 (volume in µl) |
|---|---|---|
| **10x DreamTaq Buffer** | 2.5 | 5 |
| **dNTPs (10 mM)** | 1 | 1 |
| **forward primer [#F] (10 µM)** | 1.25 | 2,5 |
| **reverse primer [#R] (10 µM)** | 1.25 | 2,5 |
| **$H_2O$, nuclease-free** | 18.375 | 37,75 |
| **DreamTaq polymerase (5 U/µl)** | 0.125 | 0,25 |
| **template DNA (10-100 ng/µl)** | 1 | 1 |
| **final reaction volume** | **25** | **50** |

**TABLE 8** PCR reaction conditions

| step | COND 1 | | COND 2 | | COND 3 | |
|---|---|---|---|---|---|---|
| | temp. (°C) | time (s) | temp. (°C) | time (s) | temp. (°C) | time (s) |
| **1 - initial denaturation** | 98 | 120 | 98 | 60 | 95 | 180 |
| **2 – denaturation** | 98 | 10 | 98 | 10 | 95 | 30 |
| **3 – annealing** | 63 – 65* | 30 | 60 | 30 | 60 | 30 |
| **4 - elongation** | 72 | 40 | 72 | 15 | 72 | 50 |
| **steps 2-4: number of repeats** | 34x | | 32x | | 34x | |
| **5 – final elongation** | 72 | 420 | 72 | 300 | 72 | 420 |

*temperature specific for primer pairs used for insert amplification in cloning

63 °C: primer pairs:

XbaI_P482_0255_F -- XhoI_P482_0255_R
XbaI_P482_0592_F -- KpnI_P482_0592_R

65 °C: primer pairs:

XbaI_P482_2408_F -- KpnI_P482_2408_R
XbaI_P482_4870_F -- KpnI_P482_4870_R
XbaI_P482_4879_F -- KpnI_P482_4879_R

All the standard PCR (non-quantitative) assays were carried out using T100 thermal cycler (Bio-Rad, USA).

### 8.4.4. Cloning

To perform directed insertion mutagenesis of the P482 strain, fragments of the genes chosen for inactivation (**TABLE 12**) were cloned into the pKNOCK-Km vector (Alexeyev, 1999) shown in **FIGURE 4**. First, the appropriate fragments of genes (430 bp to 529 bp) were amplified in a PCR reaction (see **8.4.3**: **MIX P2; COND 1**) with the use of high fidelity Hot Start II Phusion polymerase (Thermo Scientific, USA) and primer pairs details of which can be found in **SUPPLEMENTARY TABLE 2**. The primers were designed to add digestion sites to the amplified gene fragment for further sticky ends ligation with the digested vector.

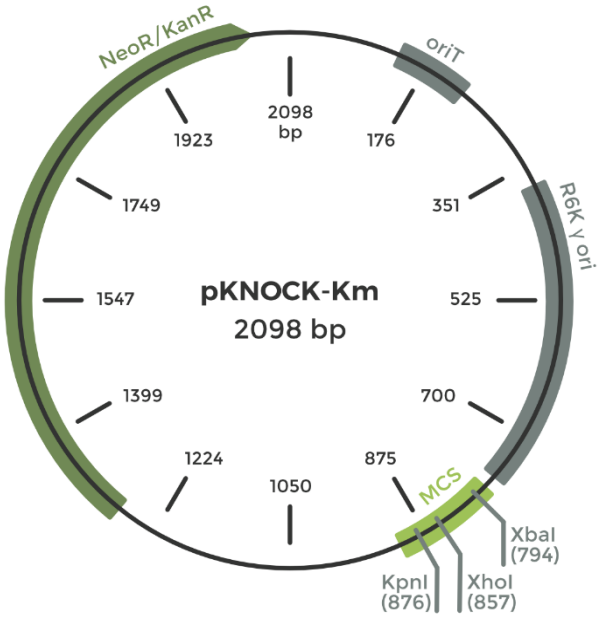


**FIGURE 7. pKNOCK-Kn vector map.** Kanamycine resistance (KanR) gene is marked with dark green. The inserts were cloned into the multiple cloning site (MCS) with the use of marked restriction sites (KpnI, XhoI and XbaI).

The PCR products were confirmed to be of the desired length by a separation on an agarose gel (1.5% agarose in 0.5 x TBE buffer) and each product was subjected to double digestion with the restriction enzymes (Thermo Scientific, USA) corresponding to the digestion sites added in the PCR reaction. Conditions of all double digestion reactions are specified in **TABLE 9**. At the same time, the previously isolated pKNOCK vector was subjected to two separate double digestion reactions, one using KpnI and XbaI enzymes, the other using XhoI and XbaI enzymes (**TABLE 9**). One 20 µl double digestion reaction used 700 ng of the vector (10 µl; 70 ng/µl) or 10 µl of the insert sample (directly post-PCR, as described in the manufacturer's protocol for the restriction enzymes). After the digestion both the insert and the vector samples were purified using Wizard SV Gel and PCR Clean-Up System (Promega, USA) following the manufacturer's protocol. The digested vector samples were purified from the agarose gel after electrophoresis (vector concentration after the purification ~20-30 ng/µl), while the inserts were purified directly from the post-digestion samples (insert concentration after the purification ~20-25 ng/µl).

**TABLE 9.** Double digestion conditions for pairs of restriction enzymes used in the study.

| | KpnI/XbaI | XhoI/XbaI |
|---|---|---|
| **enzyme 1; units/reaction** | KpnI; 0.4 | XhoI; 0.1 |
| **enzyme 2; units/reaction** | XbaI; 0.1 | XbaI; 0.2 |
| **buffer; concentration** | Tango buffer; 1x | Tango buffer; 2x |
| **reaction time; temperature** | 1 hour; 37 °C | 1 hour; 37 °C |
| **enzyme inactivation time; temperature** | 20 minutes; 80 °C | 20 minutes; 80 °C |

The inserts were then cloned into the designated restriction sites in the pKNOCK vector using Rapid DNA Ligation Kit (Thermo Scientific, USA), as described in the manufacturer's protocol. Briefly, 100 ng of the vector and 80 ng of the given insert were used per one ligation reaction (20 µl), which contained 5 units of T4 DNA Ligase in a Rapid Ligation Buffer. After the overnight ligation (incubation in room temperature), the post-ligation mixtures were used immediately for bacterial transformation or stored at -20 °C for up to three months.

### 8.4.5. Transformation, conjugation and mutagenesis confirmation

The cloning products (post-ligation mixtures **8.4.4**) were individually introduced into electrocompetent *Escherichia coli* ST18 using the electroporation method or into chemically competent ST18 cells using heat shock transformation.

#### 8.4.5.1. Transformation by electroporation

Before the electroporation transformation, the ligation mixture (buffer with ligase and pKNOCK-Km vector with the applicable insert built-in) was desalted with a drop dialysis method (Schlaak *et al.*, 2005) on a Millipore disk membrane filter (pore size: 0.025 µm, Merck, USA). The electroporation method utilised *E. coli* ST18 cells scraped from an overnight LB-agar plate culture into 1 ml of a sterile, ice-cold 10% glycerol solution. The bacterial suspension was then centrifuged (8000 x g, 5 minutes), the supernatant was discarded, and the pellet was suspended in fresh 10% glycerol solution (half of the volume of the discarded supernatant). This step was repeated twice more and lastly, the cells were suspended in 20 µl of 10% glycerol and placed in a 0.2 µm electroporation cuvette (Bio-Rad, USA). Finally, the desalted ligation mixture (8 µl) was added to the cell suspension and incubated together on ice for an hour. The electroporation was performed using Gene Pulser Xcell system (Bio-Rad, USA) in manufacturer's pre-set conditions for *E. coli*: pulse type – exponential decay; capacitance = 25 µF; voltage = 2.5 kV; PC resistance = 200 ohms.

After the electropulse, 1 ml of LB medium pre-warmed to 37 °C was immediately transferred to the cuvette containing electroporated cells. The inoculated medium was then incubated at 37 °C for an hour (shaking: 50 rpm) to recover the transformed cells. Subsequently, this recovered bacterial suspension (100 µl per plate) was plated on LB-agar plates supplemented with 5-ALA and kanamycin (30 mg/l) to select the transformants.

#### 8.4.5.2. Heat-shock transformation

The chemically competent *E. coli* ST18 cells were prepared according to Inoue *et al.* (1990). First, ST18 was cultured at 28 °C for 5 hours (until it reached OD600 of ~0.5) in 100 ml of LB medium supplemented with 5-ALA (**8.1.3.5**). The culture was then chilled on ice, centrifuged for 10 minutes at 3000 g at 4 °C and the pellet was resuspended in 10 ml of ice-cold transformation buffer [TB] (**8.1.3.6**). After 10 minutes of incubation on ice, the bacterial suspension was again centrifuged. The pellet was then resuspended in 3.72 ml of ice-cold TB buffer and 0.28 ml of DMSO was added to the suspension as a stabiliser for the storage of frozen competent cells. After another 10 minutes of incubation on ice, the suspension of competent cells was split into aliquots stored at -80 °C for up to one year or used directly for heat shock transformation (Sambrook and Russell, 2001), conducted as follows. A two hundred µl aliquot of the competent cells' suspension was transferred into a sterile, chilled 15 ml centrifuge tube. The post-ligation sample of the pKNOCK-Km vector with the applicable insert was added to the reaction tube and incubated with the ST18 competent cells on ice for 30 minutes. The heat-shock step was then carried out by placing the tube in a water bath set for 42 °C for 90 seconds and immediately moving it back to an ice bath afterwards. After a minute of cooling, 1 ml of LB medium supplemented with 5-ALA and kanamycin was added to the tube, the cells were incubated for 1 hour at 37 °C and subsequently they were plated on a corresponding selective agar medium (100 µl of post-transformation cell suspension per one LB/5-ALA/kanamycin-agar plate). The plates were incubated overnight at 37 °C.

#### 8.4.5.3. Conjugation

The colonies obtained on the selective medium were transferred to a fresh agar plate regardless of the transformation method. After overnight culture, the presence of the pKNOCK vector in the ST18 cells was confirmed with a colony PCR (see **8.4.3**: **MIX P2; COND 2**) using pKNOCK_backbone and insert flanking primers (**SUPPLEMENTARY TABLE 2**). The method quality controls were applied for each transformation performed: positive ST18 transformation control with pKNOCK-Km without an insert and negative control with nuclease-free water instead of a vector solution.

The final step of the mutagenesis was the vector transfer from the *E. coli* ST18 strain transformed with pKNOCK containing the desired insert to *P. donghuensis* P482 cells. It was achieved through biparental mating (conjugation) of the two strains as described by Krzyżanowska *et al.* (2016). First, the strains were grown in 3 ml of LB medium; for the ST18 transformants LB medium was supplemented with 5-ALA and kanamycin. Then, each culture was washed with fresh LB and resuspended in 1 ml of LB. Two suspensions (of an ST18 transformant strain and P482) were then pooled together (1:1) and centrifuged. The pellet was then resuspended in 30 µl of LB and spotted on the LB-agar plate. The plate was incubated for 16 h at 37 °C. The resulting macrocolony was fully scratched from the medium and suspended in 1 ml of LB for further serial dilutions (tenfold, up to $10^{-3}$) and plating. Finally, three 100 µl aliquots of each dilution and the undiluted suspension were plated on LB-agar deprived of 5-ALA but supplemented with kanamycin for positive selection of P482 transconjugants.

#### 8.4.5.4. Mutagenesis confirmation

The colonies of P482 transconjugants obtained were then screened for the presence of pKNOCK-Km vector insertions in their genetic material. The screening consisted of a PCR procedure (see 8.4.3: **MIX P2; COND 2**) with pKNOCK_backbone primers (**SUPPLEMENTARY TABLE 2**) with isolated gDNA of the transconjugants serving as a template. If the PCR screening results were positive, the targeted loci of pKNOCK-Km insertion were confirmed by short DNA sequencing (DNA Sequencing and Oligonucleotide Synthesis Laboratory, Institute of Biochemistry and Biophysics, Polish Academy of Sciences, Warsaw, Poland) with the F_outof_pKNOCK primer (**SUPPLEMENTARY TABLE 2**) and P482 transconjugants gDNA as a template. The sequencing results were then mapped onto the P482 genome to identify the insertion sites and confirm the inactivation of the targeted genes.

## 8.5. Gene expression analyses

### 8.5.1. RNA isolation

To perform RT-qPCR analyses, total RNA was isolated from P482 wt cultured under conditions specified in **TABLE 10**. Culture time was established with the use of growth curves for each of the nutritional conditions.

After the specified incubation time, the cultures' turbidity was measured and the calculated volumes were centrifuged to harvest ca. 2.5 x $10^8$ cells per single isolation. The cells were resuspended in 500 µl of sterile saline and 1 ml of RNAprotect Bacteria Reagent (Qiagen, Germany) was added to each sample to prevent RNA degradation.

Total RNA isolation using RNeasy Mini Kit (Qiagen, Germany) was performed immediately after this step. The RNA extraction was carried out as instructed in the manufacturer's protocol

using the provided columns, reagents and buffers. Nuclease free water (50 µl) was used to elute RNA from the column, and the RNA samples obtained were stored at -80 °C.

Each sample was subjected to a quality check procedure. First, the genomic DNA (gDNA) contamination of the samples was detected by subjecting 1 µl of an RNA sample to a PCR reaction (see 8.4.3: **MIX T2; COND 3**) with primers designed to amplify the fragment of *lexA* or *rpoB* gene in P482 DNA (**SUPPLEMENTARY TABLE 2**). In the case of gDNA contamination, the samples were subjected to additional DNA digestion before the reverse transcription step. Then, the concentration and quality of the RNA samples were assessed using NanoDrop 2000 spectrophotometer (Thermo Scientific, USA). The concentration of RNA in the samples was in the range of 100 - 700 ng/µl, and these values were later used to calculate the volume of each sample used in reverse transcription.

**TABLE 10.** Conditions of the cultures used for RNA isolation and subsequent RT-qPCR analyses.

| culture medium[a] | conditions label (results section) | incubation temperature | culture time | growth phase | RNA samples purpose[b] |
|---|---|---|---|---|---|
| M9 + glucose | glucose (no Fe) | 28 °C | 12.5 h | late log | RGs selection, GE analysis |
| M9 + glycerol | glycerol (no Fe) | 28 °C | 30 h | late log | RGs selection, GE analysis |
| M9 + glucose +30 µM $FeSO_4$ | glucose Fe(II) | 28 °C | 12.5 h | late log | RGs selection, GE analysis |
| M9 + glucose +30 µM $FeCl_3$ | glucose Fe(III) | 28 °C | 12.5 h | late log | RGs selection, GE analysis |
| M9 + glycerol +30 µM $FeSO_4$ | glycerol Fe(II) | 28 °C | 22 h | late log | RGs selection, GE analysis |
| M9 + glycerol +30 µM $FeCl_3$ | glycerol Fe(III) | 28 °C | 30 h | late log | RGs selection, GE analysis |
| M9 + glucose + maize root exudates | - | 28 °C | 12 h | late log | RGs selection |
| M9 + glucose + tomato root exudates | - | 28 °C | 12 h | late log | RGs selection |
| LB | - | 28 °C | 16 h | late log | RGs selection |
| 0.1 TSB | - | 28 °C | 10 h | mid-log | RGs selection |
| 0.1 TSB | - | 28 °C | 15 h | mid-stationary | RGs selection |
| 0.1 TSB | - | 22 °C | 16 h | late log | RGs selection |

[a]Media described in section 8.1.3;
[b]RGs – reference genes, GE – gene expression

### 8.5.2. RT-qPCR

Reverse transcription [RT] of RNA to cDNA was carried out using iScript gDNA Clear cDNA Synthesis Kit (Bio-Rad, USA). The kit reaction buffer utilises random hexamers as primers. The manufacturer's instructions were followed to obtain cDNA, the optional DNase treatment was employed prior to RT for the samples in which gDNA contamination was detected. The amount of total RNA per single RT reaction was adjusted to 500 ng. The cDNA samples after the RT procedure were immediately subjected to qPCR or stored at -20 °C for up to two months.

All qPCR reactions were carried out using CFX96 thermocycler (Bio-Rad, USA) coupled with CFX Maestro software (Bio-Rad, USA) for assay control and recording of the results. The reaction conditions were: 95 °C for 5 minutes; 40 cycles of: 95 °C (15 sec), 60 °C (30 sec), readout. After the reaction, a melting curve assay was performed for each sample to assess the primers' specificity. Melting temperatures of the amplicons were measured in the range from 65 °C to 95 °C with an increment of 0.5 °C per second.

SYBR Green dye was used for the quantification of the amplicon. The qPCR reaction mixtures (total volume of the sample: 15 µl) contained Sso Advanced Universal SYBR Green Supermix (Bio-Rad, USA), forward and reverse primers (final concentration: 200 nM) and 5 µl of cDNA template (1:3 diluted post-RT mixture). The reactions were carried out in 96-well plates, each reaction was run in 2 technical replicates and there was an inter-run calibrating sample included in each run.

Quality parameters of the qPCR assay were validated prior to experiments. Primer pairs were designed as described in **8.7.1**. Each primer pair's efficiency and assay linearity were assessed using 7-point standard curves obtained by amplifying 10-fold dilutions of corresponding templates (respective post-PCR amplicons). Primer specificity was established with the initial standard PCR reaction (see **8.4.3**: **MIX T1; COND 3**) and assessment of the products' length on an agarose gel after electrophoresis as well as with the melting curves assay. Additional quality control measures were applied in the analysis of the results. For the results to be included in the statistical analysis, the quantitation cycle [$C_q$] difference between the duplicates (replicate variability) had to be lower than 0.3 cycle. The results were excluded from the analysis if the negative controls [NCs] without added primers and no-template controls [NTCs] resulted in $C_q$ value lower than 37 (typically NCs and NTCs yielded no signal).

### 8.5.3. Selection of reference genes

The potential reference genes for gene expression analysis in *P. donghuensis* P482 were chosen following the literature concerning the topic. The list of the tested housekeeping genes and their features is presented in **TABLE 11** and the qPCR primers corresponding to these genes

designed in the study are shown in **SUPPLEMENTARY TABLE 2**. The expression of the selected housekeeping genes was tested with qPCR on the reverse transcribed RNA samples obtained from P482 cultured under twelve different conditions listed in **TABLE 10**.

The quality of qPCR results was determined using Maestro CFX software (Bio-Rad, USA) after recording the runs. The raw results obtained were exported and the stability of potential RGs was assessed using the geNorm algorithm incorporated into the qbase + software, v. 3.2 (Biogazelle NV, Belgium – www.qbaseplus.com). Furthermore, the RefFinder tool (www.heartcure.com.au/reffinder/) was utilised to support RGs expression stability analysis.

**TABLE 11.** P482 housekeeping genes tested in RT-qPCR reference genes validation study

| gene | P482 locus | protein annotation | reference gene literature |
|---|---|---|---|
| *rpoB* | BV82_1963 | sigma factor rpoB | (Ahmed *et al.*, 2019, Case *et al.*, 2007) |
| *gyrB* | BV82_2296 | DNA gyrase subunit B | (Ahmed *et al.*, 2019) |
| *mrdA* | BV82_4935 | penicillin-binding protein 2 | (Savli *et al.*, 2003) |
| *rpoD* | BV82_1895 | sigma factor RpoD | (Chang *et al.*, 2009, Savli *et al.*, 2003) |
| *lexA* | BV82_3405 | transcriptional repressor LexA | (Chang *et al.*, 2009) |
| *proC* | BV82_2548 | pyrroline-5-carboxylate reductase | (Ahmed *et al.*, 2019, Alqarni *et al.*, 2016, Savli *et al.*, 2003) |
| *recA* | BV82_0583 | DNA recombination protein RecA | (Alqarni *et al.*, 2016) |
| *algD* | BV82_3321 | GDP-mannose-6-dehydrogenase | (Alqarni *et al.*, 2016) |
| *acpP* | BV82_4055 | acyl carrier protein | (Akiyama *et al.*, 2018) |
| *tuf* | BV82_1955 | elongation factor Tu | (Cui *et al.*, 2016) |

### 8.5.4. Gene expression analysis

RT-qPCR technique (**8.5.2**) was adopted to analyse the level of expression of selected P482 genes under given conditions. The primers used in the gene expression study are listed in **SUPPLEMENTARY TABLE 2**. Once the qPCR results were recorded, the expression of the tested genes was calculated using the qbase+ software, version 3.2 (Biogazelle NV, Belgium) by applying the general ΔΔCt approach with normalisation to reference genes chosen in the study and the amplification efficiencies determined for each primer pair. The values of normalised relative quantity [NRQ] obtained were corrected with respect to the values acquired for the used inter-run calibrator sample to determine calibrated NRQ [CNRQ] values which represent the relative

expression values and have subsequently been subjected to statistical analysis, also carried out in the qbase+ software. Finally, the mean CNRQ values obtained for each tested gene in various test conditions were compared by implementing a one-way ANOVA test with correction for multiple testing and a Tukey-Kramer post-hoc analysis.

## 8.6. Biofilm formation analyses

### 8.6.1. Crystal violet assay

To assess the influence of given nutritional conditions on biofilm formation by P482 and mutants, a polystyrene 96-well plate was used as a biofilm attachment surface. *P. aeruginosa* PA01 (a thoroughly investigated model organism for biofilm development studies (Lee and Yoon, 2017)) served as the positive control strain of biofilm formation assay, while *S. epidermidis* ATCC 12228, a strain without biofilm forming abilities (Zhang *et al.*, 2003), served as a negative control in this assay.

Firstly, an overnight preculture of the tested strain was diluted in the given liquid medium in a ratio of 1:500. The inoculated medium was then distributed into a 96-well plate in portions of 200 µl per well. Bacteria were cultured overnight with shaking (100 rpm) at 28 °C. After the $OD_{600}$ of the cultures was measured (EnVision Microplate Reader, PerkinElmer, USA) the wells were washed three times with phosphate-buffered saline (PBS; Sambrook and Russell, 2001) and the biofilm was fixed with 2% sodium acetate and its evaporation in 60 °C.

To stain the biofilm, 150 µl of 0.1% crystal violet solution was added per well and incubated at room temperature for 15 minutes. After the incubation, the plate was thoroughly rinsed with distilled water, dried and the crystal violet bound to the biofilm was dissolved in 150 µl of 96% ethanol per well. Under the given conditions, the strains' biofilm formation ability was quantified using spectrophotometry by measuring the 570 nm absorption of the bound crystal violet dissolved in ethanol. All biofilm formation tests were performed in twelve biological replicates.

### 8.6.2. Colony morphology assessment (stereoscopic microscopy)

For the colony morphology evaluation, the tested strains were precultured in a liquid LB medium. The $OD_{600}$ of the precultures was measured (EnVision Microplate Reader, PerkinElmer, USA) and their optical density was adjusted to 0.5 $OD_{600}$ by centrifugation and resuspension in PBS (**8.1.3.6**). Ten microlitre drops of the PBS bacterial suspensions were placed on the biofilm inducing MSgg-agar plates prepared according to Townsley *et al.* (2018) (**8.1.3.4**). The plates were incubated for 48 hours at 28 °C and the resulting macrocolonies were observed and documented using a stereoscopic microscope (MZ10 F, Leica Microsystems, Germany).

## 8.7. *In silico* analyses

### 8.7.1. PCR/qPCR primer design and *in silico* predictive quality analyses

All PCR/qPCR primers used in the study were designed using PerlPrimer software (Marshall, 2004). The primers were generated based on the input properties and algorithms that calculated their physical properties and primer-dimer formation predictions. Primer3 algorithm (Untergasser *et al.*, 2007) incorporated into the UGENE software (Unipro, Russia; Okonechnikov *et al.*, 2012) was utilised in the case of PerlPrimer algorithm generating no fitting primer pairs. The NCBI Primer-Blast tool (https://www.ncbi.nlm.nih.gov/tools/primer-blast/; Ye *et al.*, 2012) was used to analyse the designed primers template specificity.

### 8.7.2. Gene and protein sequence and functional analyses

*In silico* nucleotide and amino acid sequence analyses were performed during various stages of the study. The NCBI databases were used for genetic/protein sequence search and analysis. The NCBI BLAST online tool (https://blast.ncbi.nlm.nih.gov/Blast.cgi; Altschul *et al.*, 1990) was used to find and compare similar genetic/protein sequences. UGENE software (Unipro, Russia; Okonechnikov *et al.*, 2012) was used to analyse genetic sequences for the presence of given sequence fragments, such as restriction sites, and for multiple gene/protein sequence alignments. The genome mining antiSMASH 5.0 and 6.0 tools were used to predict putative gene clusters involved in secondary metabolism of P482 (www.antismash.secondarymetabolites.org; Blin *et al.*, 2019, 2021). The Operon-mapper tool was used to predict the operon organisation in gene "cluster 17" (www.biocomputo.ibt.unam.mx/operon_mapper; Taboada *et al.*, 2018).

Predictive protein function analyses were carried out with the use of numerous online tools and databases provided at: UniProt (www.uniprot.org; The Uniprot Consortium, 2018), KEGG (www.genome.jp; Kanehisa and Goto, 2000), PDB (www.rcsb.org; Berman *et al.*, 2000), InterPro (www.ebi.ac.uk/interpro; Blum *et al.*, 2021) and EggNOG v5.0 (www.eggnog5.embl.de; Huerta-Cepas *et al.*, 2019).

### 8.7.3. Statistical analyses

Statistical analyses of the antibacterial activity and biofilm data were carried out with R programming language (R Core Team, 2020) using RStudio Desktop software (v2021.09.1+372.pro1). In addition, R packages dplyr (Wickham *et al.*, 2022) and ggplot2 (Wickham, 2016) were employed for data transformation and visualisation. The specific tests used in data analysis are annotated in the captions of the relevant figures.

Statistical analyses of the metabolomic data were carried out by Alessia Staropoli, MSc (IPSP-CNR, Portici, NA, Italy) using Mass Profiler Professional software (Agilent Technologies,

USA). The signal values of the entities detected in the samples included in a given analysis were normalised subjected to ANOVA analysis with Tukey's post-hoc test. They were further filtered using a fold change [FC] threshold, only samples with FC ≥ 2 were included in the analyses. These results were subjected to hierarchical clustering and principal component analysis [PCA].

# 9. Results

## 9.1. Insertion mutagenesis in P482 and characteristics of the mutants

### 9.1.1. P482 genomic loci involved in iron metabolism selected for inactivation

Previous studies on *P. donghuensis* P482 have identified several genomic regions involved in its antimicrobial activity (Krzyżanowska *et al.*, 2016). The most extensively investigated regions are involved in the iron metabolism, particularly the iron acquisition which is associated with pyoverdine [PVD] and 7-hydroxytropolone [7-HT] biosynthesis. Therefore, to extend these studies of, additional genes involved in the iron metabolism (loci BV82_0255, _0562, _2408, _4870, _4879; characterised in **TABLE 12**) were selected for further investigation. Only the loci of very high identity to iron metabolism genes found in other *Pseudomonas* spp. were selected for the study to minimise the risk of functional inaccuracy. The selected loci were subjected to insertional mutagenesis. The locus of primary interest was BV82_4870, annotated as *fur* gene which encodes for the ferric uptake regulator protein (Fur). Other chosen loci were selected for the involvement of their products in iron-sulphur cluster assembly (BV82_0255) and employment (BV82_0562 and BV82_4879), and potential engagement in siderophore transport (BV82_2408).

**TABLE 12.** P482 iron metabolism-related loci selected for the mutagenesis

| Locus (GenBank location) | Gene length (bp) | Product size (aa) | Annotation(s)[a] | KEGG [KO, EC][b] | KEGG pathway[c] | BLAST high score hits[d] |
|---|---|---|---|---|---|---|
| BV82_**4870** (CP071706.1: 5012823-5013227) | 405 | 134 | *fur* ferric uptake transcriptional regulator | K03711 | - | >100 |
| BV82_**0255** (CP071706.1: 1130659-1130982) | 324 | 107 | *iscA* iron-sulphur cluster assembly protein | K13628 | - | >100 |
| BV82_**0562** (CP071706.1: 1466186-1466509) | 324 | 107 | *fdxA* ferredoxin A | K05524 | - | >100 |
| BV82_**2408** (CP071706.1: 273700-276195) | 2496 | 838 | TonB-dependent siderophore receptor | K02014 | - | >100 |
| BV82_**4879** (CP071706.1: 5019344-5022154) | 2811 | 936 | d-lactate dehydrogenase; Fe-S oxidoreductase | K18930 | map00620 | >100 |

[a]Combined data obtained using: NCBI BLAST, KEGG BlastKOALA, EggNOG-mapper v2 and InterPro annotations
[b]KO: Kegg Orthologs, EC: enzyme classification; obtained using KEGG BlastKOALA tool
[c]Pathways: map00620 – pyruvate metabolism
[d]≥90 % query cover, 75 % identity to sequences reported for proteins of taxon *Pseudomonas* spp. (data: January 2017)

The mutants with pKNOCK-Km insertions were obtained (8.4.4; 8.4.5) and the insertions were confirmed by DNA sequencing. The mutants' phenotypes such as the colony morphology, PVD and 7-HT production, and the pathogens' growth inhibition are briefly characterised in the following sections. The aim was to select the mutant that shows significant differences with respect to P482 wt for its further inclusion in the studies on carbon/iron source influence on P482 antimicrobial activity and biofilm formation.

### 9.1.2. Colony morphology of the mutant strains

The colony morphology of P482 wt and the mutants obtained was assessed by growing their macrocolonies on MSgg agar, the biofilm-promoting minimal medium. The experiment was performed based on the assumption that the altered colony morphology in a mutant might be correlated with changes in its biofilm formation (Cabeen *et al.*, 2016). The assay was facilitated by stereoscopic light microscopy and documented using photomicrography. To exclude the artefacts produced by the minor differences in the hydration of the agar medium on different plates, each mutant was grown on at least two separate plates.

The colonies of P482 and the mutants obtained exhibited a highly similar visual appearance with few differentiating traits in certain mutants (FIGURE 5). All the macrocolonies measured up to 15 mm in diameter, aside from the macrocolonies of the KN4870 mutant which were larger and measured 20-23 mm in diameter. The distinct trait of P482 is to produce macrocolonies with a double-shaded surface when seen in magnification. They are characterised by a circular, darker centre with the fresh growth of the motile cells around the edge, sometimes discernible as light ellipsoid protrusions. However, this structure was observed to be differently pronounced in the

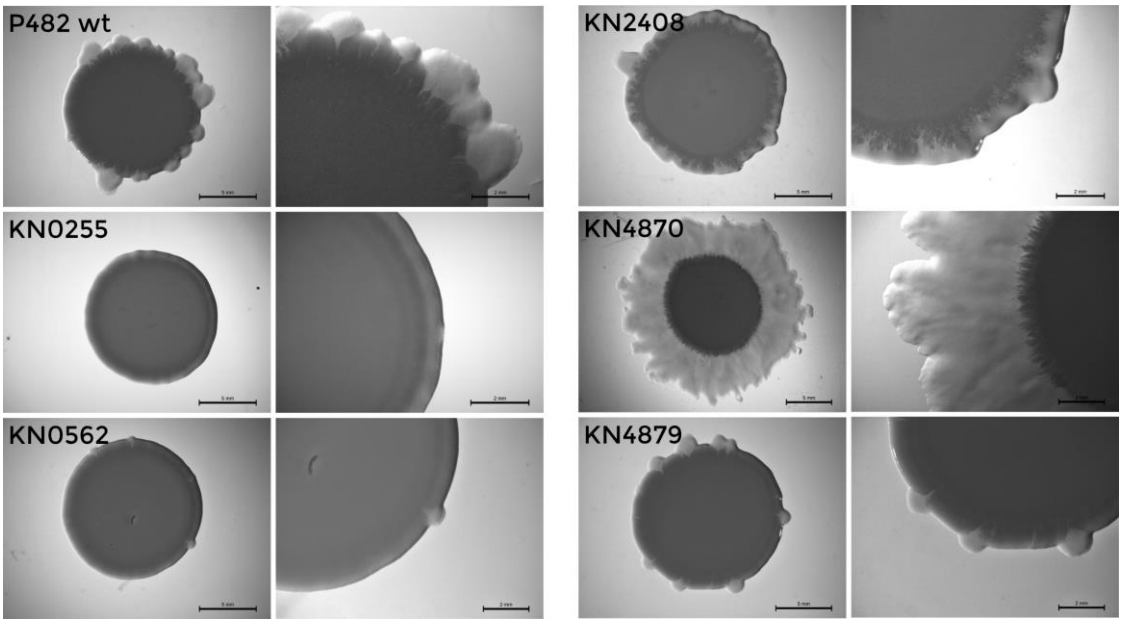


**FIGURE 8. Photomicrographs of macrocolonies formed by P482 wt and its selected mutant strains.** Photographs of entire colonies on the left (scale bar: 5 mm), the corresponding magnifications of the colonies' margins on the right (scale bar: 2 mm).

tested strains. The macrocolonies of P482 wt were on average characterised by nine to twelve of visible edge protrusions. The colony margin of the KN4879 mutant resembled that of P482 wt. A significant difference could be observed for KN4870, which produced colonies of a highly irregular and wider protruding marginal structure. In contrast to KN4870, KN0255 colonies did not form the edge irregularities at all and remained circular. KN2408 exhibited an undulated edge made of the structure forming the wild type protrusions, while the marginal structure of KN0562 resembled the regular one of KN0255 with only a few small protrusions (up to five).

### 9.1.3. 7-HT and PVD production by the mutants (rich growth medium)

UV-Vis spectrophotometry was used to examine whether the inactivation of the selected iron metabolism-related genes in P482 affects its production of the known iron chelators, namely PVD and 7-HT. The wild type *P. donghuensis* P482 produces both compounds when cultured in rich, undefined media such as LB medium. The UV-Vis absorption spectrum of the supernatant obtained from HYS$^T$ culture in King's B Medium reveals three peaks that correspond to the mentioned iron chelators: 330 nm and 392 nm for 7-HT and 405 nm for PVD (Chen M. *et al.*, 2018). In the case of P482 cultured in LB medium, the peaks are slightly shifted towards the shorter wavelengths with ca. 327 nm and 387 nm for 7-HT and ca. 398 nm for PVD. (**FIGURE 6**). Regardless of the culturing duration (22 h or 44 h), all the discussed peaks can be observed for P482 wt and the tested mutants, namely KN0255, KN0562, KN2408, KN4870 and KN4879. This indicates that the production of the mentioned iron-chelating compounds occurs in the mutants obtained in this study. Despite the varied heights of the peaks, the qualitative nature of this method of compound detection does not allow for the quantitative description of their biosynthesis levels.

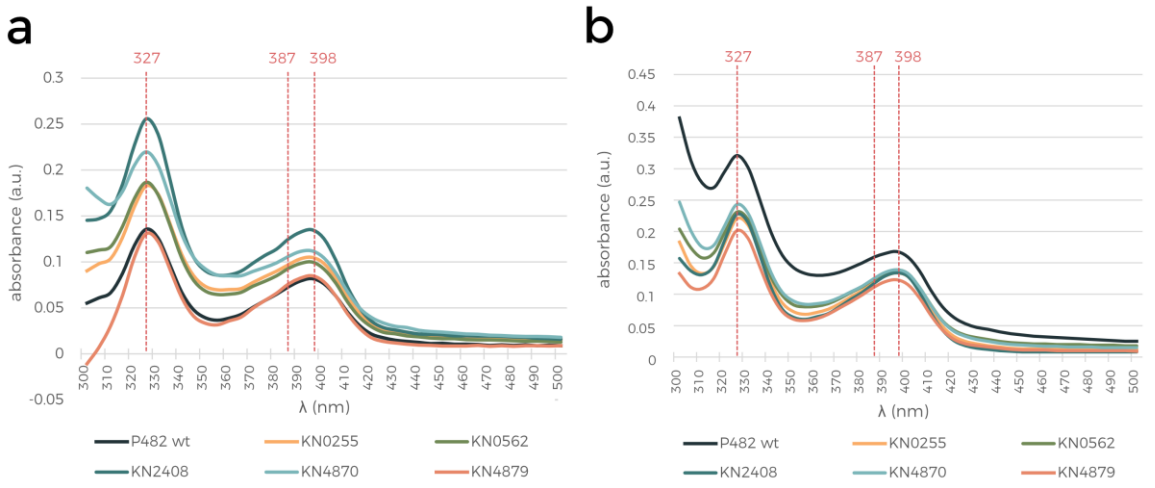


**FIGURE 11. UV-Vis absorption spectra of the LB culture supernatants of P482 wt and its mutants in genes related to iron metabolism.** The samples were the given strain's post-culture supernatants after **a**. 22 h and **b**. 44 h of culturing in LB medium. The spectra were recorded in the wavelength range 300-500 nm. The red dashed lines indicate the peak absorption wavelengths for the iron chelators: 7-HT (obtained: 327 nm and 387 nm, expected: 330 nm and 392 nm) and PVD (obtained: 398 nm, expected: 405 nm).

### 9.1.4. Antimicrobial activity of the obtained mutants (rich growth medium)

To determine whether the mutations introduced into P482 genes associated with iron metabolism influenced its overall antibacterial activity, all the mutants obtained in the study were tested for their antagonism against three bacterial plant pathogens. The selected pathogen strains were *D. solani* IFB0102, *P. brasiliense* Pcb LMG21371 and *P. syringae* pv. *syringae* Pss762. LB-agar, a rich growth medium, was used as the test environment.

The test results did not indicate any considerable change in antimicrobial activity of the mutants in comparison to the wild type strain (**FIGURE 7**). For all tested mutant vs pathogen pairs, the growth inhibition zones' diameters measured ranged from 80% to 110% of the diameters of zones caused by P482 wt under the same conditions. Considering the inaccuracy of the human factor in measurements and only two biological replicates, no significant differences were detected.

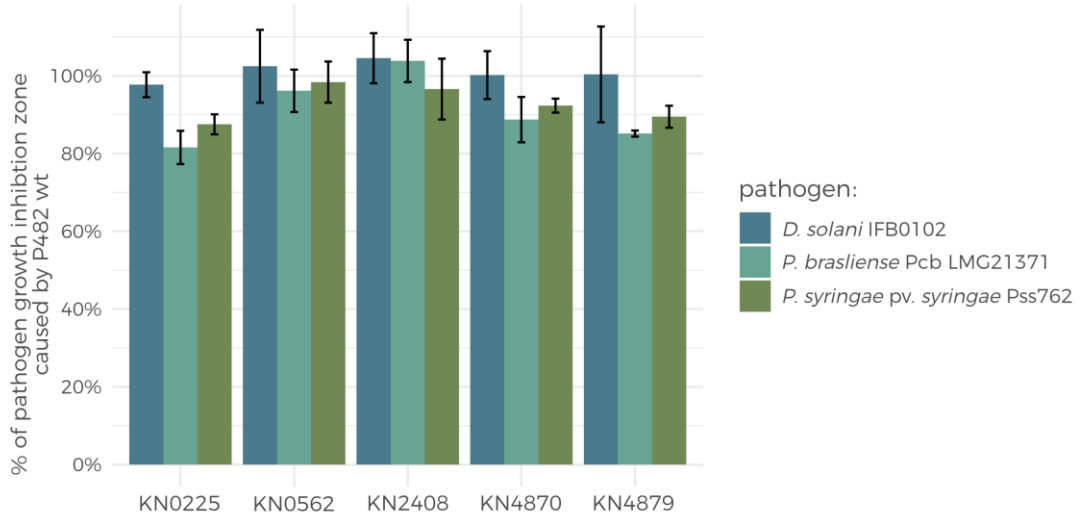


**FIGURE 14. Direct antibacterial activity of the P482 mutants with inactivated genes related to iron metabolism.** The tests utilised LB-agar medium. The bars represent antagonism (pathogen growth inhibition zones) calculated relatively to the growth inhibition zones caused by the wild type P482 under the same conditions. The error bars represent standard deviation.

Overall, none of the mutants obtained in this study differed significantly from the wild type strain regarding the performed preliminary phenotype characteristics assays. The only differences could be observed in KN0255 and KN4870 mutants in colony morphology analysis. The KN4870 mutant was selected to be included in further tests due to the assumed significance of its inactivated gene product, the Fur protein, and its distinct colony morphology. The remaining mutants constructed in this study are planned to be further explored in other projects conducted at LPM (primarily the SONATA10 project No. 2015/19/D/NZ9/03588; principal investigator: M. Rajewska, PhD; funded by Polish National Science Center, Poland).

## 9.2. Investigation of the "cluster 17" functionality

The previous studies conducted at the LPM revealed "cluster 17" as one of the genomic regions which might be interesting for their possible involvement in secondary metabolism. The mentioned cluster was particularly interesting since its antiSMASH 2.0 analysis suggested the involvement in polyketide biosynthesis (Krzyżanowska *et al.*, 2016).

In this study, the P482 gene "cluster 17" was analysed *in silico* to expand our understanding on the role of this genomic region. "Cluster 17" comprises ten open reading frames [ORFs]. Using of the Operon-mapper tool which identifies promoter sequences (Taboada *et al.*, 2018), the "cluster 17" ORFs were shown to belong to two operons (**FIGURE 8**). The first operon encompasses seven ORFs in loci BV82_4236 to BV82_4242, while the second only consists of three ORFs, namely loci BV82_4243, BV82_4244 and BV82_4245.

Furthermore, the gene orthology analysis with the use of the BlastKOALA (KEGG Orthology and Links Annotation) tool was performed for the "cluster 17" genes. This algorithm provides the comparative analysis of the input amino acid sequence to the database of protein sequences to define the putative gene product by assigning a KEGG Orthology [KO] number. In the case of "cluster 17", only four genes were assigned the KO numbers, namely BV82_4237, _4243, _4244 and _4245 (**TABLE 13**). BlastKOALA did not identify any possible orthologs to the remaining six genes of "cluster 17", thus implying that the studied region has not been studied in other organisms.

Additionally, the functional analysis of "cluster 17" genes was carried out using the eggNOG-mapper v2 tool (Huerta-Cepas *et al.*, 2019). This tool assigns gene products to functional categories incorporated into Clusters of Orthologous Genes [COG] database. The genes of "cluster 17" were identified as belonging to various categories with the highest prevalence of the genes belonging to the "lipid transport and metabolism" class (**FIGURE 8**).


**FIGURE 17. Graphic representation of the P482 gene "cluster 17" ORF organisation.** Blue dots mark the ORFs targeted in pKNOCK insertional mutagenesis. Grey arrows represent identified promoter sequences The letters above the ORFs represent functional categories of the product of each gene as in COG classification assigned by the eggNOG-mapper v2 tool: Q – secondary metabolites biosynthesis, transport and catabolism, H – coenzyme transport and metabolism, I – lipid transport and metabolism, S – function unknown, V – defence mechanisms, E – amino acid transport and metabolism, G – carbohydrate transport and metabolism, P – inorganic ion transport and metabolism, M – cell wall/membrane/envelope biogenesis, U – intracellular trafficking, secretion, and vesicular transport. Figure adapted from Matuszewska *et al.* (2021). Information concerning gene annotation can be found in **TABLE 13**.

**TABLE 13.** ***P. donghuensis*** **P482 gene "cluster 17" annotation and features (updated[a]).**

| Locus (GenBank location) | Gene length (bp) | Product size (aa) | Annotation(s)[b] | KEGG [KO, EC][c] | KEGG pathway[d] | BLAST high score hits[e] |
|---|---|---|---|---|---|---|
| BV82_**4236** (CP071706.1: 4317199-4318272) | 1074 | 357 | NAD dependent epimerase/dehydratase family protein; (RfbD domain containing) | - | - | 9 |
| BV82_**4237** (CP071706.1: 4318273-4319544) | 1,272 | 423 | *patA* aspartate aminotransferase family protein, putrescine aminotransferase | KO: K09251 EC: 2.6.1.82 | ko00310 ko00330 ko01100 ko01120 | 3 |
| BV82_**4238** (CP071706.1: 4319541-4319984) | 444 | 147 | polyketide cyclase/dehydrase family protein; (SRPBCC ligand-binding domain containing) | - | - | 3 |
| BV82_**4239** (CP071706.1: 4319990-4321135) | 1,146 | 382 | putative isobutylamine N-hydroxylase; (CaiA domain containing [acyl-CoA dehydrogenase]) | - | - | 4 |
| BV82_**4240** (CP071706.1: 4321132-4321959) | 828 | 276 | SDR family NAD(P)-dependent oxidoreductase | - | - | 62 |
| BV82_**4241** (CP071706.1: 4321970-4322962) | 993 | 330 | fatty acid desaturase family protein | - | - | 2 |
| BV82_**4242** (CP071706.1: 4322995-4323798) | 804 | 267 | hypothetical protein; DUF3050 domain containing | - | - | 4 |
| BV82_**4243** (CP071706.1: 4323879-4324943) | 1065 | 354 | *emrA* efflux transporter, MFP subunit (HlyD_D23 domain containing) | K03543 | - | 17 |
| BV82_**4244** (CP071706.1: 4324940-4326514) | 1,575 | 524 | *emrB* DHA2 family efflux MFS transporter permease subunit | K03446 | - | 74 |
| BV82_**4245** (CP071706.1: 4326478-4327827) | 1,350 | 449 | *tolC* outer membrane TolC family protein | K12340 | ko01501 ko01503 ko02020 ko03070 ko04626 | 8 |

[a]Table was revised and updated with new information with respect to the data published in Matuszewska *et al.* (2021)
[b]Combined data obtained using: NCBI BLAST, KEGG BlastKOALA, EggNOG-mapper v2 and InterPro annotations
[c]KO: Kegg Orthologs, EC: enzyme classification; obtained using KEGG BlastKOALA tool
[d]Pathways: ko00310 – lysine degradation, ko00330 – arginine and proline metabolism, ko01100 – metabolic pathways, ko01120 – microbial metabolism in diverse environments, ko01501 – beta-lactam resistance, ko01503 – cationic antimicrobial peptide (CAMP) resistance, ko02020 – two-component system, ko03070 – bacterial secretion system, ko04626 – plant-pathogen interactions
[e]≥90 % query cover, 75 % identity to sequences reported for proteins of taxon *Pseudomonas* spp., search performed in March 2022

The detailed description of the "cluster 17" ORFs revealed that only one of them is assigned as a hypothetical protein, however, no well investigated orthologs were found for any of the genes except for BV82_4237 which was annotated as a putrescine aminotransferase encoding gene, *patA* (**TABLE 13**). The BLAST nucleotide and protein searches suggest fewer than 10 closely related genes for most ORFs of "cluster 17". The low level of conservation of this genomic region pinpoints to its uniqueness and possible novelty of its product.

To test the hypothesis that "cluster 17" genes might be involved in the antimicrobial activity of P482, pKNOCK insertion mutants in genes BV82_4240 and BV82_4243 were constructed by T. Maciąg, MSc (LPM) using methods described in sections **8.4.4** and **8.4.5**. Locus BV82_4240, located in the first predicted operon, encodes an enzyme from the short chain dehydrogenase [SDR] family. The BV82_4243 locus belongs to the second operon and its predicted product is annotated as EmrA, one of the proteins building a tripartite efflux pump. The resulting pKNOCK mutants KN4240 and KN4243 were subjected to the antagonism tests towards *D. solani* IFB0102 and *P. syringae* pv. *syringae* Pss762 (**FIGURE 9**). This preliminary study, conducted upon an undefined, rich growth medium (LB-agar), showed that the tested genes do not contribute significantly to P482 antibacterial activity under these conditions, in spite of the tendency of the KN4243 mutant to exhibit lower antagonistic potential (~70% of that of P482 wt).

Overall, the P482 gene "cluster 17" is a rare genomic region that might be involved in biosynthesis of a potentially valuable metabolite. While the "cluster 17" mutants' antibacterial activity is mostly unchanged on LB-agar, the slight reduction in the antagonistic properties in KN4243 and the premise of a novel biosynthetic cluster led to inclusion of both KN4240 and KN4243 mutants in the subsequent experiments.

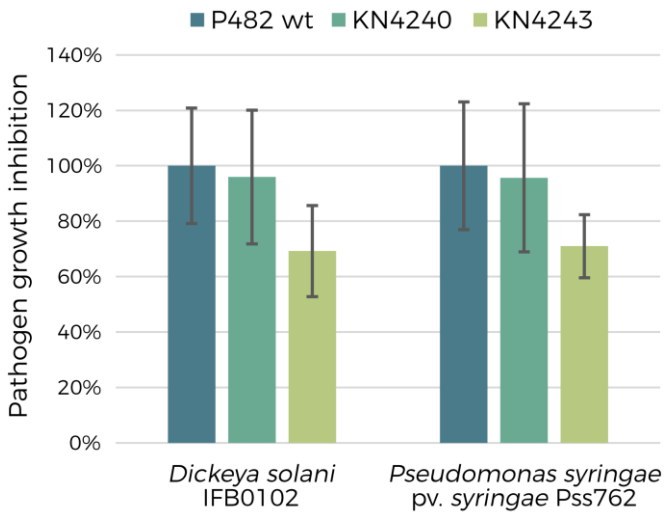


**FIGURE 20. Growth inhibition of *D. solani* IFB0102 and *P. syringae* pv. *syringae* Pss762 by P482 wt and its "cluster 17" mutants on LB-agar medium.** The bars show the percentage of the growth inhibition zone obtained for the P482 wt strain under given condition. Error bars represent standard deviation. Figure adapted from Matuszewska *et al.* (2021, supplementary material).

## 9.3. Carbon source affects growth and antimicrobial activity of P482

### 9.3.1. Glycerol induces an extended lag phase in P482 cultures

Prior to the experiments focusing on the nutritional dependency of P482 antimicrobial activity and biofilm formation, the growth of P482 and the mutants selected for the study was analysed. The mutant strains included in the analyses were KN4706, KN4709, KN3318, KN1009, KN3375, KN4870, KN4240 and KN4243. To present the data clearly, the results are divided into sections corresponding to the groups of P482 mutants with a common functionality of the inactivated genes. The mutants in genes from the 7-HT cluster (KN4706, KN4709) are grouped with a *gacA*$^-$ (KN3318) mutant since the Gac/Rsm pathway was shown to regulate 7-HT production in *P. donghuensis*. Additionally, the analyses that did not require the sample number to be limited include a KN4705 mutant (a third strain with an inactivation in the gene from the 7-HT cluster). Furthermore, the strains with inactivated genes involved in pyoverdine (PVD) synthesis (KN1009 and KN3755) are grouped with the *fur*$^-$ mutant (KN4870) since the Fur protein is responsible for the regulation of siderophore biosynthesis. Finally, the last group comprises the mutants in genes belonging to "cluster 17" (KN4240, KN4243). This division to mutant groups was also used to present other data in the results section of this thesis (when applicable).

The growth curves of P482 and mutants were obtained under the minimal nutritional conditions with glucose or glycerol as a single carbon source. All the growth curves obtained were analysed and compared in order to determine the pattern of bacterial population growth.

A significant difference was observed between the growth of P482 in glucose and in glycerol (**FIGURE 10**). When glucose was the sole carbon source in the mineral medium, the exponential growth phase started after 8(±1) hours of P482 wt culture. However, when glycerol was the carbon source, the lag phase was extended up to approximately 20 hours. This 10-hour (or longer) extension of the lag phase on glycerol versus glucose is valid for all the tested mutants of P482. Due to this phenomenon, all further protocols involving incubation of P482 under glycerol as the sole carbon source were adjusted accordingly.

Another characteristic phenotype can be observed for the KN3318 mutant (*gacA*$^-$). Compared to P482 wt, KN3318 enters the exponential growth phase earlier (~2 hours) and its culture reaches higher $OD_{600}$ values (**FIGURE 10**). This occurs regardless of the carbon source (glucose/glycerol) present in the medium, whereas the extension of KN3318 lag phase between the growth on glycerol versus glucose is comparable to the one observed in the wild type strain. Nevertheless, due to technical difficulties and sustainability issues, the assays could not be adjusted to the mutant growth abnormalities and the incubation time for the KN3318 mutant was not shortened with respect to P482 wt.

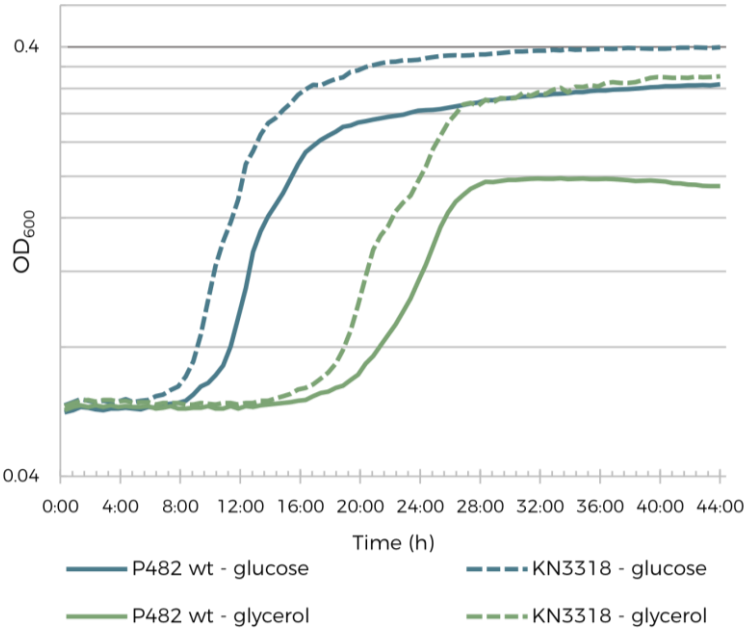


**FIGURE 21. Growth curves of P482 and KN3318 on glucose and glycerol.** The strains were cultured in M9 with either 0.4% glucose or 0.4% glycerol as a sole carbon source. The $OD_{600}$ values at each time point are the mean values of four biological replicates. The curves obtained are presented in a logarithmic scale.

The other tested mutants did not exhibit clear growth timing patterns as described in the case of KN3318. Particularly, no other mutant cultured in the glucose medium entered the logarithmic growth phase significantly later or earlier than P482 wt (**FIGURE 11**). However, the differences can be observed in the final density of the glucose cultures which for KN1009, KN4870 and KN4240 are higher than for P482 wt. In the case of KN1009 and KN4240 this phenomenon of higher final density of the culture is consistent and also detected when glycerol serves as a carbon source. Additionally, this increased cell density on glycerol can be also observed in KN4706.

Another observation of the growth of P482 mutants when utilising glycerol is that KN4709 and KN4243 tend to have a prolonged lag phase in comparison with P482 wt, whereas the KN1009 mutant exhibits a slightly shortened lag phase (**FIGURE 11**). Other mutants selected for this test did not exhibit major deviations from the wild type growth pattern.

The overall conclusion from the described growth curves is that the growth of P482 is influenced not only by the carbon source it utilises. The combination of two factors, namely carbon source and particular mutations (inactivating selected genes relevant for P482 antimicrobial activity), determines P482 growth curve shape and height in a way which cannot be predicted with our current knowledge of the factors. Nonetheless, the changes in P482 growth curves caused by the mutations were minor in comparison to the difference caused by the glucose/glycerol influence. Therefore, following this part of the study, only carbon source influence was taken into account to establish the culturing time in further experiments.

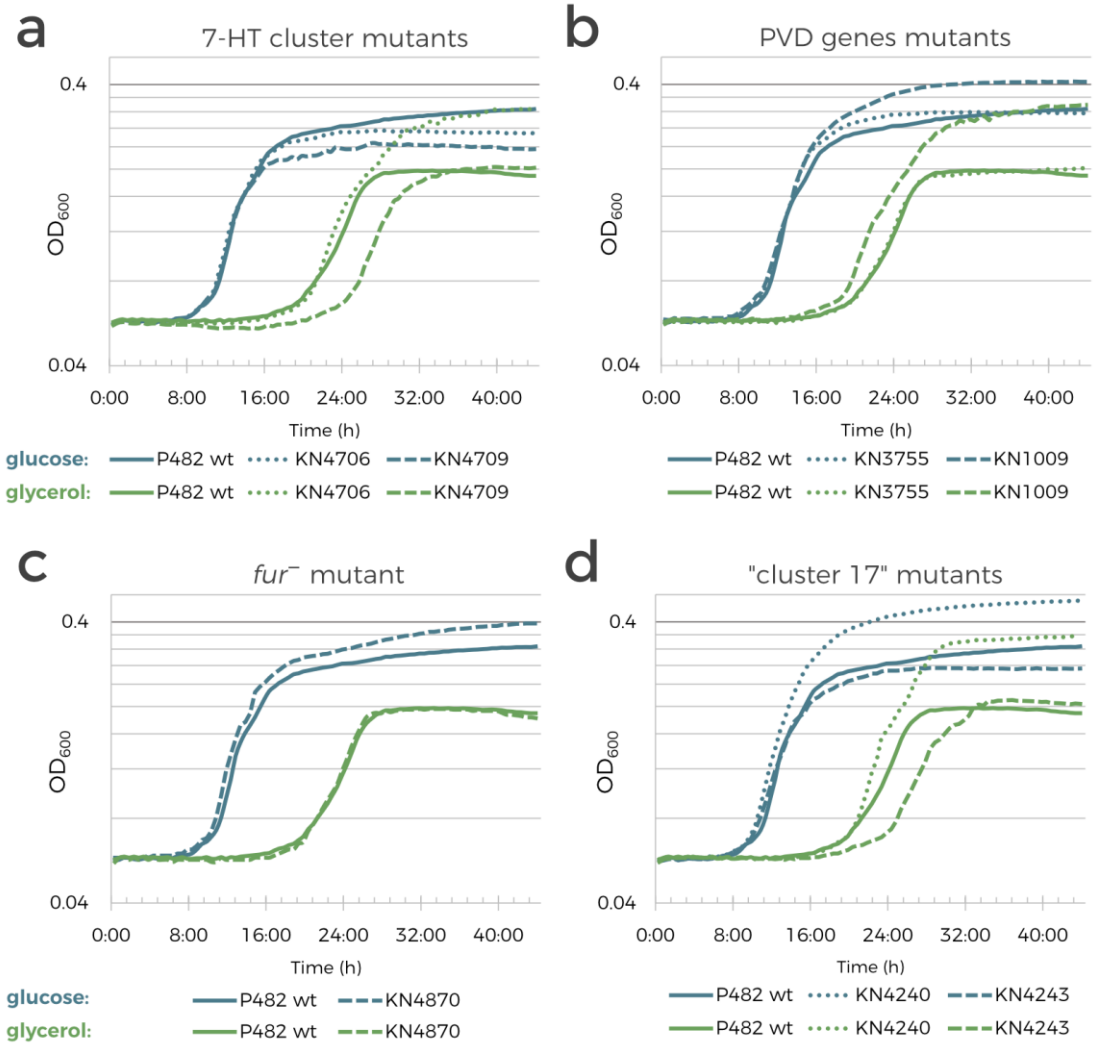


**FIGURE 22. Growth curves of P482 and its selected mutants on glucose and glycerol.** The strains were cultured in M9 with 0.4% glucose or 0.4% glycerol as a carbon source. The $OD_{600}$ values at each time point are the mean values of four biological replicates. The curves obtained are presented in a logarithmic scale.

### 9.3.2. Direct antagonistic activity of P482 depends on carbon source

To examine whether the antibacterial activity of *P. donghuensis* P482 is dependent on the carbon source (glucose or glycerol), a direct antagonism assay was used (8.2). The antagonism was tested towards plant pathogenic bacteria: *D. solani* IFB0102, *P. brasiliense* LMG21371 and *P. syringae* pv. *syringae* Pss762 (FIGURE 12).

The obtained results indicate that P482 inhibits the growth of all three pathogens used. However, the collected data show that carbon source is a significant factor determining the diameter of the pathogen growth inhibition zone caused by P482. Glucose rather than glycerol causes the growth inhibition to be more pronounced (size of the growth inhibition zones: example in SUPPLEMENTARY FIGURE 1). The growth medium composition can affect both the

antibacterial potential of P482 and the growth rate of the pathogen. Therefore, the direct comparison of the zones' diameters is redundant since it does not provide information about how carbon source influences P482 direct antibacterial activity.

Thus, the selected P482 mutant strains were also tested to determine whether the inactivated genes are essential for this antagonistic activity on given carbon sources. The following sections explore the influence of glucose and glycerol of antibacterial activity of the P482 mutants divided into functional groups as described previously.

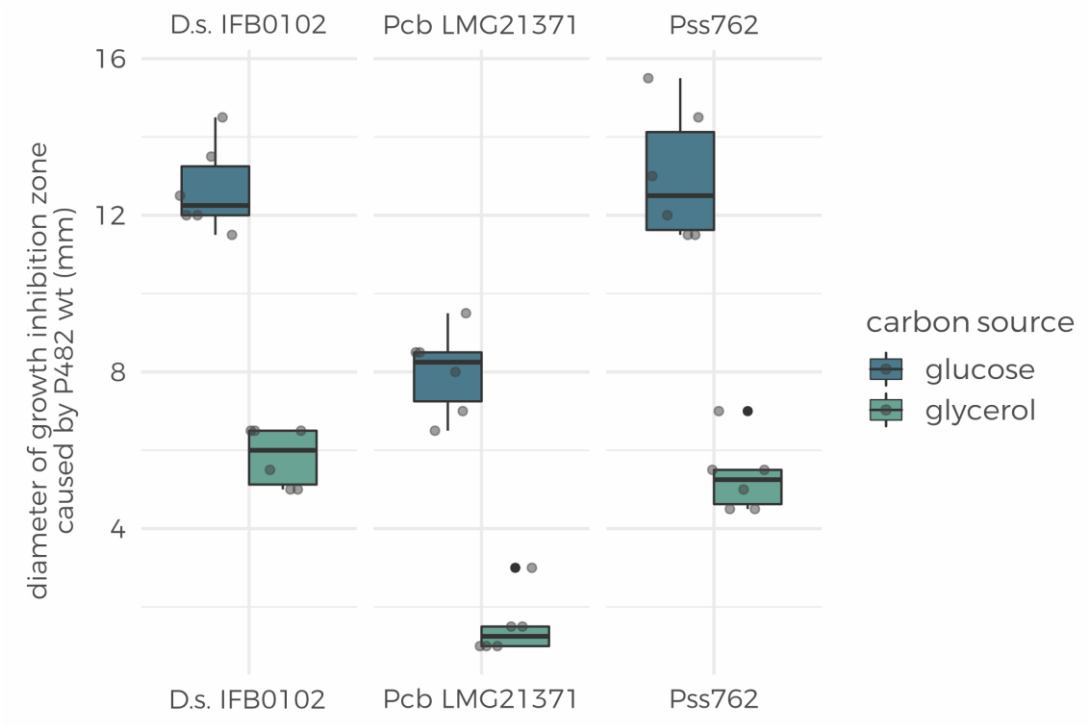


**FIGURE 25. Differences in diameters of the growth inhibition zones caused by P482 wt – carbon source and pathogen dependence.** Boxplot represents the distribution of the diameters of the pathogen (*D. solani* IFB0102, *P. brasiliense* Pcb LMG21371 and *P. syringae pv. syringae* Pss762) growth inhibition zones caused by P482 under minimal media conditions with glucose or glycerol as a sole carbon source. The dark band inside the box represents the median diameter value, the top edge of the box is the upper quartile (Q3) while the bottom edge of the box is the lower quartile (Q1). Q3 and Q1 refer to the 75th percentile and the 25th percentile, respectively, meaning that 75 or 25% of the data were at or below the point. The grey dots (●) represent individual observations. The whiskers represent the maximum and minimal values excluding outliers. Outlier data points are presented with a black dot symbol (●).

#### 9.3.2.1. Carbon source determines the antagonistic activity of the P482 7-HT cluster mutants

The P482 mutants in the 7-HT biosynthesis gene cluster, namely KN4705, KN4706 and KN4709, exhibit antibacterial activity against all tested pathogens on both glucose and glycerol. However, the levels of this activity differ depending on the carbon source and pathogen (**FIGURE 13**).

The most significant differences were recorded for the mutants' antagonism towards *D. solani* IFB0102 (**FIGURE 13a**) Glucose as a sole carbon source in the medium leads to the 7-HT cluster mutants having their IFB0102 growth inhibition capability reduced to approximately 45% of the growth inhibition caused by the wild type P482 strain. On the other hand, when glycerol is the sole carbon source, their activity towards IFB0102 remains unchanged with respect to P482 wt activity under the same conditions.

Similarly, under the glycerol medium conditions, the growth of *P. syringae* pv. *syringae* Pss762 is inhibited by the 7-HT mutants as much as by P482 wt (**FIGURE 13c**). The partial loss of the mutants' activity towards Pss762 is detectable on the glucose medium, where their growth inhibition ability is reduced to half of that of P482 wt.

While the described results are consistent for IFB102 and Pss762, the same experimental setup yielded a different outcome for the third tested pathogen, *Pectobacterium brasiliense* (Pcb) LMG21371 (**FIGURE 13b**). Regardless of the carbon source choice, the mutants exhibited a reduced antagonism against Pcb LMG2137, constituting ca. 40-60% that of P482 wt. Nevertheless, under the minimal media conditions, the choice of carbon source did not significantly affect the levels of inhibition of Pcb LMG21371 growth by the 7-HT cluster mutants.

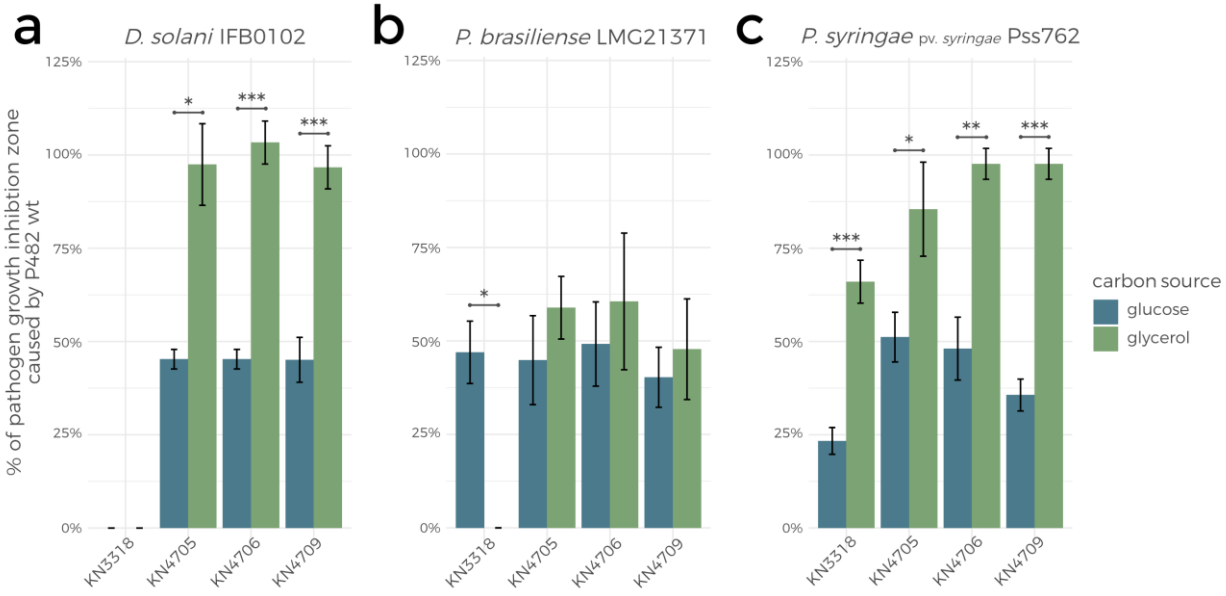


**FIGURE 28. Carbon-source dependency of the direct antibacterial activity of P482 7-HT cluster mutants and P482 *gacA*⁻ mutant.** The growth inhibition of **a**. *Dickeya solani* IFB0102, **b**. *Pectobacterium brasiliense* LMG21371 and **c**. *Pseudomonas syringae* pv. *syringae* Pss762 by *Pseudomonas donghuensis* P482 mutant strains KN3318 (*gacA*⁻), KN4705, KN4706 and KN4709 tested on minimal M9 agar medium with 0.4% glucose or 0.4% glycerol as a single carbon source. The bars represent the percentage of the growth inhibition zone obtained for P482 wt under the same conditions. The assay was performed in triplicates; error bars represent standard deviation. The statistical analysis was performed using Student's T-test, the asterisks indicate the levels of statistical significance of the differences: * - $p < 0.05$; ** - $p < 0.01$; *** - $p < 0.001$.

Taken together, in the case of 7-HT biosynthetic gene cluster mutants, the inactivation of these genes does not impact the overall antimicrobial activity of P482 but only if glycerol is the only carbon source. This observation is however not valid for antagonism towards *P. brasiliense*. Nevertheless, this indicates that the 7-HT gene cluster is not responsible (or only partially responsible) for the P482 antibacterial activity under glycerol minimal medium conditions.

Interestingly, the antagonistic activity of KN3318, a mutant with an inactivating insertion in the *gacA* gene, does not mirror that of 7-HT cluster mutants (**FIGURE 13**). Under the minimal medium conditions, KN3318 shows no antibacterial potential against *D. solani* IFB0102 regardless of the carbon source used. However, it inhibits the growth of Pcb LMG21371 (ca. 50% of P482 wt activity, but only when glucose is the carbon source) and Pss762 (constitutes about 25% and 65% of P482 wt activity on glucose and glycerol, respectively). Gac/Rsm pathway is known to control the biosynthesis of 7-HT but not PVD. Thus, this result suggests that the antibacterial activity of P482 is either based on more than these two metabolites or the Gac/Rsm pathway can, under specific conditions, influence PVD biosynthesis.

#### 9.3.2.2. Genes related to PVD synthesis are pivotal for P482 antibacterial activity on minimal media

The mutants with insertions inactivating PVD biosynthesis-related genes (KN1009 and KN3755) were examined for the carbon source dependency of their antimicrobial activity along the *fur* gene mutant obtained in this study (KN4870). Fur is a negative regulator of the PVD genes, thus, with Fur inactivation, PVD biosynthesis should be largely uninhibited.

The results revealed that the antibacterial activity of KN4870 under minimal media conditions is predominantly unchanged with respect to the activity of P482 wt (**FIGURE 14**). This is consistent with the results obtained using rich media (**9.1.4**) and the premise of the unrestrained PVD production in KN4870 caused by Fur inactivation. However, when *D. solani* IFB0102 was the pathogen and the minimal medium contained glucose as the only carbon source, the growth inhibition zones caused by KN4870 constituted approximately 75% of those caused by P482 wt.

Contrarily to KN4870, the mutants with defective PVD biosynthetic genes revealed the importance of these genes in antibacterial abilities of P482 under minimal media conditions with a single carbon source, glucose or glycerol. The growth inhibition zones caused by KN1009 and KN3755 were typically less than half in size than those caused by the wild type strain – regardless of the pathogen and carbon source (**FIGURE 14**). There were, however, several differences among them. Analogously to the case of 7-HT cluster genes' mutants, the PVD mutants under set conditions act similarly against Pss762 and IFB0102, but differently against Pcb LMG21371. Almost no activity of KN1009 and KN3755 could be detected towards Pcb LMG21371 under the test conditions. Moreover, KN3755 exhibits a slightly more pronounced antagonistic activity

towards Pss762 and IFB0102 when glucose is the carbon source rather than glycerol. This suggests that the gene in locus BV82_1009 is more significant than BV82_3755 for P482 antibacterial potential under these conditions, although both genes are associated with the PVD biosynthesis pathway.

Overall, this part of the results indicates that PVD biosynthesis genes are highly significant for the growth inhibition of bacterial plant pathogens by P482 under minimal medium conditions with glucose or glycerol as a carbon source.

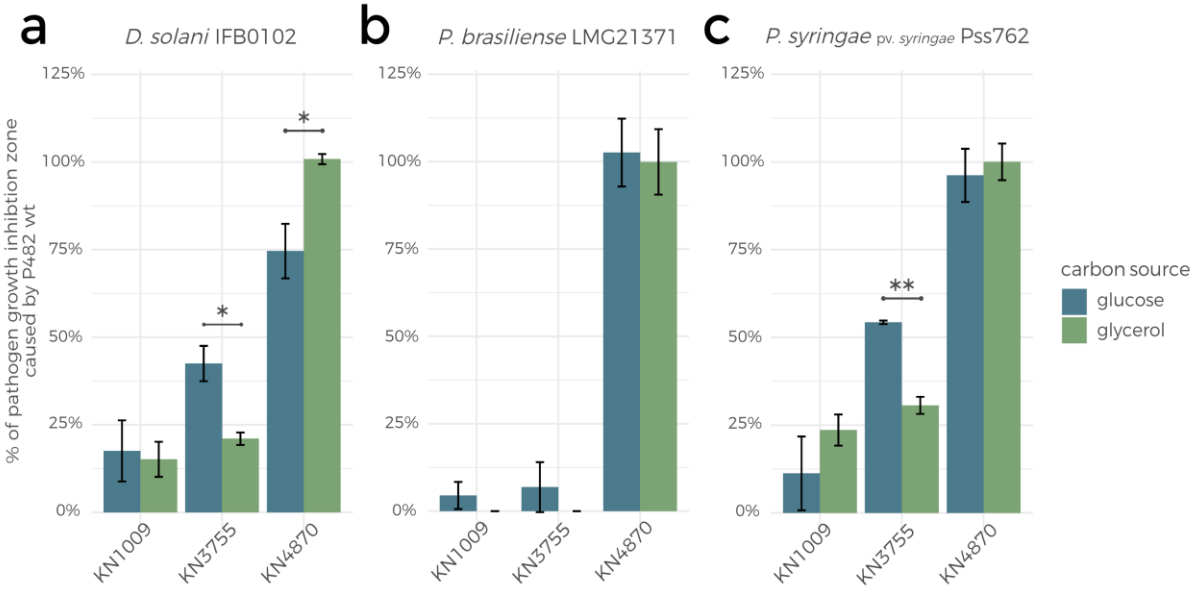


**FIGURE 29. Carbon-source dependency of the direct antibacterial activity of P482 mutants defective in PVD biosynthesis and P482 *fur*⁻ mutant.** The growth inhibition of **a.** *Dickeya solani* IFB0102, **b**. *Pectobacterium brasiliense* LMG21371 and **c**. *Pseudomonas syringae* pv. *syringae* Pss762 by *Pseudomonas donghuensis* P482 mutant strains KN1009, KN3755 and KN4870 (*fur*⁻) tested on minimal M9 agar medium with 0.4% glucose or 0.4% glycerol as a single carbon source. The bars represent the percentage of the growth inhibition zone obtained for P482 wt under the same conditions. The assay was performed in triplicates; error bars represent standard deviation. The statistical analysis was performed using Student's T-test, the asterisks indicate the levels of statistical significance of the differences: * - $p < 0.05$; ** - $p < 0.01$; *** - $p < 0.001$.

### 9.3.2.3. KN4240 and KN4243, the "cluster 17" mutants, reveal distinct phenotypes

The last group of P482 mutants in the analysis of carbon source influence on their antibacterial activity were the strains with insertions inactivating genes from "cluster 17", namely KN4240 and KN4243.

Interestingly, when tested on minimal medium, the KN4240 mutant manifested contrasting impact of carbon source (glucose or glycerol) on its antagonistic activity towards all three pathogens (**FIGURE 15**). When glucose was the only carbon source, the activity of KN4240 remained unchanged with respect to P482 wt. Conversely, when glycerol was the carbon source, KN4240 showed zero or slight activity (ca. 12% of the wild type strain activity) towards all three

tested pathogens. These results indicate that BV82_4240, a gene inactivated in KN4240 mutant, is predominantly responsible for P482 antibacterial activity when glycerol is a sole carbon source.

The other mutant from the "cluster 17" group, KN4243, exhibits a different antimicrobial phenotype when compared to KN4240 (**FIGURE 15**). Its antibacterial activity on minimal medium is low on glucose, between 25-45% of the P482 wt activity recorded. Furthermore, this antimicrobial potential of KN4243 is even lower (towards IFB0102 and Pss762) or entirely lost (towards Pcb LMG21371) on glucose. This pattern resembles the results documented for KN3755, a PVD biosynthesis mutant.

Together the results described in this section provide important information about carbon source importance in the modulation of antibacterial activity of P482. This part of the study suggests that P482 antagonism towards bacterial phytopathogens is highly dependent on genes in three different biosynthetic clusters, while the functioning of these clusters is also affected by the carbon source in the medium. Therefore, the following section, progresses to show how adding iron ions to these environments affects the discussed traits of P482.

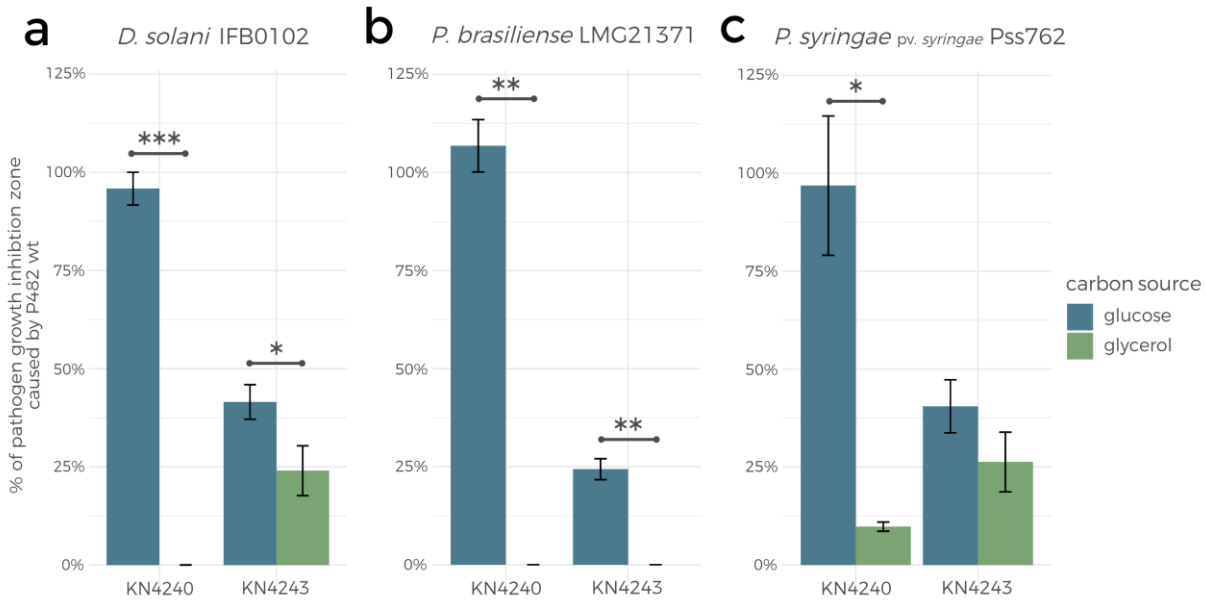


**FIGURE 32. Carbon-source dependency of the direct antibacterial activity of P482 'cluster 17' mutants.** The growth inhibition of **a**. *Dickeya solani* IFB0102, **b**. *Pectobacterium brasiliense* LMG21371 and **c**. *Pseudomonas syringae* pv. *syringae* Pss762 by *Pseudomonas donghuensis* P482 mutant strains KN4240 and KN4243 tested on minimal M9 agar medium with 0.4% glucose or 0.4% glycerol as a single carbon source. The bars represent the percentage of the growth inhibition zone obtained for P482 wt under the same conditions. The assay was performed in triplicates; error bars represent standard deviation. The statistical analysis was performed using Student's T-test, the asterisks indicate the levels of statistical significance of the differences: * - $p < 0.05$; ** - $p < 0.01$; *** - $p < 0.001$.

## 9.4. Iron abundance reduces P482 antibacterial activity

### 9.4.1. The addition of iron diminishes the P482 lag phase

In this part of the study, two types of iron ions, ferrous (Fe(II); 30 μM $FeSO_4$) and ferric (Fe(III); 30 μM $FeCl_3$) iron were added to the M9 minimal medium with either glucose or glycerol as a carbon source. The concentration of iron ions was adjusted in a preliminary study according to a literature research showing the universal working concentration of Fe(II) and Fe(III) to obtain non-toxic, iron-abundant media for pseudomonads ranges from 10 to 100 μM. The studies used in the adjustment included Manninen and Mattila-Sandholm (1994), Meyer and Abdallah (1978) and Neilands (1984). The two types of iron ions were used since they vary in their availability for the bacteria, Fe(II) ions are readily available for the uptake, while the poorly soluble Fe(III) require the aid of iron chelators or siderophores. The aim of this part of the study was to observe how iron supplementation and availability modulate the direct antimicrobial activity of P482.

First, the P482 wild type strain growth curves were obtained to determine how the iron ions influence the bacterial growth (**FIGURE 16**). The curves show that the presence of both ferrous and ferric ions markedly shortens the initial lag phase in P482 wt growth, regardless of the carbon source. However, when glycerol is the only carbon source in the medium, P482 reaches the stationary phase later (~12-hour delay compared to glucose) and displays diauxic-like growth curves. Surprisingly, this growth pattern modification occurs despite no additional carbon source being present in the medium. It is also detected, albeit less pronounced, when P482 is grown on glucose with Fe(III). Nevertheless, this phenomenon remains unexplained and requires further research.

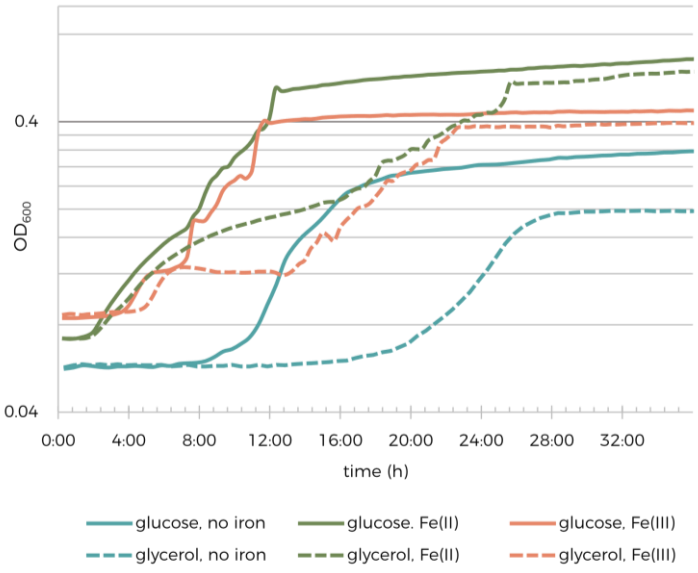


**FIGURE 35. P482 wt growth curves – carbon/iron source dependence.** P482 wt was cultured in M9 with 0.4% glucose or 0.4% glycerol as a sole carbon source with or without iron supplementation (30 μM Fe(II) ($Fe_2SO_4$) or 30 μM Fe(III) ($FeCl_3$)). The $OD_{600}$ values of the cultures at each time point are the mean values of four biological replicates. The curves obtained are presented in a logarithmic scale.

The P482 mutants were also subjected to the growth curve analysis under the same conditions as P482 wt. The comparisons of the P482 wt growth curves with the mutants revealing atypical growth patterns (>2 h shifts in entering any growth phase) are presented in **FIGURE 17**. For clarity of results visualisation, the growth curves of the remaining mutants are not shown as they do not differ from the curve obtained for P482 wt. In the case of KN4243 considerable differences were detected under all iron-supplemented conditions. KN3318 (*gacA*$^-$) was observed to have different growth patterns than P482 wt under all the tested conditions apart from the minimal medium with glucose and Fe(III). Moreover, the addition of iron diminishes the effect noticeable under single carbon source conditions without iron supplementation, that is the earlier start of the log phase in KN3318 that P482 wt. The results presented in **FIGURE 17d** revealed that glycerol and Fe(III) cause the highest number of mutants to show abnormal growth, however it is unclear what causes the delay of their log phase onset.

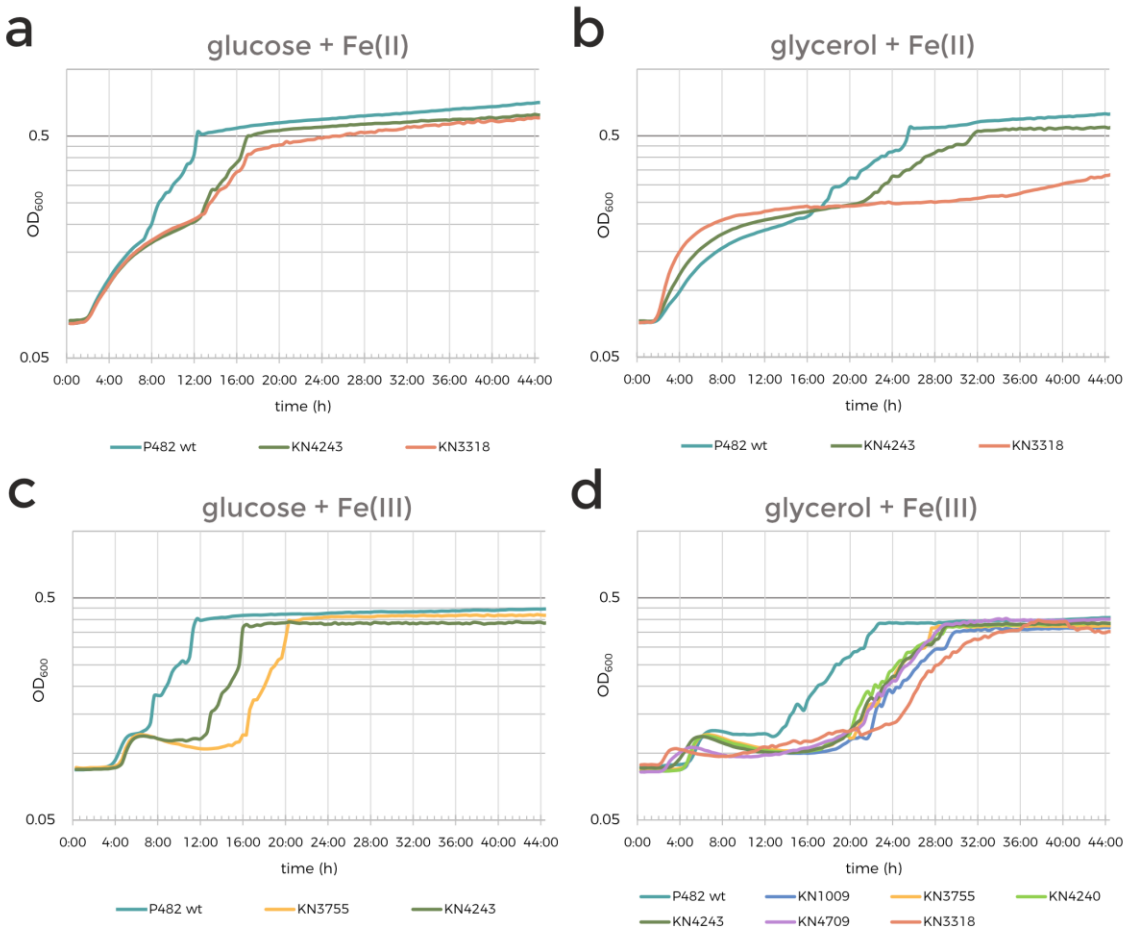


**FIGURE 38. Growth curve alterations in P482 mutants– carbon/iron source dependence.** The charts show the comparisons of growth curves between P482 wt and its mutants for which abnormal growth curves were observed under the given conditions. P482 wt and its mutants were cultured for 44 hours in:
**a.** M9 medium with 0.4% glucose and 30 μM Fe(II) ($Fe_2SO_4$);
**b.** M9 medium with 0.4% glycerol and 30 μM Fe(II) ($Fe_2SO_4$);
**c.** M9 medium with 0.4% glucose and 30 μM Fe(III) ($FeCl_3$);
**d.** M9 medium with 0.4% glycerol and 30 μM Fe(III) ($FeCl_3$).
The $OD_{600}$ values of the cultures at each time point are the mean values of four biological replicates. The curves obtained are presented in a logarithmic scale.

Further experiments on P482 wt that required the cells to reach a specific growth phase were adjusted according to the described growth curves results in **FIGURE 16**. However, analogously to a previous report concerning P482 mutant KN3318 in section **9.2.1**, the growth durations could not be adjusted for each mutant due to the sustainability and technical issues concerning the assay execution.

### 9.4.2. Direct antagonistic activity of P482 is dependent on the iron source

The iron source-dependent differences in the antibacterial potential of P482 were measured as described for the previous experiments against *D. solani* IFB0102, *P. brasiliense* Pcb LMG21371 and *P. syringae* pv. *syringae* Pss762. The test (**8.2**) was performed using M9-agar medium with glucose or glycerol as a single carbon source with the iron supplementation of the medium with either 30 μM Fe(II) ($FeSO_4$) or 30 μM Fe(III) ($FeCl_3$). The results obtained in the experiment without iron supplementation were added to the comparison. Thus, the effect of six carbon source-iron source combinations on P482 antibacterial activity was tested overall.

The wild type strain's antagonistic activity was analysed prior to assessing the consequences of the tested environmental conditions for the P482 mutants. **FIGURE 18** shows the comparison of the diameters of pathogens' growth inhibition zones caused by P482 wt. Glucose as a carbon source generally promotes the inhibition of the pathogens' growth, however when Fe(II) ions are present in the glucose medium, the antagonistic activity of P482 is considerably weaker towards IFB0102 and Pss672. This may be caused by the fact that the primary source of P482 antibacterial activity are siderophores, the production of which is repressed by the readily available iron ions in the environment. However, the other explanation of the smaller growth inhibition zones is the intensified growth of pathogens once they are not depleted of iron. Therefore, the presented data must be interpreted carefully.

With glycerol as the only carbon source, iron (ferric and ferrous ions) supplementation does not cause a substantial change in the antibacterial activity (**FIGURE 18**). Nonetheless, there is a noticeable trend in which Fe(III) addition to the glycerol medium causes the partial loss of antibacterial potential in P482. Moreover, it is crucial to note that the *P. brasiliense* Pcb LMG21371 growth inhibition zones caused by P482 when glycerol is a sole carbon source are particularly small (less than 4 mm in diameter). Due to this fact, the diameter readings were problematic and thus, the results of the tests performed under these conditions on Pcb LMG21371 yield sizable standard deviation values and shall be interpreted with caution.

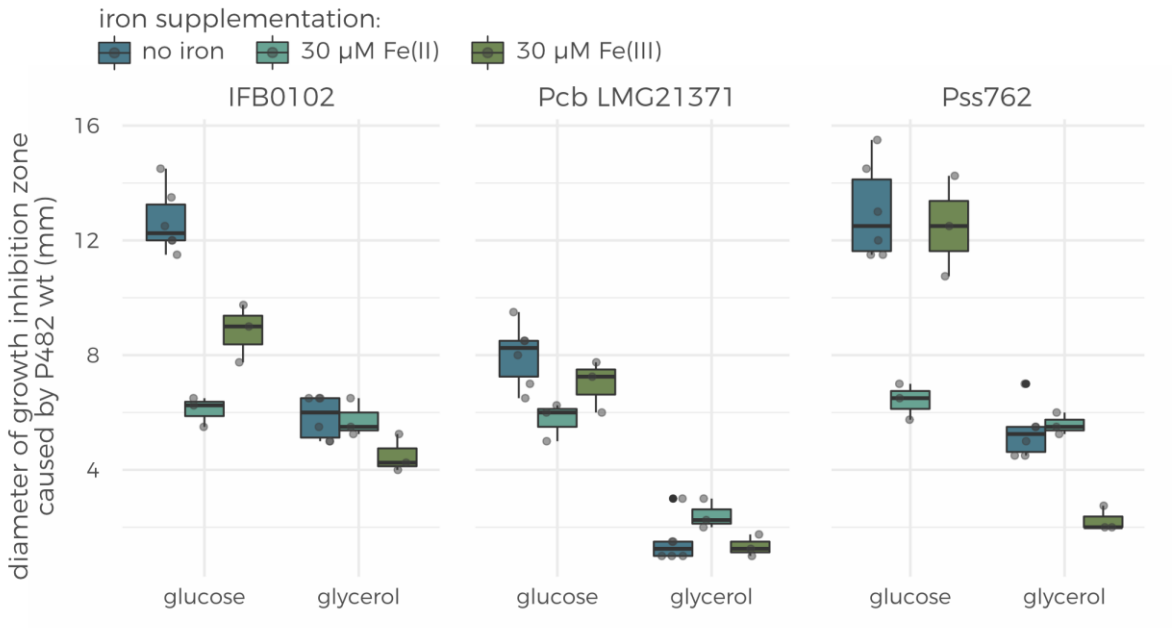


**FIGURE 41. Differences in diameters of the growth inhibition zones caused by P482 wt – carbon/iron source and pathogen dependence.** Boxplot represents the distribution of the diameters of the pathogen (*D. solani* IFB0102, *P. brasiliense* Pcb LMG21371 and *P. syringae pv. syringae* Pss762) growth inhibition zones caused by P482 under minimal media conditions with glucose or glycerol as a sole carbon source with or without iron supplementation (30 µM Fe(II) ($Fe_2SO_4$) or 30 µM Fe(III) ($FeCl_3$)). The dark band inside the box represents the median diameter value, the top edge of the box is the upper quartile (Q3) while the bottom edge of the box is the lower quartile (Q1). Q3 and Q1 refer to the 75th percentile and the 25th percentile, respectively, meaning that 75 or 25% of the data were at or below the point. The grey dots (●) represent individual observations. The whiskers represent the maximum and minimal values excluding outliers. Outlier data points are presented with a black dot symbol (●).

#### 9.4.2.1. Iron ions varied effects on 7-HT cluster mutants

The P482 mutants with inactivation of genes from the 7-HT cluster (KN4705, KN4706, KN4709) and the *gacA*⁻ mutant (KN3318) were utilised to determine how P482 antimicrobial activity is affected by iron supplementation when it is not dependent on the 7-HT biosynthesis genes and Gac/Rsm signalling pathway. The results were compared to those obtained under similar minimal medium conditions but without iron supplementation (**FIGURE 19**).

When glucose was the only carbon source in the medium, iron supplementation did not significantly influence the antibacterial activity of the 7-HT cluster mutants. However, when glycerol was used as the carbon source, the changes in the mutants' antagonistic potential against the tested pathogens were more pronounced. This effect was particularly apparent towards Pss762 when Fe(III) was supplemented in the medium (**FIGURE 19c**). Surprisingly, in this case, the 7-HT cluster mutants exhibit antibacterial activity twice as high as the wild type strain. A possible explanation for this might be a Fe(III)-dependent stimulation of another pathway in the mutants leading to their more robust antimicrobial capability. This effect might be also dependent on the biology of the pathogen since it was only observed towards Pss762.

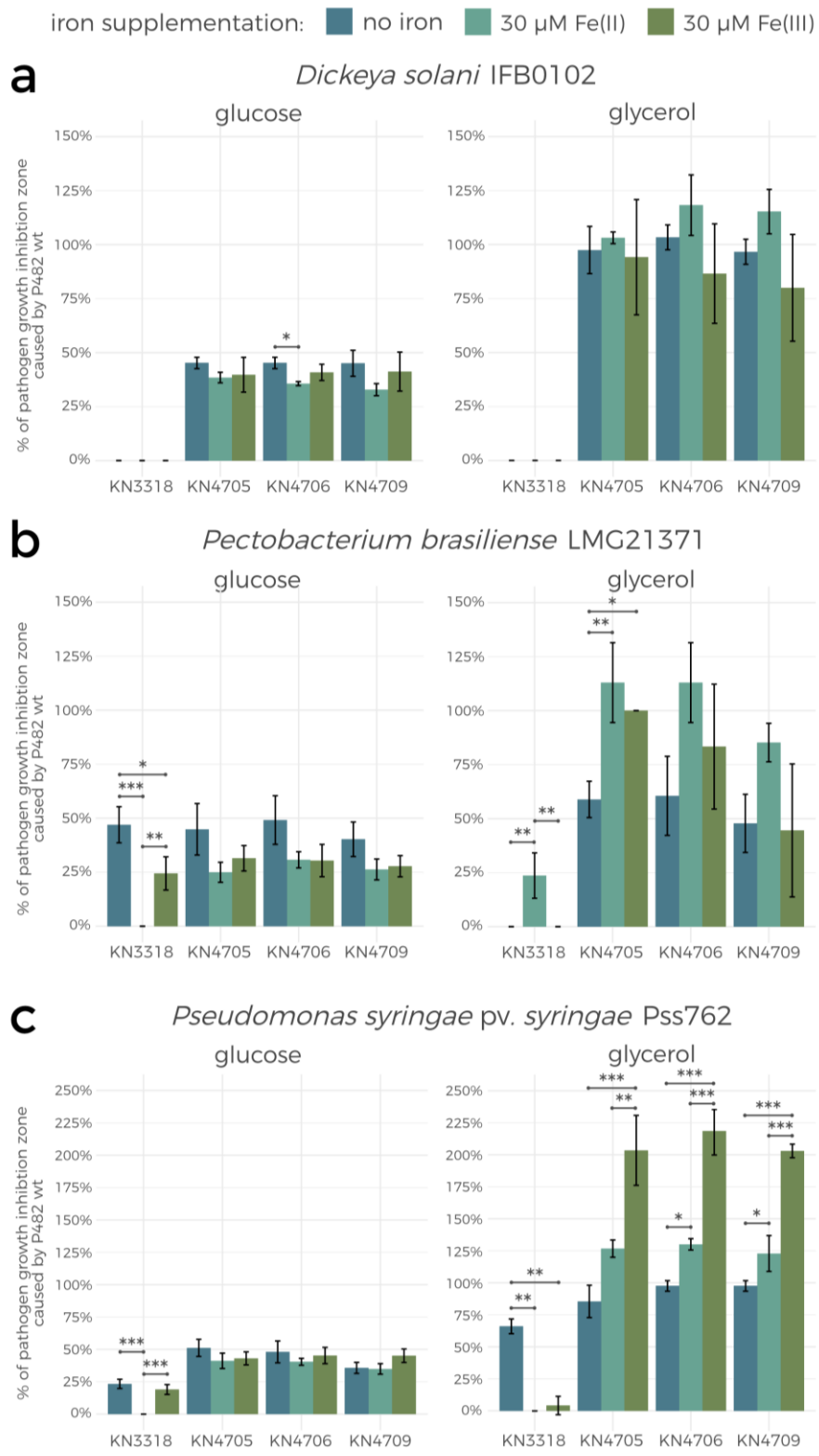


**FIGURE 44. Iron source-dependency of the direct antibacterial activity of P482 7-HT cluster mutants and *gacA*⁻ mutant.** The growth inhibition of **a**. *D. solani* IFB0102, **b**. *P. brasiliense* LMG21371 and **c**. *P. syringae* pv. *syringae* Pss762 by *P. donghuensis* P482 mutant strains KN3318, KN4705, KN4706 and KN4709 tested on minimal M9 agar medium with 0.4% glucose or 0.4% glycerol as a carbon source. The iron supplementation comprised 30 μM Fe(II) ($Fe_2SO_4$) or 30 μM Fe(III) ($FeCl_3$). The bars represent the percentage of the growth inhibition zone obtained for P482 wt under the same conditions. The assay was performed in triplicates; error bars represent standard deviation. The statistical analysis was performed using one-way ANOVA test with Tukey's post-hoc analysis, the asterisks indicate the levels of statistical significance of the differences: * - $p < 0.05$; ** - $p < 0.01$; *** - $p < 0.001$.

Furthermore, the *gacA*⁻ mutant (KN3318) displays no activity towards *D. solani* IFB0102 under given conditions regardless of the carbon/iron source (**FIGURE 19a**). The outcome is different in the case of Pss762, the loss of activity in KN3318 is partial unless the medium is supplemented with Fe(II) (**FIGURE 19c**). Ferrous ions in the environment, rather than ferric ones, completely abolished the KN3318 inhibitory effect on Pss762. The analogous tests on Pcb LMG21371 yielded even more remarkable results for KN3318 (**FIGURE 19b**). They revealed zero antibacterial activity of this mutant towards Pcb LMG21371 under glucose/Fe(II) conditions whereas the same Fe(II) ions stimulated this activity if glycerol was the carbon source. Additionally, the Fe(III) supplementation diminished the KN3318 mutant's activity towards Pss762 on glycerol, but does not affect it on glucose. This is different in case of other tested pathogens, which suggests that the iron-dependency of GacA-deficient P482 is highly influenced by the pathogen itself. These results, however, cannot be conclusively explained, as the inactivation of the *gacA* gene disrupts the Gac/Rsm global regulatory pathway and causes innumerable changes in P482 metabolism.

Together, these findings reveal that the iron influence on the antagonistic activity of P482 7-HT cluster mutants is highly context-dependent and strongly affected by other factors like carbon source and the strain it is directed towards.

#### 9.4.2.2. The antagonism of P482 PVD biosynthesis mutants is only partially restored by iron supplementation

The availability of iron ions in the environment has a suppressive effect on pyoverdine [PVD] biosynthesis, which is a process partially responsible for P482 antibacterial activity. Under iron-depleted conditions, PVD production is intensified, and this iron chelator constitutes a sizable portion of the antagonistic potential of P482. Thus, the P482 mutants with inactivated genes in PVD biosynthesis revealed a substantial loss of this activity under iron-depleted conditions (**9.3.2.2**). Therefore, the presence of iron ions should partially restore their antibacterial capabilities with respect to P482 wt tested under the same conditions.

The results obtained confirmed this hypothesis only partially. The PVD mutants (KN1009 and KN3755) exhibit different phenotypes and their activity varies depending on the carbon source and the iron sources, and the pathogen (**FIGURE 20**). Nevertheless, the most consistent results were recorded for the KN3755 mutant. When cultured with glucose, the addition of readily available Fe(II) caused the antibacterial activity of KN3755 to increase in relation to the wild type strain's activity. This trend was observable independently of the pathogen. However, no such tendency can be identified for KN1009.

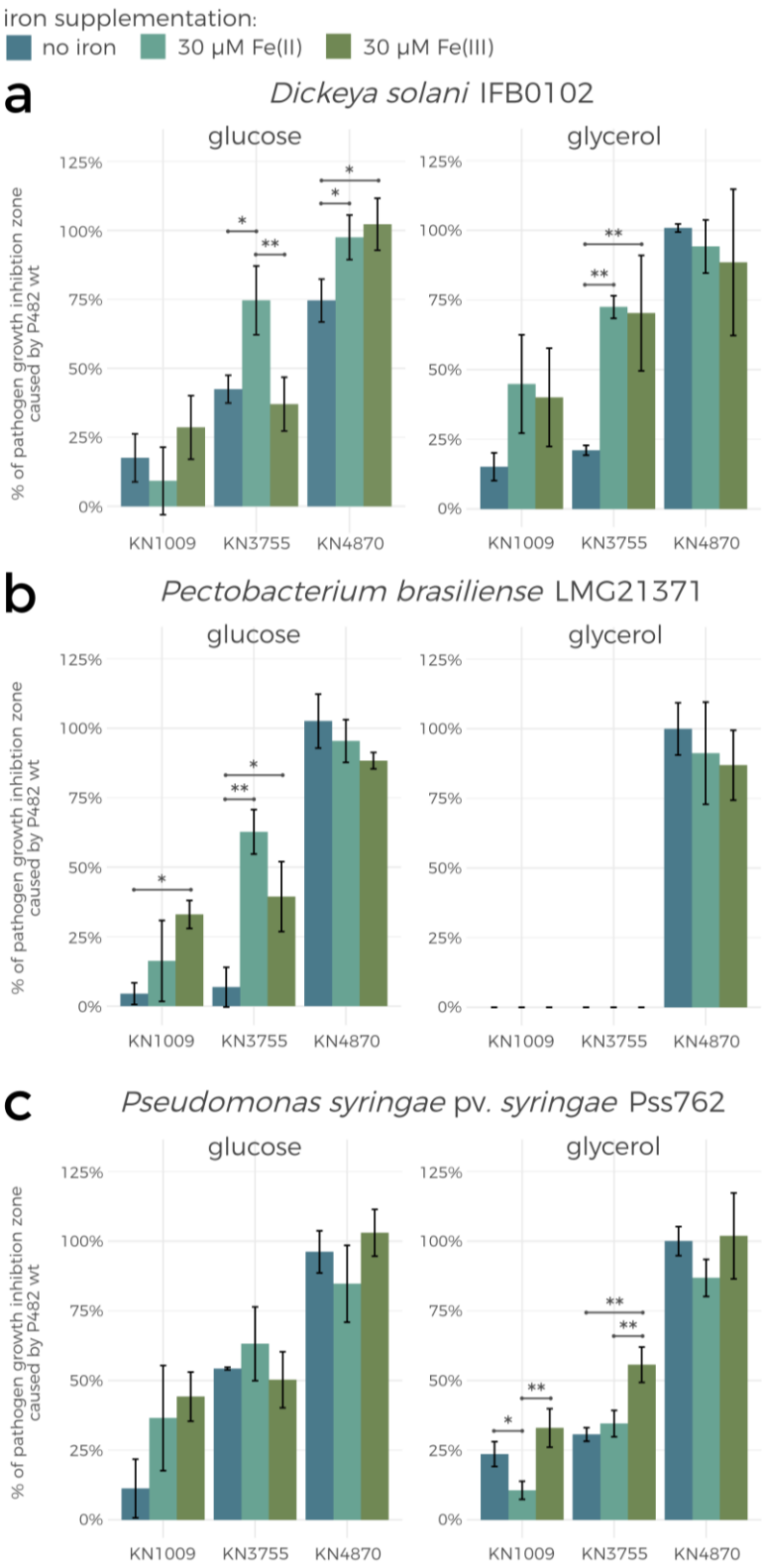


**FIGURE 47. Iron source-dependency of the direct antibacterial activity of P482 PVD genes mutants and *fur*⁻ mutant.** The growth inhibition of **a**. *D. solani* IFB0102, **b**. *P. brasiliense* LMG21371 and **c**. *P. syringae* pv. *syringae* Pss762 by *P. donghuensis* P482 mutant strains KN1009, KN3755 and KN4870 tested on minimal M9 agar medium with 0.4% glucose or 0.4% glycerol as a carbon source. The iron supplementation comprised 30 µM Fe(II) ($Fe_2SO_4$) or 30 µM Fe(III) ($FeCl_3$). The bars represent the percentage of the growth inhibition zone obtained for P482 wt under the same conditions. The assay was performed in triplicates; error bars represent standard deviation. The statistical analysis was performed using one-way ANOVA test with Tukey's post-hoc analysis, the asterisks indicate the levels of statistical significance of the differences: * - $p < 0.05$; ** - $p < 0.01$; *** - $p < 0.001$.

In the case of iron supplementation, when glycerol is the carbon source, the documented observations are less regular. Markedly, this experiment involves a complex system of two living organisms, a P482 mutant and a pathogen, and each of them reacts to the environmental stimuli and each other's secretome. The antagonism of KN1009 and KN3755 towards the three tested phytopathogens is differently influenced by Fe(II) and Fe(III). It is worth noting that both of the mutants do not exhibit any antibacterial activity towards Pcb LMG21371 on glycerol and it does not change with the iron supplementation (**FIGURE 20b**). On the other hand, the addition of Fe(III) enhances the inhibitory activity of KN1009 and KN3755 towards IFB0102 and Pss762 (**FIGURE 20ac**), although the levels of this change vary and not all of the deviations yield statistical significance.

KN4870, the P482 mutant with inactivation in gene encoding ferric uptake regulator protein (Fur), was also tested in the experiment alongside the PVD mutants. The only significant difference in its antimicrobial activity was a slight increase in the antibacterial activity against *D. solani* IFB0102 with the addition of iron ions to the glucose medium (**FIGURE 20a**). Nevertheless, the results indicate that, under the tested conditions, the antagonistic potential of P482 is not dependent on the *fur* gene. These results are not surprising since Fur protein typically inhibits the PVD biosynthesis when iron is available in the environment. Under the iron-deficient conditions, Fur does not block PVD biosynthesis, so its production is unrestricted in the wild type and in the *fur*$^-$ mutant. This should provide similar outcomes when it comes to the antibacterial activity of both strains. On the other hand, under the iron-abundant conditions, Fur stops PVD production in the wild type. Therefore, in this situation, the antimicrobial activity of P482 is not as highly dependent on PVD. In addition, the overproduction of PVD in the *fur*$^-$ mutant should not be of high significance to the antagonistic profile of P482 since the access to readily available iron makes the mutant versus pathogen competition for iron less relevant.

Overall, these findings demonstrate that the PVD-dependent P482 antagonism towards the tested bacterial plant pathogens is highly susceptible to nutritional conditions. Furthermore, the presence of different strains of pathogens and iron ions complicates the situation even further, what shows the importance of external conditions in any case of antibacterial activity of P482 and its potential application. There is, however, no consequence of nutritional changes in the behaviour of the P482 *fur*$^-$ mutant, which suggests that Fur protein itself is not engaged in the P482 antimicrobial activity under the tested conditions.

#### 9.4.2.3. The antibacterial activity of "cluster 17" mutants is only marginally dependent on the iron ions

The last group of mutants tested in this part of the study were the P482 mutants with inactivated genes in "cluster 17" (KN4240, KN4243). Although the genes (loci: BV82_4240 and

BV82_4243) represent one potential biosynthetic cluster, they belong to different operons. The implications of this fact are apparent in how the inactivation of these genes affects the antimicrobial activity of P482 and its dependence on carbon/iron sources.

The KN4240 mutant was not strongly affected by iron ions in terms of its antibacterial activity (**FIGURE 21**). The only measurable tendency was a partial loss of activity of this mutant when the glucose medium is supplemented with Fe(II). This decrease occurs regardless of the pathogen tested and it does not apply to the conditions with glycerol as a carbon source since KN4240 exhibits no or almost no activity under these conditions. A gain of KN4240 antagonistic potential was observed on the glycerol medium when supplemented with Fe(II), however it is pathogen-dependent and occurs only towards Pcb LMG21371.

The second mutant from the "cluster 17" group, KN4243 does not match the performance of KN4240 in its antagonism under minimal media conditions (**FIGURE 21**). Firstly, its antibacterial activity on glucose is much lower than that of both KN4240 and P482 wt and it tends to decrease even more with iron supplementation, with the most significant differences observed in its antagonism towards *D. solani* IFB0102. Secondly, on the glycerol medium, KN4243 does not inhibit the growth of Pcb LMG21371, but marginally (up to 25% of the wild type strain activity) inhibits the growth of Pss762, regardless of the iron ions presence. This mutant also slightly inhibits the growth of IFB0102, but only when the glycerol medium is supplemented with neither Fe(II) nor Fe(III) ions.

Overall, the antagonism of KN4240 and KN4243 shows only slight dependence on the abundance of iron in the environment. The antimicrobial activity results obtained for these P482 mutants confirm the previous conclusion that the antibacterial activity of KN4240 and KN4243 is diversely modulated by the variables of the experiment. Therefore, these two genes belonging to different operons might be considered to perform different roles in the antagonistic phenotype of P482.

Taken together, in this chapter, the influence of two iron ion types on the antibacterial activity P482 and its relevant mutants was explored. The impact of iron was combined with the changes determined by two other factors, namely, the pathogen and the carbon source. The results included in this section strongly vary between mutants and the factors tested. This illustrates the complexity of the P482 antagonism towards bacterial plant pathogens. Thus, further experiments such as metabolomic analyses and gene expression investigation were performed in this study and their outcomes are presented in the following sections.

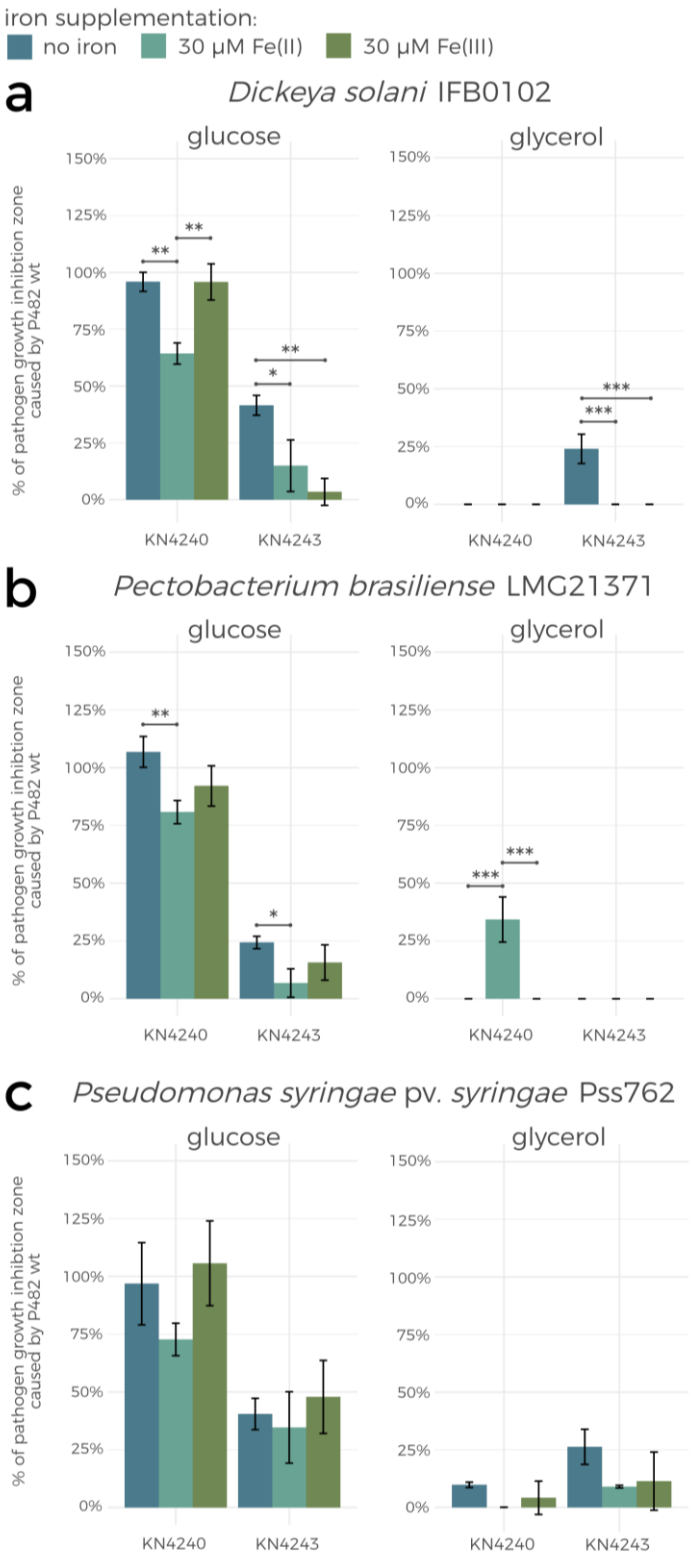


**FIGURE 50. Iron source-dependency of the direct antibacterial activity of P482 "cluster 17" mutants.** The growth inhibition of **a.** *D. solani* IFB0102, **b.** *P. brasiliense* LMG21371 and **c.** *P. syringae* pv. *syringae* Pss762 by *P. donghuensis* P482 mutant strains KN4240 and KN4243 tested on minimal M9 agar medium with 0.4% glucose or 0.4% glycerol as a carbon source. The iron supplementation comprised 30 µM Fe(II) ($Fe_2SO_4$) or 30 µM Fe(III) ($FeCl_3$). The bars represent the percentage of the growth inhibition zone obtained for P482 wt under the same conditions. The assay was performed in triplicates; error bars represent standard deviation. The statistical analysis was performed using one-way ANOVA test with Tukey's post-hoc analysis, the asterisks indicate the levels of statistical significance of the differences: * - $p < 0.05$; ** - $p < 0.01$; *** - $p < 0.001$.

## 9.5. Nutritional dependencies of P482 secondary metabolism

The analyses of secondary metabolite profiles of P482 and mutants were performed to observe the differences between them under rich media (LB, 0.1 TSB) and minimal media conditions with either glucose or glycerol as a carbon source.

### 9.5.1. UV-Vis spectra of post-culture supernatants reveal metabolic differences between mutants

The differences observed between the effects of glucose and glycerol on antimicrobial activity of P482 and its mutants were substantial. Therefore, UV-Vis spectrophotometry was employed to preliminarily determine the production of antimicrobials. Two potentially antibacterial compounds can be detected with this method in *P. donghuensis* post-culture supernatants or filtrates: 7-HT and PVD. The measurements were carried out identically to those described in section **9.1.3**.

The UV-Vis spectra in the wavelength range 300-500 nm were obtained for supernatants from strains cultured in a rich medium LB (Lysogeny broth, 44 h of culture) and minimal medium M9 with 0.4% glucose or 0.4% glycerol as the sole carbon source (96 h of culture for both variants of the medium) (**FIGURE 22**). The P482 culture duration in M9 medium variants was prolonged with respect to the LB medium culture duration due to the expected lower metabolic activity of P482 in minimal media. The incubation time was therefore adjusted with preliminary experiments which showed that no compounds are detected in the M9 culture supernatants even after 72 hours post-inoculation.

The spectra obtained in the study differ between P482 wt and the mutants (**FIGURE 22**). The growth media are an important factor influencing the appearance of the absorption peaks of the metabolites (the expected peak wavelengths were 330 nm and 392 nm for 7-HT; 405 nm for PVD). The expected spectra were obtained only for P482 wt and the KN4870, KN1009, KN3755 and KN4240 mutants under the rich growth medium conditions (LB, green line on the chart). The LB spectra for P482 wt, KN4870 and KN4240 contain three peaks, at wavelengths 326 nm and 387 nm (a slightly shifted spectrum of 7-HT), and at 399 nm (slightly shifted peak of PVD). The second peak for 7-HT and the PVD peak are superimposed and non-distinguishable under the conditions applied. No distinct PVD peak is present in the KN1009 and KN3755 LB spectra, which agrees with the fact that these mutants are defective in PVD biosynthesis. The remaining mutants (KN3318, KN4705, KN4706, KN4709, KN4243) do not produce/secrete any detectable levels of 7-HT and PVD when cultured in LB medium.

The outcome of the spectrophotometry is different in the case of the minimal medium used for the culture P482 wt and mutants (**FIGURE 22**). No peak at 330 nm (nor 327 nm) was observed for the supernatants obtained from minimal media cultures regardless of the carbon source. Thus,

no 7-HT biosynthesis/secretion was detected in the minimal media. However, for P482 wt and all the mutants except for KN4243, KN1009 and KN3755, there are two main peaks present in the spectra. One of the peaks matches the PVD peak (at ca. 400 nm). The other peak, at 387 nm, could potentially match the second peak for 7-HT. Nevertheless, the lack of the first 7-HT peak in spectra of supernatants from minimal media cultures leads to the conclusion that the 387 nm peak detected is another compound synthesised by P482 under these conditions.

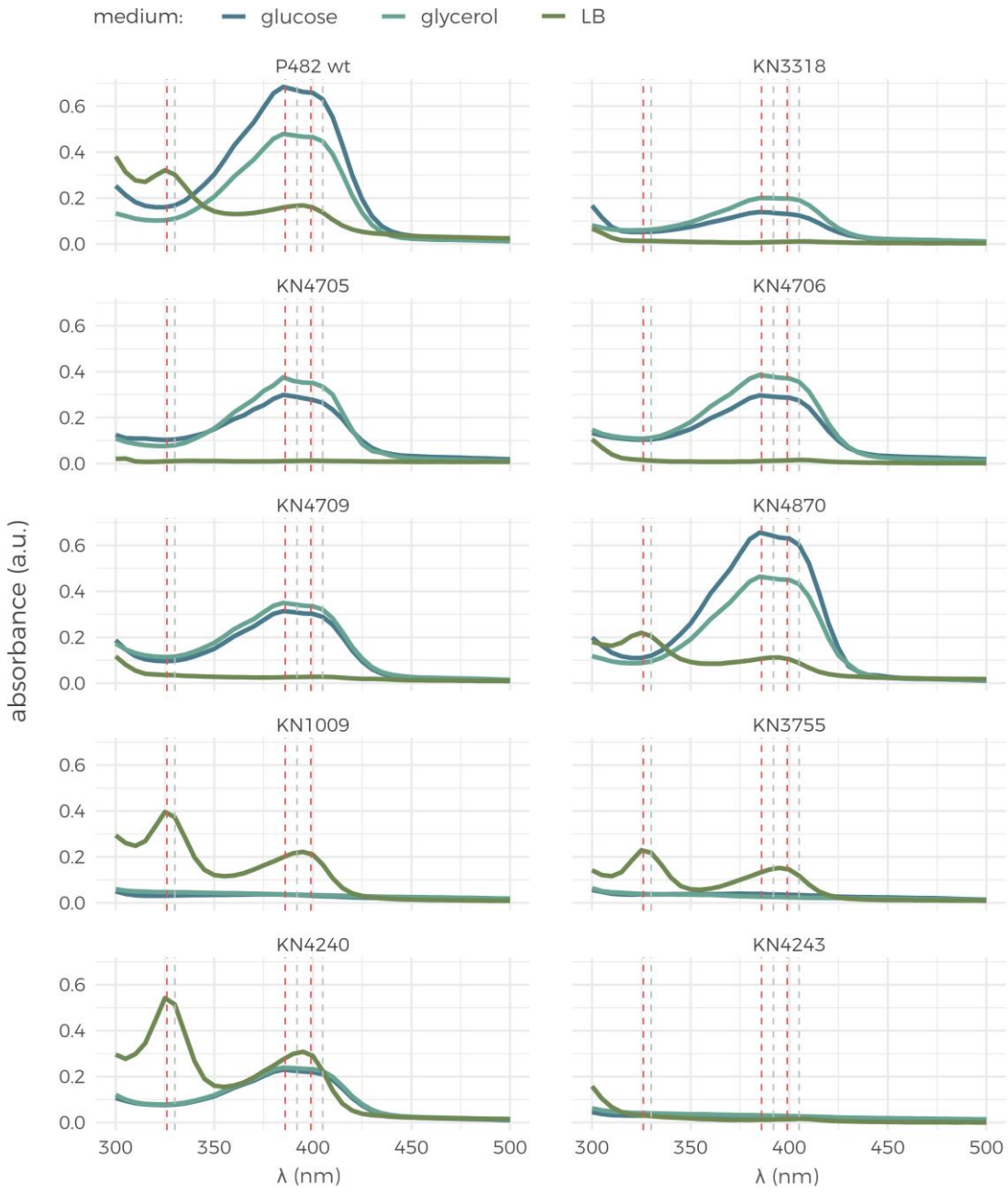


**FIGURE 53. UV-Vis absorption spectra of post-culture supernatants of P482 wt and its mutants – growth medium influence.** The samples measured were the given strain's post-culture supernatants, the colour of the line indicates the growth conditions: **glucose (blue)** – M9 minimal medium + 0.4% glucose, **glycerol (teal)** – M9 minimal medium + 0.4% glycerol, **LB (green)** – Lysogeny broth. The spectra were recorded in the wavelength range 300-500 nm. The dashed vertical lines indicate the peak absorption wavelengths for the iron chelators typical for *P. donghuensis*: 7-HT (obtained (red): 326 nm and 387 nm, expected (grey): 330 nm and 392 nm) and PVD (obtained (red): 399 nm, expected (grey): 405 nm).

Moreover, the mutants KN1009, KN3755 and KN4243 cultured in minimal media do not produce/secrete any compound that would be detectable by UV-Vis spectrophotometry in the given wavelength range. The lack of PVD peak is expected in KN1009 and KN3755 because these strains were obtained by targeted mutagenesis at the PVD biosynthesis loci. However, the KN4243 is a "cluster 17" mutant with a yet unexplained partial loss of antimicrobial activity. The UV-Vis spectra for this mutant show lack of both 7-HT and PVD biosynthesis/secretion under all tested conditions. Therefore, it suggests that the absence of these compounds is responsible for the antibacterial activity decrease in KN4243.

Overall, the 7-HT and PVD production or secretion seem to be linked in the 7-HT mutants of P482. Moreover, the production of 7-HT by P482 was only detected in rich medium. This suggests that 7-HT is not the main compound responsible for the antibacterial activity of P482 under minimal media conditions.

### 9.5.2. Metabolomic analyses of organic extracts from P482 cultures

The metabolomic analyses were performed using EtOAc extracts obtained from the P482 and its mutants post-culture supernatants. The extracts were subjected to the preliminary TLC separation (**8.3.3**) to visualise the polarity of main compounds in the extracts to select the most suitable HPLC program. The best separation of the compounds present in all the extracts was obtained in the RP-TLC setup, and, as a result, reverse phase was selected for the HPLC assay. The 0.1 TSB culture extracts were rich in various metabolites (more than 20 compounds) detected on TLC plate with the use of UV light, while in the minimal media culture extracts only max. five compounds were detected. Subsequently, the RP-HPLC-ESI-qTOF (LC-MS) analyses were conducted (**8.3.4**). The data obtained in the study were subjected to statistical analyses. The LC-MS spectra were also examined using the available databases of bacterial metabolites and other organic compounds, and searched for the presence of m/z expected for 7-HT.

Only a limited number of samples could be included in the LC-MS analyses. Therefore, only the effect of carbon source in minimal medium on P482 wt metabolome, and the effects of mutations in 7-HT cluster and "cluster 17" in P482 grown in the rich medium were explored.

#### 9.5.2.1. LC-MS analyses support the lack of 7-HT biosynthesis by P482 in minimal media

In order to determine the influence of the studied carbon sources on P482 metabolome, the metabolites' extracts were obtained from the 96-hour cultures of P482 wt in three growth media: 0.1 TSB (undefined, rich medium), M9 (minimal medium) + 0.4% glucose and M9 + 0.4% glycerol. The 0.1 TSB medium was used in this experiment in accordance with the studies by A. Ossowicki, PhD (LPM, unpublished) which revealed that extracts from P482 grown in 0.1 TSB have the highest antimicrobial potential out of the tested media. The extracts were tested for their

antibacterial activity in a qualitative disk-diffusion assay, the results mirrored those obtained in the previous study and described in the introduction section of this thesis (**5.2.2, FIGURE 2**). The LC-MS analysis of the extracts shows the growth media influence on P482 metabolome even without the mass spectra analysis. The HPLC chromatograms look differently (in amount and retention time of the peaks) depending on whether P482 was cultured in a rich, undefined 0.1 TSB medium or M9 minimal medium, whereas the carbon source selection in M9 medium shows a smaller impact on the overall P482 metabolome (**FIGURE 23**)

The LC-MS data obtained from the tested samples were further subjected to statistical analysis (**FIGURE 24**). The hierarchically clustered heatmap shows the results of the ANOVA analysis revealing the growth medium-dependent $\log_2$ fold change [FC] in the normalised concentrations of the compounds detected in the samples (**FIGURE 24a**). The heatmap visualises the striking differences between the contents of the tested extracts. Overall, 205 compounds were detected in the 0.1 TSB-cultured P482 extracts samples that were detected in the minimal media samples. Furthermore, 22 and 30 unique compounds were detected in the glycerol and glucose culture extracts, respectively. The principal component analysis [PCA] additionally confirms the statistical differences between the overall metabolite profiles of the samples (**FIGURE 24b**). The first component (x-axis, 91.51%) distinguishes the effect of the rich medium from the effect of minimal media on the metabolome of P482. The second component (y-axis, 7.16%) further separates the minimal media extracts by the difference in the P482 metabolome caused by the carbon source (glucose/glycerol). The variation between the biological replicates on the PCA plot is insignificant, which suggests there is no observable effect of other, possibly uncontrollable conditions of the experiment.

The m/z data obtained in the study were transformed into mass and compound formula and used as queries against microbial metabolic databases. Unfortunately, very few detected compounds could be structurally matched by the databases search, both automated and manual. Additionally, the majority of the automatically matched bioactive compounds have never been reported in *Pseudomonas* spp. thus correct annotation is highly uncertain. Of these automatically annotated metabolites, only two compounds have been previously described as antimicrobials of pseudomonads: 7-HT (m/z 139) and zafrin (m/z 213). While 7-HT is known to be a metabolite of *P. donghuensis* and can be additionally detected with UV-Vis spectrophotometry, the efforts to isolate and identify zafrin following the study by Uzair *et al.*, (2008) were unsuccessful. Furthermore, PVD also could not be explored in this part of the study due to its, at that time, unknown structure and molecular mass. Thus, only 7-HT, which was hypothesised to contribute significantly to P482 antimicrobial activity, was explored in the following analyses.

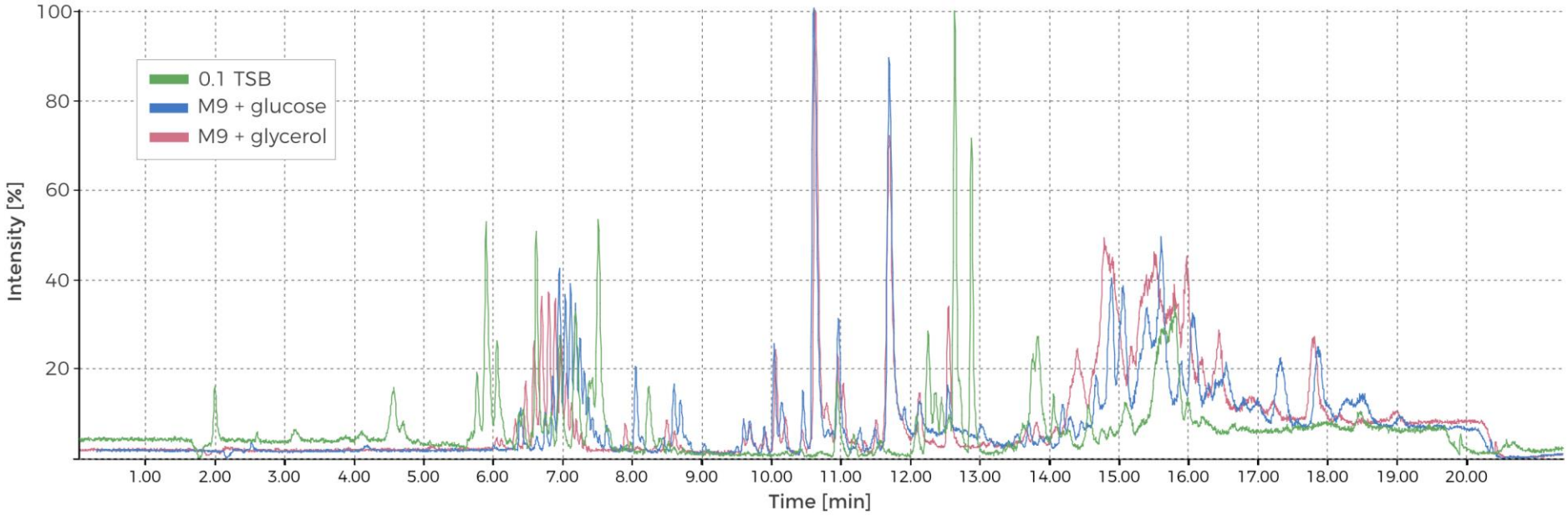


**FIGURE 56. The overlay of the representative LC-MS chromatograms of the P482 wt extracts.** The tested extracts were obtained from the post-culture supernatants of P482 wt cultured in 0.1 TSB (**green line**), M9 + 0.4% glucose (**blue line**) or M9 + 0.4% glycerol (**red line**). The spectra are scaled to the highest peak obtained in each of the presented samples.

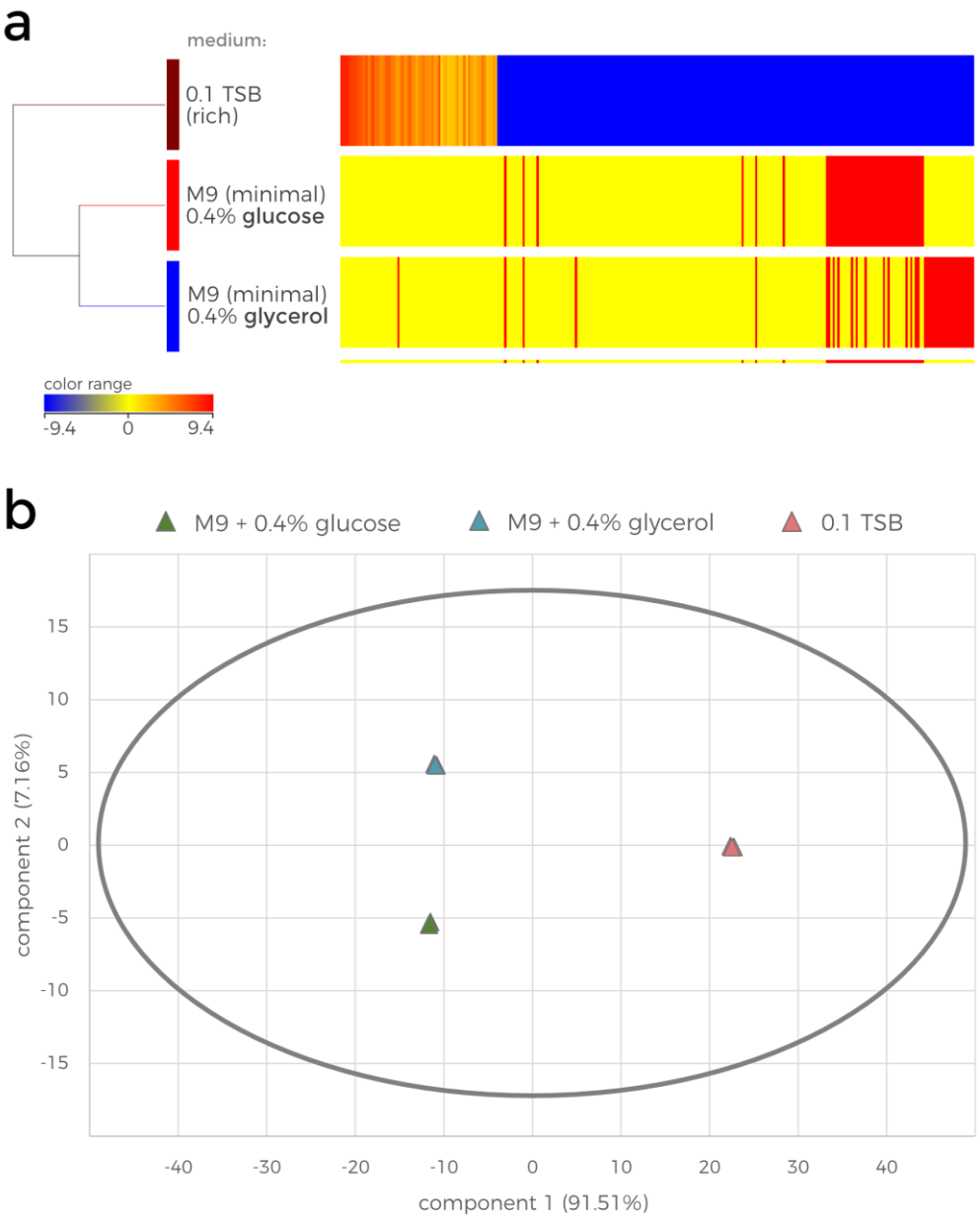


**FIGURE 57. Statistical analysis of the LC-MS data obtained for the metabolite extracts of P482 wt cultured in 0.1 TSB, M9 + 0.4% glucose or M9 + 0.4% glycerol.**

**a.** Heatmap with hierarchical clustering showing the diverse metabolic profile of P482 wt depending on the nutritional conditions. The color range represents log2 fold change (FC) of the normalised intensity values for compounds detected in the samples (compounds with FC > 2 were included in the analysis, ANOVA, $p < 0.01$)
**b.** Principal component analysis (PCA) biplot representing the similarity between all the samples included in the analysis (three biological replicates of each extract conditions).

The presence of 7-HT in the tested P482 wt post-culture extracts was assessed using LC-MS spectra. The UV-Vis results (9.5.1) obtained for the culture supernatants of P482 wt suggested that while 7-HT is indeed produced under rich medium conditions (LB in the case of UV-Vis spectrophotometry experiments), its biosynthesis is inhibited in minimal media, regardless of the carbon source used (glucose or glycerol). The LC-MS investigation confirmed this hypothesis. Peaks of mass spectra corresponding with the 7-HT formula were found in the chromatograms obtained for the 0.1 TSB-grown P482 wt post-culture extracts (rich medium) as seen in the

excerpts from the obtained data (**FIGURE 25**). Moreover, no trace of 7-HT presence was detected in the extracts from P482 wt grown in M9 minimal media with either glucose or glycerol as the carbon source. This outcome reinforces the assumption that P482 requires nutrients other than those included in the M9 medium formulation or a specific molecular signalisation in order to biosynthesise 7-HT.

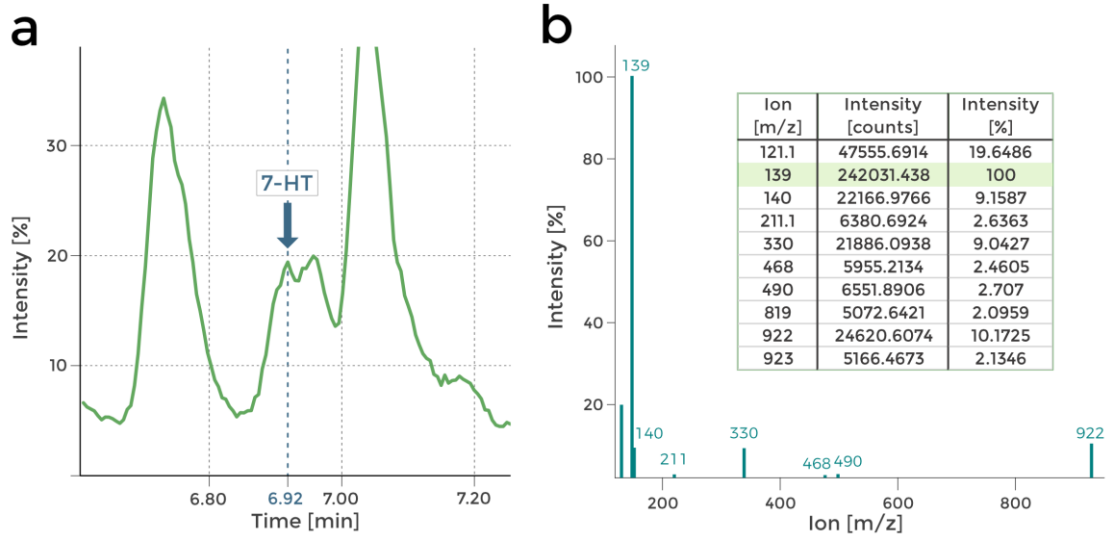


| Ion [m/z] | Intensity [counts] | Intensity [%] |
|---|---|---|
| 121.1 | 47555.6914 | 19.6486 |
| 139 | 242031.438 | 100 |
| 140 | 22166.9766 | 9.1587 |
| 211.1 | 6380.6924 | 2.6363 |
| 330 | 21886.0938 | 9.0427 |
| 468 | 5955.2134 | 2.4605 |
| 490 | 6551.8906 | 2.707 |
| 819 | 5072.6421 | 2.0959 |
| 922 | 24620.6074 | 10.1725 |
| 923 | 5166.4673 | 2.1346 |

**FIGURE 60. LC-MS confirmation of 7-hydroxytropolone presence in 0.1 TSB P482 wt extracts.**
**a.** Representative HPLC chromatogram peak (RT = 6.92) for which the ion m/z (139) corresponding with the mass of 7-HT was detected with the highest counts.
**b.** Mass spectrum for scan at RT = 6.92 with the table presenting raw counts and intensity values for each detected ion. The row corresponding to 7-HT m/z is highlighted.

The PVD production by P482 was not tested in this part of study due to the limitation of the method. However, it is worth noting that the UV-Vis spectral analysis suggests that PVD is present in the supernatants obtained from P482 cultured in minimal medium. It occurs unless the P482 mutant is defective in PVD production, which can be observed in KN1009, KN3755 (PVD biosynthesis genes mutants) and KN4243 (efflux pump gene mutant). This result implies that the BV82_4243 gene product (EmrA) might play a role in the secretion of PVD.

Overall, these analyses established the immense effect of the nutritional environment on the metabolome of P482, while the single carbon source as a component of a minimal medium does not prove to be as instrumental. Moreover, 7-HT was found to be produced by P482 only in the rich, undefined medium. Since the antagonism of 7-HT cluster mutants of P482 is affected by the carbon source in the minimal medium (**9.3.2.1**), this issue needs further investigation.

### 9.5.2.2. Mutations in four of P482 key antimicrobial loci have an unpredicted influence on P482 metabolome

To test whether and how the mutations in the 7-HT biosynthesis cluster and "cluster 17" affect the metabolome of P482, the extracts from the 0.1 TSB-post-culture supernatants of P482 wt

and the mutants (KN4706, KN4709, KN4240 and KN4243) were analysed with LC-MS. The 0.1 TSB medium was chosen for this experiment as the production of the crucial metabolite, 7-HT, was observed for P482 cultured under rich medium conditions.

First metabolic differences between the mutants can be observed in the HPLC chromatograms (**FIGURE 26**). The comparison of the chromatograms of P482 wt and the 7-HT cluster mutants is the first confirmation of 7-HT biosynthesis ability loss in the mutant strains (no peak at approx. 6.92 min; **FIGURE 26c**). The only other difference between the mutants seems to lie in the ratios of normalised concentrations of the numerous detected compounds, although it is not clearly visible in the chromatograms. Nevertheless, it suggests that the production of other metabolites can be influenced by the introduced mutations. Therefore, a statistical analysis was needed to fully discern the results for all the detected compounds.

The statistical analyses on the extracts' metabolomic data were performed similarly to those in the previous section. The charts in **FIGURE 27** present their results. The hierarchically clustered heatmap represents the mutant-dependent difference in abundance of the ions detected in the extracts (**FIGURE 27a**). Featured in this analysis were only the compounds for which at least a 2-fold change in abundance between at least one pair of the strains (wild type or mutants) was calculated. This resulted in only 32 compounds being included. Out of these 32, only 8 are present in the extracts from P482 wt cultures, 4 of which are not present in any mutant culture extract. None of the 32 compounds except 7-HT could be fully identified based on the database search, however the mass was used to calculate the formula of these metabolites. The metabolites present only in the wild type strain culture were: C17 H13 N O (mass: 247.0993), C19 H15 N11 O11 (mass: 573.0944), C19 H39 Cl O3 S2 (mass: 414.2035) and C19 H31 Cl N4 O4 (mass: 414.2032).

Furthermore, three metabolites were only present in P482 wt and KN4240, a "cluster 17" gene mutant. These metabolites were C27 H49 N (mass: 387.3852), C27 H15 S4 (mass: 467.0057) and the antimicrobial iron chelator, 7-HT (mass: 138.0312). Unsurprisingly, 7-HT is not produced by the P482 mutants designed to be defective in its biosynthesis, namely, KN4706 and KN4709 (**FIGURE 27b**). In addition, one biological replicate of the KN4243 (a "cluster 17" mutant) extract contains 7-HT, yet in concentration much lower than in KN4240 and P482 wt. This result suggests that the gene in the BV82_4243 locus is linked also to 7-HT biosynthesis. Since it encodes a part of an efflux pump (EmrA), it might be engaged in 7-HT secretion. This explains the detection of 7-HT in one of the replicates of KN4243 extract as it could come from the cells broken in centrifuge.

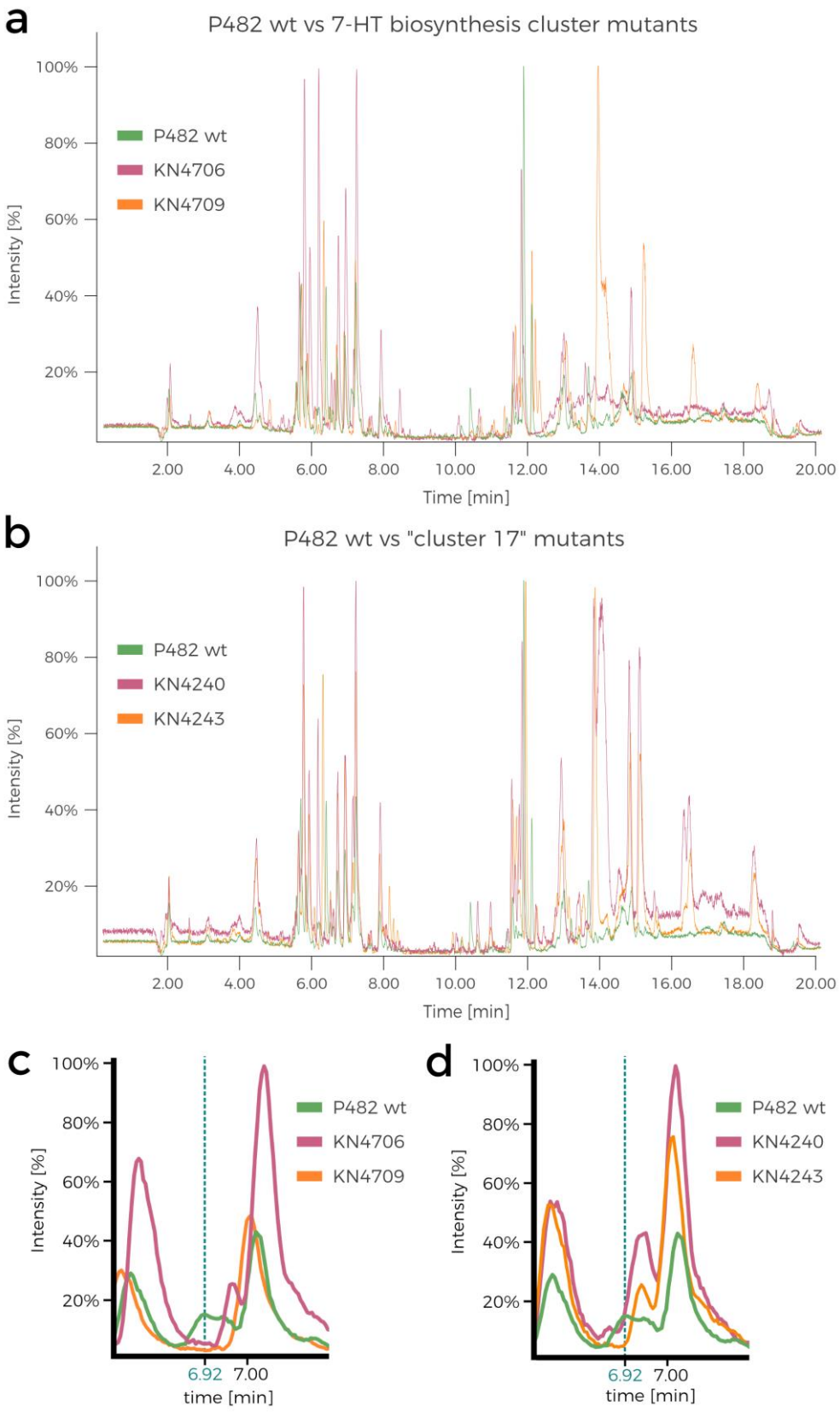


**FIGURE 63. The overlay of the representative LC-MS chromatograms of the studied extracts.**
The analysed extracts were obtained from 0.1 TSB post-culture supernatants of: **a.** P482 wt (**green line**) and its 7-HT biosynthesis cluster mutants: KN4706 (**pink line**) and KN4709 (**orange line**); **b.** P482 wt (**green line**) and its "cluster 17" mutants: KN4240 (**pink line**) and KN4243 (**orange line**). The spectra are scaled to the highest peak obtained in each of the presented samples; **c.** and **d.** are excerpts of chromatograms **a.** and **b.** (respectively) presenting the zoom on peaks at **6.92 min** retention time corresponding with the detection of **7-HT** in the mass spectra.

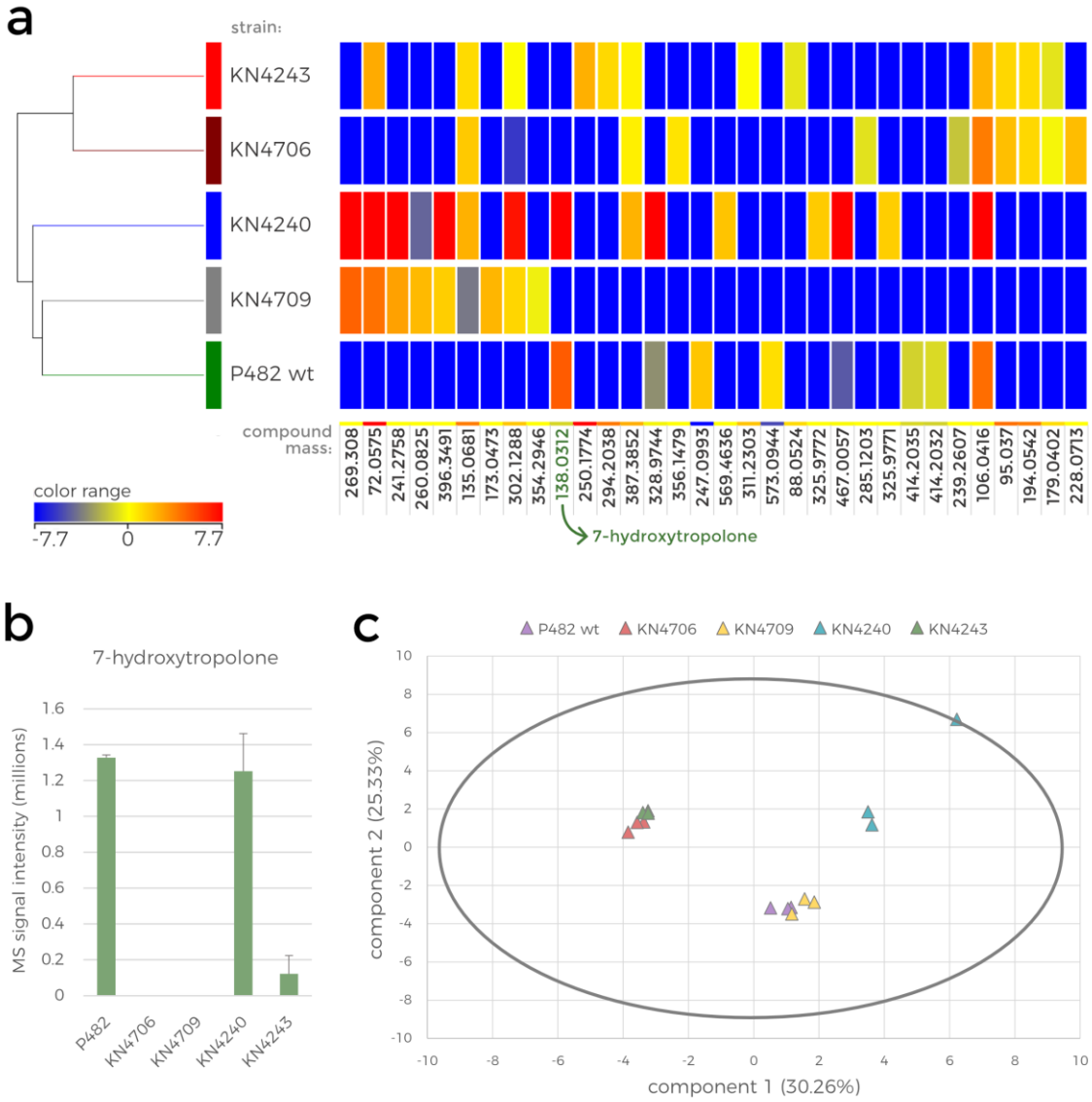


**FIGURE 66. Statistical analysis of the LC-MS data obtained for the metabolite extracts of P482 wt and its mutants cultured in 0.1 TSB.**

**a.** Heatmap with hierarchical clustering showing the diverse metabolic profile of P482 and its selected mutants (KN4706, KN4709, KN4240 and KN4243). The color range represents log2 fold change (FC) of the normalised intensity values for compounds detected in the samples, a calculated mass of the compared compound is below each column (compounds with FC > 2 were included in the analysis, ANOVA, $p < 0.01$). **b.** Bar plot showing the mean raw MS signal intensity obtained for the m/z 139 ions (7-HT) for P482 wt and each of the investigated mutants. The error bars represent standard deviation. **c.** Principal component analysis (PCA) biplot representing the similarity between all the samples included in the analysis (three biological replicates for each mutant).

The PCA of the data obtained in this part of the study is presented in a biplot showing the two first principal components scores for each sample (**FIGURE 27c**). These two principal components together are responsible for only ca. 55.5% of the variance in the analysed data, meaning that the other two components, omitted in the biplot, might also be useful for understanding the correlations, thus they are included in the **SUPPLEMENTARY TABLE 4**. Since each biological replicate was scored separately, the plot presents three data points for each strain. It shows the variance in metabolome between the mutants and the variance between biological

replicates. The correlations between the mutants are similar to what was observed in the hierarchical clustering (**FIGURE 27a**): the metabolomes of the KN4706 and KN4243 mutants resemble each other and the metabolome of KN4709 is similar to that of P482 wt. However, the metabolic profile of the KN4240 mutant is substantially different to other tested strains, including KN4243. Although the genes inactivated in these mutants were classified into one biosynthetic cluster, the lack of correlation between these mutants' metabolomes (as well as their antibacterial activity) clearly suggests that they serve various functions in P482 metabolism. What is more, the metabolic profiles of KN4706 and KN4709, while both missing 7-HT, differ from each other significantly, which implies the involvement of the 7-HT cluster genes in distinct additional processes.

Taken together, the results of the selected P482 mutants' metabolomic analysis do not comply with the predictions which would have clustered the mutants in the neighbouring genes together. The KN4243 mutant from "cluster 17" shares the metabolomic similarity with KN4706, a 7-HT biosynthesis cluster mutant, although their carbon source-dependent antagonism towards bacterial plant pathogens differs substantially. Moreover, it was revealed that the levels of 7-HT in KN4243 are not or barely detectable suggesting that the gene in locus BV82_4243 is involved in 7-HT secretion.

### 9.5.3. 7-HT biosynthesis is not stimulated by the substances secreted by the pathogen

The production of 7-HT could not be confirmed for P482 in minimal media. However, the 7-HT biosynthesis cluster mutants (KN4705, KN4706, KN4709) show reduced antimicrobial abilities in the direct antagonism tests performed on the same, albeit solidified, media. This suggests the contribution of this cluster's product in P482 antibacterial activity against plant pathogens. Furthermore, since the direct antagonism tests are performed in a way that allows for the antagonist-pathogen contact (mostly indirect, through secreted substances), the hypothesis emerged that pathogen signalling might be responsible for the 7-HT biosynthesis by P482 under minimal media conditions.

EtOAc extracts from P482 post-culture supernatants were obtained to test this hypothesis. To prepare the extract, P482 was cultured for 96 hours in minimal medium M9 with either glucose or glycerol as a carbon source and supplemented with the filtrate of *Dickeya solani* IFB0102 48-hour culture [DsFIL] in the corresponding minimal medium (M9 + glucose or M9 + glycerol).

Prior to the extraction of secondary metabolites, the post-culture supernatants were sampled for the preliminary UV-Vis spectrophotometry test. The obtained spectra of the supernatants of the P482 cultures with added DsFIL exhibit substantial differences that depend on the carbon source in the medium (**FIGURE 28**). When glycerol was the carbon source for P482 in the DsFIL-supplemented M9 medium, the amounts of produced compounds absorbing 350-425 nm light wavelengths were much higher than their production under the conditions with glucose. The absorption peaks found in the glycerol/DsFIL P482 culture supernatant are analogous to those found in the corresponding P482 supernatant but obtained from the culture without added compounds secreted by the pathogen (**FIGURE 22**). Thus, no detectable peak at ~330 nm suggests no 7-HT production by P482 in the presence of glycerol and DsFIL. However, a vague shape of the typical 7-HT 330 nm peak is observed in the glucose/DsFIL culture supernatant of P482 (**FIGURE 28**). This contrasts with the absorption spectrum obtained for P482 cultured under corresponding conditions without DsFIL supplementation, where no peak at 330 nm was detected (**FIGURE 22**). Although the method does not allow for quantitative analysis, the flat shape of the P482 glucose/DsFIL supernatant spectrum is unexpected.

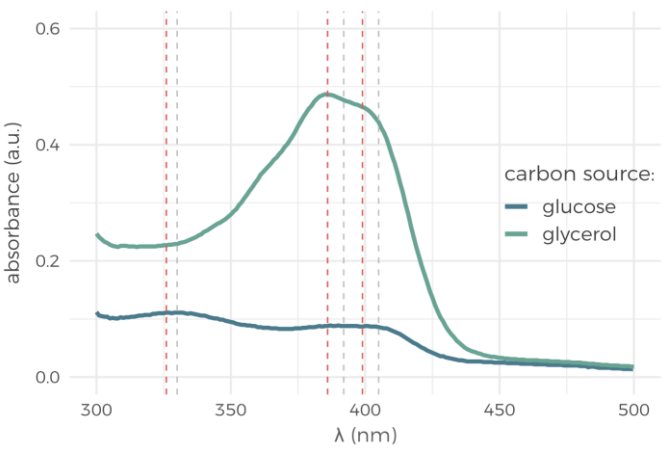


**FIGURE 69. UV-Vis absorption spectra of culture supernatants of P482 wt cultured with *D. solani* IFB0102 culture filtrate.** The samples were P482 wt post-culture supernatants, the colour of the line indicates growth conditions: **glucose (blue)** – M9 + 0.4% glucose + 10% DsFIL, **glycerol (teal)** – M9 + 0.4% glycerol +10% DsFIL. The spectra were recorded in the wavelength range 300-500 nm. The dashed vertical lines indicate the peak absorption wavelengths for the iron chelators typical for *P. donghuensis*: 7-HT (obtained (red): 326 nm and 387 nm, expected (grey): 330 nm and 392 nm) and PVD (obtained (red): 399 nm, expected (grey): 405 nm).

Furthermore, the organic extracts from the described P482 culture supernatants were subjected to the LC-MS analysis. This part of the study was performed to ultimately determine whether the addition of DsFIL stimulates the 7-HT production by P482 under minimal media conditions. The comprehensive analysis of the spectra directed towards the detection of ions with m/z in the range 138.5-139.5 showed that 7-HT (m/z = 139; [M+H]+) is present in trace amounts in the tested extracts regardless of the carbon source being glucose (**FIGURE 29**) or glycerol (**FIGURE 30**). For all the MS peaks with possible 7-HT ion mass detected, m/z 139 was one of the minor ions in the spectrum and the fragmentation did not show the pattern that was obtained in the previous experiments. Moreover, the m/z value of several detected ions found in the query range was 139.1. This does not agree with the calculated 7-HT m/z (139.038) and does not indicate the presence of this compound in the analysed extracts. These results suggest that the DsFIL

supplementation of M9 minimal media with either glucose or glycerol does not cause any noteworthy changes in 7-HT biosynthesis by P482.

Together, the analyses do not support the hypothesis that the compounds secreted by the pathogen might be stimulating the production of 7-HT by P482 and thus the antibacterial activity of this strain under the minimal medium conditions. However, only the limited experimental data obtained in this study is available to be considered and further investigation is needed in order to fully eliminate the possibility of pathogen-dependent regulation of 7-HT biosynthesis in P482.

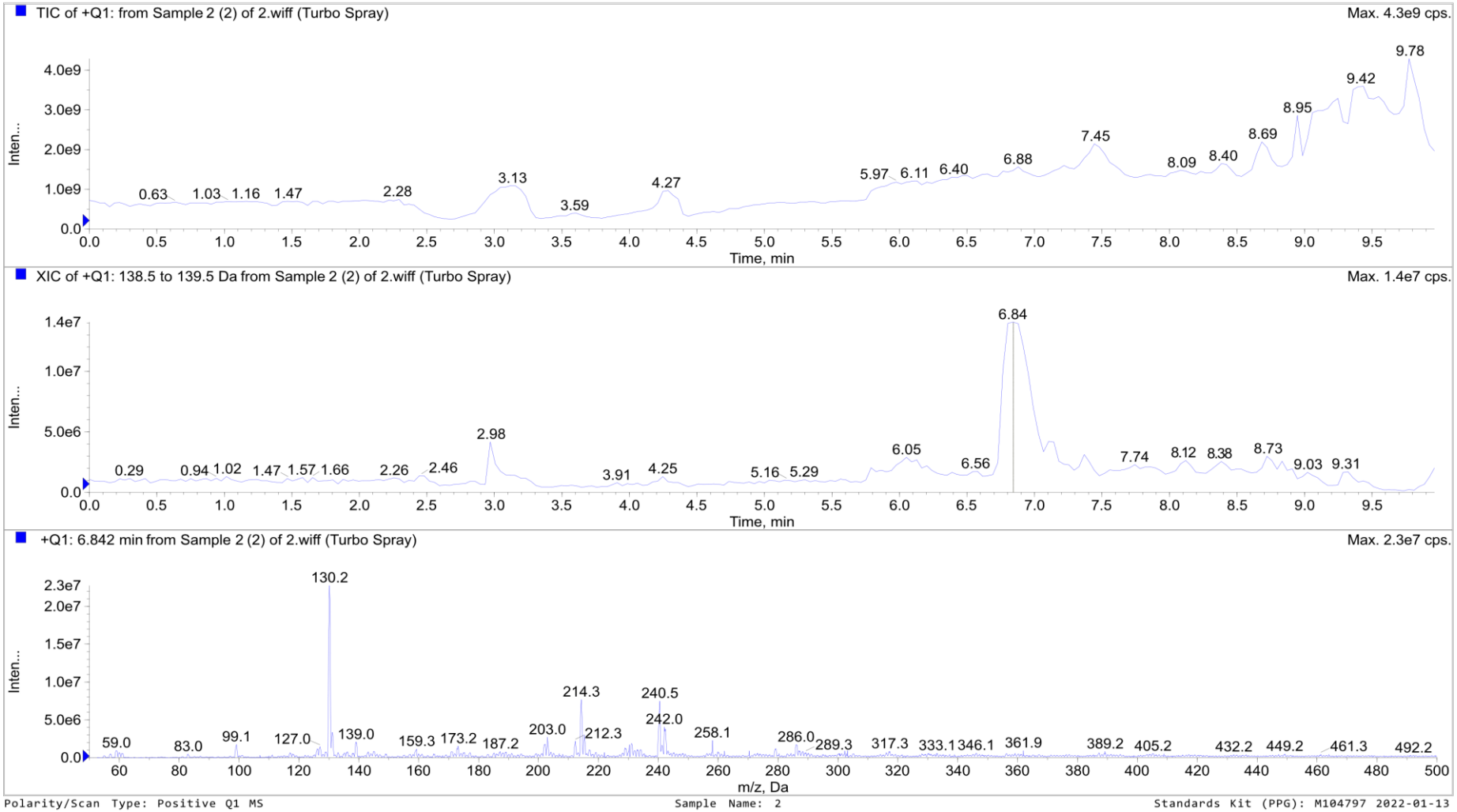


**FIGURE 72. The results of 7-HT detection in the metabolite extracts from P482 cultured in M9 + 0.4% glucose supplemented with *D. solani* culture filtrate.**
The charts present (from the top): HPLC-MS total ion count [TIC] chromatogram of the sample; HPLC-MS extracted ion count [XIC] chromatogram for ions of m/z138.5 to 139.5; the mass spectrum of the peak with the highest intensity of ion of m/z 139. The charts were generated in Sciex Analyst software.

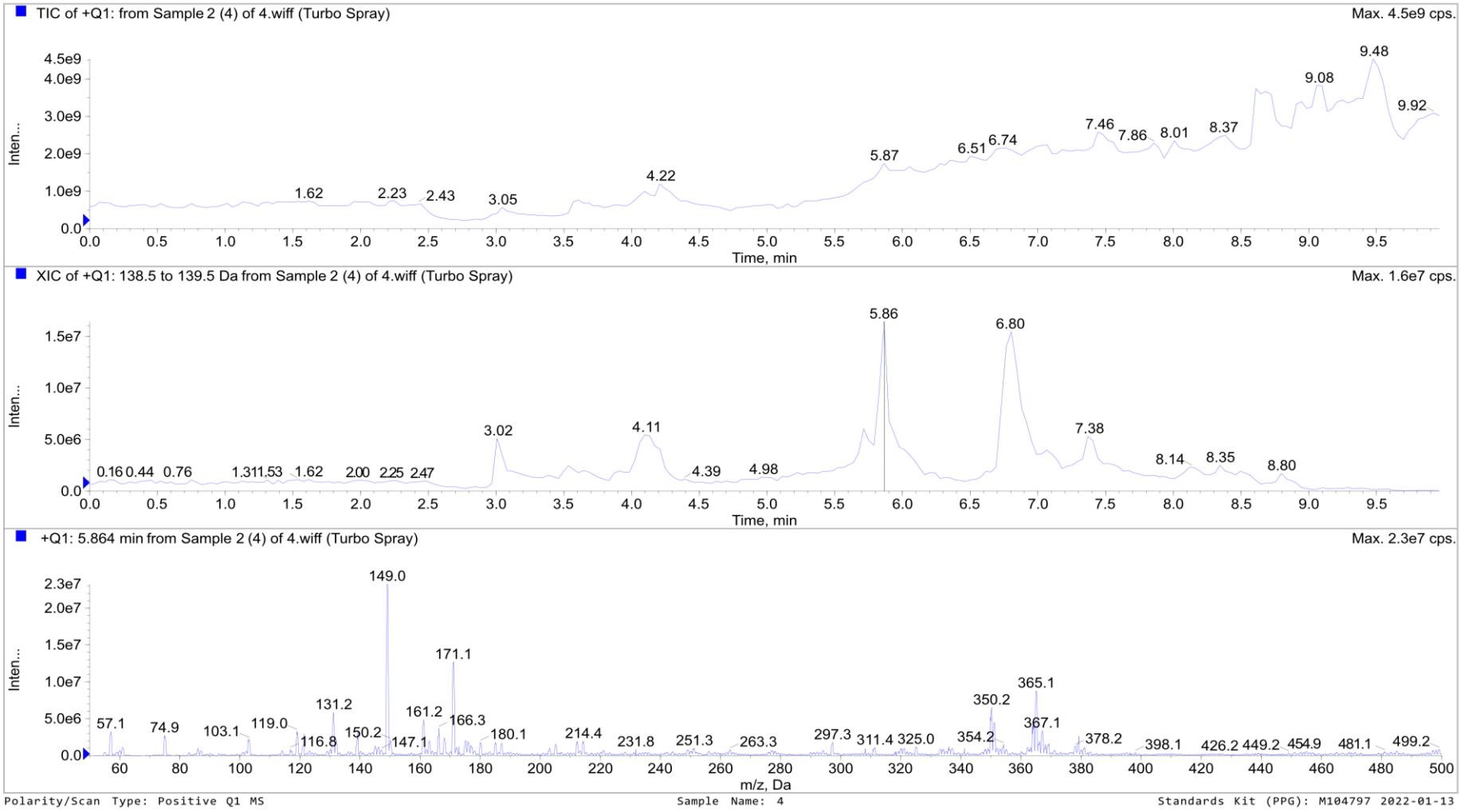


**FIGURE 75. The results of 7-HT detection in the metabolite extracts from P482 cultured in M9 + 0.4% glycerol supplemented with *D. solani* culture filtrate.**
The charts present (from the top): HPLC-MS total ion count [TIC] chromatogram of the sample; HPLC-MS extracted ion count [XIC] chromatogram for ions of m/z138.5 to 139.5; the mass spectrum of the peak with the highest intensity of ion of m/z 139. The charts were generated in Sciex Analyst software.

## 9.6. Gene expression of selected P482 genes is dependent on carbon and iron source availability

### 9.6.1. RT-qPCR reference gene selection

Prior to the gene expression RT-qPCR assays, the set of reference genes [RGs] has been selected during a comprehensive study of their expression stability. Ten housekeeping genes (named together with references in **TABLE 11**) were chosen based on literature reports focusing on *Pseudomonas* spp. RGs, apart from the *tuf* gene for which no reports on stability in Gram-negative bacteria had existed in the literature. However, *tuf* was widely explored in Gram-positive bacteria such as *Lactococcus* spp. and *Staphylococcus* spp. as the RG.

The stability of expression of the potential P482 RGs was tested under twelve culture conditions differing in media composition, incubation temperature and endpoint growth phase (**TABLE 10**). To select and validate best RGs in P482, the concentrations of cDNA templates were standardised and RT-qPCR reactions were conducted with primers designed for each of the tested genes (primers were validated prior to the assay as described in section 8.5.2; list of primers can be found in **SUPPLEMENTARY TABLE 2**). The validation of the primer pairs confirmed their specificity using the melting curve analysis. Furthermore, the standard curves revealed the amplification efficiencies of the primers, which were in the acceptable range from 90 to 111%, apart from the primer pair for the *algD* gene, which showed efficiency of 120% (**SUPPLEMENTARY TABLE 5**). The RT-qPCR results obtained as Cq (threshold cycle) data (**FIGURE 31**) were further processed using different algorithms. The first of the employed tools was RefFinder, a web-based tool that utilises four individual algorithms (ΔCT, BestKeeper, NormFinder and geNorm) that calculate the stability of reference genes using raw Cq data. In this analysis, each of the algorithms yields

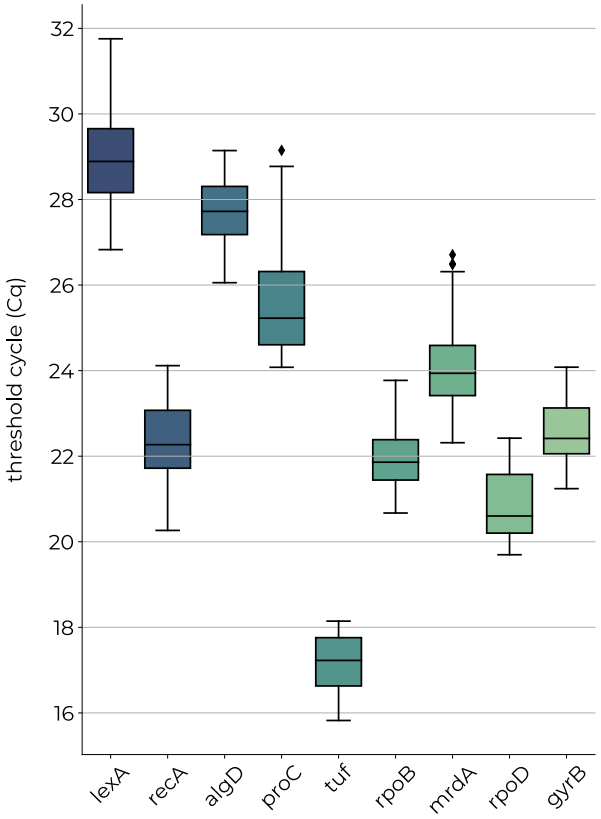


**FIGURE 78. RGs threshold cycle (Cq) data distribution.** Boxplot represents the distribution of Cq data obtained for the potential RGs during the study on their expression stability. The dark band inside the box represents the median value, the top edge of the box is the upper quartile (Q3) while the bottom edge of the box is the lower quartile (Q1). Q3 and Q1 refer to the 75th percentile and the 25th percentile, respectively, meaning that 75 or 25% of the data were at or below the point. The whiskers represent the maximum and minimal values excluding outliers. Outlier data is presented with black diamond symbol (♦).

individual results of gene expression stability (**FIGURE 32abcd**). NormFinder and ΔCT algorithms generated identical RGs rankings, favouring *gyrB*, *mrdA* and *tuf* as the most stably expressed among the ten tested potential RGs (NormFinder stability values, respectively: 0.535, 0.681, 0.710); ΔCT average standard deviation, respectively: 1.09, 1.14, 1.15). BestKeeper found *gyrB*, *tuf* and *rpoD* the most stable (Best Keeper stability values, respectively: 0.527, 0.656, 0688), whereas geNorm ranking found both *mrdA* and *rpoD* most stable (geNorm stability value: 0.833), followed by gyrB (0.925). The stability rankings obtained were further processed into a comprehensive ranking of the genes calculated as a geometric mean of the rankings obtained by the four algorithms. This global RefFinder ranking found *gyrB* the most stably expressed among the tested genes (ranking geometric mean: 1.32), followed by *mrdA* (2.3) and *rpoD* (2.63) (**FIGURE 32e**).

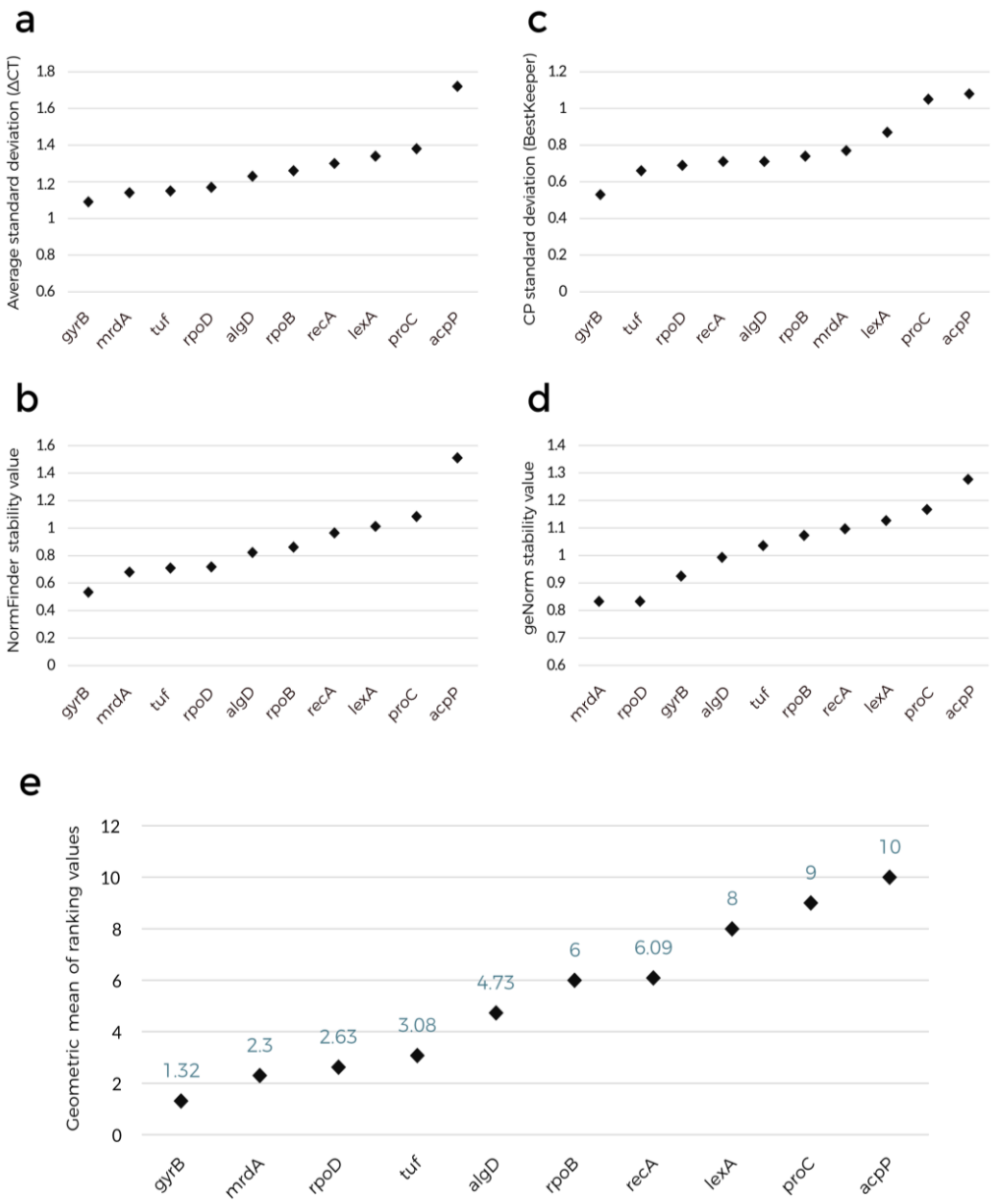


**FIGURE 81. RefFinder analysis results**. Potential RGs expression stability as calculated by each of the algorithms employed by the RefFinder tool: **a.** ΔCT, **b.** NormFinder, **c.** BestKeeper, **d.** geNorm and **e**. the comprehensive RefFinder ranking values for the tested genes.

RefFinder calculations do not utilise the primer efficiency and inter-run calibration data. Therefore, this tool was used only in preliminary data analysis and as an additional confirmation of the results described further, obtained in qbase+ geNorm analysis.

The qbase+ software was employed for all the steps of qPCR data analysis. The comprehensive framework of this tool includes assay quality control, primer efficiency calculations, inter-run calibration to the standard sample. These factors are also considered prior to the RGs selection which is calculated with the geNorm algorithm. In this analysis, quality control excluded the *acpP* gene due to insufficient data quality (replicate Cq variability was higher than 0.3), therefore nine instead of ten potential RGs were investigated further. The results obtained were consistent with the RGs expression stability ranking obtained with the RefFinder analysis. The expression stability was represented by the geNorm M value. The lower the value of this parameter, the more stable the given gene's expression. The most stably expressed of the tested housekeeping genes was found to be *gyrB* (geNorm M value: 0.485), closely followed by *rpoD* and *mrdA*, which ranked second (geNorm M value: 0.518) and third (geNorm M value: 0.532), respectively (**FIGURE 33a**).

Furthermore, the geNorm algorithm employed in qbase+ software calculates an additional parameter called geNorm V. It is based on pairwise variation analysis and indicates the number of RGs that should be incorporated into a given RT-qPCR experiment in order to obtain a reliable and optimal normalisation factor. geNorm V is a value that represents how much the final, normalised gene expression results would change if an additional RG was included in the analysis. The general threshold for the significance of the experimental outcome change assessment by geNorm V parameter is Vn/n+1 > 0.15 (n – number of RGs used for normalisation).

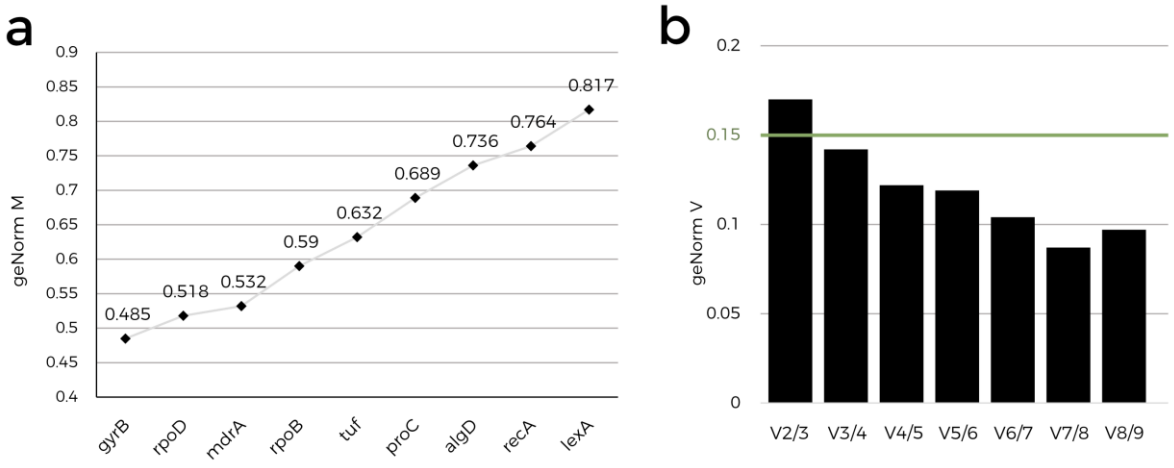


**FIGURE 84. qbase+ geNorm analysis results.**

**a.** Average expression stability of the tested P482 housekeeping genes represented by the geNorm M value. Lower M values indicate more stable genes.

**b.** Pairwise variation (geNorm V) chart for determination of the optimal number of RGs in the gene expression study. Vn/n+1 value below 0.15 indicates no significant change in experimental normalisation factor when using n+1 of RGs instead of n RGs and n RGs are sufficient for the RT-qPCR experiment normalisation.

In the presented study, a significant change in the experimental situation was shown when the normalisation factor was calculated for two and for three RGs (V2/3 = 0.17; **FIGURE 33b**). It means that two RGs are insufficient to analyse the RT-qPCR results reliably. However, adding the fourth RG to the normalisation factor calculation did not cause a significant change in the outcome of the analysis (V3/4 = 0.142; **FIGURE 33b**). Thus, geNorm V analysis suggests that in the case of P482 three RGs are sufficient for the optimal normalisation of the RT-qPCR results.

Taken together, all the described RGs analyses revealed that the most stably expressed housekeeping genes in P482 under various tested conditions are *gyrB*, *mrdA* and *rpoD*. Moreover, it was shown that these three RGs should be used together as RGs to optimally normalise the results of RT-qPCR gene expression analyses in P482. Thus, *gyrB*, *mrdA* and *rpoD* were incorporated into all further gene expression analyses presented in this thesis.

### 9.6.2. Gene expression analyses setup and quality assessment

The expression of the selected P482 genes was analysed in minimal media with glucose or glycerol as a carbon source and supplemented or not with iron(II) or iron(III) source (**TABLE 10**). The culture conditions with glucose as a single carbon source and no iron source served as a reference for the gene expression analyses since the "untreated control" was unapplicable. Thus, all the results shown in the figures were scaled/referenced to the results obtained from samples labelled as "glucose (no Fe)".

The selected genes belonged to the gene groups of interest which comprised the 7-HT biosynthetic cluster (genes in loci: BV82_4705, BV82_4706, BV82_4709), the pyoverdine biosynthetic genes (loci: BV82_1009, BV82_3755), the genes of "cluster 17" (loci: BV82_4240, BV82_4243), *gacA* gene (locus BV82_3318), and *fur* gene (locus BV82_4870). RT-qPCR was performed on RNA samples isolated from P482 wt cultured under the conditions described above. Primer pairs designed for each gene (**SUPPLEMENTARY TABLE 2**) were validated (**8.5.2**). The validation of the primers confirmed their specificity with the melting curve analysis (**SUPPLEMENTARY FIGURE 2**) The amplification efficiencies of the primers were in the range from 95% to 107% as calculated using the standard curves (**SUPPLEMENTARY TABLE 5**)

### 9.6.3. 7-HT cluster expression is regulated by both iron and carbon source

The expression of the selected P482 genes from the 7-HT biosynthetic cluster (loci: BV82_4705, BV82_4706 and BV82_4709; for simplicity referred to as: *4705*, *4706* and *4709* respectively) and the *gacA* gene (locus: BV82_3318, referred to as *3318*) was examined under all six selected nutritional conditions. In addition, the expression of *gacA* was analysed together with the 7-HT biosynthesis genes since the Gac/Rsm system is involved in the regulation of 7-HT production in *P. donghuensis*.

The results of this analysis are presented as the relative expression levels (CNRQ) (**FIGURE 34a**). Moreover, a heatmap in **FIGURE 34b** presents the expression fold change [FC] transformed logarithmically ($log_2$) for visualisation, while the untransformed FC is given in the main text body with the annotation of down- or up-regulation. All three genes from the 7-HT biosynthetic cluster exhibited the highest expression levels when P482 was cultured in medium with glucose. The addition of Fe(II) to the minimal medium with glucose had a profound suppressive effect on the expression of all tested 7-HT biosynthetic cluster genes. The downregulation was 16.5-fold for *4705*, 18.5-fold for *4706* and 23.6-fold for *4709*. Furthermore, the addition of Fe(III) to the glucose medium downregulated the expression of *4705* (3.78-fold) and *4706* (3.19-fold), however it did not have the same effect on the expression of *4709* (1.97-fold, non-significant downregulation). The expression dissimilarities can be explained by the fact that genes *4705, 4706* and *4709* belong to three separate operons which was confirmed by the Operon-mapper analysis of the P482 7-HT biosynthetic cluster (Krzyżanowska *et al.*, 2016). The downregulation of 7-HT biosynthesis genes' expression with the addition of Fe(II) suggests that their product might be involved in iron acquisition.

Interestingly, the expression results for *4706* and *4709* under glycerol conditions were similar to those obtained when glucose was a single carbon source in the medium, no matter the addition of iron. Glycerol, compared to glucose, downregulates the expression of *4706* 16-fold and *4709* 39.9-fold. Yet, the *4705* gene expression level was only 4.9-fold lower in glycerol than in glucose, which is comparable to its expression under glucose + Fe(III) conditions. Since 4705 encodes a transcriptional regulator (TetR/AcrR family), these results are in agreement with the reports showing that TetR/AcrR regulator positively regulates the transcription of 7-HT biosynthetic genes like 4706 and 4709. The lower the *4705* transcription level, the less *4706* and *4709* transcript copies should be observed. However, this effect is not observable in the case of glucose medium, which suggests a more complex transcriptional regulation of P482 7-HT biosynthesis under these conditions. Furthermore, the addition of iron ions to the glycerol medium did not cause a significant change in the expression of any of the tested 7-HT biosynthesis genes compared to the iron depleted glycerol medium. This result implies that when glycerol is the carbon source, the 7-HT cluster does not play a substantial role in the biology of P482. This confirms the antibiosis test results, in which the 7-HT cluster mutants did not lose their antibacterial potential, but only when glycerol was the carbon source (**9.3.2.1**).

The *gacA* (*3318*) gene expression remained statistically unchanged with Fe(II) addition to the medium with glucose. However, adding Fe(III) to the glucose medium slightly (1.95-fold) downregulated the *3318* expression. In comparison to glucose, glycerol caused the most prominent change observed for *3318* expression, although the downregulation was only 2.6-fold. It validates the reports of Gac/Rsm system positively regulating the TetR/AcrR regulator expression, which in turn positively regulates the expression of 7-HT genes. This regulatory cascade means that

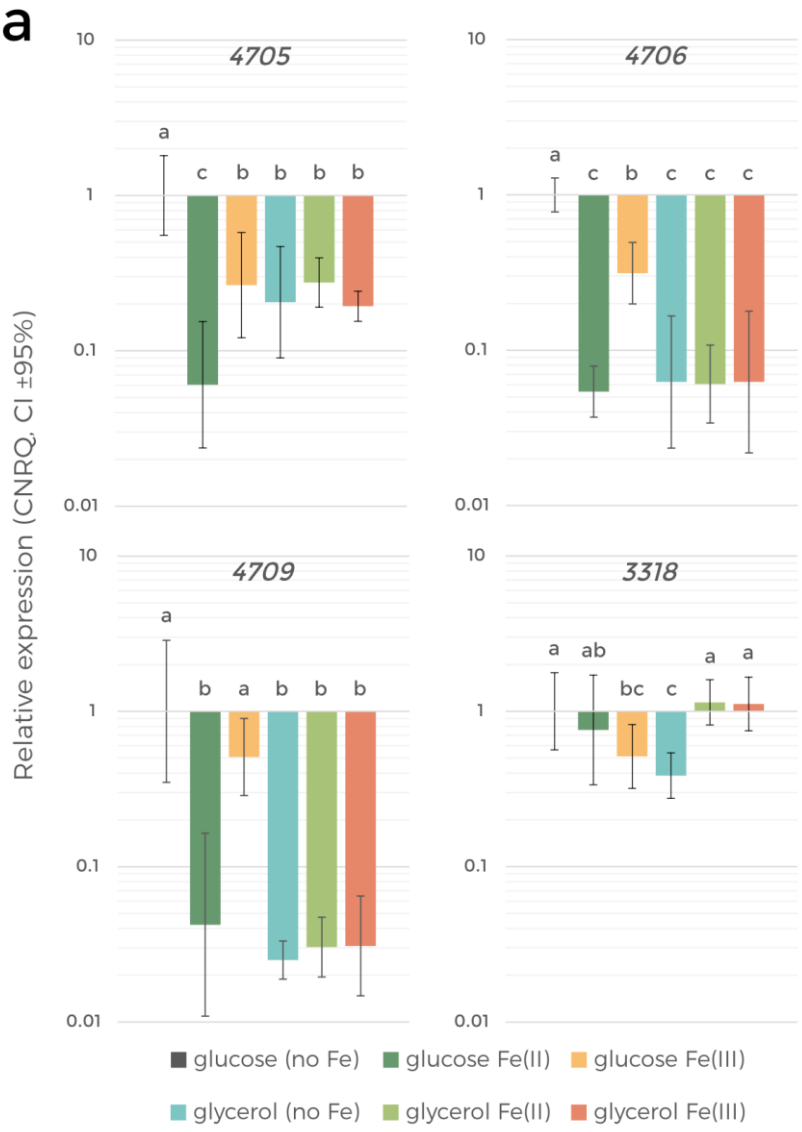


**b**

| | glucose Fe(II) | glucose Fe(III) | glycerol | glycerol Fe(II) | glycerol Fe(III) |
|---|---|---|---|---|---|
| *4705* | -4.05 | -1.92 | -2.28 | -1.86 | -2.37 |
| *4706* | -4.21 | -1.67 | -4.00 | -4.05 | -4.00 |
| *4709* | -4.56 | -0.97 | -5.32 | -5.04 | -5.02 |
| *3318* | -0.40 | -0.96 | -1.38 | 0.19 | 0.16 |



**FIGURE 87. 7-HT biosynthesis genes' expression results.**

**a.** Bar plot showing the relative P482 gene expression results as **CNRQ values** (scaled to the CNRQ for the given gene under the conditions with glucose as a carbon source and iron depletion). Error bars represent the 95% confidence interval (CI ± 95%). Statistical analysis was performed using two-way ANOVA. Differing letters above the bars denote significant differences ($p < 0.05$).

**b.** Heatmap and table of **$\log_2$ fold-change** value of the given P482 genes in comparison to their expression under the conditions with glucose as a carbon source and iron depletion ($\log_2$ fold change = 0).

For clarity of the figure, loci references are represented by numbers only.

with the downregulation of *gacA* (*3318*) expression, we shall observe stronger downregulation of *4705* and even more pronounced downregulation of *4706* and *4709*. This agrees with the expression results obtained for the 7-HT cluster genes on glycerol. The addition of iron ions (regardless of their valence) to the glycerol medium caused a modest upregulation 2.95-fold for iron(II) and 2.89-fold for Fe(III) in *3318* expression when compared to the levels obtained under iron-depleted glycerol conditions. These levels are however comparable to those obtained for an iron-depleted glucose medium.

Overall, these results suggest that glycerol, compared to glucose serving as a carbon source, substantially downregulates the expression of 7-HT biosynthesis cluster genes and causes a minor downregulation of the *gacA* gene. This, together with the antibacterial activity results, indicates that not 7-HT but other antibacterial metabolites are important for P482 activity on glycerol. The iron supplementation of the minimal medium (with either ferric or ferrous iron) negatively modulates 7-HT cluster genes expression when glucose is a sole carbon source, but it has no effect when glycerol substitutes for glucose. Of all tested iron supplementation combinations, Fe(III) supplementation of the glucose medium has a marginally negative effect on *gacA* expression and the addition of either Fe(II) or Fe(III) to the glycerol media, albeit slightly, upregulates the *gacA* expression.

### 9.6.4. The standard iron-dependent pattern of PVD biosynthesis genes' expression – an exemplary case

The P482 PVD biosynthesis genes (loci BV82_1009 and BV82_3755, further referred to as *1009* and *3755*, respectively) and a ferric uptake regulator gene (*fur*; locus BV82_4870, further referred to as *4870*) expression under the previously described conditions was analysed collectively due to the Fur involvement in the general regulation of PVD biosynthesis. The results of these gene expression analyses are presented in **FIGURE 35**.

Unsurprisingly, the expression of PVD biosynthesis genes is downregulated with the addition of Fe(II) ions, regardless of the carbon source. In the M9 medium with glucose, the Fe(II)-related negative regulation of the *1009* gene was 19.6-fold and *3755* gene – 13.8-fold. Although less pronounced, corresponding results were obtained for the glycerol medium, where the addition of Fe(II) downregulated the expression of both *1009* and *3755* 4.1-fold (compared to iron-depleted glycerol medium).

Since Fe(III) ions in the neutral pH of the M9 medium are practically unavailable for uptake without iron chelators, the manifested reaction of the bacteria is producing PVD, a siderophore. Thus, the resulting transcript amounts of PVD biosynthesis genes should be the same as in the medium without iron supplementation. As expected, ferric ions (Fe(III)) had no significant effect on the expression of *1009* and *3755* regardless of the carbon source which was present in the

medium (when compared to the iron-depleted medium with the same carbon source). Moreover, in the iron-depleted M9 medium, no significant difference in *1009* and *3755* expression was caused by the applied carbon source modification (glucose/glycerol substitution).

A contradictory outcome was observed for the expression of the P482 *fur* gene (*4870*). No significant differences were detected in the expression of *4870* under the compared conditions. However, the substantial variability in the relative amount of *fur* transcript (CI ± 95%), but also the *1009* and *3755* transcripts, detected among the biological replicates suggests that the regulation of their expression is not as stringent as in the case of other tested genes and can substantially vary even under technically the same conditions.

In summary, these results confirm the association of Fe(II) ions presence with the lower expression of PVD biosynthesis genes. It was also shown that Fe(III) ions supplementation causes the expression of iron chelator genes on the same level as when no iron is present in the medium. The expression of the gene encoding Fur regulator was not observed to be regulated by any of the manipulated nutritional factors.

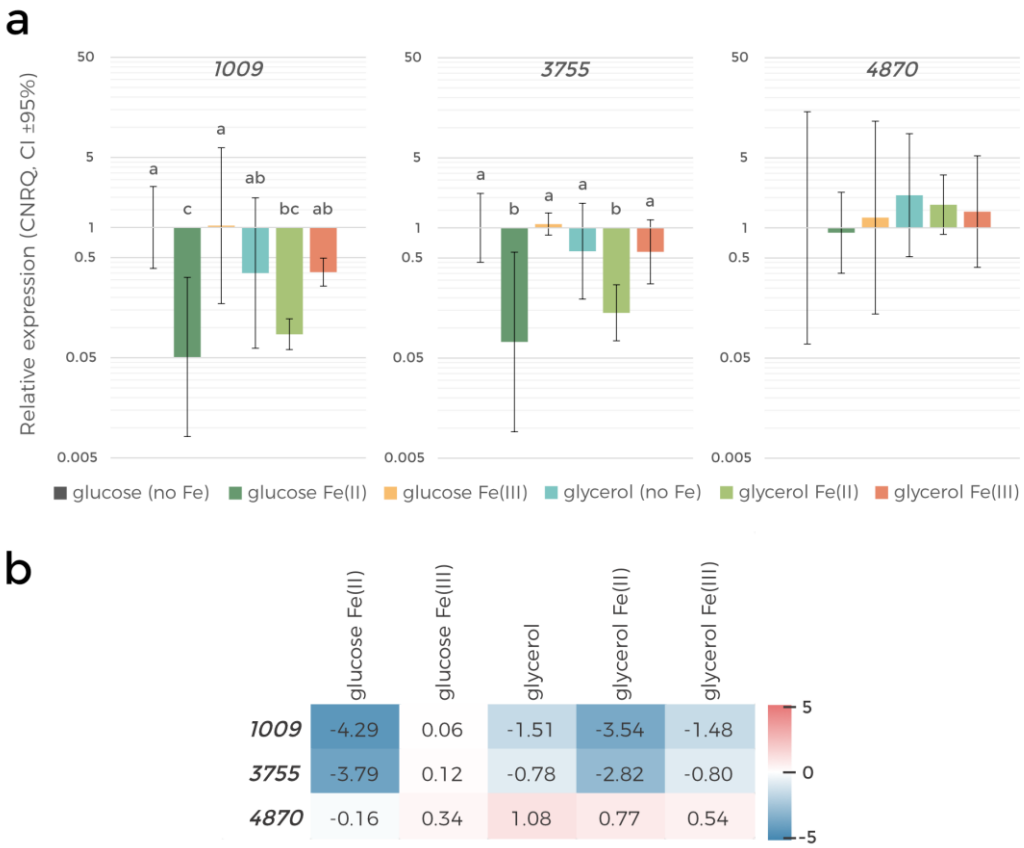


**FIGURE 90. PVD biosynthesis and *fur* genes' expression results.**

**a.** Bar plot showing the relative P482 gene expression results as **CNRQ values** (scaled to the CNRQ for the given gene under the conditions with glucose as a carbon source and iron depletion). Error bars represent the 95% confidence interval (CI ± 95%). Statistical analysis was performed using two-way ANOVA. Differing letters above the bars denote significant differences ($p < 0.05$).

**b.** Heatmap and table of **log2 fold-change** value of the given P482 genes in comparison to their expression under the conditions with glucose as a carbon source and iron depletion (log2 fold change = 0).

For clarity of the figure, loci references are represented by numbers only.

### 9.6.5. The divergent expression of two ‘cluster 17’ genes.

The expression of the ‘cluster 17’ genes of P482 was tested for two selected genes that belong to two different operons: loci BV82_4240 and BV82_4243 (further referred to as *4240* and *4243*, respectively).

The expression of *4240* in P482 was relatively stable among all of the applied nutritional conditions (**FIGURE 36**). The statistical amount of the *4240* transcripts under the given conditions is characterised by the 95% confidence interval that predicts this gene’s expression under any given conditions can be maximally 3-fold higher or lower than the mean result. This means that the *4240* expression among the biological replicates is reasonably stable and neither iron nor carbon sources affected it in this experiment.

Contrary to *4240*, the *4243* expression exhibits moderate changes under varying conditions (**FIGURE 36**). The addition of Fe(III) ions to the minimal medium upregulates the *4243* expression 2.9-fold (for the medium with glucose serving as a carbon source) or 2.4-fold (medium with glycerol). This might be explained in the light of the conclusions reached in the previous sections.

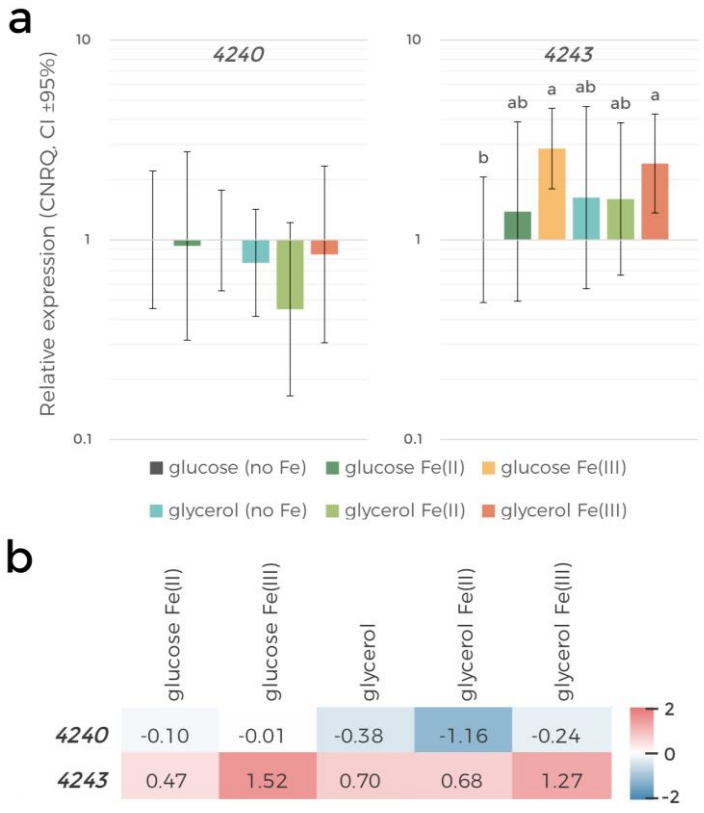


**FIGURE 93. ‘Cluster 17’ genes’ expression results.**
**a.** Bar plot showing the relative P482 gene expression results as **CNRQ values** (scaled to the CNRQ for the given gene under the conditions with glucose as a carbon source and iron depletion). Error bars represent the 95% confidence interval (CI ± 95%). Statistical analysis was performed using two-way ANOVA. Differing letters above the bars denote significant differences ($p < 0.05$).
**b.** Heatmap and table of **log2 fold-change** value of the given P482 genes in comparison to their expression under the conditions with glucose as a carbon source and iron depletion (log2 fold change = 0). For clarity of the figure, loci references are represented by numbers only.

It was unveiled that the *4243* gene encodes an efflux pump protein EmrA, which might be responsible for the PVD transport out of the cell. Therefore, the Fe(III)-abundant conditions can positively affect the expression of *4243* as its product is relevant to the iron uptake. However, similar *4243* transcript levels should also be observed in iron-depleted conditions. Surprisingly, this does not occur and the expression of *4243* without iron supplementation is similar to the results obtained with Fe(II) supplementation. This would suggest that not just the lack of readily available iron, but also the Fe(II) supplementation causes the upregulation of *4243* expression. No other statistically significant changes in *4243* transcript amounts in P482 were observed under the tested conditions.

Taken together, these results show differences in the regulation of what is supposed to be a gene cluster of P482. The *4240* gene from the first operon of 'cluster 17' was not observed to be significantly regulated by the applied nutritional conditions, while the *4243* gene, belonging to the second operon of 'cluster 17', was shown to be slightly upregulated by the ferric iron presence in the medium. This confirms the previous results showing the divergent phenotype of the two mutants in these neighbouring regions and thus suggesting that these loci are not functionally linked to each other.

## 9.7. Carbon and iron source dependency of P482 biofilm formation

The carbon/iron source-dependent differences in the abiotic biofilm formation by P482 and its mutants were examined using the crystal violet staining assay with spectrophotometric quantification. The test determines the relative biomass of the biofilm formed on the polystyrene surface of the 96-well plate by measuring the absorption of crystal violet ($OD_{570}$) bound to the biofilm cells and dissolved in a given volume of the solvent (EtOH).

The changes were first assessed in P482 wt under the conditions used throughout the study, namely M9 minimal medium with single carbon source (glucose or glycerol) and with or without iron ions supplementation (either ferrous or ferric iron ions). The results obtained suggest no evident influence of carbon and iron on the biofilm production by P482 (**FIGURE 37**). The only statistically significant difference can be observed in the case of iron supplementation of the glucose medium. Under these circumstances, Fe(II) in the medium slightly reduces the abiotic biofilm production by P482 compared to Fe(III) supplementation of the same medium. However, given that the purpose of this semi-quantitative assay was to detect only the substantial disparities in biofilm formation capabilities, the minor changes in P482 biofilm production caused by the tested carbon/iron sources should not be interpreted as conclusive.

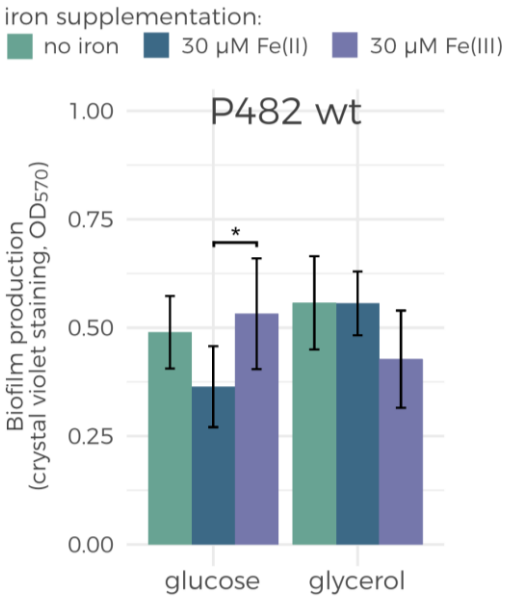


**FIGURE 96. Quantification of P482 wt biofilm formation – carbon/iron source dependency.** P482 wt was cultured in M9 minimal medium with either 0.4% glucose or 0.4% glycerol as a carbon source. Each medium had three variants: without added iron, supplemented with 30 μM Fe(II) or with 30 μM Fe(III). The biofilm biomass produced by P482 under each of the conditions was quantified by crystal violet staining ($OD_{570}$). Error bars represent standard deviation. The asterisks indicate the levels of statistical significance of the differences: * - $p < 0.05$ (Student's t-test).

### 9.7.1. Gac/Rsm pathway is involved in biofilm formation by P482 on glycerol

Following the P482 wt biofilm formation tests, the previously introduced P482 mutants were also examined for their abiotic biofilm production capabilities under different nutritional conditions. The mutants selected for the test were KN4706 and KN4709 (the 7-HT cluster mutants), KN3318 (*gacA*⁻ mutant), KN4240 and KN4243 (the "cluster 17" mutants), KN1009 and KN3755 (the PVD genes mutants) and KN4870 (*fur*⁻ mutant). First, their abiotic biofilm formation capabilities were evaluated on glucose and glycerol minimal media (without iron supplementation). These measurements were then compared to those obtained for P482 wt cultured under the same conditions. Moreover, each strain's biofilm production was analysed for the carbon source dependencies.

The outcome of the described analyses is presented in **FIGURE 38**. The most notable reduction in biofilm accumulation with respect to P482 wt was observed for the *gacA*⁻ mutant in a glycerol medium. The $OD_{570}$ values obtained for this strain were approximately 2x lower than those of P482 wt. Similar results (ca. 60% of the mean $OD_{570}$ measured for P482 wt) were obtained for KN4240 and KN1009, under conditions with glycerol as a sole carbon source. The biofilm formation abilities of these two mutants also significantly differ from those of P482 wt on glucose, however under these conditions their biofilm production was slightly increased (ca. 130% of the mean $OD_{570}$ obtained for P482 wt).

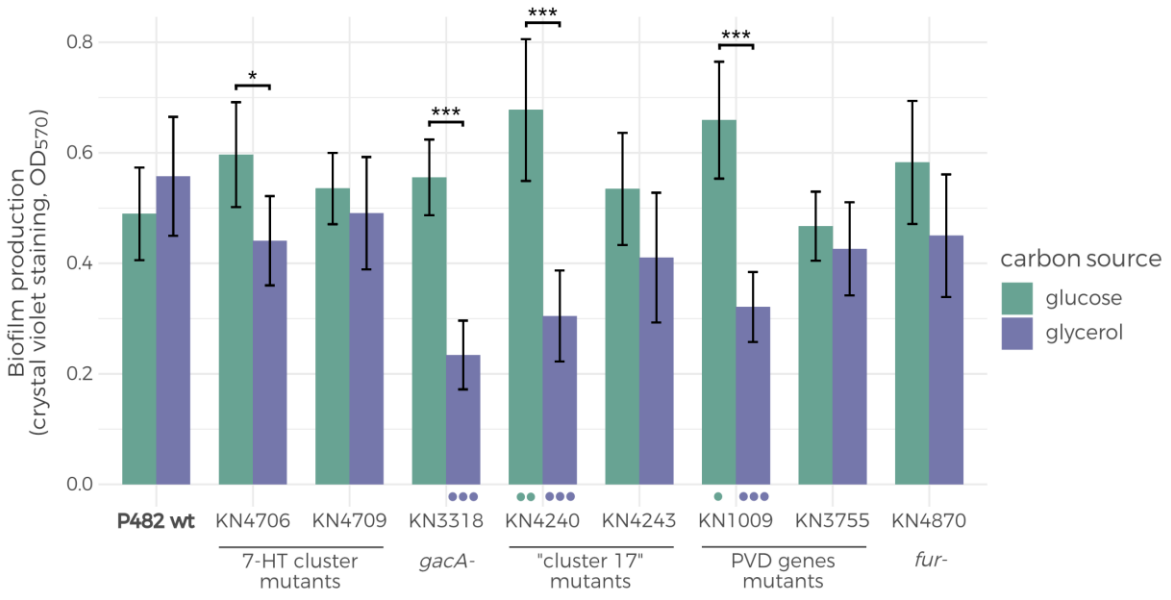


**FIGURE 97. Quantification of the biofilm formation of P482 mutants- carbon source dependency.**
P482 wt and its mutants were cultured in M9 minimal medium with either 0.4% glucose or 0.4% glycerol as a carbon source. The biofilm biomass produced in each sample was quantified by crystal violet staining ($OD_{570}$). Error bars represent standard deviation. The asterisks indicate the levels of statistical significance of the differences between the same strain samples (carbon source influence): * - $p < 0.05$, ** - $p < 0.01$; *** - $p < 0.001$ (Student's t-test). The green and purple dots below the bars indicate the statistical significance of the differences between the result obtained for a given strain and P482 wt under the same conditions (revealing the mutation influence): • - $p < 0.05$, •• - $p < 0.01$, ••• - $p < 0.001$ (Student's t-test).

Furthermore, the differences in biofilm formation caused by the carbon source influence were also analysed in each mutant (**FIGURE 38**). The results suggest that the three mutants that significantly differed from P482 wt in their biofilm development, that is KN3318, KN4240 and KN1009, also significantly differ in their biofilm biomass yield depending on the carbon source (glycerol or glucose). Glycerol, in their case, has an inhibitory effect on biofilm production. This is also true for the KN4706 mutant; however, the influence of glycerol is not as pronounced in this strain.

Taken together, these results provide valuable information about the P482 biofilm. First of all, this trait is not highly dependent on any of the genes inactivated in the examined P482 mutants. The biofilm is formed by the mutants despite their deficits in antibacterial activity, although some of the mutations (such as *gacA*$^{-}$) can affect the level of biofilm formation under certain nutritional conditions. The carbon source variation also modulates the biofilm formation by the P482 mutants, but only to some extent, which shows that the mutants retain their basic capability to develop biofilms.

### 9.7.2. Iron source effects on biofilm formation by P482 and its mutants

In addition to the investigated carbon sources and their effects on biofilm formation, iron supplementation was also considered as a factor that might influence this aspect of P482 biology. This experiment was carried out on the same growth media previously used for the biofilm formation assessment in the wild type strain. In the following description, the mutants subjected to the assay are divided into three groups to simplify the analysis of the obtained results.

Furthermore, statistical analyses were performed to compare the impact of iron ion supplementation. Thus, to minimise the effect of other variables, each statistical analysis was carried out within a group of samples of a given mutant under a given carbon source conditions and the only variable was the iron supplementation. Following the analyses, the effect of carbon sources combined with iron supplementation was considered in the interpretation of the results.

#### 9.7.2.1. Fe(II) supplementation restores biofilm forming capabilities of the glycerol-grown P482 *gacA*$^{-}$ mutant

The first group of mutants studied for the iron-dependency of biofilm formation were the mutants with deactivated genes from the 7-HT biosynthesis cluster (KN4706 and KN4709) and the *gacA*$^{-}$ mutant (KN3318).

The mean $OD_{570}$ values obtained from the crystal violet staining measurements for each of the mutants under the examined conditions are presented in **FIGURE 39**. The data suggest a tendency of Fe(II) ions to modulate the biofilm production of the given mutants. However, the outcome of this modulatory effect is dependent on the carbon source. For example, when glucose

is the carbon source, Fe(II) addition tends to decrease the biofilm biomass detected, whereas adding the same iron ions increases biofilm production when glycerol is the carbon source. Another trend that can be recognised both in the wild type P482 strain (**FIGURE 37**) and the 7-HT cluster mutants (**FIGURE 39**) is the minor reduction of relative biofilm biomass with the addition of Fe(III) to the glycerol medium.

Moreover, a substantial modification can be observed in the case of the KN3318 mutant. When cultured on glycerol, KN3318 has a reduced ability to form biofilm with respect to the situation when it is cultured on glucose. The addition of Fe(II) ions to the glycerol medium, restores this ability to the levels observable in KN3318 cultured on glucose. However, the supplementation of the Fe(III) ions does not yield any change in KN3318 glycerol culture biofilm production.

Overall, the P482 mutants defective in 7-HT biosynthesis genes (KN4706, KN4709) present a characteristic pattern of biofilm response to the tested carbon/iron source combinations. However, this pattern is also observable for P482 wt, therefore no mutant-specific iron influence was detected. This is different for the *gacA*$^-$ mutant (KN3318), in which biofilm formation abilities seem to strongly rely on iron supplementation, although only in its bioavailable, ferrous ion form.

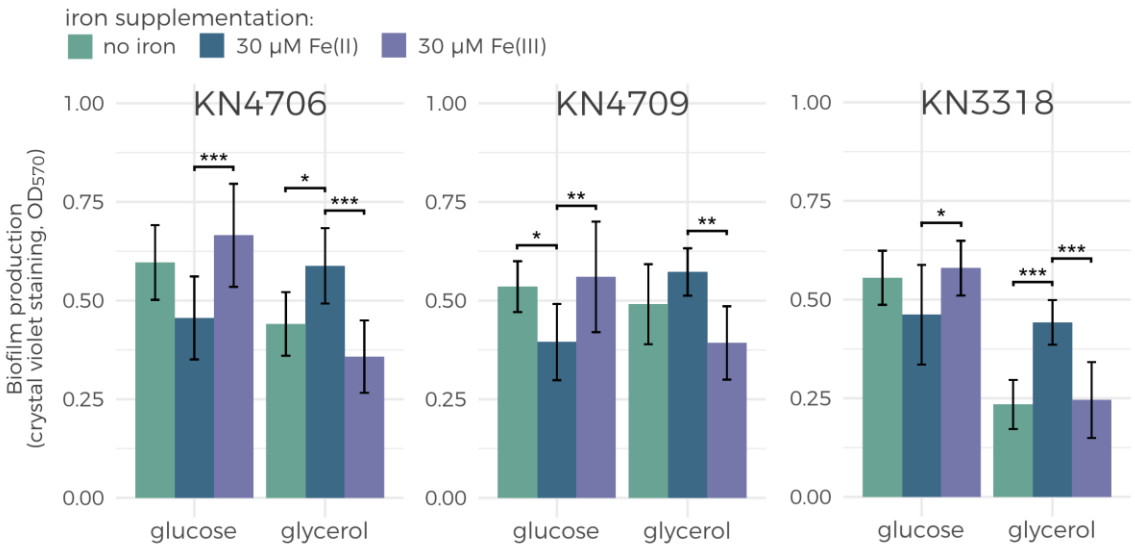


**FIGURE 100. Quantification of the biofilm formation by the P482 7-HT cluster and *gacA*$^-$ mutants – iron source dependency.** The strains KN4706, KN4709 and KN3318 were cultured in M9 minimal medium with either 0.4% glucose or 0.4% glycerol as a carbon source. Each medium had three variants: without added iron, supplemented with 30 μM Fe(II) or with 30 μM Fe(III). The biofilm biomass produced by the mutants under each of the conditions was quantified by crystal violet staining ($OD_{570}$). Error bars represent standard deviation. The asterisks indicate the levels of statistical significance of the differences between the samples: * - $p < 0.05$; ** - $p < 0.01$; *** - $p < 0.001$ (one-way ANOVA, Tukey's post-hoc test).

### 9.7.2.2. The biofilm regulation in the PVD mutants of P482 is highly dependent on iron ions availability.

The second group of mutants tested for their iron-dependency of abiotic biofilm formation included the strains of P482 with inactivation of genes relevant to the iron chelator, PVD,

biosynthesis (KN1009 and KN3755) and the mutant in the gene encoding the iron acquisition regulator Fur (KN4870).

The results of the crystal violet staining for these strains grown under the test conditions reveal some common characteristics for this group of mutants (**FIGURE 40**), but also resemble the P482 wt biofilm profile (**FIGURE 37**). What stands out is that the glucose medium supplementation with Fe(II) ions causes the reduction in biofilm biomass of all these strains when compared with the iron-depleted glucose medium and Fe(III) supplemented glucose medium. This trend can be observed for all the mutants in the study. Another interesting observation concerns the notably high value of standard deviation obtained for the biofilm measurements of the PVD genes mutants cultured in glucose medium with Fe(III). This is mainly true for KN1009 and KN3755, however, KN4870 and one of the "cluster 17" mutants (KN4243; described in the following section: **9.6.2.3**), also seems to exhibit a high variability of its biofilm biomass under these nutritional conditions.

Under the glycerol medium conditions, Fe(II) supplementation causes a slight increase in the biofilm production in KN1009 and KN3755. Contrastingly, no iron supplementation of the glycerol medium impacts the biofilm formation levels in KN4870.

Overall, the main findings for this mutant group confirm the suggestion of the P482 biofilm modulation by Fe(II) ions and reveal that this modulatory activity of Fe(II) is enhanced in PVD-related mutants.

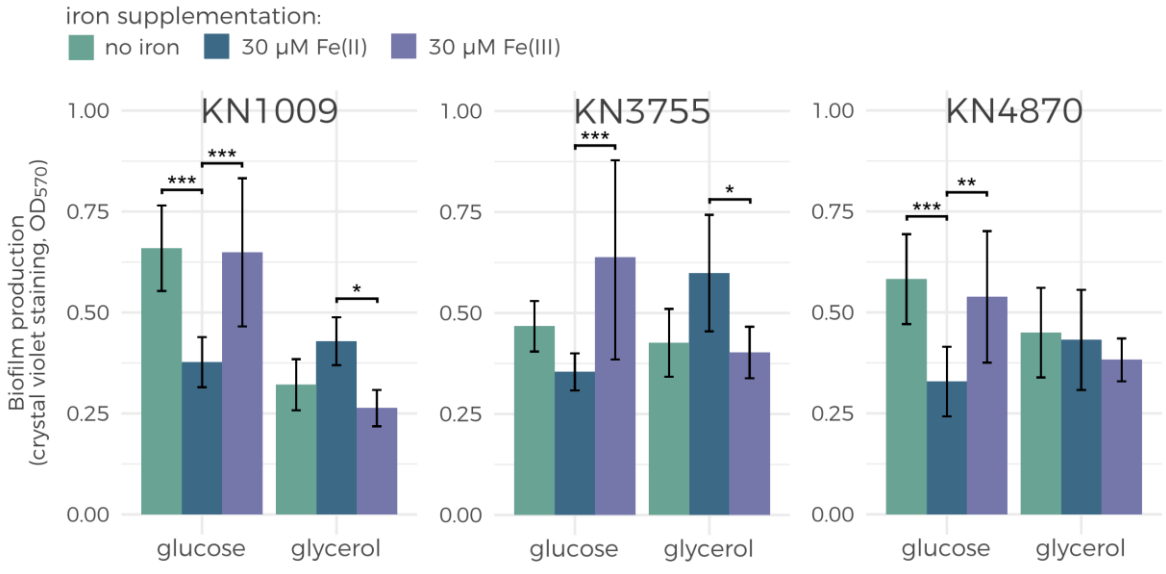


**FIGURE 101. Quantification of the biofilm formation by the P482 PVD biosynthesis genes and *fur* mutants – iron source dependency.** The strains KN1009, KN3755 and KN4870 were cultured in M9 minimal medium with either 0.4% glucose or 0.4% glycerol as a carbon source. Each medium had three variants: without added iron, supplemented with 30 μM Fe(II) or with 30 μM Fe(III). The biofilm biomass produced by the mutants under each of the conditions was quantified by crystal violet staining ($OD_{570}$). Error bars represent standard deviation. The asterisks indicate the levels of statistical significance of the differences between the samples: * - $p < 0.05$; ** - $p < 0.01$; *** - $p < 0.001$ (one-way ANOVA, Tukey's post-hoc test).

### 9.7.2.3. KN4240, rather than KN4243, exhibits strong biofilm formation dependency on Fe(II) ions.

The last group of mutants analysed for their biofilm formation dependency on iron ions consists of KN4240 and KN4243.

These analyses show that KN4240 strain biofilm production levels are strongly controlled by the nutritional combinations used in the study (**FIGURE 41**). Fe(II) supplementation seems to be a leading influential factor, however, it shows opposing trends depending on the carbon source in the medium. The outcome of the ferrous iron ions influence on KN4240 biofilm biomass is positive when paired with glycerol, but negative when paired with glucose. The results obtained for KN4240 show the most substantial influence of Fe(II) on biofilm formation in all tested mutants.

The biofilm formation by KN4243, in contrast to KN4240, is not enhanced by Fe(II) ions supplementation of its glycerol medium cultures. However, the influence of Fe(II) addition to the glucose medium causes a marginal decrease of KN4243 biofilm forming abilities. Furthermore, the Fe(III) addition does not cause significant differences in the biofilm of both KN4240 and KN4243 in comparison to the iron-depleted medium.

Overall, the difference between the impact of iron ions on the biofilm formation in KN4240 and KN4243 reiterate the previously shown functional divergence between the genes inactivated in these mutants.

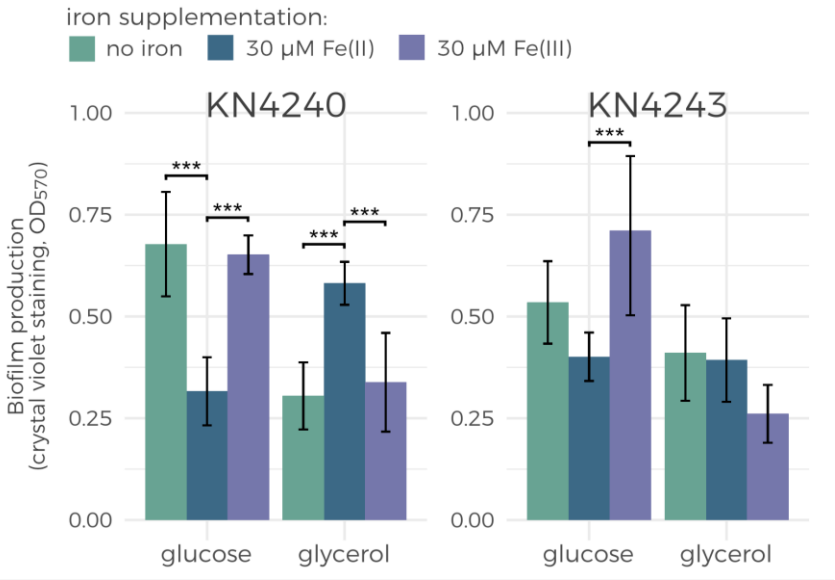


**FIGURE 104. Quantification of the biofilm formation by the P482 "cluster 17" mutants – iron source dependency.** The strains KN4240 and KN4243 were cultured in M9 minimal medium with either 0.4% glucose or 0.4% glycerol as a carbon source. Each medium had three variants: without added iron, supplemented with 30 μM Fe(II) or with 30 μM Fe(III). The biofilm biomass produced by the mutants under each of the conditions was quantified by crystal violet staining ($OD_{570}$). Error bars represent standard deviation. The asterisks indicate the levels of statistical significance of the differences between the samples: * - $p < 0.05$; ** - $p < 0.01$; *** - $p < 0.001$ (one-way ANOVA, Tukey's post-hoc test).

Taken together, the results gathered in this section demonstrate that P482 biofilm formation is a trait to some extent controlled by the studied nutritional conditions and the genetic makeup of the strain. Strikingly, the iron influence studies revealed that the bioavailable ferrous iron (Fe(II)) is a factor of a substantial impact on the P482 biofilm formation capabilities. On the other hand, Fe(III) supplementation shows almost no influence over this trait of P482, regardless of the carbon source conditions. This implies the importance of iron bioavailability for biofilm formation in P482 wt and its mutants. Nevertheless, this study is limited because it only explores several factors, that might interact with P482 biofilm development.

# 10. Discussion

The research presented in this thesis can be divided into three groups of experiments of different aims:

1. Development of "tools" that could be implemented in the subsequent experiments.
2. Assessment of the effect of carbon source (glucose/glycerol) on P482, its antimicrobial activity and biofilm formation.
3. Assessment of the effect of iron source (Fe(II) or Fe(III)) on P482, its antimicrobial activity and biofilm formation.

The following discussion adheres to this order, and it is summed up with a short overview on the significance of the study in terms of the potential application of P482 as a biocontrol agent.

## 10.1. Development of applicable "tools" as a part of the study

Parts of the presented study were based on the implementation of particular "tools" which had to be created specifically for the *Pseudomonas donghuensis* P482 research. The developed set of implements includes:

- the iron metabolism-related mutants of P482,
- the functional information about the ORFs of the gene "cluster 17",
- the set of reference genes for the RT-qPCR gene expression analysis.

The generation and analyses of these "tools" are discussed in the following subsections.

### 10.1.1. Targeted iron metabolism genes are not essential for P482 antibacterial activity

To investigate the nutritional dependencies of *P. donghuensis* P482 antimicrobial activity and biofilm formation, its mutants with insertions inactivating certain genes were used throughout the study. Particular mutants (KN4705, KN4706, KN4709, KN1009, KN3755) were derived by Krzyżanowska *et al.*, 2016, in the investigation which revealed the regions of the P482 genome that are involved in its antagonism against bacterial plant pathogens. These regions were found to be responsible for the biosynthesis of 7-hydroxytropolone [7-HT] and pyoverdine [PVD] – compounds that share a common trait, namely, they are both iron scavengers (Jiang *et al.*, 2016, Visca *et al.*, 2007). Following this lead, iron metabolism had been assumed to contribute to the antimicrobial activity of P482. The fact that iron availability, acquisition and management can influence the production of secondary metabolites by *Pseudomonas* spp. is well established (Escolar *et al.*, 1999, Lim *et al.*, 2012). This premise prompted this study not only to include iron ions as a

variable in the environment, but also to use P482 mutants with disrupted iron metabolism to find out how it affects the analysed attributes of this strain.

Among the genes selected as the candidates for inactivation were those encoding i.a., the ferric uptake regulator [Fur] protein, ferredoxins and iron ion transport proteins. The mutants (KN0255, KN0562, KN2408, KN4870, KN4879) were obtained during the study, however, under the standard culture conditions (rich, undefined growth medium), their antibacterial activity and production of 7-HT and PVD remained unchanged with respect to P482 wt. Little is known about the way these genes may contribute to the biocontrol traits of P482. However, the *fur* gene disruption was hypothesised to considerably interfere with P482 physiology as in various *Pseudomonas* spp. the Fur repressor is known to control numerous cellular processes, such as quorum sensing, biofilm formation, pathogenicity (Banin *et al.*, 2005, Cha *et al.*, 2008, Zhou *et al.*, 2015). The *fur*⁻ mutant of P482 (KN4870) does not seem to be affected in the antibacterial activity and iron chelators production under the rich medium conditions. However, it is important to note that Fur inactivation effect might be nutrient- and strain-dependent. P482 is the first *P. donghuensis* strain in which Fur is explored. Meanwhile, the substantial difference in Fur function among various *Pseudomonas* species was reported as this regulator is essential for growth and survival of *P. aeruginosa* on solid media, while it is not essential in other species of *Pseudomonas* (Pasqua *et al.*, 2017). This was shown to be a result of the toxicity of pyochelin, a siderophore which is produced excessively in *fur*⁻ mutants of *P. aeruginosa* and accumulated in the spot of colony formation on solid medium.

The only trait that significantly diversified the mutants of P482 obtained in the study from the wild type strain was the altered morphology of the macrocolonies, especially those formed by the *fur*⁻ mutant. The distinct structure of KN4870 colonies might indicate the involvement of Fur in biofilm formation processes in P482. This correlation of macrocolony structure and biofilm was observed in the case of various mutants of *P. aeruginosa* (Cabeen *et al.*, 2016). The mechanism of Fur involvement in biofilm formation was described in detail for *Yersinia pestis* (Sun *et al.*, 2012). Fur, being a transcriptional repressor, inhibits the biosynthesis of HmsT, a diguanylate cyclase which is crucial for the production of 3′, 5′-cyclic diguanylic acid [c-di-GMP], a signalling molecule. An important role of c-di-GMP in *Y. pestis* is the activation of biofilm formation by triggering exopolysaccharide biosynthesis. Thus, a mutation in *fur* gene region can intensify biofilm formation. These findings agree with studies on *P. aeruginosa* which showed that its Fur mutant, producing ample amounts of pyoverdine, forms more complex ("mushroom-like") biofilm structures (Banin *et al.*, 2005).

Although the other mutant exhibiting changed colony morphology, *iscA*⁻ (KN0255) was not selected for further tests, it is worth noting that the iron-dependent biofilm formation can be influenced by the proteins taking part in iron-sulphur cluster assembly. Such finding was reported

for *Escherichia coli*, in which the *iscR* mutation inactivating the IscR (iron-sulphur cluster regulator protein) production caused biofilm disruption by the decrease in type I fimbriae-related gene expression (Wu and Outten, 2009).

Due to the general importance of the Fur repressor for *Pseudomonas* biology, the KN4870 mutant was selected for further experiments under controlled nutritional conditions which are presented in this thesis and discussed in the following sections. To date, the presented study is the only account of *fur* gene inactivation in *P. donghuensis,* therefore more research is needed to fully understand the role of this gene in P482 biology.

### 10.1.2. The first analysis and description of gene "cluster 17" and its novel traits

In the course of this study, a previously underinvestigated gene cluster, called "cluster 17" was explored due to its potential involvement in P482 antimicrobial activity. This group of genes was initially singled out during the previous studies conducted at the LPM. These analyses used antiSMASH 2.0, which is a web-based tool for identifying novel gene clusters possibly engaged in biosynthesis of secondary metabolites (Blin *et al.*, 2013). This genome mining investigation of *P. donghuensis* P482 with an additional use of the ClusterFinder algorithm (Cimermancic *et al.*, 2014) revealed 23 interesting genomic regions, most of them potentially engaged in a production of a novel or atypical metabolite (Krzyżanowska *et al.*, 2016). Among them, one cluster, "cluster 17", was annotated as possibly involved in polyketide synthesis.

Sequences of most of the genes belonging to this cluster are highly uncommon among the genomic databases. The uniqueness of "cluster 17" was also confirmed with further antiSMASH analyses (versions 5.0 and 6.0), which did not recognise this group of ORFs as a candidate biosynthetic cluster. The gene annotated as the polyketide synthase/cyclase [PKS], BV82_4238 (**TABLE 13**), is surrounded by other ORFs that might be involved in the process of polyketide production, however the functional information about them is yet insufficient to present any conclusions. On one hand, the nonmodular, type II and III polyketide synthase clusters are common in pseudomonads and reveal a substantial diversity in ORFs function and organisation (Gross and Loper, 2009). On the other hand, the potential fatty acid desaturase (BV82_4241, **TABLE 13**) could point to the cluster being involved in fatty acid synthesis [FAS]. Moreover, in one curious case, a hybrid cluster discovered in *Serratia plymuthica* encodes enzymes related to PKS, FAS and non-ribosomal peptide synthase [NRPS] (Masschelein *et al.*, 2013). This interesting combination of biosynthetic potential is used by *S. plymuthica* to produce three zeamine-related antibiotics.

Herein, the gene "cluster 17" was shown to be involved in the antibacterial activity of P482. This study focused on investigating two loci of "cluster 17" – BV82_4240 and BV82_4243, both to some extent responsible for the antagonistic phenotype of P482. The BV82_4240 locus encodes an enzyme of the short chain dehydrogenase/reductase [SDR] family. This group of NAD(P)H-

dependent enzymes is ubiquitous in all prokaryotes and eukaryotes, being vital catalysts of many metabolic reactions with a diverse range of substrates (Jörnvall *et al.*, 1995). Several SDRs have been described to take part in the synthesis of secondary metabolites (i.e., antimicrobials) by various microorganisms including pseudomonads (Cao *et al.*, 2019, Mattheus *et al.*, 2010, Mo *et al.*, 2020). Moreover, the 7-HT biosynthetic gene cluster of P482 also includes a gene encoding an SDR (Krzyżanowska *et al.*, 2016).

The second explored ORF, BV82_4243, encodes a protein predicted to a part of an efflux pump system. It is an ortholog of EmrA from *E. coli*, a membrane adapter protein in the tripartite transport system. The two other ORFs building the operon together with BV82_4243 encode the remaining components of the efflux pump system. The product of gene in locus BV82_4244 was annotated as EmrB, the inner cell membrane transporter protein, while the product of BV82_4245 is an ortholog of a TolC protein, the part of the transporter located in the outer membrane of the bacterial cell. Together they form the pseudomonad counterpart to the EmrAB-TolC system, an efflux pump belonging to the major facilitator superfamily [MFS], best described for *E. coli* (Alav *et al.*, 2021, Lomovskaya and Lewis, 1992). Interestingly, the EmrAB orthologs have not been well researched in *Pseudomonas* s. Up to date, the only report of their activity in *P. aeruginosa* suggests that they participate in its resistance to carbenicillin, chloramphenicol and nalidixic acid (Heacock-Kang *et al.*, 2018). In general, the MFS pumps are known to transport a wide range of compounds out of Gram-negative and Gram-positive bacterial cells. They can pump out antibiotics, siderophores, toxic metabolites and more, however deciphering their specific functions in pseudomonads still requires more research (Alav *et al.*, 2021). In this study, the mutation of the putative *emrA* gene in P482 (KN4243 mutant) resulted in the absence of 7-HT and PVD in the post-culture supernatant. Thus, it is possible that this inactivated MFS transport system participates in the secretion of these compounds by P482. It is especially interesting in the case of PVD secretion. Up to date, the PVD release by pseudomonads was linked with the resistance-nodulation-division [RND] transporters (MdtABC-OpmB and MexAB-OprK; Henríquez *et al.*, 2019, Poole *et al.*, 1993), the ATP-binding cassette [ABC] transporters (PvdRT-OpmQ; Hannauer *et al.*, 2010) and the type 6 secretion system [T6SS] (Chen *et al.*, 2016). However, no reports exist connecting the MFS-type transporters with PVD. Therefore, this part of the study, published in Matuszewska *et al.* (2021), presents the first suggestion of the EmrAB-TolC-like transporter involvement in PVD secretion by *Pseudomonas* spp. Upon that, more research elucidating information on the actual products of ORFs from "cluster 17" and their biosynthetic mechanism could be a fruitful area of further work.

### 10.1.3. A set of three RT-qPCR reference genes was established for P482

Prior to the gene expression studies, it was fundamental to perform a comprehensive evaluation of the most suitable and stably expressed reference genes [RGs] in *P. donghuensis* P482.

Among the ten preselected P482 housekeeping genes, three were found to be the most stable, namely *gyrB*, *mrdA*, and *rpoD*.

The importance of the stringent RG selection lies in the fact that the expression stability of the selected genes affects the entire result datasets of the target gene expression studies. Since the publication of the MIQE guidelines for designing RT-qPCR studies (Bustin *et al.*, 2009) it has become a more popular practice to perform detailed research to determine the most stable RGs, however, it is still overlooked in many published, peer-reviewed studies (Rocha *et al.*, 2015). Moreover, it is a common misconception that one RG is enough to obtain reliable RT-qPCR results. The flaw of such study design and the importance of using multiple well validated RGs instead of just one peer-recommended RG has been demonstrated in various studies (Van Acker *et al.*, 2019, Linardić and Braybrook, 2021, Vandesompele *et al.*, 2002). In the presented study, the malpractice of selecting only one RG was counteracted with using the geNorm V algorithm to predict how the number of the selected RGs would affect the future data. The geNorm V results put together with an interpretation offered by the developers (Vandesompele *et al.*, 2002) showed that adding a third RG to a set of two would change the outcome of the gene expression studies significantly, whereas adding a fourth RG would not affect it. This suggestion led to using the three selected genes as a reference throughout the following RT-qPCR experiments on P482 RNA samples.

Among other reasons for a proper selection of multiple RGs are the studies which show that factors other than expression stability, such as disproportion in RGs transcript abundance and differences in chemical stability between rRNA and mRNA, may influence the outcome of an RT-qPCR analysis (Desroche *et al.*, 2005, Deutscher, 2006). These conclusions contradict the prevalent use of 16s rRNA as an arbitrarily selected RG. In order not to introduce this possible distortion of the results, the P482 16s rRNA gene was not included in the RGs evaluation study.

Nowadays, the proper identification of RGs is slowly becoming a rather standard practice in the microbiological research on gene expression. Thus, multiple reports on various bacterial strains, including *Pseudomonas* spp., are being published that focus solely on this task (*i.a.* Bai *et al.*, 2020, García-Laviña *et al.*, 2019, Krzyżanowska *et al.*, 2019). The presented investigation is a part of this good practice adjustment and it is the first account of RGs selection in *P. donghuensis*. Moreover, it was successfully published as a part of the main paper containing findings from this PhD project (Matuszewska *et al.*, 2021).

## 10.2. Role of glucose and glycerol in the antagonistic profile of P482

Glucose and glycerol are among the simplest, most used and best studied carbon sources in microbiology, both in industry and research sectors. Although the nutritional situation in the plant rhizosphere is much more complex than in the laboratory, the plant exudates often contain these

compounds and the root colonising bacteria get affected by their presence (Bais *et al.*, 2006, Neumann *et al.*, 2014, Sasse *et al.*, 2018). In turn, this influence leads to the development of various metabolic/transcriptomic responses to the carbon sources in the rhizosphere isolates (Mavrodi *et al.*, 2021). While the complexity of the root exudates as a growth medium would allow for observing their overall effect on the microorganism's phenotype, using a minimal medium formulation with a single carbon source (in this study this was either glucose or glycerol) can provide insight into specific mechanisms which are employed by bacteria utilising it.

The secondary metabolism of *Pseudomonas* spp. has been repeatedly shown to be influenced by the carbon sources explored in this study. The most common carbohydrate, glucose, as a sole carbon source in the medium, represses the production of such noteworthy compounds as pyoluteorin (Schnider *et al.*, 1995) and pyocyanin (Korth, 1973) in various pseudomonads. Interestingly, in *P. protegens* CHA0, glucose positively regulates the synthesis of 2,4-DAPG, however at the same time it represses the production of pyoluteorin (Duffy and Défago, 1999). Glucose was also found to be an effective carbon source for the synthesis of phenazine-1-carboxylic acid in *P. fluorescens* 2-79 (Slininger and Shea-Wilbur, 1995).

Glycerol, on the other hand, affects the pseudomonad secondary metabolism in a different manner than glucose. It positively influences the synthesis of pyoluteorin in *P. protegens* Pf-5 and CHA0 (Duffy and Défago, 1999, Kraus and Loper, 1995), synthesis of rhamnose in *P. fluoresecens* HW-6 and the formation of biofilm by *P. aeruginosa* (Scoffield and Silo-Suh, 2016). Recently glycerol gained attention as a redundant byproduct of biodiesel fuel production. In order to eliminate the problem of excess glycerol waste, substantial efforts are undertaken to develop sustainable ways of its application (Monteiro *et al.*, 2018). One of such methods is utilising glycerol as a cost-effective substrate for industrial microorganisms to convert it into valuable products (Almeida *et al.*, 2012). *Pseudomonas* spp. are among the most promising biocatalysts and have already been employed as such in multiple studies (Borrero-de Acuña *et al.*, 2021, Liu *et al.*, 2018, Pappalardo *et al.*, 2014)

Although the diverse effects of glucose and glycerol utilisation on the production of valuable secondary metabolites by *Pseudomonas* spp. are indisputable, they have not been explored in *P. donghuensis* prior to this study. Thus, the presented conclusions from the experimental work on P482 are the first reports of how this regulation might look in this species.

### 10.2.1. Glycerol as the lag phase inducer in minimal media

*Pseudomonas* spp. are often recognised for the versatility of nutritional conditions they tolerate. *P. donghuensis* P482 exhibits efficient growth in the undefined media, abundant in various amino acids and carbohydrates, but also in minimal media containing only necessary inorganic ions and single carbon and nitrogen sources which it is capable of utilising. Among these carbon sources are the ones explored in this study: glucose and glycerol. The growth curves obtained show

that P482 proliferates catabolising both of these carbon sources, but in the case of glycerol the onset of the log phase is delayed by ~12 hours relative to when glucose serves as a carbon source. This phenomenon was studied before in *Pseudomonas putida* KT2440 and the transcriptomic rearrangement of the catabolism was proven to take place in KT2440 cells during the prolonged lag phase on glycerol (Nikel *et al.*, 2015a). Moreover, Nikel *et al.* (2014) showed that the commonly observed prolonged lag phase in *P. putida* grown on glycerol might result from a general regulatory rearrangement of metabolic pathways to optimise growth efficiency. This systemic reorganisation undoubtedly affects the microbial secondary metabolism and other physiological traits. Additionally, the expression of the KT2440 genes responsible for stress response is decreased when measured during the lag phase and it is hypothesised that glycerol might have a positive effect on *P. putida* general cell fitness and physiology (Poblete-Castro *et al.*, 2020). Both aspects of glycerol utilisation, the reorganisation of catabolism and the reduced stress, can, in turn, in various ways influence the production of certain secondary metabolites by the bacteria (Poblete-Castro *et al.*, 2020, Sarniguet *et al.*, 1995).

An interesting observation was made in the case of growth of the *gacA*⁻ mutant of P482 (KN3318) as its lag phase under minimal media conditions without iron supplementation was markedly shortened in comparison with the wild type. This phenomenon has already been discerned in *P. protegens* CHA0 *gacA*⁻ mutant cultured in MG medium, another type of a defined growth medium (Takeuchi, 2018). Gac/Rsm pathway is one of the components of the pseudomonad stress response and the mutations inactivating this pathway may cause increased sensitivity to various stress factors (Heeb and Haas, 2001, Heeb *et al.*, 2005). It also plays key roles in secondary metabolism, iron acquisition, biofilm formation and motility which are all crucial traits of the plant-associated *Pseudomonas* spp. (Ferreiro and Gallegos, 2021). Because of the wide range of molecular processes controlled by the Gac/Rsm pathway, the reduced time of the *gacA*⁻ mutants lag phase cannot be easily explained without additional experimental research. Nonetheless, it poses a question about the GacA protein importance in control of proliferation and general fitness of pseudomonads which can be a suggestion of the future studies' direction.

### 10.2.2. Glucose and glycerol as carbon sources modulate secondary metabolism and biofilm formation in the wild type P482

While this study's main insight results from the exploration of the carbon/iron source impact on the relevant P482 mutants, the first analyses of each experiment always concerned the wild type strain. The P482 wt antimicrobial activity, metabolome and biofilm formation are all to some extent dependent on the carbon source. Analysing these traits under minimal nutritional conditions with glucose or glycerol allowed not only for the comparison of the carbon source effect on them, but also provided reference for the further mutant studies.

The antimicrobial activity of P482 wt on glycerol was shown to be weaker than on glucose. However, the most probable cause for this result is not the decreased level of antimicrobials' biosynthesis, but simply the issue of the growth rate of P482 on glycerol being much slower than this of a pathogen. The additional analyses carried out to verify if the hypothesis might be viable suggest that e.g., *Dickeya solani* utilises glycerol in a minimal medium more efficiently than *P. donghuensis*, without the prolonged lag phase (**SUPPLEMENTARY FIGURE 3**). However, the hypothesis of this being the reason for P482 having weaker anti-pathogen activity on glycerol requires further research.

The metabolomic analysis of extracts of P482 wt secondary metabolites produced in three different media (0.1 TSB, M9 + glucose and M9 + glycerol) visualises the immense difference between microbial secondary metabolism in an environment abundant in various nutrients and in a simple one with nutritional limitations. These results expectedly show that numerous compounds are produced by P482 only in a nutrient rich environment, where all the essential precursors are present and the energy supply is sufficient for more than primary metabolism (Breitling *et al.*, 2013, Frimmersdorf *et al.*, 2010, Ruiz *et al.*, 2010). The analyses also reveal the difficulties of investigating the effects of single carbon sources on bacterial metabolome. On one hand, minimal media provide too little nutrients to switch on the robust secondary metabolism. On the other hand, the direct comparison of the carbon sources effects on microbial phenotype is impossible when the media are more complex. Nevertheless, the fact that the difference between glucose and glycerol as sole carbon sources did not significantly affect the P482 metabolome builds on the comprehensive analysis by Van Der Werf *et al.* (2008). Their study on *P. putida* S12 presented evidence that the metabolic profiles after S12 growth on four various carbon sources (fructose, glucose, gluconate and succinate) are very similar, differing mostly in concentration of several detected compounds. Additionally, a study on the metabolome of *P. aeruginosa* showed that during the growth under minimal nutritional conditions, bacteria mostly engage the metabolic pathways directly related to the utilisation of the given carbon source, while the secondary metabolism is reduced (Frimmersdorf *et al.*, 2010). This notion was the basis for the subsequent part of this study in which the metabolome of P482 mutants was compared, however, the profiles were obtained from rich media cultures, to provide more robust secondary metabolism.

In the last part of this study, the influence of carbon sources on the biofilm formation by P482 wt was assessed using the crystal violet staining assay. No significant differences were observed between P482 wt biofilm on glucose and on glycerol. The crystal violet staining assay is commonly analysed in a quantitative way but the flaws of this approach have been criticised (Azeredo *et al.*, 2017). In this study, multiple biological replicates were used and cells were washed avoiding their contact with air-liquid interface to assure the assay's reliability (Gómez-Suárez *et al.*, 2001). Nevertheless, the standard deviation values were relatively high. The imperfection of the

assay might be a result of uncontrollable external conditions; thus, all the data interpretation should be approached cautiously.

Although no previous studies on the conditions influence on biofilm in *P. donghuensis* were published, this study does not fully support the conclusions of similar studies in other *Pseudomonas* spp. For example, in *P. aeruginosa,* biofilm formation seems to be considerably promoted by glycerol as the carbon source (Scoffield and Silo-Suh, 2016). Glycerol was also observed to enhance biofilm formation in *P. fluorescens* WCS365 (O'Toole and Kolter, 1998). Despite the fact that P482 wt does not form biofilm more effectively on glycerol compared to glucose, the differences were observed for the biofilm formed by its mutants, and they are discussed in the following sections.

### 10.2.3. Vital P482 genomic regions and their relation to carbon sources

*P. donghuensis* P482 exhibits antagonistic behaviour which varies in its intensity depending on the available nutrients, the pathogen towards which the antagonism is displayed, but also the inactivating mutations in particular genomic regions. It is known that antibacterial activity of P482 is complex due to the fact that not just one, but several genomic regions are responsible for biosynthesis of potentially antimicrobial metabolites (**SUPPLEMENTARY TABLE 1**). One of these regions is the 7-HT biosynthesis gene cluster (described together with the *gacA* gene), another "region" is in fact three distant loci encoding proteins significant in PVD biosynthesis and the Fur regulator. The presented study shows that a third region called "cluster 17" is more vital to P482 antibacterial activity than it was previously believed (Maciąg, MSc thesis, 2015), however, its importance is revealed only under specific nutritional conditions. The following paragraphs discuss all three regions/functions and their importance in the light of carbon source influence on P482.

#### 10.2.3.1. 7-hydroxytropolone: 7-HT biosynthetic gene cluster and Gac/Rsm pathway

7-hydroxytropolone [7-HT] is the most often reported metabolite of *P. donghuensis*, it has been described as a broad-range antimicrobial, nematicide and an iron chelator (Gui *et al.*, 2020, Jiang *et al.*, 2016, Muzio *et al.*, 2020, Tao *et al.*, 2020). Its biosynthesis has been linked to a particular gene cluster – the inactivation of genes located in this cluster attenuates all the *P. donghuensis* traits attributed to 7-HT and such mutants are shown not to secrete this compound under rich medium conditions (Chen M. *et al.*, 2018, Krzyżanowska *et al.*, 2016, Muzio *et al.*, 2020). These mutants of P482 (KN4705, KN4706 and KN4709) have been used during this study to explore the effect that glucose and glycerol as carbon sources might have on 7-HT-dependent antimicrobial potential of P482. The direct antagonism tests showed that the antibacterial activity of these mutants is indeed reduced by about 50% with respect to the wild type's activity, but only when the tests were performed under conditions with glucose as a sole carbon source. When glycerol was the carbon

source, the antagonism of the 7-HT-deficient mutants was comparable to that of the wild type strain. It suggests that the 7-HT-related antibacterial activity is insignificant in P482 under glycerol conditions, but since this activity is still present, alternative antagonistic mechanisms take over. The reduced significance of the 7-HT cluster in P482 cultured in glycerol medium was confirmed in the gene expression tests, which revealed that glycerol decreases the expression of the 7-HT biosynthesis cluster genes in P482 in comparison to glucose.

Surprisingly however, 7-HT production was not detected at all in P482 wt cultured in minimal medium M9, regardless of the carbon source. Moreover, although the 7-HT genes were found to be important for the P482 antibacterial activity on M9 with glucose towards i.a., *Dickeya solani* IFB0102, the filtrate from the minimal medium culture of this pathogen also does not stimulate 7-HT production in P482. The hypothesis that compounds secreted by IFB0102 might modulate antimicrobials production by P482 came from the published reports of such interspecies interactions between various microorganisms (Bertrand *et al.*, 2014, Ezaki *et al.*, 1993, Traxler *et al.*, 2013, Vinale *et al.*, 2017), although it did not prove right in the case of P482 and IFB0102. The puzzling lack of 7-HT in P482 secondary metabolites extracts might have several causes. Firstly, the addition of IFB0102 supernatant does not take the other direction of signalisation into account – P482 might be releasing compounds that trigger IFB0102 to produce modulators of P482 activity. A co-culture would be an optimal way to test this idea (Bertrand *et al.*, 2014), however it is problematic due to the fact that P482 substantially inhibits the growth of IFB0102. Nevertheless, it is an intriguing topic for further studies on metabolic pathways of P482. It is also plausible that the 7-HT production might be induced only on the solid media, as the regulation of bacterial metabolism might be significantly rearranged due to the colony formation (Pasqua *et al.*, 2017). Another explanation of the 7-HT absence in the described extracts is that M9 minimal medium might not contain the necessary precursors for 7-HT biosynthesis, thus the gene expression alone would not equal the synthesis of the final product (Iwai and Ömura, 1982, Pan *et al.*, 2019). However, in the case of P482 it is unclear as the biochemical pathway of 7-HT biosynthesis in *P. donghuensis* is not well understood and needs further research. The future studies could be based on the recently elucidated dihydroxytropolone biosynthetic pathway in *Streptomyces* spp. (Chen X. *et al.*, 2018). Interestingly, glucose is shown to be a substrate in this process, which supports the conclusion of glucose rather than glycerol promoting the 7-HT genes' expression and their importance in antimicrobial activity of P482.

The expression of 7-HT gene cluster *P. donghuensis* HYS$^{T}$ is known to be regulated by a mechanism involving Gac/Rsm global regulatory pathway (Yu *et al.*, 2014). GacA and GacS positively regulate the expression of further regulators: LysR and TetR/AcrR which in turn induce the expression of 7-HT (Chen M. *et al.*, 2018). This positive regulation is observable also in this study on *P. donghuensis* P482. The *gacA*$^{-}$ mutant of P482 (KN3318) does not produce 7-HT when

cultured in the rich medium and the situation is analogous for all the mutants in genes from the 7-HT cluster. Even though the final product is not present in minimal media, the gene expression of 7-HT biosynthesis genes is lower on glycerol than on glucose and this also applies to *gacA* gene. Based on the regulatory pathway described by Chen M. *et al.* (2018) and the levels of the downregulation of tested genes' expression, the results suggest that the reduction of antimicrobial significance of the P482 7-HT cluster in the glycerol medium (compared to the glucose medium) starts with the reduced expression of GacA, which leads to the reduced expression of BV82_4705 (encoding the TetR/AcrR regulator), which eventually leads to the reduced expression of BV82_4706 and BV82_4709 (encoding the biosynthetic proteins).

In the case of P482 biofilm formation abilities on glucose and glycerol, no abnormal biofilm formation performance was observed in the tested 7-HT cluster mutants (KN4706 and KN4709). The current literature does not report any exploration of the *P. donghuensis* 7-HT biosynthetic cluster in biofilm formation; hence, this analysis is the first showing that inactivation of these genes does not affect the P482 capability to develop abiotic biofilm. It is, however, worth noting that the *gacA*$^{-}$ mutant (KN3318) exhibits a clear reduction in biofilm formation abilities when cultured on glycerol, but not on glucose. Gac/Rsm signal transduction pathway in biofilm formation has been most extensively described for the clinically relevant *P. aeruginosa*, where GacA was established as an essential regulator for the development of biofilms (Parkins *et al.*, 2001). In plant-associated pseudomonads the situation with Gac/Rsm contribution to biofilm formation process is not yet settled (Ferreiro and Gallegos, 2021). In *P. chlororaphis* O6, the biofilm formed by the *gacS*$^{-}$ mutant was found to be controlled by the carbon source. In this case, mannitol, as opposed to sucrose, promoted biofilm formation by the GacS-deficient O6 mutant (Kim *et al.,* 2014). In *P. putida,* the closest relative of *P. donghuensis* for whom data can be found, the defective Gac/Rsm system (by *gacS* inactivation) causes a partial deficit in biofilm forming abilities (López-Sánchez *et al.*, 2016). Nevertheless, the data were obtained only for the LB medium environment and no nutritional regulation was tested in this case, thus the apparent importance of *gacA* in P482 biofilm formation only when glycerol serves as a carbon source is an unprecedented result.

Up to date, all the known studies on *P. donghuensis* and its production of 7-HT have utilised rich, undefined growth media which contain numerous carbon source compounds, such as LB or King's B medium [MKB], which is typically used to obtain high levels of siderophore production and was utilised to obtain high yields of 7-HT and other secondary metabolites (Jiang *et al.*, 2016, Muzio *et al.*, 2020). Prior to this study, the nutritional regulation of 7-HT biosynthesis remained unexplored. Nevertheless, further research is needed to fully understand which steps of the regulation pathway of 7-HT biosynthesis are impacted by glucose and glycerol.

#### 10.2.3.2. Pyoverdine: PVD biosynthesis genes and Fur regulator

One of the features of fluorescent pseudomonads that might be influenced by the carbon source is siderophore production. *P. donghuensis* P482 produces fluorescent pyoverdine [PVD], however the carbon source regulation of its biosynthesis has not been researched prior to this study (Krzyżanowska *et al.*, 2016). Here, two P482 mutants in the genes responsible for PVD biosynthesis, KN1009 and KN3755 were used. Both of the mutants have insertions in genes encoding non-ribosomal peptide synthase components. The inactivation of these genes was highly influential under both glucose and glycerol conditions without iron supplementation. The KN1009 and KN3755 mutants exhibited from zero to maximum 50% of the wild type strain's antimicrobial activity depending on the pathogen and the carbon source. This shows that in the iron-depleted conditions, the PVD-mediated pathogen's growth inhibition is remarkably important. This concept is not novel and it has been discussed in the most prominent literature regarding this topic (Haas and Défago, 2005, Visca *et al.*, 2007).

An intriguing finding was revealed in the UV-Vis spectra of the post-culture supernatants of KN1009 and KN3755. As expected, the mutants do not produce PVD under any of the tested nutritional conditions. What is striking, is that they appear not to produce also 7-HT. While we are aware of the Gac/Rsm LysR and TetR/AcrR regulatory pathways' roles in the 7-HT biosynthesis (Chen M. *et al.*, 2018), we have not yet elucidated the entire biochemistry behind it. The lack of 7-HT production in PVD mutants of P482 might be a result of the 7-HT biosynthesis being regulated (directly or indirectly) by PVD or its biosynthetic enzymes. This observation might be a noteworthy direction for the future studies.

In *Pseudomonas* spp., the PVD biosynthesis regulation relies on ferric uptake regulator [Fur] and a number of other regulators (Cornelis *et al.*, 2022, Frangipani *et al.*, 2014, Venturi *et al.*, 1995). This suggests that the regulatory mechanism of PVD production might be as complex in *P. donghuensis*. Nevertheless, the Fur-deficient P482 mutant was also included in the study to observe the effects of Fur on relevant functions of P482 under the tested conditions of carbon and iron source availability.

Iron deficiency is the most straightforward way to enhance the yields of siderophores (Neilands, 1984). Thus, the role of carbon sources in this process has not been particularly widely researched. Moreover, the literature gathered on the carbon source regulation of siderophore biosynthesis presents the research on the role of glucose and glycerol as inconclusive. This is because the definition of a siderophore encompasses a vast array of compounds which can differ significantly in their structure (hydroxamate, catecholate, mixed and other), depending on their producer and the biosynthetic genes/proteins (comprehensively reviewed by Hider and Kong, 2010). Thus, the nutritional regulation of their biosynthesis can vary. Glycerol as a carbon source was shown to enhance siderophore biosynthesis in *P. aeruginosa* (Braud *et al.*, 2007). It is also an

ingredient of King's B, a popular medium used for enhanced production of fluorescent siderophores by *Pseudomonas* spp. (King *et al.*, 1954). However, the primary carbon sources in King's B are the amino acids from peptone, which are utilised before glycerol due to carbon catabolism repression [CCR] (Rojo, 2010). It has been proposed that succinate-containing media, rather than King's B, are more appropriate for siderophore production in *P. fluorescens* (Meyer and Abdallah, 1978, Vindeirinho *et al.*, 2020). In a metabolomic study of the influence of carbon metabolism on siderophore production, Mendonca *et al.* (2020) proposed a hierarchy of metabolic pathways used by *P. putida* and *P. protegens* to favour the efficient siderophore biosynthesis and iron acquisition. They presented a comprehensive model, showing that under iron-deficient conditions, bacteria rearrange their metabolism to favour gluconeogenic substrates over the glycolytic ones. The utilisation of gluconeogenic carbon sources, such as succinate and other organic acids, results in higher siderophore secretion by pseudomonads as opposed to glycolytic substrates (e.g., glucose). The role of glucose, the other tested carbon source, in siderophore yield regulation in pseudomonads is not clear. On one hand glucose, when compared to glycerol and other carbon sources, was shown to increase the production of iron chelators in various strains of fluorescent *Pseudomonas* spp. belonging to, e.g., *P. fluorescens* and *P. protegens* species (Advinda *et al.*, 2019, Duffy and Défago, 1999). On the other hand, some studies present distinct conclusions, such as the fact that addition of glucose to the medium with succinate causes lower levels of PVD production (Barbhaiya and Rao, 1985).

In this study, the use of either glucose or glycerol did not particularly influence the outcome of the antimicrobial activity tests of the PVD genes' mutants of P482. There was also no change in the Fur-deficient mutant's activity. Moreover, these findings are supported by the P482 gene expression measurements. The levels of expression obtained for the PVD biosynthesis genes (BV82_1009, BV82_3755) and the *fur* gene are similar regardless of the carbon source. This, combined with the literature data, does not allow for establishing one universal carbon source for the production of PVD in all fluorescent pseudomonads. Thus, if necessary, the determination of the best carbon source for the siderophore biosynthesis, shall be strain-specific and resolved experimentally.

Another interesting point of the study was the carbon source dependency of the biofilm formation in the PVD genes' mutants of P482. The extensive research on *P. aeruginosa* provided data pointing to association and interplay between biofilm formation and iron acquisition (Kang and Kirienko, 2018, Llamas *et al.*, 2014). The induction of both functions, PVD biosynthesis and transition to biofilm, is caused by, *i.a.,* high intracellular levels of c-di-GMP (Coggan and Wolfgang, 2012, Frangipani *et al.*, 2014). This interdependence was also revealed in *P. putida*, which produces biofilm more efficiently when its PVD biosynthesis levels are high (Ponraj *et al.*, 2012). In this thesis, the presented results showed that carbon source metabolism might be woven into this

network of biofilm regulation in *P. donghuensis* P482. When the PVD-deficient mutant of P482, KN1009, grows on minimal medium, it forms biofilm more efficiently on glucose than on glycerol. This might indicate that glucose metabolism launches the biofilm formation when no product of BV82_1009 gene is synthesised. Surprisingly, this is not the case for KN3755, another PVD-deficient mutant of P482, implicating that the lack of PVD is not the cause of this disparity, but rather the lack of NRPS components encoded specifically by the BV82_1009 gene.

#### 10.2.3.3. "Cluster 17": differential effect of carbon source on two "cluster 17" mutants

First described by Maciąg (MSc thesis, Gdańsk, 2015), the P482 mutants with inactivating insertions in the genes of "cluster 17" did not significantly differ from the wild type strain in the levels of their direct antibacterial activity towards plants pathogens. However, the mentioned results were obtained only for the rich medium conditions (LB-agar plates). As it emerged in this study, using only one type of nutritional conditions for the antagonism tests could have led to the underestimation of this cluster's importance in P482 antibacterial activity. During the work presented in this thesis, the "cluster 17" mutants (KN4240 and KN4243) were included in the preliminary screening test (data not shown) of their antagonism towards *D. solani* IFB0102 on minimal media with glucose or glycerol as a carbon source. Surprisingly, the screening showed that both mutants are impaired in their antibacterial capabilities, although KN4240 exhibits this defective phenotype only when glycerol is the sole carbon source. These results were further confirmed with more extensive tests (section **9.3.2.3**) which showed that the antagonism of KN4243 is largely weakened regardless of the carbon source, while KN4240 entirely or almost entirely lost its ability to inhibit bacterial phytopathogens, but solely when cultured on glycerol. This suggests that these two mutated genes are not regulated by glucose/glycerol in the same way. Indeed, the bioinformatic analysis of "cluster 17" shows that genes in loci BV82_4240 and BV82_4243 belong to two different operons which possibly have very distinct functions. Thus, although these genes were investigated together, their importance will be discussed separately.

The P482 BV82_4240 insertion mutant (KN4240) has a significantly impaired antibacterial activity, but only when utilising glycerol as a carbon source. This leads to the hypothesis that an SDR encoded by this gene might be participating in a glycerol-induced biosynthesis pathway of an antimicrobial compound. What is more, this result for KN4240 contrasts with those obtained for the 7-HT cluster genes mutants (KN4705, KN4706, KN4709) whose antagonistic activity is impaired only on glucose. The corresponding gene expression results also show significant differences between the carbon source regulation of these two genomic regions in P482 – the 7-HT cluster genes are notably downregulated on glycerol in comparison with glucose, while the expression of BV82_4240 remains unchanged. Such disparities suggest that BV82_4240 gene and 7-HT

biosynthesis genes are possibly involved in unrelated, differently regulated secondary metabolism pathways.

The implication that the BV82_4240 gene product might be a part of a pathway for biosynthesis of a novel antibacterial compound is supported by the fact that both known P482 antimicrobials (7-HT and PVD) were detected in the UV-Vis spectral analysis of KN4240 post-culture supernatant (LB medium). Nevertheless, the comparison between the rich-medium (0.1 TSB) metabolome of P482 wt and KN4240 did not identify the potential novel antimicrobial. However, in the antagonism tests, the rich medium was observed not to promote the exploitation of the antimicrobial pathway involving the BV82_4240 locus, as the KN4240 mutant's antibacterial activity was not reduced compared to P482 wt. Thus, any further work on identification of the metabolite would primarily require creating the P482 growth conditions which effectively promote the biosynthesis of this compound, especially using glycerol as the carbon source.

The insertion in BV82_4240 gene resulted also in different biofilm formation levels depending on the carbon source. Glucose rather than glycerol as a carbon source caused KN4240 to form biofilm much more efficiently. Therefore, it can be concluded that under the glycerol conditions the SDR encoded in BV82_4240 locus contributes to both antagonism and abiotic biofilm formation of P482. The wide variety of roles played by SDRs in metabolism of all earthly life (Jörnvall *et al.*, 1995) shows that it is highly possible that the BV82_4240 gene product is intertwining the antagonism and biofilm formation pathways, although no particular example of it has yet been described in the literature. However, it is worth noting that the concept of the SDRs importance in *Pseudomonas* spp. biofilm has already been introduced, e.g., in a study on *P. protegens* and its unique SDR, PelX (Marmont *et al.*, 2020).

KN4243, the second P482 mutant in a "cluster 17" gene (insertion in the BV82_4243 gene encoding a component of an MFS efflux pump), exhibited markedly reduced levels of antimicrobial activity regardless of the carbon source in the medium. Furthermore, no 7-HT and PVD were detected in the post-culture supernatants of KN4243 and the levels of 7-HT detected in the KN4243 extracts were negligible, which implies that the MFS pump inactivated in KN4243 is involved in the secretion or, indirectly, in the biosynthesis of these compounds. The expression of the efflux pumps is known to be tightly controlled and only upregulated in the stress conditions which require secretion or detoxification (Pasqua *et al.*, 2019). Their regulation involving carbon sources has not been well explored, but it was found that carbohydrates can promote efflux pump expression depending on their uptake routes (Villagra *et al.*, 2012). However, in this study, no substantial carbon source (glucose/glycerol) influence was observed for any of the traits tested for the KN4243 mutant nor the expression of the BV82_4243 gene. Thus, although this region is crucial for P482 antagonism on minimal media, it is not directly affected by the glucose/glycerol alteration as the carbon source.

## 10.3. Iron ions and their regulatory impact on P482 antagonism and biofilm formation

Iron is a key element to understanding the antagonistic potential of pseudomonads. Their elaborate and efficient iron acquisition systems are among their most lethal weapons in the competition with other microorganisms (Deveau *et al.*, 2016, Dowling and O'Gara, 1994, Duijff *et al.*, 1993). Apart from the microbial interactions, iron availability has been found to modulate various functions and activities of different *Pseudomonas* spp., such as motility, biofilm formation or virulence (Banin *et al.*, 2005, Cornelis and Dingemans, 2013, Jimenez *et al.*, 2010, Kang and Kirienko, 2018, Ponraj *et al.*, 2012). Thus, the investigation of iron modulation of the most prominent traits of P482 became an important step to characterise the strain's application potential. Although the iron source and availability seem to have a profound impact on the biology of pseudomonads in general, this study revealed that in the case of P482 and its biocontrol traits it was not as pronounced as the effect of the carbon sources. On this account, the iron influence on P482 will be discussed in a briefer manner than that of glucose/glycerol.

### 10.3.1. Iron deficits enhance P482 antibacterial activity

The antimicrobial activity of P482 and other strains of *P. donghuensis* is based mainly on two compounds, 7-HT and PVD. They were both previously described as iron chelators and their biosynthesis was characterised as iron-dependent with 7-HT production being less sensitive to iron levels than PVD (Jiang *et al.*, 2016). Pseudomonads are widely known for their phenotypic plasticity, also in the case of iron chelation. *P. aeruginosa* produces two known siderophores, PVD and pyochelin (Cornelis, 2010). While this might seem redundant, it was shown to be a balanced system of a trade-off siderophore switching (Dumas *et al.*, 2013). PVD, compared to pyochelin, is metabolically more expensive, but also more efficient in iron uptake. Thus, it is produced by *P. aeruginosa* in the severely iron-limited environments. Pyochelin, on the other hand, is produced when the iron-limitation is moderate and *P. aeruginosa* can dedicate less of its energy to iron uptake. Therefore, 7-HT in *P. donghuensis* might play a role of secondary iron chelator, with a production regulation similar to that of pyochelin in *P. aeruginosa*.

The antagonistic activity of P482 wt was shown to decline after the addition of Fe(II) ions to the glucose medium. This further reinforces the claim that the iron chelators, 7-HT and PVD, play the roles of main antagonistic compounds of P482. However, this cannot be applied to the situation when the only carbon source for P482 and pathogens is glycerol. In this case, the addition of iron ions does not cause a reduction in antimicrobial activity of P482 wt, which reinforces the suggestion that the glycerol-related activity of P482 is based on other compound(s), whose biosynthesis is not regulated by iron levels. The antagonism tests using the KN4240 mutant from

"cluster 17" indicate that it the BV82_4240 gene is the most plausible genomic region responsible for this activity.

Furthermore, the tests using P482 mutants revealed that the antibacterial activity based on the genes from 7-HT cluster is only slightly, often insignificantly, modulated with the iron availability. Under the glucose conditions, this activity is about half of that of P482 wt, regardless of the iron source and availability. Surprisingly, these finding was not confirmed by the P482 gene expression results. The 7-HT biosynthesis cluster genes exhibit reduced expression when growth medium is supplemented with Fe(II). Nevertheless, just the gene expression results do not fully confirm the iron chelator role of 7-HT postulated by Jiang *et al.* (2016), whereas the mutants' antibacterial activity results suggest that the antimicrobial effect of the 7-HT cluster product is based on a mechanism other than the competition for iron. This supports the report of Muzio *et al.* (2020) on the direct antifungal activity of 7-HT. Prior to the *P. donghuensis* studies, the most researched biological role of 7-HT was the inhibition of aminoglycoside adenylyltransferases, a group of enzymes providing some bacteria with resistance to aminoglycoside antibiotics (Allen *et al.*, 1982, Kirst *et al.*, 1982). Hydroxytropolones are often recognised for their metalloenzyme inhibition (Bentley, 2008, Meck *et al.*, 2014). For example, in a recent study, a few α-hydroxytropolones (a group of compounds to which 7-HT also belongs) were characterised as the inhibitors of RNase H1 of human immunodeficiency virus [HIV] and hepatitis B virus [HBV] (Ponzar *et al.*, 2022). Therefore, it seems possible that the inhibition of some crucial enzyme in the tested plant pathogenic bacteria might be the cause for 7-HT's antimicrobial activity.

PVD is a compound the biosynthesis of which can be directly associated with the absence of readily available iron in the environment. The addition of iron was shown to diminish the antagonistic effects of various fluorescent *Pseudomonas* strains on plant pathogens (Thomashow and Weller, 1990) and this is also true for P482 cultured on glucose, but not on glycerol. Moreover, under the glucose conditions, the disruption of PVD biosynthesis genes in P482 causes its antimicrobial potential to significantly decrease, while the supplementation with iron ions makes this reduction less substantial. These results are supported by the detected changes in gene expression. The PVD biosynthesis genes are significantly downregulated by the presence of readily available Fe(II) ions in the environment. This situation represents the typical iron-related regulation of PVD biosynthesis combined with the importance of the siderophore in the antibacterial activity mechanism of P482. It is a known phenomenon that has been previously reported for, i.a., *P. fluorescens* (Leeman *et al.*, 1995), *P. chlororaphis* (Liu *et al.*, 2021a) and *P. aeruginosa* (Sass *et al.*, 2018). The surprisingly different levels of iron influence on antibacterial activity of the KN1009 and KN3755 mutants (both impaired in PVD biosynthesis) may be a result of the fact that the disrupted genes belong to separate operons (Krzyżanowska *et al.*, 2021). During the *in silico* studies, these two genes of P482, BV82_1009 and BV82_3755, were found to be related

to PVD biosynthesis as parts of the NRPS gene clusters and orthologs of *psvA/pvdL* and a part of *pvdD,* respectively (Krzyżanowska *et al.*, 2016). However, the mentioned study did not find significant association of the PVD biosynthesis genes with the antibacterial activity of P482. Moreover, the addition of 15 μM of Fe(II) did not change the outcome where KN1009 and KN3755 exhibited antagonistic activity comparable to P482 wt. The most plausible cause of the disparity between the results presented in this dissertation and the results obtained by Krzyżanowska *et al.* (2016) is the growth medium (minimal medium M9 vs LB-agar). LB-agar is an undefined growth medium, classified as iron-rich with iron content ~16 μM (Rodríguez-Rojas *et al.*, 2015). This concentration of iron is suggested to inhibit the PVD biosynthesis well enough so this compound would not contribute to the overall P482 antimicrobial potential on LB-agar.

Iron plays a minor role in the antimicrobial activity of P482 dependent on the "cluster 17" genes. The two genes explored, BV82_4240 and BV82_4243 do not seem to be related to each other in terms of their functions. Little is known about the functional characteristics of BV82_4240 thus the slight effects of iron supplementation of the medium cannot be attributed to a specific purpose of this gene. However, more functional associations were identified during this study for the other gene from "cluster 17", BV82_4243. The previously hinted function of BV82_4243 as a part of an MFS efflux pump transporting PVD, a siderophore, could suggest that iron ions would profoundly affect its expression and activity. For example, we know that a loss of another type of efflux pumps, the RND family members, can lead to iron starvation in *P. aeruginosa* (Adamiak *et al.*, 2021), but no data can be found that provide insight into how iron regulates the efflux pump biosynthesis and activity. However, we know that efflux pumps are much more versatile. Not only can they export siderophores, but also various other compounds, *i.e.*, antibiotics, which facilitates the multidrug resistance in bacteria, or virulence factors (Nishino *et al.*, 2021). Therefore, it is expected that simply the iron ion content in the environment would not be enough to stop the expression of efflux pump proteins and this seems to be true in case of BV82_4243 in P482.

### 10.3.2. P482 biofilm and its iron-dependent regulation requires detailed inquiry

Bacterial biofilm formation is known to be affected by iron levels in the environment. However, the effects of this element's presence differ between the species. While it was shown that the environmental availability of iron supports and promotes formation of biofilm in *Vibrio cholerae* (Mey *et al.*, 2005) and *E. coli* (Wu and Outten, 2009), it was also concluded that it acts otherwise in *Staphylococcus aureus* (Lin *et al.*, 2012) and *Streptococcus mutans* (Berlutti *et al.*, 2004). Since *Pseudomonas* spp. are acknowledged for the robust iron dependence of their metabolism, their biofilms were also studied with this notion in mind. The literature data indisputably attribute the environmental availability of iron with its promotion of biofilm formation in *P. aeruginosa* (Banin *et al.*, 2005, Patriquin *et al.*, 2008). Jimenez *et al.* (2010) found that the PVD biosynthesis

pathway is also involved in the process of biofilm development in *P. aeruginosa*. The most recent studies confirm this finding and show that mutations in genes encoding PVD-biosynthetic NRPSs can impact biofilm structure in *P. aeruginosa* (Díaz-Pérez *et al.*, 2022).

This study presents a basic search of the associations between biofilm formation by *P. donghuensis* P482, its genetic background (inactivation of genes involved in its antagonistic behaviour) and carbon/iron sources in the growth medium. While no remarkable differences in biofilm were found among the P482 mutants under the tested nutritional conditions, there was an observable tendency dependent on the carbon/iron source pairing. The addition of iron(II) to the glucose medium weakened the biofilm production, while when added to the glycerol medium it promoted biofilm formation. Nevertheless, this trend in results was barely observable and it requires further, more detailed exploration to be confirmed. In pseudomonads, biofilm formation and its iron dependency has been primarily researched in the clinically relevant species and isolates, human pathogens. This topic has not been extensively studied in plant-associated bacteria, even though the biofilm formation is a highly significant process for the plant colonisation (Zboralski and Filion, 2020) and despite the fact that the microbe-plant interactions are known to be regulated by iron availability (Lemanceau *et al.*, 2009). The most comprehensive study concerning the influence of iron on bacterial plant colonisation explored the TonB system of iron uptake in *P. putida* KT2440 (Molina *et al.*, 2005). When the ferrisiderophore receptor protein TonB was inactivated, KT2440 had a reduced ability to colonise maize roots and seeds. The intracellular iron content was found to be an important signal for biofilm formation. Further research in *P. putida* S11 confirmed these findings by showing that that the increased pyoverdine-mediated iron uptake results in better biofilm formation (Ponraj *et al.*, 2012). Overall, more research is needed to fully explore the impact that environmental iron has on biofilm formation and plant colonisation by plant-associated pseudomonads.

## 10.4. Significance of the study in the light of P482 application potential

One of the most remarkable attributes of *P. donghuensis* P482 is its direct antagonism towards a broad range of bacterial plant pathogens (Krzyzanowska *et al.*, 2012a, Krzyżanowska *et al.*, 2016, Matuszewska *et al.*, 2021). Although in the 20$^{th}$ century the research on fluorescent pseudomonads was predominantly dedicated towards finding the most potent agents against the fungal plant pathogens (reviewed by i.a.: Bloemberg and Lugtenberg, 2001, Raaijmakers *et al.*, 2002), the accounts of the antibacterial role *Pseudomonas* spp. metabolites also sporadically emerged in the literature (Cronin *et al.*, 1997, Lavermicocca *et al.*, 2002). In the recent years, there has been a notable surge of reports concerning pseudomonads as potential allies in combating numerous crop-infecting bacteria, such as *Xanthomonas*, *Acidovorax, Erwinia* or the pathogenic *Pseudomonas*

species – *P. syringae* (Ali *et al.*, 2022, Dagher *et al.*, 2021, Liu *et al.*, 2021b, Yan *et al.*, 2017, Yang *et al.*, 2021). Moreover, a *P. donghuensis* isolate, strain JS1, was recently established as an antagonist of *Xathomonas citri* subsp. *citri* [Xcc], however its antibacterial activity was only confirmed *in vitro* and no reduction in bacterial canker symptoms caused by Xcc on citrus plants was observed (Villamizar *et al.*, 2020). Overall, the research in this field shows the largely untapped potential of the *Pseudomonas* spp. as a diverse genus rich in bioactive metabolites. This worldwide effort also suggests that there is a need to develop more strategies to control bacterial plant pathogens.

Practical biological plant protection with the use of microorganisms including *Pseudomonas* spp. faces numerous challenges, for instance, biocontrol agent formulation, issues with agent implementation, efficacy of the given strategy, and the risk-aversion of the society. Therefore, a good understanding of the biocontrol candidate's biology and the mechanisms of its activity are necessary to provide an effective strategy of plant protection with a given agent (Barratt *et al.*, 2018, Weller *et al.*, 2007). Gaining the basic understanding about how the external conditions may affect the potential biocontrol agent could be of high significance to its eventual application. Thus, the presented study is an *in vitro* exploration of some of the basic metabolic dependencies in *P. donghuensis* P482 and their effect on its crucial biocontrol traits.

# 11. Conclusions

The presented study:

1. Partially characterised the **P482 mutants** in five genes related to **iron metabolism** (*fur*⁻ and *iscA*⁻, among others), finding **no conclusive differences** between the mutants and the wild type strain.
2. Investigated the P482 gene „**cluster 17**". BV82_4240 and BV82_4243, the two studied genes partially responsible for P482 antimicrobial activity were found to be involved in **two different mechanisms** of antagonism.
3. Found the **contribution of the principal genetic components of P482 antimicrobial activity to differ** depending on the carbon source in the minimal medium, with **7-HT genes** being **crucial** for this activity on **glucose**, **gene BV82_4240** on **glycerol**, and **PVD genes** playing a vital role on **both carbon sources**. **PVD-related** activity was also found to be **less significant** under iron-abundant conditions, while the other components were not significantly changed by the iron addition.
4. Analysed the **metabolome of P482** depending on the genetic background and the medium. **The absence of 7-HT** in all extracts of P482 **minimal media** cultures, also those stimulated with the pathogen's excretions, suggests that other antimicrobial pathway might also rely on the 7-HT biosynthesis genes.
5. Established the set of **reference genes** for RT-qPCR in *P. donghuensis* P482. Three out of ten tested housekeeping genes, namely ***gyrB, rpoD*** and ***mrdA***, were found to be most stably expressed in P482 under eleven test conditions.
6. Characterised **the expression** of the major genes contributing to the antimicrobial activity of P482 under minimal medium conditions with either **glucose** or **glycerol** as the carbon source and with or without **Fe(II)** or **Fe(III)** supplementation. The 7-HT biosynthesis genes were found to be downregulated in P482 by the utilisation of glycerol instead of glucose while the expression of other tested genes did not reveal carbon source dependencies. The abundance of easily available iron was found to downregulate the expression of PVD-related genes in P482.
7. Investigated the **abiotic biofilm of P482** and its mutants in the genes related to its antibacterial properties. The P482 biofilm formation was found to be only to an extent dependent on the nutritional conditions tested, with the addition of **Fe(II)** generally slightly **enhancing biofilm formation** in combination with **glycerol**, but **reducing** it when combined with **glucose**.

# 12. References


1. Van Acker, S. I., Van Acker, Z. P., Haagdorens, M., Pintelon, I., Koppen, C., and Zakaria, N., "Selecting appropriate reference genes for Quantitative Real-Time Polymerase Chain Reaction studies in isolated and cultured ocular surface epithelia" *Sci. Rep.*, vol. 9, no. 1, pp. 1–11, **2019**, doi: 10.1038/s41598-019-56054-1.
2. Adamiak, J. W. *et al.*, "Loss of RND-type Multidrug Efflux Pumps triggers iron starvation and Lipid A modifications in *Pseudomonas aeruginosa*" *Antimicrob. Agents Chemother.*, vol. 65, no. 10, **2021**, doi: 10.1128/AAC.00592-21.
3. Advinda, L., Pratama, I., Fifendy, M., Anhar, A., and Armaleni, "The addition of various carbon sources on growing media to increase the siderophore level of fluorescent pseudomonad bacteria" *J. Phys. Conf. Ser.*, vol. 1317, p. 012078, **2019**, doi: 10.1088/1742-6596/1317/1/012078.
4. Agaras, B. C., Iriarte, A., and Valverde, C. F., "Genomic insights into the broad antifungal activity, plant-probiotic properties, and their regulation, in *Pseudomonas donghuensis* strain SVBP6" *PLoS One*, vol. 13, no. 3, pp. 1–32, **2018**, doi: 10.1371/journal.pone.0194088.
5. Ahmed, S. A. K. S., Rudden, M., Smyth, T. J., Dooley, J. S. G., Marchant, R., and Banat, I. M., "Natural quorum sensing inhibitors effectively downregulate gene expression of *Pseudomonas aeruginosa* virulence factors" *Appl. Microbiol. Biotechnol.*, vol. 103, pp. 3521–3535, **2019**, doi: 10.1007/s00253-019-09618-0.
6. Ahn, B. E., Cha, J., Lee, E. J., Han, A. R., Thompson, C. J., and Roe, J. H., "Nur, a nickel-responsive regulator of the Fur family, regulates superoxide dismutases and nickel transport in *Streptomyces coelicolor*" *Mol. Microbiol.*, vol. 59, no. 6, pp. 1848–1858, **2006**, doi: 10.1111/J.1365-2958.2006.05065.X.
7. Akiyama, T., Williamson, K. S., and Franklin, M. J., "Expression and regulation of the *Pseudomonas aeruginosa* hibernation promoting factor" *Mol. Microbiol.*, vol. 110, no. 2, pp. 161–175, **2018**, doi: 10.1111/mmi.14001.
8. Alav, I., Kobylka, J., Kuth, M. S., Pos, K. M., Picard, M., Blair, J. M. A., and Bavro, V. N., "Structure, assembly, and function of tripartite efflux and Type 1 Secretion Systems in Gram-negative bacteria" *Chem. Rev.*, vol. 121, no. 9, pp. 5479–5596, **2021**, doi: 10.1021/acs.chemrev.1c00055.
9. Alexeyev, M. F., "The pKNOCK series of broad-host-range mobilizable suicide vectors for gene knockout and targeted DNA insertion into the chromosome of Gram-negative bacteria" *Biotechniques*, vol. 26, no. 5, pp. 824–828, **1999**, doi: 10.2144/99265bm05.
10. Ali, M. A. *et al.*, "*Pseudomonas bijieensis* Strain XL17 within the *P. corrugata* subgroup producing 2,4-diacetylphloroglucinol and lipopeptides controls bacterial canker and gray mold pathogens of kiwifruit" *Microorganisms*, vol. 10, no. 2, p. 425, **2022**, doi: 10.3390/microorganisms10020425.
11. Allen, N. E., Alborn Jr., W. E., Hobbs Jr., J. E., and Kirst, H. A., "Inhibitor of aminoglycoside-2"-O-adenylyltransferase" *Antimicrob. Agents Chemother.*, vol. 22, no. 5, pp. 824–831, **1982**, doi: 10.1128/AAC.22.5.824.
12. Almeida, J. R. M., Fávaro, L. C. L., and Quirino, B. F., "Biodiesel biorefinery: opportunities and challenges for microbial production of fuels and chemicals from glycerol waste" *Biotechnol. Biofuels*, vol. 5, p. 48, **2012**, doi: 10.1186/1754-6834-5-48.
13. Alqarni, B., Colley, B., Klebensberger, J., McDougald, D., and Rice, S. A., "Expression stability of 13 housekeeping genes during carbon starvation of *Pseudomonas aeruginosa*" *J. Microbiol. Methods*, vol. 127, pp. 182–187, **2016**, doi: 10.1016/j.mimet.2016.06.008.
14. Altschul, S. F., Gish, W., Miller, W., Myers, E. W., and Lipman, D. J., "Basic local alignment search tool" *J. Mol. Biol.*, vol. 215, no. 3, pp. 403–410, **1990**, doi: 10.1016/S0022-2836(05)80360-2.
15. Andersen, C. L., Jensen, J. L., and Ørntoft, T. F., "Normalization of Real-Time Quantitative Reverse Transcription-PCR data: A model-based variance estimation approach to identify genes suited for normalization, applied to bladder and colon cancer data sets" *Cancer Res.*, vol. 64, pp. 5245–5250, **2004**, doi: 10.1158/0008-5472.CAN-04-0496.
16. Andrews, S. C., Robinson, A. K., and Rodríguez-Quiñones, F., "Bacterial iron homeostasis" *FEMS Microbiol. Rev.*, vol. 27, no. 2–3, pp. 215–237, **2003**, doi: 10.1016/S0168-6445(03)00055-X.
17. Arseneault, T., Goyer, C., and Filion, M., "Biocontrol of potato common scab is associated with high *Pseudomonas fluorescens* LBUM223 populations and phenazine-1-carboxylic acid biosynthetic transcript accumulation in the potato geocaulosphere" *Phytopathology*, vol. 106, no. 9, pp. 963–970, **2016**, doi: 10.1094/phyto-01-16-0019-r.
18. Azeredo, J. *et al.*, "Critical review on biofilm methods" *Crit. Rev. Microbiol.*, vol. 43, no. 3, pp. 313–351, **2017**, doi: 10.1080/1040841X.2016.1208146.

19. Backer, R. *et al.*, "Plant Growth-Promoting Rhizobacteria: context, mechanisms of action, and roadmap to commercialization of biostimulants for sustainable agriculture" *Front. Plant Sci.*, vol. 9, p. 1473, **2018**, doi: 10.3389/FPLS.2018.01473.
20. Badri, D. V. and Vivanco, J. M., "Regulation and function of root exudates" *Plant. Cell Environ.*, vol. 32, no. 6, pp. 666–681, **2009**, doi: 10.1111/J.1365-3040.2009.01926.X.
21. Bai, B., Ren, J., Bai, F., and Hao, L., "Selection and validation of reference genes for gene expression studies in *Pseudomonas brassicacearum* GS20 using Real-Time Quantitative Reverse Transcription PCR" *PLoS One*, vol. 15, no. 1, pp. 1–15, **2020**, doi: 10.1371/journal.pone.0227927.
22. Bais, H. P., Weir, T. L., Perry, L. G., Gilroy, S., and Vivanco, J. M., "The role of root exudates in rhizosphere interactions with plants and other organisms" *Annu. Rev. Plant Biol.*, vol. 57, pp. 233–266, **2006**, doi: 10.1146/annurev.arplant.57.032905.105159.
23. Banin, E., Vasil, M. L., and Greenberg, E. P., "Iron and *Pseudomonas aeruginosa* biofilm formation" *Proc. Natl. Acad. Sci. U.S.A.*, vol. 102, no. 31, pp. 11076–11081, **2005**, doi: 10.1073/PNAS.0504266102.
24. Barbhaiya, H. B. and Rao, K. K., "Production of pyoverdine, the fluorescent pigment of *Pseudomonas aeruginosa* PAO1" *FEMS Microbiol. Lett.*, vol. 27, no. 2, pp. 233–235, **1985**, doi: 10.1111/j.1574-6968.1985.tb00673.x.
25. Barratt, B. I. P., Moran, V. C., Bigler, F., and van Lenteren, J. C., "The status of biological control and recommendations for improving uptake for the future" *BioControl 2017 631*, vol. 63, pp. 155–167, **2018**, doi: 10.1007/S10526-017-9831-Y.
26. Beinert, H., Holm, R. H., and Münck, E., "Iron-sulfur clusters: nature's modular, multipurpose structures" *Science*, vol. 277, no. 5326, pp. 653–659, **1997**, doi: 10.1126/science.277.5326.653.
27. Bentley, R., "A fresh look at natural tropolonoids" *Nat. Prod. Rep.*, vol. 25, no. 1, pp. 118–138, **2008**, doi: 10.1039/b711474e.
28. Berlutti, F., Ajello, M., Bosso, P., Morea, C., Petrucca, A., Antonini, G., and Valenti, P., "Both lactoferrin and iron influence aggregation and biofilm formation in *Streptococcus mutans*" *BioMetals*, vol. 17, no. 3, pp. 271–278, **2004**, doi: 10.1023/B:BIOM.0000027704.53859.d3.
29. Berman, H. M. *et al.*, "The Protein Data Bank" *Nucleic Acids Res.*, vol. 28, no. 1, pp. 235–242, **2000**, doi: 10.1093/nar/28.1.235.
30. Bertrand, S., Bohni, N., Schnee, S., Schumpp, O., Gindro, K., and Wolfender, J. L., "Metabolite induction via microorganism co-culture: A potential way to enhance chemical diversity for drug discovery" *Biotechnol. Adv.*, vol. 32, no. 6, pp. 1180–1204, **2014**, doi: 10.1016/j.biotechadv.2014.03.001.
31. Biessy, A. and Filion, M., "Phloroglucinol derivatives in plant-beneficial *Pseudomonas* spp.: Biosynthesis, regulation, and functions" *Metabolites*, vol. 11, no. 3, **2021**, doi: 10.3390/metabo11030182.
32. Blin, K., Medema, M. H., Kazempour, D., Fischbach, M. A., Breitling, R., Takano, E., and Weber, T., "antiSMASH 2.0 — a versatile platform for genome mining of secondary metabolite producers" *Nucleic Acids Res.*, vol. 41, no. W1, pp. 204–212, **2013**, doi: 10.1093/nar/gkt449.
33. Blin, K. *et al.*, "AntiSMASH 5.0: Updates to the secondary metabolite genome mining pipeline" *Nucleic Acids Res.*, vol. 47, no. W1, pp. W81–W87, **2019**, doi: 10.1093/nar/gkz310.
34. Blin, K., Shaw, S., Kloosterman, A. M., Charlop-Powers, Z., Van Wezel, G. P., Medema, M. H., and Weber, T., "antiSMASH 6.0: improving cluster detection and comparison capabilities" *Nucleic Acids Res.*, vol. 49, no. W1, pp. W29–W35, **2021**, doi: 10.1093/nar/gkab335.
35. Bloemberg, G. V. and Lugtenberg, B. J., "Molecular basis of plant growth promotion and biocontrol by rhizobacteria" *Curr. Opin. Plant Biol.*, vol. 4, no. 4, pp. 343–350, **2001**, doi: 10.1016/S1369-5266(00)00183-7.
36. Blum, M. *et al.*, "The InterPro protein families and domains database: 20 years on" *Nucleic Acids Res.*, vol. 49, no. D1, pp. D344–D354, **2021**, doi: 10.1093/nar/gkaa977.
37. Blumer, C. and Haas, D., "Mechanism, regulation, and ecological role of bacterial cyanide biosynthesis" *Arch. Microbiol.*, vol. 173, pp. 170–177, **2000**, doi: 10.1007/s002039900127.
38. Bonneau, A., Roche, B., and Schalk, I. J., "Iron acquisition in *Pseudomonas aeruginosa* by the siderophore pyoverdine: an intricate interacting network including periplasmic and membrane proteins" *Sci. Rep.*, vol. 10, p. 120, **2020**, doi: 10.1038/s41598-019-56913-x.
39. Borrero-de Acuña, J. M., Rohde, M., Saldias, C., and Poblete-Castro, I., "Fed-batch *mcl*- polyhydroxyalkanoates production in *Pseudomonas putida* KT2440 and *ΔphaZ* mutant on biodiesel-derived crude glycerol" *Front. Bioeng. Biotechnol.*, vol. 9, no. March, pp. 1–10, **2021**, doi: 10.3389/fbioe.2021.642023.

40. Braud, A., Jézéquel, K., and Lebeau, T., "Impact of substrates and cell immobilization on siderophore activity by Pseudomonads in a Fe and/or Cr, Hg, Pb containing-medium" *J. Hazard. Mater.*, vol. 144, no. 1–2, pp. 229–239, **2007**, doi: 10.1016/j.jhazmat.2006.10.014.
41. Breitling, R., Ceniceros, A., Jankevics, A., and Takano, E., "Metabolomics for secondary metabolite research" *Metabolites*, vol. 3, no. 4, pp. 1076–1083, **2013**, doi: 10.3390/metabo3041076.
42. Budzikiewicz, H., "Secondary metabolites from fluorescent pseudomonads" *FEMS Microbiol. Rev.*, vol. 104, pp. 209–228, **1993**, doi: 10.1016/0378-1097(93)90597-U.
43. Budzikiewicz, H., "Siderophores of fluorescent pseudomonads" *Zeitschrift fur Naturforsch. C*, vol. 52, pp. 713–720, **1997**, doi: 10.1515/znc-1997-11-1201.
44. Bustin, S. and Nolan, T., "Talking the talk, but not walking the walk: RT-qPCR as a paradigm for the lack of reproducibility in molecular research" *Eur. J. Clin. Invest.*, vol. 47, no. 10, pp. 756–774, **2017**, doi: 10.1111/eci.12801.
45. Bustin, S. A. *et al.*, "The MIQE guidelines: Minimum information for publication of quantitative real-time PCR experiments" *Clin. Chem.*, vol. 55, no. 4, pp. 611–622, **2009**, doi: 10.1373/clinchem.2008.112797.
46. Bustin, S. A. (Ed.), *The PCR Revolution.* Cambridge: Cambridge University Press, **2009**
47. Cabeen, M. T., Leiman, S. A., and Losick, R., "Colony-morphology screening uncovers a role for the *Pseudomonas aeruginosa* nitrogen-related phosphotransferase system in biofilm formation" *Mol. Microbiol.*, vol. 99, no. 3, pp. 557–570, **2016**, doi: 10.1111/MMI.13250.
48. Cao, Z. *et al.*, "Biosynthesis of clinically used antibiotic fusidic acid and identification of two short-chain dehydrogenase/reductases with converse stereoselectivity" *Acta Pharm. Sin. B*, vol. 9, no. 2, pp. 433–442, **2019**, doi: 10.1016/j.apsb.2018.10.007.
49. Case, R. J., Boucher, Y., Dahllöf, I., Holmström, C., Doolittle, W. F., and Kjelleberg, S., "Use of 16S rRNA and *rpoB* genes as molecular markers for microbial ecology studies" *Appl. Environ. Microbiol.*, vol. 73, no. 1, pp. 278–288, **2007**, doi: 10.1128/AEM.01177-06.
50. Caspi, R. *et al.*, "The MetaCyc database of metabolic pathways and enzymes" *Nucleic Acids Res.*, vol. 46, no. D1, pp. D633–D639, **2018**, doi: 10.1093/nar/gkx935.
51. Cha, J. Y., Lee, J. S., Oh, J. Il, Choi, J. W., and Baik, H. S., "Functional analysis of the role of Fur in the virulence of *Pseudomonas syringae* pv. *tabaci* 11528: Fur controls expression of genes involved in quorum-sensing" *Biochem. Biophys. Res. Commun.*, vol. 366, no. 2, pp. 281–287, **2008**, doi: 10.1016/j.bbrc.2007.11.021.
52. Chang, Q., Amemiya, T., Liu, J., Xu, X., Rajendran, N., and Itoh, K., "Identification and validation of suitable reference genes for quantitative expression of *xylA* and *xylE* genes in *Pseudomonas putida* mt-2" *J. Biosci. Bioeng.*, vol. 107, no. 2, pp. 210–214, **2009**, doi: 10.1016/j.jbiosc.2008.09.017.
53. Chen, M., Wang, P., and Xie, Z., "A complex mechanism involving LysR and TetR/AcrR that regulates iron scavenger biosynthesis in *Pseudomonas donghuensis* HYS," *J. Bacteriol.*, vol. 200, no. 13, pp. e00087-18, **2018**, doi: 10.1128/JB.00087-18.
54. Chen, W. J. *et al.*, "Involvement of type VI secretion system in secretion of iron chelator pyoverdine in *Pseudomonas taiwanensis*" *Sci. Rep.*, vol. 6, no. 32950, **2016**, doi: 10.1038/srep32950.
55. Chen, X. *et al.*, "Biosynthesis of tropolones in *Streptomyces* spp.: Interweaving biosynthesis and degradation of phenylacetic acid and hydroxylations on the tropone ring" *Appl. Environ. Microbiol.*, vol. 84, no. 12, pp. e00349–18, **2018**, doi: 10.1128/AEM.00349-18.
56. Cimermancic, P. *et al.*, "Insights into secondary metabolism from a global analysis of prokaryotic biosynthetic gene clusters" *Cell*, vol. 158, no. 2, pp. 412–421, **2014**, doi: 10.1016/J.CELL.2014.06.034.
57. Coggan, K. A. and Wolfgang, M. C., "Global regulatory pathways and cross-talk control *Peudomonas aeruginosa* environmental lifestyle and virulence phenotype" *Curr. Issues Mol. Biol.*, vol. 14, no. 2, pp. 47–70, **2012**, doi: 10.21775/cimb.014.047.
58. Collier, D. N., Hager, P. W., and Phibbs, P. V., "Catabolite repression control in the Pseudomonads" *Res. Microbiol.*, vol. 147, no. 6–7, pp. 551–561, **1996**, doi: 10.1016/0923-2508(96)84011-3.
59. Cornelis, P., "Iron uptake and metabolism in pseudomonads" *Appl. Microbiol. Biotechnol.*, vol. 86, no. 6, pp. 1637–45, **2010**, doi: 10.1007/s00253-010-2550-2.
60. Cornelis, P., Wei, Q., Andrews, S. C., and Vinckx, T., "Iron homeostasis and management of oxidative stress response in bacteria" *Metallomics*, vol. 3, no. 6, pp. 540–549, **2011**, doi: 10.1039/C1MT00022E.

61. Cornelis, P., Tahrioui, A., Lesouhaitier, O., Bouffartigues, E., Feuilloley, M., Baysse, C., and Chevalier, S., "High affinity iron uptake by pyoverdine in *Pseudomonas aeruginosa* involves multiple regulators besides Fur, PvdS, and FpvI" *BioMetals*, **2022**, doi: 10.1007/s10534-022-00369-6.
62. Cornelis, P. and Dingemans, J., "*Pseudomonas aeruginosa* adapts its iron uptake strategies in function of the type of infections" *Front. Cell. Infect. Microbiol.*, vol. 4, p. 75, **2013**, doi: 10.3389/fcimb.2013.00075.
63. Cronin, D., Moënne-Loccoz, Y., Fenton, A., Dunne, C., Dowling, D. N., and O'Gara, F., "Ecological interaction of a biocontrol *Pseudomonas fluorescens* strain producing 2,4-diacetylphloroglucinol with the soft rot potato pathogen *Erwinia carotovora* subsp. *atroseptica*" *FEMS Microbiol. Ecol.*, vol. 23, no. 2, pp. 95–106, **1997**, doi: 10.1111/j.1574-6941.1997.tb00394.x.
64. Cui, B., Smooker, P. M., Rouch, D. A., and Deighton, M. A., "Selection of suitable reference genes for gene expression studies in *Staphylococcus capitis* during growth under erythromycin stress" *Mol. Genet. Genomics*, vol. 291, no. 4, pp. 1795–1811, **2016**, doi: 10.1007/s00438-016-1197-9.
65. Dagher, F., Nickzad, A., Zheng, J., Hoffmann, M., and Déziel, E., "Characterization of the biocontrol activity of three bacterial isolates against the phytopathogen *Erwinia amylovora*" *MicrobiologyOpen*, vol. 10, no. 3, p. e1202, **2021**, doi: 10.1002/MBO3.1202.
66. Desroche, N., Beltramo, C., and Guzzo, J., "Determination of an internal control to apply reverse transcription quantitative PCR to study stress response in the lactic acid bacterium *Oenococcus oeni*" *J. Microbiol. Methods*, vol. 60, no. 3, pp. 325–333, **2005**, doi: 10.1016/j.mimet.2004.10.010.
67. Deutscher, M. P., "Degradation of RNA in bacteria: comparison of mRNA and stable RNA" *Nucleic Acids Res.*, vol. 34, no. 2, pp. 659–666, **2006**, doi: 10.1093/NAR/GKJ472.
68. Deveau, A. *et al.*, "Role of secondary metabolites in the interaction between *Pseudomonas fluorescens* and soil microorganisms under iron-limited conditions" *FEMS Microbiol. Ecol.*, vol. 92, no. 8, **2016**, doi: 10.1093/femsec/fiw107.
69. Díaz-Pérez, S. P., Solis, C. S., López-Bucio, J. S., Valdez Alarcón, J. J., Villegas, J., Reyes-De la Cruz, H., and Campos-Garcia, J., "Pathogenesis in *Pseudomonas aeruginosa* PAO1 biofilm-associated is dependent on the pyoverdine and pyocyanin siderophores by quorum sensing modulation" *Microb. Ecol.*, vol. 1, pp. 1–15, **2022**, doi: 10.1007/s00248-022-02095-5.
70. Dolan, S. K., Kohlstedt, M., Trigg, S., Ramirez, P. V., Kaminski, C. F., Wittmann, C., and Welch, M., "Contextual flexibility in *Pseudomonas aeruginosa* central carbon metabolism during growth in single carbon sources" *MBio*, vol. 11, no. 2, **2020**, doi: 10.1128/mBio.02684-19.
71. Dowling, D. N. and O'Gara, F., "Metabolites of *Pseudomonas* involved in the biocontrol of plant disease" *Trends Biotechnol.*, vol. 12, no. 4, pp. 133–141, **1994**, doi: 10.1016/0167-7799(94)90091-4.
72. Duffy, B. K. and Défago, G., "Environmental factors modulating antibiotic and siderophore biosynthesis by *Pseudomonas fluorescens* biocontrol strains" *Appl. Environ. Microbiol.*, vol. 65, no. 6, pp. 2429–2438, **1999**, doi: 10.1128/aem.65.6.2429-2438.1999.
73. Duijff, B. J., Meijer, J. W., Bakker, P. A. H. M., and Schippers, B., "Siderophore-mediated competition for iron and induced resistance in the suppression of fusarium wilt of carnation by fluorescent *Pseudomonas* spp." *Netherlands J. Plant Pathol.*, vol. 99, no. 5–6, pp. 277–289, **1993**, doi: 10.1007/BF01974309.
74. Dumas, Z., Ross-Gillespie, A., and Kümmerli, R., "Switching between apparently redundant iron-uptake mechanisms benefits bacteria in changeable environments" *Proc. R. Soc. B Biol. Sci.*, vol. 280, no. 1764, **2013**, doi: 10.1098/rspb.2013.1055.
75. Escolar, L., Pérez-Martín, J., and De Lorenzo, V., "Opening the iron box: Transcriptional metalloregulation by the Fur protein" *J. Bacteriol.*, vol. 181, no. 20, pp. 6223–6229, **1999**, doi: 10.1128/JB.181.20.6223-6229.1999.
76. Ezaki, M., Shigematsu, N., Yamashita, M., Komori, T., Umehara, K., and Imanaka, H., "Biphenomycin C, a precursor of biphenomycin A in mixed culture" *J. Antibiot. (Tokyo).*, vol. 46, no. 1, pp. 135–139, **1993**, doi: 10.7164/antibiotics.46.135.
77. Fernando, W. G. D., Ramarathnam, R., Krishnamoorthy, A. S., and Savchuk, S. C., "Identification and use of potential bacterial organic antifungal volatiles in biocontrol" *Soil Biol. Biochem.*, vol. 37, pp. 955–964, **2005**, doi: 10.1016/j.soilbio.2004.10.021.
78. Ferreiro, M.-D. and Gallegos, M.-T., "Distinctive features of the Gac-Rsm pathway in plant-associated *Pseudomonas*" *Environ. Microbiol.*, pp. 1462-2920.15558, **2021**, doi: 10.1111/1462-2920.15558.
79. Francis, V. I., Stevenson, E. C., and Porter, S. L., "Two-component systems required for virulence in *Pseudomonas aeruginosa*" *FEMS Microbiol. Lett.*, vol. 364, no. 11, p. 104, **2017**, doi: 10.1093/femsle/fnx104.
80. Frangipani, E., Visaggio, D., Heeb, S., Kaever, V., Cámara, M., Visca, P., and Imperi, F., "The Gac/Rsm and cyclic-di-GMP signalling networks coordinately regulate iron uptake in *Pseudomonas aeruginosa*" *Environ. Microbiol.*, vol. 16, no. 3, pp. 676–688, **2014**, doi: 10.1111/1462-2920.12164.

81. Frasson, D., Opoku, M., Picozzi, T., Torossi, T., Balada, S., Smits, T. H. M., and Hilber, U., "*Pseudomonas wadenswilerensis* sp. nov. and *Pseudomonas reidholzensis* sp. nov., two novel species within the *Pseudomonas putida* group isolated from forest soil" *Int. J. Syst. Evol. Microbiol.*, vol. 67, no. 8, pp. 2853–2861, **2017**, doi: 10.1099/IJSEM.0.002035.
82. Fravel, D. R., "Role of Antibiosis in the Biocontrol of Plant Diseases," *Annu. Rev. Phytopathol.*, vol. 26, pp. 75–91, **2003**, doi: 10.1146/annurev.py.26.090188.000451.
83. Frimmersdorf, E., Horatzek, S., Pelnikevich, A., Wiehlmann, L., and Schomburg, D., "How *Pseudomonas aeruginosa* adapts to various environments: A metabolomic approach" *Environ. Microbiol.*, vol. 12, no. 6, pp. 1734–1747, 2010, doi: 10.1111/j.1462-2920.2010.02253.x.
84. Gao, J., Xie, G., Peng, F., and Xie, Z., "*Pseudomonas donghuensis* sp. nov., exhibiting high-yields of siderophore" *Antonie Van Leeuwenhoek*, vol. 107, no. 1, pp. 83–94, **2015**, doi: 10.1007/s10482-014-0306-1.
85. Gao, J., Yu, X., and Xie, Z., "Draft genome sequence of high-siderophore-yielding *Pseudomonas* sp. strain HYS" *J. Bacteriol.*, vol. 194, no. 15, p. 4121, **2012**, doi: 10.1128/JB.00688-12.
86. García-Laviña, C. X., Castro-Sowinski, S., and Ramón, A., "Reference genes for real-time RT-PCR expression studies in an Antarctic *Pseudomonas* exposed to different temperature conditions" *Extremophiles*, vol. 23, pp. 625–633, **2019**, doi: 10.1007/s00792-019-01109-4.
87. Georgia, F. R. and Poe, C. F., "Study of bacterial fluorescence in various media: I. Inorganic substances necessary for bacterial fluorescence.," *J. Bacteriol.*, vol. 22, no. 5, pp. 349–361, **1931**.
88. Ghysels, B., Dieu, B. T. M., Beatson, S. A., Pirnay, J. P., Ochsner, U. A., Vasil, M. L., and Cornelis, P., "FpvB, an alternative type I ferripyoverdine receptor of *Pseudomonas aeruginosa*" *Microbiology*, vol. 150, no. 6, pp. 1671–1680, **2004**, doi: 10.1099/mic.0.27035-0.
89. Van Gijsegem, F., Toth, I. K., and van der Wolf, J. M., "Soft Rot *Pectobacteriaceae*: A brief overview" in *Plant Diseases Caused by Dickeya and Pectobacterium Species*, 1st ed., F. Van Gijsegem, I. K. Toth, and J. M. van der Wolf (Eds.), Springer Nature Switzerland AG , **2021**, pp. 1–11.
90. Girard, L. *et al.*, "The ever-expanding *Pseudomonas* genus: Description of 43 new species and partition of the *Pseudomonas putida* group" *Microorganisms*, vol. 9, no. 8, **2021**, doi: 10.3390/microorganisms9081766.
91. Golanowska, M., Ankiewicz, H., Taraszkiewicz, A., Kamysz, W., Czajkowski, R., Krolicka, A., and Jafra, S., "Combined effect of the antagonistic potential of selected *Pseudomonas* spp. strains and the synthetic peptide 'CAMEL' on *Pseudomonas syringae* pv. *syringae* and *P. syringae* pv. *morsprunorum*" *J. Plant Pathol.*, vol. 94, **2012**, doi: 10.4454/jpp.v94i1sup.012.
92. Gómez-Suárez, C., Busscher, H. J., and Van Der Mei, H. C., "Analysis of bacterial detachment from substratum surfaces by the passage of air-liquid interfaces," *Appl. Environ. Microbiol.*, vol. 67, no. 6, pp. 2531–2537, **2001**, doi: 10.1128/AEM.67.6.2531-2537.2001.
93. Gomila, M., Peña, A., Mulet, M., Lalucat, J., and García-Valdés, E., "Phylogenomics and systematics in *Pseudomonas*" *Front. Microbiol.*, vol. 6, p. 214, **2015**, doi: 10.3389/FMICB.2015.00214.
94. Gottesman, S., "Bacterial regulation: Global regulatory networks" *Ann. Rev. Genet*, vol. 18, no. 1, p. 441, **1984**, doi: 10.1146/annurev.ge.18.120184.
95. Gross, H. and Loper, J. E., "Genomics of secondary metabolite production by *Pseudomonas* spp." *Nat. Prod. Rep.*, vol. 26, no. 11, pp. 1408–46, **2009**, doi: 10.1039/b817075b.
96. Gui, Z., You, J., Xie, G., Qin, Y., Wu, T., and Xie, Z., "*Pseudomonas donghuensis* HYS 7-hydroxytropolone contributes to pathogenicity toward *Caenorhabditis elegans* and is influenced by pantothenic acid" *Biochem. Biophys. Res. Commun.*, vol. 533, no. 1, pp. 50–56, **2020**, doi: 10.1016/j.bbrc.2020.08.067.
97. Guo, J. *et al.*, "Comparative genomic and functional analyses: unearthing the diversity and specificity of nematicidal factors in *Pseudomonas putida* strain 1A00316" *Sci. Rep.*, vol. 6, no. 1, **2016**, doi: 10.1038/srep29211.
98. Haas, D. and Défago, G., "Biological control of soil-borne pathogens by fluorescent pseudomonads" *Nat. Rev. Microbiol.*, vol. 3, no. 4, pp. 307–19, **2005**, doi: 10.1038/nrmicro1129.
99. Haas, H., "Molecular genetics of fungal siderophore biosynthesis and uptake: The role of siderophores in iron uptake and storage" *Appl. Microbiol. Biotechnol.*, vol. 62, no. 4, pp. 316–330, **2003**, doi: 10.1007/s00253-003-1335-2.
100. Hannauer, M., Yeterian, E., Martin, L. W., Lamont, I. L., and Schalk, I. J., "An efflux pump is involved in secretion of newly synthesized siderophore by *Pseudomonas aeruginosa*" *FEBS Lett.*, vol. 584, no. 23, pp. 4751–4755, **2010**, doi: 10.1016/j.febslet.2010.10.051.

101. Heacock-Kang, Y., Sun, Z., Zarzycki-Siek, J., Poonsuk, K., McMillan, I. A., Chuanchuen, R., and Hoang, T. T., "Two regulators, PA3898 and PA2100, modulate the *Pseudomonas aeruginosa* multidrug resistance MexAB-OprM and EmrAB efflux pumps and biofilm formation," *Antimicrob. Agents Chemother.*, vol. 62, no. 12, pp. e01459-18, **2018**, doi: 10.1128/AAC.01459-18.
102. Heeb, S. and Haas, D., "Regulatory roles of the GacS/GacA two-component system in plant-associated and other Gram-negative bacteria" *Mol. Plant-Microbe Interact.*, vol. 14, no. 12, pp. 1351–1363, **2001**, doi: 10.1094/MPMI.2001.14.12.1351.
103. Heeb, S., Valverde, C., Gigot-Bonnefoy, C., and Haas, D., "Role of the stress sigma factor RpoS in GacA/RsmA-controlled secondary metabolism and resistance to oxidative stress in *Pseudomonas fluorescens* CHA0" *FEMS Microbiol. Lett.*, vol. 243, no. 1, pp. 251–258, **2005**, doi: 10.1016/j.femsle.2004.12.008.
104. Henríquez, T., Stein, N. V., and Jung, H., "PvdRT-OpmQ and MdtABC-OpmB efflux systems are involved in pyoverdine secretion in *Pseudomonas putida* KT2440" *Environ. Microbiol. Rep.*, vol. 11, pp. 98–106, **2019**, doi: 10.1111/1758-2229.12708.
105. Hider, R. C. and Kong, X., "Chemistry and biology of siderophores" *Nat. Prod. Rep.*, vol. 27, no. 5, pp. 637–657, **2010**, doi: 10.1039/b906679a.
106. Höfte, M., "The use of *Pseudomonas* spp. as bacterial biocontrol agents to control plant diseases" in *Microbial bioprotectants for plant disease-management*, J. Köhl and W. J. Ravensberg (Eds.), Burleigh Dodds Science Publishing, **2021**, pp. 301–374.
107. Holloway, B. W., "Genetic recombination in *Pseudomonas aeruginosa*" *J. Gen. Microbiol.*, vol. 13, no. 3, pp. 572–81, **1955**, doi: 10.1099/00221287-13-3-572.
108. Howell, C. R. and Stipanovic, R. D., "Control of *Rhizoctonia solani* on cotton seedlings with *Pseudomonas fluorescens* and with an antibiotic produced by the bacterium" *Phytopathology*, vol. 69, pp. 480–482, **1979**, doi: 10.1094/phyto-69-480.
109. Huerta-Cepas, J. *et al.*, "eggNOG 5.0: a hierarchical, functionally and phylogenetically annotated orthology resource based on 5090 organisms and 2502 viruses" *Nucleic Acids Res.*, vol. 47, no. D1, pp. D309–D314, **2019**, doi: 10.1093/NAR/GKY1085.
110. Inoue, H., Nojima, H., and Okayama, H., "High efficiency transformation of *Escherichia coli* with plasmids" *Gene*, vol. 96, no. 1, pp. 23–28, **1990**, doi: 10.1016/0378-1119(90)90336-P.
111. Iwai, Y. and Ömura, S., "Culture conditions for screening of new antibiotics" *J. Antibiot. (Tokyo).*, vol. 35, no. 2, pp. 123–141, **1982**, doi: 10.7164/antibiotics.35.123.
112. Jamali, F., Sharifi-Tehrani, A., Lutz, M. P., and Maurhofer, M., "Influence of host plant genotype, presence of a pathogen, and coinoculation with *Pseudomonas fluorescens* strains on the rhizosphere expression of hydrogen cyanide and 2,4-diacetylphloroglucinol biosynthetic genes in *P. fluorescens* biocontrol strain CHA0" *Microb. Ecol.*, vol. 57, pp. 267–275, **2009**, doi: 10.1007/s00248-008-9471-y.
113. James, D. W. J. and Gutterson, N. I., "Multiple antibiotics produced by *Pseudomonas fluorescens* HV37a and their differential regulation by glucose" *Appl. Environ. Microbiol.*, vol. 52, no. 5, pp. 1183–9, **1986**, doi: 10.1128/aem.52.5.1183-1189.1986.
114. Jiang, Z., Chen, M., Yu, X., and Xie, Z., "7-Hydroxytropolone produced and utilized as an iron-scavenger by *Pseudomonas donghuensis*" *BioMetals*, vol. 29, no. 5, pp. 817–826, **2016**, doi: 10.1007/s10534-016-9954-0.
115. Jimenez, P. N. *et al.*, "Role of PvdQ in *Pseudomonas aeruginosa* virulence under iron-limiting conditions" *Microbiology*, vol. 156, no. 1, pp. 49–59, **2010**, doi: 10.1099/mic.0.030973-0.
116. Jörnvall, H., Krook, M., Persson, B., Atrian, S., Gonzàlez-Duarte, R., Jeffery, J., and Ghosh, D., "Short-Chain Dehydrogenases/Reductases (SDR)" *Biochemistry*, vol. 34, no. 18, pp. 6003–6013, **1995**, doi: 10.1021/bi00018a001.
117. Joshi, H., Dave, R., and Venugopalan, V. P., "Pumping iron to keep fit: Modulation of siderophore secretion helps efficient aromatic utilization in *Pseudomonas putida* KT2440" *Microbiology*, vol. 160, no. 7, pp. 1393–1400, **2014**, doi: 10.1099/mic.0.079277-0.
118. Kałużna, M., Puławska, J., and Sobiczewski, P., "The use of PCR melting profile for typing of *Pseudomonas syringae* isolates from stone fruit trees" *Eur. J. Plant Pathol.*, vol. 126, no. 4, pp. 437–443, **2009**, doi: 10.1007/s10658-009-9553-9.
119. Kanehisa, M. and Goto, S., "KEGG: Kyoto Encyclopedia of Genes and Genomes" *Nucleic Acids Res.*, vol. 28, no. 1, pp. 27–30, **2000**, doi: 10.3892/ol.2020.11439.
120. Kang, D. and Kirienko, N. V., "Interdependence between iron acquisition and biofilm formation in *Pseudomonas aeruginosa*" *J. Microbiol.*, vol. 56, no. 7, pp. 449–457, **2018**, doi: 10.1007/s12275-018-8114-3.
121. Keel, C. *et al.*, "Suppression of root disease by *Pseudomonas fluorescens* CHA0: Importance of the bacterial secondary metabolite 2,4-diacetylphloroglucinol" *Molecular Plant-Microbe Interactions*, vol. 5, no. 1. pp. 4–13, **1992**, doi: 10.1094/MPMI-5-004.

122. Kim, J. S., Kim, Y. H., Park, J. Y., Anderson, A. J., and Kim, Y. C., "The global regulator GacS regulates biofilm formation in *Pseudomonas chlororaphis* O6 differently with carbon source" *Can. J. Microbiol.*, vol. 60, no. 3, pp. 133–138, **2014**, doi: 10.1139/cjm-2013-0736.
123. Kim, S. *et al.*, "PubChem in 2021: new data content and improved web interfaces" *Nucleic Acids Res.*, vol. 49, **2021**, doi: 10.1093/nar/gkaa971.
124. King, E. O., Ward, M. K., and Raney, D. E., "Two simple media for the demonstration of pyocyanin and fluorescin" *J. Lab. Clin. Med.*, **1954**, doi: 10.5555/uri:pii:002221435490222X.
125. Kirst, H. A. *et al.*, "Synthesis and characterization of a novel inhibitor of an aminoglycoside-inactivating enzyme" *J. Antibiot. (Tokyo).*, vol. 35, no. 12, pp. 1651–1657, **1982**, doi: 10.7164/antibiotics.35.1651.
126. Kloepper, J. W. and Schroth, M. N., "Plant growth-promoting rhizobacteria on radishes" in *Proceedings of the 4th International Conference on Plant Pathogenic Bacteria*, **1978**, vol. 2, pp. 879–882.
127. Köhl, J., Kolnaar, R., and Ravensberg, W. J., "Mode of action of microbial biological control agents against plant diseases: Relevance beyond efficacy" *Front. Plant Sci.*, vol. 10, no. July, pp. 1–19, **2019**, doi: 10.3389/fpls.2019.00845.
128. Korth, H., "Carbon source regulation of the phenazine-α-carboxylic acid synthesis in *Pseudomonas aureofaciens*" *Arch. Mikrobiol.*, vol. 92, pp. 175–177, **1973**, doi: 10.1007/BF00425015.
129. Kraus, J. and Loper, J. E., "Characterization of a genomic region required for production of the antibiotic pyoluteorin by the biological control agent *Pseudomonas fluorescens* Pf-5" *Appl. Environ. Microbiol.*, vol. 61, no. 3, p. 854, **1995**, doi: 10.1128/aem.61.3.849-854.1995.
130. Krzyzanowska, D. M., Potrykus, M., Golanowska, M., Polonis, K., Gwizdek-Wisniewska, A., Lojkowska, E., and Jafra, S., "Rhizosphere bacteria as potential biocontrol agents against soft rot caused by various *Pectobacterium* and *Dickeya* spp. strains" *J. Plant Pathol.*, vol. 94, no. 2, pp. 367–378, **2012a**, doi: 10.4454/JPP.FA.2012.042.
131. Krzyzanowska, D. M., Obuchowski, M., Bikowski, M., Rychlowski, M., and Jafra, S., "Colonization of potato rhizosphere by GFP-tagged *Bacillus subtilis* MB73/2, *Pseudomonas* sp. P482 and *Ochrobactrum* sp. A44 shown on large sections of roots using enrichment sample preparation and confocal laser scanning microscopy" *Sensors*, vol. 12, no. 12, pp. 17608–19, **2012b**, doi: 10.3390/s121217608.
132. Krzyżanowska, D. M., Supernat, A., Maciąg, T., Matuszewska, M., and Jafra, S., "Selection of reference genes for measuring the expression of aiiO in *Ochrobactrum quorumnocens* A44 using RT-qPCR" *Sci. Rep.*, vol. 9, no. 13129, p. 13129, **2019**, doi: 10.1038/s41598-019-49474-6.
133. Krzyżanowska, D. M., Iwanicki, A., Czajkowski, R., and Jafra, S., "High-quality complete genome resource of tomato rhizosphere strain *Pseudomonas donghuensis* P482, a representative of a species with biocontrol activity against plant pathogens" *Mol. Plant-Microbe Interact.*, vol. 34, no. 12, pp. 1450–1454, **2021**, doi: 10.1094/MPMI-06-21-0136-A.
134. Krzyzanowska, D. M., Ossowicki, A., and Jafra, S., "Genome sequence of *Pseudomonas* sp. strain P482, a tomato rhizosphere isolate with broad-spectrum antimicrobial activity" *Genome Announc.*, vol. 2, no. 3, **2014**, doi: 10.1128/genomeA.00394-14.
135. Krzyżanowska, D. M. *et al.*, "When genome-based approach meets the 'Old but Good': Revealing genes involved in the antibacterial activity of *Pseudomonas* sp. P482 against soft rot pathogens" *Front. Microbiol.*, vol. 7, p. 782, **2016**, doi: 10.3389/fmicb.2016.00782.
136. Kwak, Y.-S., Bakker, P. A. H. M., Glandorf, D. C. M., Rice, J. T., Paulitz, T. C., and Weller, D. M., "Diversity, virulence, and 2,4-diacetylphloroglucinol sensitivity of *Gaeumannomyces graminis* var. *tritici* isolates from Washington state" *Phytopathology*, vol. 99, no. 5, pp. 472–9, **2009**, doi: 10.1094/phyto-99-5-0472.
137. Lamont, I. L. and Martin, L. W., "Identification and characterization of novel pyoverdine synthesis genes in *Pseudomonas aeruginosa*" *Microbiology*, vol. 149, no. 4, pp. 833–842, **2003**, doi: 10.1099/MIC.0.26085-0.
138. Lanteigne, C., Gadkar, V. J., Wallon, T., Novinscak, A., and Filion, M., "Production of DAPG and HCN by *Pseudomonas* sp. LBUM300 contributes to the biological control of bacterial canker of tomato" *Phytopathology*, vol. 102, no. 10, pp. 967–973, **2012**, doi: 10.1094/phyto-11-11-0312.
139. Latour, X., "The evanescent GacS signal" *Microorganisms*, vol. 8, no. 11, p. 1746, **2020**, doi: 10.3390/microorganisms8111746.
140. Lavermicocca, P., Lonigro, S. L., Valerio, F., Evidente, A., and Visconti, A., "Reduction of olive knot disease by a bacteriocin from *Pseudomonas syringae* pv. *ciccaronei*" *Appl. Environ. Microbiol.*, vol. 68, no. 3, pp. 1403–1407, **2002**, doi: 10.1128/AEM.68.3.1403-1407.2002.
141. Lee, K. and Yoon, S. S., "*Pseudomonas aeruginosa* biofilm, a programmed bacterial life for fitness" *J. Microbiol. Biotechnol.*, vol. 27, no. 6, pp. 1053–1064, **2017**, doi: 10.4014/jmb.1611.11056.

142. Leeman, M., van Pelt, J. A., den Ouden, F. M., Heinsbroek, M., Bakker, P. A. H. M., and Schippers, B., "induction of systemic resistance against fusarium wilt of radish by lipopolysccharides of *Pseudomonas fluorescens*" *Phytopathology*, vol. 85, pp. 1021–1027, **1995**.
143. Lemanceau, P., Bauer, P., Kraemer, S., and Briat, J.-F., "Iron dynamics in the rhizosphere as a case study for analyzing interactions between soils, plants and microbes" *Plant Soil*, vol. 321, pp. 513–535, **2009**, doi: 10.1007/s11104-009-0039-5.
144. Leong, J., "Siderophores: their biochemistry and possible role in the biocontrol of plant pathogens" *Annu. Rev. Phytopath.*, vol. 24, pp. 187–209, **2003**, doi: 10.1146/annurev.py.24.090186.001155.
145. Lessie, T. G. and Phibbs, Jr., P. V., "Alternative pathways of carbohydrate utilization in pseudomonads" *Annu. Rev. Microbiol.*, vol. 38, pp. 359–87, **1984**, doi: 10.1146/annurev.mi.38.100184.002043.
146. Li, Y., Jiang, H., Xu, Y., and Zhang, X., "Optimization of nutrient components for enhanced phenazine-1-carboxylic acid production by *gacA*-inactivated *Pseudomonas* sp. M18G using response surface method" *Appl. Microbiol. Biotechnol.*, vol. 77, no. 6, pp. 1207–17, **2008**, doi: 10.1007/s00253-007-1213-4.
147. Lim, C. K., Hassan, K. A., Tetu, S. G., Loper, J. E., and Paulsen, I. T., "The effect of iron limitation on the transcriptome and proteome of *Pseudomonas fluorescens* Pf-5" *PLoS One*, vol. 7, no. 6, p. e39139, **2012**, doi: 10.1371/journal.pone.0039139.
148. Lin, M. H., Shu, J. C., Huang, H. Y., and Cheng, Y. C., "Involvement of iron in biofilm formation by *Staphylococcus aureus*" *PLoS One*, vol. 7, no. 3, pp. 3–9, **2012**, doi: 10.1371/journal.pone.0034388.
149. Linardić, M. and Braybrook, S. A., "Identification and selection of optimal reference genes for qPCR-based gene expression analysis in *Fucus distichus* under various abiotic stresses" *PLoS One*, vol. 16, no. 4, p. e0233249, **2021**, doi: 10.1371/journal.pone.0233249.
150. Liu, M.-H., Chen, Y.-J., and Lee, C.-Y., "Characterization of medium-chain-length polyhydroxyalkanoate biosynthesis by *Pseudomonas mosselii* TO7 using crude glycerol" *Biosci. Biotechnol. Biochem.*, vol. 82, no. 3, pp. 532–539, **2018**, doi: 10.1080/09168451.2017.1422386.
151. Liu, Y. *et al.*, "Pyoverdines are essential for the antibacterial activity of *Pseudomonas chlororaphis* YL-1 under low-iron conditions" *Appl. Environ. Microbiol.*, vol. 87, no. 7, pp. e02840-20, **2021a**, doi: 10.1128/AEM.02840-20.
152. Liu, Y. *et al.*, "Phenazine-1-carboxylic acid produced by *Pseudomonas chlororaphis* YL-1 is effective against *Acidovorax citrulli*" *Microorganisms*, vol. 9, no. 10, p. 2012, **2021b**, doi: 10.3390/microorganisms9102012.
153. Llamas, M. A., Imperi, F., Visca, P., and Lamont, I. L., "Cell-surface signaling in *Pseudomonas*: Stress responses, iron transport, and pathogenicity" *FEMS Microbiol. Rev.*, vol. 38, no. 4, pp. 569–597, **2014**, doi: 10.1111/1574-6976.12078.
154. Lomovskaya, O. and Lewis, K., "*emr*, an *Escherichia coli* locus for multidrug resistance" *Proc. Natl. Acad. Sci. U.S.A.*, vol. 89, no. 19, pp. 8938–8942, **1992**, doi: 10.1073/pnas.89.19.8938.
155. Loper, J. E. and Buyer, J. S., "Siderophores in microbial interactions on plant surfaces," *Mol. Plant-Microbe Interact.*, vol. 4, no. 1, pp. 5–13, **1991**, doi: 10.1094/mpmi-4-005.
156. Loper, J. E. *et al.*, "Comparative genomics of plant-associated *Pseudomonas* spp.: insights into diversity and inheritance of traits involved in multitrophic interactions" *PLoS Genet.*, vol. 8, no. 7, p. e1002784, **2012**, doi: 10.1371/journal.pgen.1002784.
157. López-Sánchez, A. *et al.*, "Biofilm formation-defective mutants in *Pseudomonas putida*" *FEMS Microbiol. Lett.*, vol. 363, no. 13, **2016**, doi: 10.1093/femsle/fnw127.
158. Lugtenberg, B. and Kamilova, F., "Plant-growth-promoting rhizobacteria" *Annu. Rev. Microbiol.*, vol. 63, pp. 541–556, **2009**, doi: 10.1146/annurev.micro.62.081307.162918.
159. Maciąg, T. "Podłoże genetyczne właściwości przeciwdrobnoustrojowych szczepu *Pseudomonas* sp. P482", MSc thesis, **2015**, University of Gdańsk, Poland.
160. Manninen, M. and Mattila-Sandholm, T., "Methods for the detection of *Pseudomonas* siderophores" *J. Microbiol. Methods*, vol. 19, no. 3, pp. 223–234, **1994**, doi: 10.1016/0167-7012(94)90073-6.
161. Mansfield, J. *et al.*, "Top 10 plant pathogenic bacteria in molecular plant pathology" *Mol. Plant Pathol.*, vol. 13, no. 6, pp. 614–29, **2012**, doi: 10.1111/j.1364-3703.2012.00804.x.
162. Marin-Bruzos, M., Grayston, S. J., Forge, T., and Nelson, L. M., "Isolation and characterization of streptomycetes and pseudomonad strains with antagonistic activity against the plant parasitic nematode *Pratylenchus penetrans* and fungi associated with replant disease" *Biol. Control*, vol. 158, p. 104599, **2021**, doi: 10.1016/j.biocontrol.2021.104599.
163. Marmont, L. S. *et al.*, "PelX is a UDP-N-acetylglucosamine C4-epimerase involved in Pel polysaccharide-dependent biofilm formation" *J. Biol. Chem.*, vol. 295, no. 34, pp. 11949–11962, **2020**, doi: 10.1074/jbc.RA120.014555.
164. Marshall, O. J., "PerlPrimer: Cross-platform, graphical primer design for standard, bisulphite and real-time PCR" *Bioinformatics*, vol. 20, no. 15, pp. 2471–2472, **2004**, doi: 10.1093/bioinformatics/bth254.

165. Masschelein, J. *et al.*, "A PKS/NRPS/FAS hybrid gene cluster from *Serratia plymuthica* RVH1 encoding the biosynthesis of three broad spectrum, zeamine-related antibiotics" *PLoS One*, vol. 8, no. 1, **2013**, doi: 10.1371/journal.pone.0054143.
166. Mattheus, W. *et al.*, "Isolation and purification of a new kalimantacin/batumin-related polyketide antibiotic and elucidation of its biosynthesis gene cluster" *Chem. Biol.*, vol. 17, pp. 149–159, **2010**, doi: 10.1016/j.chembiol.2010.01.014.
167. Matuszewska M. "Wpływ warunków hodowli (rodzaj pożywki, temperatura i pH) na syntezę czynników przeciwdrobnoustrojowych przez szczep *Pseudomonas* sp. P482", MSc thesis, **2016**, University of Gdańsk, Poland.
168. Matuszewska, M., Maciąg, T., Rajewska, M., Wierzbicka, A., and Jafra, S., "The carbon source-dependent pattern of antimicrobial activity and gene expression in *Pseudomonas donghuensis* P482" *Sci. Rep.*, vol. 11, p. 10994, **2021**, doi: 10.1038/s41598-021-90488-w.
169. Mavrodi, D. V, Parejko, J. A., Mavrodi, O. V, Kwak, Y.-S., Weller, D. M., Blankenfeldt, W., and Thomashow, L. S., "Recent insights into the diversity, frequency and ecological roles of phenazines in fluorescent *Pseudomonas* spp." *Environ. Microbiol.*, vol. 15, no. 3, pp. 675–86, **2013**, doi: 10.1111/j.1462-2920.2012.02846.x.
170. Mavrodi, D. V, Blankenfeldt, W., and Thomashow, L. S., "Phenazine compounds in fluorescent *Pseudomonas* spp. biosynthesis and regulation" *Annu. Rev. Phytopathol.*, vol. 44, pp. 417–45, **2006**, doi: 10.1146/annurev.phyto.44.013106.145710.
171. Mavrodi, O. V. *et al.*, "root exudates alter the expression of diverse metabolic, transport, regulatory, and stress response genes in rhizosphere *Pseudomonas*" *Front. Microbiol.*, vol. 12, **2021**, doi: 10.3389/fmicb.2021.651282.
172. Mazurier, S., Corberand, T., Lemanceau, P., and Raaijmakers, J. M., "Phenazine antibiotics produced by fluorescent pseudomonads contribute to natural soil suppressiveness to *Fusarium* wilt" *ISME J.*, vol. 3, no. 8, pp. 977–91, **2009**, doi: 10.1038/ismej.2009.33.
173. Meck, C., D'Erasmo, M. P., Hirsch, D. R., and Murelli, R. P., "The biology and synthesis of α-hydroxytropolones" *Medchemcomm*, vol. 5, no. 7, pp. 842–852, **2014**.
174. Mendonca, C. M. *et al.*, "Hierarchical routing in carbon metabolism favors iron-scavenging strategy in iron-deficient soil *Pseudomonas* species" *Proc. Natl. Acad. Sci. U.S.A.*, vol. 117, no. 51, pp. 32358–32369, **2020**, doi: 10.1073/PNAS.2016380117.
175. Mey, A. R., Craig, S. A., and Payne, S. M., "Characterization of *Vibrio cholerae* RyhB: The RyhB regulon and role of *ryhB* in biofilm formation" *Infect. Immun.*, vol. 73, no. 9, pp. 5706–5719, **2005**, doi: 10.1128/IAI.73.9.5706-5719.2005.
176. Meyer, J. M. and Abdallah, M. A., "The fluorescent pigment of *Pseudomonas fluorescens*: Biosynthesis, purification and physicochemical properties" *Microbiology*, vol. 107, no. 2, pp. 319–328, **1978**, doi: 10.1099/00221287-107-2-319.
177. Miller, J. H. [Ed.], *Experiments in Molecular Genetics*. Cold Spring Harbor, New York: Cold Spring Harbor Laboratory, 1972.
178. Mo, X., Zhang, H., Du, F., and Yang, S., "Short-chain dehydrogenase NcmD is responsible for the C-10 oxidation of nocamycin F in nocamycin biosynthesis" *Front. Microbiol.*, vol. 11, p. 3180, **2020**, doi: 10.3389/FMICB.2020.610827.
179. Molina, M. A., Godoy, P., Ramos-González, M. I., Muñoz, N., Ramos, J. L., and Espinosa-Urgel, M., "Role of iron and the TonB system in colonization of corn seeds and roots by *Pseudomonas putida* KT2440" *Environ. Microbiol.*, vol. 7, no. 3, pp. 443–449, **2005**, doi: 10.1111/j.1462-2920.2004.00720.x.
180. Molina, M. A., Ramos, J. L., and Espinosa-Urgel, M., "A two-partner secretion system is involved in seed and root colonization and iron uptake by *Pseudomonas putida* KT2440" *Environ. Microbiol.*, vol. 8, no. 4, pp. 639–647, **2006**, doi: 10.1111/j.1462-2920.2005.00940.x.
181. Molina, M. A., Ramos, J.-L., and Espinosa-Urgel, M., "Plant-associated biofilms" *Rev. Environ. Sci. Bio/Technology*, vol. 2, pp. 99–108, **2003**.
182. Monteiro, M. R., Kugelmeier, C. L., Pinheiro, R. S., Batalha, M. O., and da Silva César, A., "Glycerol from biodiesel production: Technological paths for sustainability" *Renew. Sustain. Energy Rev.*, vol. 88, pp. 109–122, **2018**, doi: 10.1016/j.rser.2018.02.019.
183. Muzio, F. M., Agaras, B. C., Masi, M., Tuzi, A., Evidente, A., and Valverde, C., "7-hydroxytropolone is the main metabolite responsible for the fungal antagonism of *Pseudomonas donghuensis* strain SVBP6" *Environ. Microbiol.*, vol. 22, no. 7, pp. 2550–2563, **2020**, doi: 10.1111/1462-2920.14925.
184. Nabhan, S., De Boer, S. H., Maiss, E., and Wydra, K., "Taxonomic relatedness between *Pectobacterium carotovorum* subsp. *carotovorum*, *Pectobacterium carotovorum* subsp. *odoriferum* and *Pectobacterium carotovorum* subsp. *brasiliense* subsp. nov." *J. Appl. Microbiol.*, vol. 113, no. 4, pp. 904–913, **2012**, doi: 10.1111/j.1365-2672.2012.05383.x.
185. Narayanasamy, P., "Factors influencing mechanisms of biocontrol (*Pseudomonas*)," in *Biological Management of Diseases of Crops (Vol. 1: Characteristics of Biological Control Agents)*, H. M. T. Hokkanen [Ed.], Dodrecht, NL: Springer Science+Business Media, **2013**, pp. 347–350.

186. Neilands, J. B., "Iron and its role in microbial physiology" in *Microbial Iron Metabolism: A Comprehensive Treatise*, 1st ed., J. B. Neilands [Ed.], London: Academic Press, **1974**, pp. 4–35.
187. Neilands, J. B., "Siderophores: structure and function of microbial iron transport compounds" *J. Biol. Chem.*, vol. 270, no. 45, pp. 26723–26726, **1995**, doi: 10.1074/jbc.270.45.26723.
188. Neilands, J. B., "Methodology of siderophores" in *Siderophores from Microorganisms and Plants. Structure and Bonding*, **1984**, vol. 58, pp. 1–24, doi: 10.1007/bfb0111309.
189. Neumann, G., Bott, S., Ohler, M. A., Mock, H. P., Lippmann, R., Grosch, R., and Smalla, K., "Root exudation and root development of lettuce (*Lactuca sativa* L. cv. Tizian) as affected by different soils" *Front. Microbiol.*, vol. 5, p. 2, **2014**, doi: 10.3389/fmicb.2014.00002.
190. Nikel, P. I., Chavarría, M., Fuhrer, T., Sauer, U., and Lorenzo, V. de, "*Pseudomonas putida* KT2440 strain metabolizes glucose through a cycle formed by enzymes of the Entner-Doudoroff, Embden-Meyerhof-Parnas, and pentose phosphate pathways" *J. Biol. Chem.*, vol. 290, no. 43, pp. 25920–25932, **2015**, doi: 10.1074/JBC.M115.687749.
191. Nikel, P. I., Kim, J., and de Lorenzo, V., "Metabolic and regulatory rearrangements underlying glycerol metabolism in *Pseudomonas putida* KT2440" *Environ. Microbiol.*, vol. 16, no. 1, pp. 239–254, **2014**, doi: 10.1111/1462-2920.12224.
192. Nikel, P. I., Romero-Campero, F. J., Zeidman, J. A., Goñi-Moreno, Á., and de Lorenzo, V., "The glycerol-dependent metabolic persistence of *Pseudomonas putida* KT2440 reflects the regulatory logic of the GlpR repressor" *MBio*, vol. 6, no. 2, **2015**, doi: 10.1128/mBio.00340-15.
193. Nishino, K., Yamasaki, S., Nakashima, R., Zwama, M., and Hayashi-Nishino, M., "Function and inhibitory mechanisms of multidrug efflux pumps" *Front. Microbiol.*, vol. 12, p. 737288, **2021**, doi: 10.3389/fmicb.2021.737288.
194. Notz, R., Maurhofer, M., Schnider-Keel, U., Duffy, B., Haas, D., and Défago, G., "Biotic factors affecting expression of the 2,4-diacetylphloroglucinol biosynthesis gene *phlA* in *Pseudomonas fluorescens* biocontrol strain CHA0 in the rhizosphere" *Phytopathology*, vol. 91, no. 9, pp. 873–881, **2007**, doi: 10.1094/phyto.2001.91.9.873.
195. Nowak-Thompson, B., Gould, S. J., Kraus, J., and Loper, J. E., "Production of 2,4-diacetylphloroglucinol by the biocontrol agent *Pseudomonas fuorescens* Pf-5" *Can. J. Microbiol.*, vol. 40, pp. 1064–1066, **1994,** doi: 10.1139/m94-168.
196. Nybroe, O. and Sørensen, J., "Production of cyclic lipopeptides by fluorescent pseudomonads" in *Pseudomonas: Volume 3 Biosynthesis of Macromolecules and Molecular Metabolism*, J.-L. Ramos [Ed.] Boston, MA: Springer US, **2004**, pp. 147–172.
197. O'Toole, G. A. and Kolter, R., "Initiation of biofilm formation in *Pseudomonas fluorescens* WCS365 proceeds via multiple, convergent signalling pathways: A genetic analysis" *Mol. Microbiol.*, vol. 28, no. 3, pp. 449–461, **1998**, doi: 10.1046/j.1365-2958.1998.00797.x.
198. Oh, W. T. *et al.*, "*Pseudomonas tructae* sp. nov., novel species isolated from rainbow trout kidney" *Int. J. Syst. Evol. Microbiol.*, vol. 69, no. 12, pp. 3851–3856, **2019**, doi: 10.1099/ijsem.0.003696.
199. Okonechnikov, K. *et al.*, "Unipro UGENE: A unified bioinformatics toolkit" *Bioinformatics*, vol. 28, no. 8, pp. 1166–1167, **2012**, doi: 10.1093/bioinformatics/bts091.
200. Ossowicki, A., Jafra, S., and Garbeva, P., "The antimicrobial volatile power of the rhizospheric isolate *Pseudomonas donghuensis* P482" *PLoS One*, vol. 12, no. 3, pp. 1–13, **2017**, doi: 10.1371/journal.pone.0174362.
201. Palleroni, N. J., "Genus: *Pseudomonas*" in *Bergey's Manual of Systematic Bacteriology, vol. 2: Proteobacteria, Part B: The Gammaproteobacteria*, 2nd ed., D. J. Brenner, N. R. Krieg, J. T. Staley, and G. M. Garrity [Eds.] New York, NY: Springer US, **2005**, pp. 323–379.
202. Pan, R., Bai, X., Chen, J., Zhang, H., and Wang, H., "Exploring structural diversity of microbe secondary metabolites using OSMAC strategy: A literature review" *Front. Microbiol.*, vol. 10, p. 294, **2019**, doi: 10.3389/fmicb.2019.00294.
203. Pappalardo, F., Fragalà, M., Mineo, P. G., Damigella, A., Catara, A. F., Palmeri, R., and Rescifina, A., "Production of filmable medium-chain-length polyhydroxyalkanoates produced from glycerol by *Pseudomonas mediterranea*" *Int. J. Biol. Macromol.*, vol. 65, pp. 89–96, **2014**, doi: 10.1016/j.ijbiomac.2014.01.014.
204. Park, H., McGill, S. L., Arnold, A. D., and Carlson, R. P., "Pseudomonad reverse carbon catabolite repression, interspecies metabolite exchange, and consortial division of labor" *Cell. Mol. Life Sci.*, vol. 77, pp. 395–413, **2020**, doi: 10.1007/s00018-019-03377-x.
205. Park, J. Y., Oh, S. A., Anderson, A. J., Neiswender, J., Kim, J.-C., and Kim, Y. C., "Production of the antifungal compounds phenazine and pyrrolnitrin from *Pseudomonas chlororaphis* O6 is differentially regulated by glucose" *Lett. Appl. Microbiol.*, vol. 52, no. 5, pp. 532–537, **2011**, doi: 10.1111/j.1472-765X.2011.03036.x.
206. Parkins, M. D., Ceri, H., and Storey, D. G., "*Pseudomonas aeruginosa* GacA, a factor in multihost virulence, is also essential for biofilm formation" *Mol. Microbiol.*, vol. 40, no. 5, pp. 1215–1226, **2001**, doi: 10.1046/j.1365-2958.2001.02469.x.

207. Parret, A. H. A., Temmerman, K., and De Mot, R., "Novel lectin-like bacteriocins of biocontrol strain *Pseudomonas fluorescens* Pf-5" *Appl. Environ. Microbiol.*, vol. 71, no. 9, pp. 5197–5207, **2005**, doi: 10.1128/AEM.71.9.5197-5207.2005.
208. Pasqua, M., Visaggio, D., Lo Sciuto, A., Genah, S., Banin, E., Visca, P., and Imperi, F., "Ferric uptake regulator Fur is conditionally essential in *Pseudomonas aeruginosa*" *J. Bacteriol.*, vol. 199, no. 22, pp. e00472-17, **2017**, doi: 10.1128/JB.00472-17.
209. Pasqua, M. *et al.*, "The varied role of efflux pumps of the mfs family in the interplay of bacteria with animal and plant cells" *Microorganisms*, vol. 7, no. 9, pp. 10–12, **2019**, doi: 10.3390/microorganisms7090285.
210. Paterson, J., Jahanshah, G., Li, Y., Wang, Q., Mehnaz, S., and Gross, H., "The contribution of genome mining strategies to the understanding of active principles of PGPR strains" *FEMS Microbiol. Ecol.*, vol. 93, no. 3, p. 249, **2017**, doi: 10.1093/femsec/fiw249.
211. Patriquin, G. M., Banin, E., Gilmour, C., Tuchman, R., Greenberg, E. P., and Poole, K., "Influence of quorum sensing and iron on twitching motility and biofilm formation in *Pseudomonas aeruginosa*" *J. Bacteriol.*, vol. 190, no. 2, pp. 662–671, **2008**, doi: 10.1128/JB.01473-07.
212. Patzer, S. I. and Hantke, K., "The ZnuABC high-affinity zinc uptake system and its regulator Zur in *Escherichia coli*" *Mol. Microbiol.*, vol. 28, no. 6, pp. 1199–1210, **1998**, doi: 10.1046/J.1365-2958.1998.00883.X.
213. Pfaffl, M. W., Tichopad, A., Prgomet, C., and Neuvians, T., "Determination of most stable housekeeping genes, differentially regulated target genes and sample integrity: BestKeeper – Excel-based tool using pair-wise correlations" *Biotechnol. Lett.*, vol. 26, pp. 509–515, 2004, doi: 10.1023/b:bile.0000019559.84305.47
214. Poblete-Castro, I., Wittmann, C., and Nikel, P. I., "Biochemistry, genetics and biotechnology of glycerol utilization in *Pseudomonas* species" *Microb. Biotechnol.*, vol. 13, no. 1, pp. 32–53, **2020**, doi: 10.1111/1751-7915.13400.
215. Ponraj, P., Shankar, M., Ilakkiam, D., and Gunasekaran, P., "Influence of siderophore pyoverdine synthesis and iron uptake on abiotic and biotic surface colonization of *Pseudomonas putida* S11" *BioMetals*, vol. 25, no. 6, pp. 1113–1128, **2012**, doi: 10.1007/s10534-012-9574-2.
216. Ponzar, N. L., Tajwar, R., Pozzi, N., and Tavis, J. E., "Alpha-hydroxytropolones are noncompetitive inhibitors of human RNase H1 that bind to the active site and modulate substrate binding" *J. Biol. Chem.*, vol. 298, no. 4, p. 101790, **2022**, doi: 10.1016/j.jbc.2022.101790.
217. Poole, K., Krebes, K., McNally, C., and Neshat, S., "Multiple antibiotic resistance in *Pseudomonas aeruginosa*: Evidence for involvement of an efflux operon" *J. Bacteriol.*, vol. 175, no. 22, pp. 7363–7372, **1993**, doi: 10.1128/jb.175.22.7363-7372.1993.
218. R Core Team, "R: A language and environment for statistical computing" R Foundation for Statistical Computing, Vienna, Austria, **2020**, [Online]. Available: https://www.r-project.org/.
219. Raaijmakers, J. M., Vlami, M., and Souza, J. T. de, "Antibiotic production by bacterial biocontrol agents" *Antonie Van Leeuwenhoek*, vol. 81, no. 1–4, pp. 537–547, **2002**, doi: 10.1023/A:1020501420831.
220. Raaijmakers, J. M., Sluis, V. Der, Koster, M., Bakker, P. A. H. M., Weisbeek, P. J., and Schippers, B., "Utilization of heterologous siderophores and rhizosphere competence of fluorescent *Pseudomonas* spp." *Can. J. Microbiol.*, vol. 135, pp. 126–135, **1995**, doi: 10.1139/m95-017.
221. Raaijmakers, J. M. and Weller, D. M., "Natural plant protection by 2,4-diacetylphloroglucinol – producing *Pseudomonas* spp. in take-all decline soils" *Mol. Plant-Microbe Interact,* vol. 11, no. 2, pp. 144–152, **1998**, doi: 10.1094/MPMI.1998.11.2.144.
222. Raaijmakers, J. M., de Bruijn, I., and de Kock, M. J. D., "Cyclic lipopeptide production by plant-associated *Pseudomonas* spp.: diversity, activity, biosynthesis, and regulation" *Mol. Plant-Microbe Interact.*, vol. 19, no. 7, pp. 699–710, **2006**, doi: 10.1094/MPMI-19-0699.
223. Rajewska, M., Matuszewska, M., and Jafra, S., "Cellular and environmental factors influencing biofilm formation and colonization of plant tissue by a beneficial strain of bacteria, *Pseudomonas donghuensis* P482" in *biofilms 9 conference*, **2020**, doi: 10.5194/biofilms9-108.
224. Rasmussen, R., "Quantification on the LightCycler" in *Rapid Cycle Real-Time PCR*, Berlin, Heidelberg: Springer Berlin Heidelberg, **2001**, pp. 21–34.
225. Rezzonico, F., Zala, M., Keel, C., Duffy, B., Moënne-Loccoz, Y., and Défago, G., "Is the ability of biocontrol fluorescent pseudomonads to produce the antifungal metabolite 2,4-diacetylphloroglucinol really synonymous with higher plant protection?" *New Phytol.*, vol. 173, no. 4, pp. 861–872, **2007**, doi: 10.1111/j.1469-8137.2006.01955.x.
226. van Rij, E. T., Wesselink, M., Chin-A-Woeng, T. F. C., Bloemberg, G. V., and Lugtenberg, B. J. J., "Influence of environmental conditions on the production of phenazine-1-carboxamide by *Pseudomonas chlororaphis* PCL1391" *Mol. Plant-Microbe Interact.*, vol. 17, no. 5, pp. 557–566, **2004**, doi: 10.1094/MPMI.2004.17.5.557.

227. Rocha, D. J. P., Santos, C. S., and Pacheco, L. G. C., "Bacterial reference genes for gene expression studies by RT-qPCR: survey and analysis" *Antonie van Leeuwenhoek*, vol. 108, no. 3, pp. 685–693, **2015**, doi: 10.1007/S10482-015-0524-1.
228. Rocha, D. J. P. G., Castro, T. L. P., Aguiar, E. R. G. R., and Pacheco, L. G. C., "Gene expression analysis in bacteria by RT-qPCR" in *Quantitative Real-Time PCR: Methods and Protocols*, 2nd ed., R. Biassoni and A. Raso [Eds.], Springer New York, **2020**, pp. 119–138.
229. Rodríguez-Rojas, A., Makarova, O., Müller, U., and Rolff, J., "Cationic peptides facilitate iron-induced mutagenesis in bacteria" *PLoS Genet.*, vol. 11, no. 10, pp. 1–16, **2015**, doi: 10.1371/journal.pgen.1005546.
230. Rojo, F., "Carbon catabolite repression in *Pseudomonas*: Optimizing metabolic versatility and interactions with the environment" *FEMS Microbiol. Rev.*, vol. 34, no. 5, pp. 658–684, **2010**, doi: 10.1111/j.1574-6976.2010.00218.x.
231. Ruiz, B. *et al.*, "Production of microbial secondary metabolites: Regulation by the carbon source" *Crit. Rev. Microbiol.*, vol. 36, no. 2, pp. 146–167, **2010**, doi: 10.3109/10408410903489576.
232. Sambrook, J. and Russell, D., [Eds.] "Molecular Cloning: A Laboratory Manual" *Cold Spring Harb. Lab. Press. NY*, **2001**.
233. Sánchez, S. *et al.*, "Carbon source regulation of antibiotic production" *J. Antibiot. (Tokyo).*, vol. 63, no. 8, pp. 442–59, **2010**, doi: 10.1038/ja.2010.78.
234. Santoyo, G., Urtis-Flores, C. A., Loeza-Lara, P. D., Orozco-Mosqueda, M. D. C., and Glick, B. R., "Rhizosphere colonization determinants by plant growth-promoting rhizobacteria (PGPR)" *Biology (Basel).*, vol. 10, no. 6, **2021**, doi: 10.3390/biology10060475.
235. Sarniguet, A., Kraus, J., Henkels, M. D., Muehlchen, A. M., and Loper, J. E., "The sigma factor σs affects antibiotic production and biological control activity of *Pseudomonas fluorescens* Pf-5" *Proc. Natl. Acad. Sci. U. S. A.*, vol. 92, no. 26, pp. 12255–12259, **1995**, doi: 10.1073/PNAS.92.26.12255.
236. Sasnow, S. S., Wei, H., and Aristilde, L., "Bypasses in intracellular glucose metabolism in iron-limited *Pseudomonas putida*" *MicrobiologyOpen*, vol. 5, no. 1, pp. 3–20, **2016**, doi: 10.1002/mbo3.287.
237. Sass, G. *et al.*, "Studies of *Pseudomonas aeruginosa* mutants indicate pyoverdine as the central factor in inhibition of *Aspergillus fumigatus* biofilm" *J. Bacteriol.*, vol. 200, no. 1, pp. e00345-17, **2018**, doi: 10.1128/JB.00345-17.
238. Sasse, J., Martinoia, E., and Northen, T., "Feed your friends: Do plant exudates shape the root microbiome?" *Trends Plant Sci.*, vol. 23, no. 1, pp. 25–41, **2018**, doi: 10.1016/j.tplants.2017.09.003.
239. Savli, H., Karadenizli, A., Kolayli, F., Gundes, S., Ozbek, U., and Vahaboglu, H., "Expression stability of six housekeeping genes: A proposal for resistance gene quantification studies of *Pseudomonas aeruginosa* by real-time quantitative RT-PCR" *J. Med. Microbiol.*, vol. 52, no. 5, pp. 403–408, **2003**, doi: 10.1099/jmm.0.05132-0.
240. Schaaf, G., Erenoglu, B. E., and von Wirén, N., "Physiological and biochemical characterization of metal-phytosiderophore transport in *Graminaceous* species" *Soil Sci. Plant Nutr.*, vol. 50, no. 7, pp. 989–995, **2004**, doi: 10.1080/00380768.2004.10408565.
241. Schlaak, C., Hoffmann, P., May, K., and Weimann, A., "Desalting minimal amounts of DNA for electroporation in *E. coli*: a comparison of different physical methods" *Biotechnol. Lett.*, vol. 27, pp. 1003–1005, **2005**, doi: 10.1007/s10529-005-7867-z.
242. Schnider, U., Keel, C., Voisard, C., Défago, G., and Haas, D., "Tn5-directed cloning of *pqq* genes from *Pseudomonas fluorescens* CHA0: mutational inactivation of the genes results in overproduction of the antibiotic pyoluteorin" *Appl. Environ. Microbiol.*, vol. 61, no. 11, pp. 3856–3864, **1995**, doi: 10.1128/AEM.61.11.3856-3864.1995.
243. Scoffield, J. and Silo-Suh, L., "Glycerol metabolism promotes biofilm formation by *Pseudomonas aeruginosa*" *Can. J. Microbiol.*, vol. 62, no. 8, pp. 704–710, **2016**, doi: 10.1139/cjm-2016-0119.
244. Shanahan, P., Sullivan, D. J. O., Simpson, P., and Jeremy, D., "Isolation of 2,4-diacetylphloroglucinol from a fluorescent pseudomonad and investigation of physiological parameters influencing its production" *Appl. Environ. Microbiol.*, vol. 58, no. 1, pp. 353–358, **1992**, doi: 10.1128/aem.58.1.353-358.1992
245. Sławiak, M., Łojkowska, E., and Van Der Wolf, J. M., "First report of bacterial soft rot on potato caused by *Dickeya* sp. (syn. *Erwinia chrysanthemi*) in Poland" *Plant Pathol.*, vol. 58, no. 4, p. 794, **2009**, doi: 10.1111/j.1365-3059.2009.02028.x.
246. Slininger, P. J. and Shea-Wilbur, M. A., "Liquid-culture pH, temperature, and carbon (not nitrogen) source regulate phenazine productivity of the take-all biocontrol agent *Pseudomonas fluorescens* 2-79" *Appl. Microbiol. Biotechnol.*, vol. 43, no. 5, pp. 794–800, **1995**, doi: 10.1007/s002530050487.
247. Sonnleitner, E. and Bläsi, U., "Regulation of Hfq by the RNA CrcZ in *Pseudomonas aeruginosa* carbon catabolite repression" *PLoS Genet.*, vol. 10, no. 6, p. e1004440, **2014**, doi: 10.1371/journal.pgen.1004440.
248. Spiers, A. J., Buckling, A., and Rainey, P. B., "The causes of *Pseudomonas* diversity" *Microbiology*, vol. 146, pp. 2345–2350, **2000**, doi: 10.1099/00221287-146-10-2345.

249. Staunton, J. and Weissman, K. J., "Polyketide biosynthesis: A millennium review" *Nat. Prod. Rep.*, vol. 18, no. 4, pp. 380–416, **2001**, doi: 10.1039/a909079g.
250. Sun, F. *et al.*, "Fur is a repressor of biofilm formation in Yersinia pestis" *PLoS One*, vol. 7, no. 12, p. e52392, **2012**, doi: 10.1371/journal.pone.0052392.
251. Taboada, B., Estrada, K., Ciria, R., and Merino, E., "Operon-mapper: A web server for precise operon identification in bacterial and archaeal genomes" *Bioinformatics*, vol. 34, no. 23, pp. 4118–4120, **2018**, doi: 10.1093/bioinformatics/bty496.
252. Takeuchi, K., "GABA, a primary metabolite controlled by the gac/rsm regulatory pathway, favors a planktonic over a biofilm lifestyle in *Pseudomonas protegens* CHAO" *Mol. Plant-Microbe Interact.*, vol. 31, no. 2, pp. 274–282, 2018, doi: 10.1094/MPMI-05-17-0120-R.
253. Tao, X., Zhang, H., Gao, M., Li, M., Zhao, T., and Guan, X., "*Pseudomonas* species isolated via high-throughput screening significantly protect cotton plants against *Verticillium* wilt" *AMB Express*, vol. 10, no. 193, **2020**, doi: 10.1186/s13568-020-01132-1.
254. Taylor, S. C., Nadeau, K., Abbasi, M., Lachance, C., Nguyen, M., and Fenrich, J., "The ultimate qPCR experiment: Producing publication quality, reproducible data the first time" *Trends Biotechnol.*, vol. 37, no. 7, pp. 761–774, **2019**, doi: 10.1016/j.tibtech.2018.12.002.
255. Temple, L. M., Sage, A. E., Schweizer, H. P., and Phibbs, P. V., "Carbohydrate catabolism in *Pseudomonas aeruginosa*" in *Pseudomonas*, Boston, MA: Springer US, **1998**, pp. 35–72.
256. Thoma, S. and Schobert, M., "An improved *Escherichia coli* donor strain for diparental mating" *FEMS Microbiol. Lett.*, vol. 294, no. 2, pp. 127–132, **2009**, doi: 10.1111/j.1574-6968.2009.01556.x.
257. Thomashow, L. S. and Weller, D. M., "Role of a phenazine antibiotic from *Pseudomonas fluorescens* in biological control of *Gaeumannomyces graminis* var. *tritici*" *J. Bacteriol.*, vol. 170, no. 8, pp. 3499–508, **1988**, doi: 10.1128/jb.170.8.3499-3508.1988
258. Thomashow, L. S. and Weller, D. M., "Role of antibiotics and siderophores in biocontrol of take-all disease of wheat" *Plant Soil*, vol. 129, no. 1, pp. 93–99, **1990**, doi: 10.1007/BF00011695.
259. Townsley, L., Yannarell, S. M., Huynh, T. N., Woodward, J. J., and Shank, E. A., "Cyclic di-AMP acts as an extracellular signal that impacts *Bacillus subtilis* biofilm formation and plant attachment" *MBio*, vol. 9, no. 2, pp. e00341-18, 2018, doi: 10.1128/mBio.00341-18.
260. Traxler, M. F., Watrous, J. D., Alexandrov, T., Dorrestein, P. C., and Kolter, R., "Interspecies interactions stimulate diversification of the *Streptomyces coelicolor* secreted metabolome" *MBio*, vol. 4, no. 4, pp. e00459-13, **2013**, doi: 10.1128/MBIO.00459-13.
261. Tripathi, R. K. and Gottlieb, D., "Mechanism of action of the antifungal antibiotic pyrrolnitrin" *J. Bacteriol.*, vol. 100, no. 1, pp. 310–8, **1969,** doi: 10.1128/jb.100.1.310-318.1969.
262. Tupe, S. G., Kulkarni, R. R., Shirazi, F., Sant, D. G., Joshi, S. P., and Deshpande, M. V, "Possible mechanism of antifungal phenazine-1-carboxamide from *Pseudomonas* sp. against dimorphic fungi *Benjaminiella poitrasii* and human pathogen *Candida albicans*" *J. Appl. Microbiol.*, vol. 118, no. 1, pp. 39–48, **2015**, doi: 10.1111/jam.12675.
263. Tvrzová, L. *et al.*, "*Pseudomonas moraviensis* sp. nov. and *Pseudomonas vranovensis* sp. nov., soil bacteria isolated on nitroaromatic compounds, and emended description of *Pseudomonas asplenii*" *Int. J. Syst. Evol. Microbiol.*, vol. 56, no. 11, pp. 2657–2663, **2006**, doi: 10.1099/ijs.0.63988-0.
264. The UniProt Consortium, "UniProt: the universal protein knowledgebase" *Nucleic Acids Res.*, vol. 46, no. 5, pp. 2699–2699, **2018**, doi: 10.1093/nar/gky092.
265. Untergasser, A., Nijveen, H., Rao, X., Bisseling, T., Geurts, R., and Leunissen, J. A. M., "Primer3Plus, an enhanced web interface to Primer3" *Nucleic Acids Res.*, vol. 35, pp. 71–74, **2007**, doi: 10.1093/nar/gkm306.
266. Uzair, B., Ahmed, N., Ahmad, V. U., Mohammad, F. V., and Edwards, D. H., "The isolation, purification and biological activity of a novel antibacterial compound produced by *Pseudomonas stutzeri*" *FEMS Microbiol. Lett.*, vol. 279, no. 2, pp. 243-250, **2008**, doi: 10.1111/J.1574-6968.2007.01036.X.
267. Vandesompele, J., De Preter, K., Pattyn, F., Poppe, B., Van Roy, N., De Paepe, A., and Speleman, F., "Accurate normalization of real-time RT-PCR data by geometric averaging of multiple internal control genes" *Genome Biol.*, vol. 3, no. 7, p. research0034.1, **2002**, doi: 10.1186/gb-2002-3-7-research0034.
268. Venturi, V., Weisbeek, P., and Koster, M., "Gene regulation of siderophore-mediated iron acquisition in *Pseudomonas*: not only the Fur repressor" *Mol. Microbiol.*, vol. 17, no. 4, pp. 603–610, *1995*, doi: 10.1111/j.1365-2958.1995.mmi_17040603.x.
269. Vidaver, A. K., "Prospects for control of phytopathogenic bacteria by bacteriophages and bacteriocins" *Annu. Rev. Phytopathol.*, vol. 14, pp. 451–465, **1976**, doi: 10.1146/annurev.py.14.090176.002315.

270. Villagra, N. A., Fuentes, J. A., Jofré, M. R., Hidalgo, A. A., García, P., and Mora, G. C., "The carbon source influences the efflux pump-mediated antimicrobial resistance in clinically important Gram-negative bacteria" *J. Antimicrob. Chemother.*, vol. 67, no. 4, pp. 921–927, **2012**, doi: 10.1093/jac/dkr573.
271. Villamizar, S., Ferro, J. A., Caicedo, J. C., and Alves, L. M. C., "Bactericidal effect of entomopathogenic bacterium *Pseudomonas entomophila* against *Xanthomonas citri* reduces citrus canker disease severity" *Front. Microbiol.*, vol. 11, p. 1431, **2020**, doi: 10.3389/fmicb.2020.01431.
272. Vinale, F. *et al.*, "Co-culture of plant beneficial microbes as source of bioactive metabolites" *Sci. Reports*, vol. 7, p. 14330, **2017**, doi: 10.1038/s41598-017-14569-5.
273. Vindeirinho, J. M., Soares, H. M. V. M., and Soares, E. V., "Modulation of siderophore production by *Pseudomonas fluorescens* through the manipulation of the culture medium composition" *Appl. Biochem. Biotechnol.*, 193, pp. 607–618, **2020**, doi: 10.1007/s12010-020-03349-z.
274. Visca, P., Imperi, F., and Lamont, I. L., "Pyoverdine siderophores: from biogenesis to biosignificance" *Trends Microbiol.*, vol. 15, no. 1, pp. 22–30, **2007**, doi: 10.1016/j.tim.2006.11.004.
275. Voisard, C., Keel, C., Haas, D., and Dèfago, G., "Cyanide production by *Pseudomonas fluorescens* helps suppress black root rot of tobacco under gnotobiotic conditions" *EMBO J.*, vol. 8, pp. 351–358, **1989**, doi: 10.1002/J.1460-2075.1989.TB03384.X.
276. Wang, Z., Huang, X., Jan, M., Kong, D., Pan, J., and Zhang, X., "The global regulator Hfq exhibits far more extensive and intensive regulation than Crc in *Pseudomonas protegens* H78" *Mol. Plant Pathol.*, vol. 22, no. 8, pp. 921–938, **2021**, doi: 10.1111/MPP.13070.
277. Weller, D. M. *et al.*, "Role of 2,4-diacetylphloroglucinol-producing fluorescent *Pseudomonas* spp. in the defense of plant roots" *Plant Biol.*, vol. 9, no. 1, pp. 4–20, **2007**, doi: 10.1055/s-2006-924473.
278. Weller, D. M., "*Pseudomonas* biocontrol agents of soilborne pathogens: looking back over 30 years" *Phytopathology*, vol. 97, no. 2, pp. 250–6, **2007**, doi: 10.1094/phyto-97-2-0250.
279. Van Der Werf, M. J. *et al.*, "Comprehensive analysis of the metabolome of *Pseudomonas putida* S12 grown on different carbon sources" *Mol. Biosyst.*, vol. 4, no. 4, pp. 315–327, **2008**, doi: 10.1039/b717340g.
280. Wickham, H., François, R., Henry, L., and Müller, K., "dplyr: A grammar of data manipulation", **2022**, [Online]. Available: https://dplyr.tidyverse.org.
281. Wickham, H., *ggplot2: Elegant graphics for data analysis*, 2nd ed. Springer-Verlag New York, **2016**.
282. Wu, Y. and Outten, F. W., "IscR controls iron-dependent biofilm formation in *Escherichia coli* by regulating type I fimbria expression" *J. Bacteriol.*, vol. 191, no. 4, pp. 1248–1257, **2009**, doi: 10.1128/JB.01086-08
283. Yan, Q., Philmus, B., Chang, J. H., and Loper, J. E., "Novel mechanism of metabolic co-regulation coordinates the biosynthesis of secondary metabolites in *Pseudomonas protegens*" *ELife*, vol. 6, p. e22835, **2017**, doi: 10.7554/elife.22835.
284. Yang, R., Li, S., Li, Y., Yan, Y., Fang, Y., Zou, L., and Chen, G., "Bactericidal effect of *Pseudomonas oryziphila* sp. nov., a novel *Pseudomonas* species against *Xanthomonas oryzae* reduces disease severity of bacterial leaf streak of rice" *Front. Microbiol.*, vol. 12, p. 3234, **2021**, doi: 10.3389/FMICB.2021.759536
285. Ye, J., Coulouris, G., Zaretskaya, I., Cutcutache, I., Rozen, S., and Madden, T. L., "Primer-BLAST: a tool to design target-specific primers for polymerase chain reaction" *BMC Bioinformatics*, vol. 13, p. 134, **2012**, doi: 10.1186/1471-2105-13-134.
286. Yu, X., Chen, M., Jiang, Z., Hu, Y., and Xie, Z., "The two-component regulators GacS and GacA positively regulate a nonfluorescent siderophore through the Gac/Rsm signaling cascade in high-siderophore-yielding *Pseudomonas* sp. strain HYS" *J. Bacteriol.*, vol. 196, no. 18, pp. 3259–3270, **2014**, doi: 10.1128/JB.01756-14.
287. Zboralski, A. and Filion, M., "Genetic factors involved in rhizosphere colonization by phytobeneficial *Pseudomonas* spp." *Comput. Struct. Biotechnol. J.*, vol. 18, pp. 3539–3554, **2020**, doi: 10.1016/j.csbj.2020.11.025.
288. Zhang, Y. Q. *et al.*, "Genome-based analysis of virulence genes in a non-biofilm-forming *Staphylococcus epidermidis* strain ATCC 12228" *Mol. Microbiol.*, vol. 49, no. 6, pp. 1577–1593, **2003**, doi: 10.1046/J.1365-2958.2003.03671.X.
289. Zhou, Z. J., Zhang, L., and Sun, L., "*Pseudomonas fluorescens*: Fur is required for multiple biological properties associated with pathogenesis" *Vet. Microbiol.*, no. 175, pp. 145–149, **2015**, doi: 10.1016/j.vetmic.2014.11.001.

# 13. Appendix

## 13.1. Supplementary tables

**SUPPLEMENTARY TABLE 1.** Annotation of P482 genes inactivated in the mutants used in this study.

| gene locus | product annotation | Genbank coordinates | protein id (NCBI) |
|---|---|---|---|
| | *7-HT biosynthesis cluster* | | |
| **BV82_4705** | TetR/AcrR family transcriptional regulator | CP071706.1: 4837282..4837974 | KDN97472.2 |
| **BV82_4706** | CitE, CoA ester lyase | CP071706.1: 4837954..4838868 | KDN97473.1 |
| **BV82_4709** | acyl-CoA dehydrogenase family protein | CP071706.1: 4840633..4841775 | KDN97476.1 |
| | *PVD biosynthesis genes* | | |
| **BV82_1009** | non-ribosomal peptide synthetase | CP071706.1: 1923188..1936150 | KDO01142.1 |
| **BV82_3755** | non-ribosomal peptide synthetase | CP071706.1: 3790348..3798909 | KDN98381.2 |
| | *"cluster 17"* | | |
| **BV82_4240** | SDR family NAD(P)-dependent oxidoreductase | CP071706.1: 4321132..4321959 | KDN97935.1 |
| **BV82_4243** | EmrA, HlyD family secretion protein | CP071706.1: 4323879..4324943 | KDN97938.1 |
| | *genes encoding regulatory proteins* | | |
| **BV82_3318** | GacA, Gac/Rsm pathway response regulator | CP071706.1: 2605593..2606231 | KDN98590.2 |
| **BV82_4870** | Fur (ferric iron uptake transcriptional regulator) | CP071706.1: 5012823..5013227 | KDN97319.1 |

**SUPPLEMENTARY TABLE 2.** Primers used in the study.

| **Target gene/sequence** (GenBank locus tag) | **Encoded protein/Description** | **Primers** | **Primer sequences** | **Amplicon length (bp)** |
|---|---|---|---|---|
| | | ***RT-qPCR reference gene selection primers*** | | |
| *rpoB* (BV82_1963) | RpoB, the β subunit of bacterial RNA polymerase | P482_rpoB_F<br>P482_rpoB_R | 5' TTCACCACGATCCACATCCA<br>5' CTTCAGCACCCACATAAACGA | 147 |
| *rpoD* (BV82_1895) | RpoD ($\sigma^{70}$), a "housekeeping" sigma factor involved in initiation of transcription | P482_rpoD _F<br>P482_rpoD_R | 5' CCACGACGGTATTCGAACTT<br>5' CGTGCCAAGAAAGAAATGGT | 152 |
| *gyrB* (BV82_2296) | DNA gyrase subunit B | P482_gyrB_F<br>P482_gyrB_R | 5' ATCGACAAGCTGCGCTATCA<br>5' CGGCTGAGCGATGTAGATGT | 144 |
| *mrdA/pbp-2* (BV82_4935) | Penicillin binding protein 2 | P482_mrdA_F<br>P482_mrdA_R | 5' CTTGATCGCTACCACCTGAG<br>5'vCAAGTCGGACTGGAACAAGG | 138 |
| *recA* (BV82_0583) | Recombinase A | P482_recA_F<br>P482_recA_R | 5' CTACCTGTGCCTTCGTTGAC<br>5' CAGCATGTCGGTGATTTCCA | 133 |
| *lexA* (BV82_3405) | Transcriptional repressor LexA | P482_lexA_F<br>P482_lexA_R | 5' CGTTCAAAGCGCTTGATGGT<br>5' CCGACTACCTGCTCAAGGTG | 153 |
| *tuf* (BV82_0583) | Elongation factor Tu | P482_tuf_F<br>P482_tuf_R | 5' CCCTACATCGTGGTCTTCCT<br>5' GAACCAATGATGATCGGAGTG | 136 |
| *algD* (BV82_3321) | GDP-mannose 6-dehydrogenase | P482_algD_F<br>P482_algD_R | 5' GAATATCAGCATCTTTGGATTGGG<br>5' CTGGTTGATCATGTCGATCTTGG | 120 |
| *proC* (BV82_2548) | Pyrroline-5-carboxylate reductase | P482_proC_F<br>P482_proC_R | 5' CAATCGAGACCACCAGTTGC<br>5' GCATCGAGATGTTCGCAGAC | 140 |
| *acpP* (BV82_4055)[2] | Acyl carrier protein | P482_acpP_F<br>P482_acpP_R | 5' GTCGATAGCAGCTTGAACAG<br>5' AGAAGTGAAGAACGAATCTTCC | 150 |

| **Target gene/sequence** (GenBank locus tag) | **Encoded protein/Description** | **Primers** | **Primer sequences** | **Amplicon length (bp)** |
|---|---|---|---|---|
| | | ***Primers for RT-qPCR targets of interest*** | | |
| BV82_1009 | A putative NRPS for pyoverdine chromophore synthesis | P482_1009_F<br>P482_1009_R | 5' CAATGGCAGAGCGAATAC<br>5' CCGTCCTCAACCAGTAAG | 140 |
| BV82_3755 | Partially similar to the PvdD pyoverdine synthase of *P.aeruginosa* | P482_3755_F<br>P482_3755_R | 5' AAAGCGAACGACATGAACAG<br>5' CTGGCGTACCTGATCTACAC | 151 |
| BV82_4705 | Bacterial regulatory s, tetR family protein (7-HT biosynthesis cluster) | P482_4705_F<br>P482_4705_R | 5' CTTCCTCAGCAACGAATCCA<br>5' GACCATCGAGGTGATCATCTG | 150 |
| BV82_4706 | HpcH/HpaI aldolase/citrate lyase family protein (7-HT biosynthesis cluster) | P482_4706_F<br>P482_4706_R | 5' AGGGCAGTTTCGATATTCGG<br>5' GTCATGATGTCCAAGGTCGAG | 127 |
| BV82_4709 | Acyl-CoA dehydrogenase, C-terminal domain protein (7-HT biosynthesis cluster) | P482_4709_F<br>P482_4709_R | 5' GATTTCATGCTGATCGTGACC<br>5' AGGTTGTCGAAATACAGCGG | 157 |
| BV82_4240 | SDR family NAD(P)-dependent oxidoreductase ("cluster 17") | P482_4240_F<br>P482_4240_R | 5' AACCTGATGAACAAGACCGTG<br>5' TAGAAGGCATCCAAGTGCAG | 145 |
| BV82_4243 | Efflux transporter, RND family, MFP subunit ("cluster 17") | P482_4243_F<br>P482_4243_R | 5' CGCCAATTTCAAGGAAACCC<br>5' CTACCTTGGTGAAGTTGCCG | 178 |
| *gacA* (BV82_3318) | GacA, a response regulator of the two-component GacS/GacA system | P482_3318_F<br>P482_3318_R | 5' CAATTTGCGGGCTGATGTAG<br>5' GGTGACCGTCTGTGAAGAAG | 148 |
| *fur* (BV82_4870) | Fur, ferric uptake regulator protein | P482_4870_F<br>P482_4870_R | 5' CTTCGAACTGGGTCAGAACAC<br>5' TCTACAGATGCTCGACTCTACC | 124 |
| | | ***Primers used in site-directed mutagenesis*** | | |
| BV82_0255 | BV82_0255 gene (*iscA*) fragment for cloning into pKNOCK vector | F_XbaI_KN0255<br>R_XhoI_KN0255 | 5' GCGCGCTCTAGA_GCGATTACAAGCAGAAGAAAGG<br>5' GCGCGCCTCGAG_GAGATCCAGACGGAAGCCAG | 451 |

| **Target gene/sequence** (GenBank locus tag) | **Encoded protein/Description** | **Primers** | **Primer sequences** | **Amplicon length (bp)** |
|---|---|---|---|---|
| BV82_0562 | BV82_0562 gene fragment for cloning into pKNOCK vector | F_XbaI_KN0562<br>R_KpnI_KN0562 | 5’ GCGCGCTCTAGA_CAGCCGAACAACCAAACCGA<br>5’ GCGCGCGGTACC_GATGATGAAAGGGAACAAAGGGA | 517 |
| BV82_2408 | BV82_2408 gene fragment for cloning into pKNOCK vector | F_XbaI_KN2408<br>R_KpnI_KN2408 | 5’ GCGCGCTCTAGA_TACGAGGCCTATCATCAAGTCC<br>5’ GCGCGCGGTACC_TACACCTGGTCCATCTTCAC | 466 |
| BV82_4870 | BV82_4870 gene (*fur*) fragment for cloning into pKNOCK vector | F_XbaI_KN4870<br>R_KpnI_KN4870 | 5’ GCGCGCTCTAGA_CGACTTCCACTATCTTGGCT<br>5’ GCGCGCGGTACC_CGCCTTCAGTACTTATGCAG | 529 |
| BV82_4879 | BV82_4879 gene fragment for cloning into pKNOCK vector | F_XbaI_KN4879<br>R_KpnI_KN4879 | 5’ GCGCGCTCTAGA_ACCTCGCTGCTGGACAAGAC<br>5’ GCGCGCGGTACC_ATGCCTTCGGGAATCACCAC | 430 |
| pKNOCK vector | pKNOCK-Km backbone | F_pKNOCK_backbone<br>R_pKNOCK_backbone | 5’ GGTGCCCTGAATGAACTCCA<br>5’ AAAAGCGGCCATTTTCCAC | - |
| pKNOCK vector | pKNOCK insert flanking region | F_outof_pKNOCK<br>R_outof_pKNOCK | 5’ CACGTACTAAGCTCTCATGTTTGAACA<br>5’ CTGGCAATTCCGGTTCGCT | - |

**SUPPLEMENTARY TABLE 3. Principal component analysis of the LC-MS results of extracts from P482 wt cultures in M9 + 0.4% glucose, M9+ 0.4% glycerol and 0.1 TSB.** The LC-MS dataset for PCA included only entities (detected compounds) for which the fold change between the conditions was higher than 2.

| sample (biol. replicate) | component 1 (91.51%) | component 2 (7.16%) | component 3 (0.63%) | component 4 (0.3%) |
|---|---|---|---|---|
| **P482 wt – glucose (1)** | -11.6437 | -5.46949 | -0.0211 | -1.68957 |
| **P482 wt – glucose (2)** | -11.5069 | -5.29038 | 0.061313 | 2.102384 |
| **P482 wt – glucose (3)** | -11.6854 | -5.46143 | -0.0238 | -0.37397 |
| **P482 wt – glycerol (1)** | -11.074 | 5.575677 | -0.04812 | -0.13541 |
| **P482 wt – glycerol (2)** | -10.7888 | 5.481601 | 0.043515 | 0.110469 |
| **P482 wt – glycerol (3)** | -10.9582 | 5.489966 | -0.01655 | -0.002 |
| **P482 wt – 0.1 TSB (1)** | 22.36511 | -0.06462 | 2.337248 | -0.01286 |
| **P482 wt – 0.1 TSB (2)** | 22.76204 | -0.11937 | 0.793236 | -0.03869 |
| **P482 wt – 0.1 TSB (3)** | 22.52972 | -0.14195 | -3.12577 | 0.039644 |

**SUPPLEMENTARY TABLE 4. Principal component analysis of the LC-MS results of P482 wt and mutants 0.1 TSB culture extract samples.** The LC-MS dataset for PCA included only entities (detected compounds) for which the fold change between the conditions was higher than 2.

| sample (biol. replicate) | component 1 (30.26%) | component 2 (25.33%) | component 3 (19.87%) | component 4 (15.1%) |
|---|---|---|---|---|
| **KN4243 (1)** | -3.23425 | 1.906899 | -1.27539 | 3.187482 |
| **KN4243 (2)** | -3.39246 | 1.812226 | -1.32219 | 3.210302 |
| **KN4243 (3)** | -3.23026 | 1.773586 | -1.04258 | 3.462186 |
| **KN4240 (1)** | 6.223362 | 6.684866 | 1.334103 | -0.1845 |
| **KN4240 (2)** | 3.620874 | 1.169709 | -0.85038 | -0.44475 |
| **KN4240 (3)** | 3.504559 | 1.848443 | -0.34529 | -0.32984 |
| **KN4706 (1)** | -3.36476 | 1.318671 | 0.800491 | -3.25717 |
| **KN4706 (2)** | -3.56611 | 1.294228 | 0.809998 | -3.43463 |
| **KN4706 (3)** | -3.84608 | 0.785221 | 1.209437 | -3.44102 |
| **KN4709 (1)** | 1.558677 | -2.70486 | -3.75247 | -0.81108 |
| **KN4709 (2)** | 1.853718 | -2.87043 | -3.19544 | -0.58136 |
| **KN4709 (3)** | 1.165435 | -3.48902 | -3.99934 | -0.77746 |
| **P482 wt (1)** | 1.144664 | -3.14615 | 4.069778 | 1.169581 |
| **P482 wt (2)** | 1.045411 | -3.21308 | 3.989043 | 1.155917 |
| **P482 wt (3)** | 0.517228 | -3.17031 | 3.570231 | 1.07635 |

**SUPPLEMENTARY TABLE 5.** **PCR efficiencies and slopes of the qPCR primer pairs for both test and reference targets, calculated from the standard curves.**

| Target | E* | E (SE)** | $R^2$ | Slope | Slope error |
|---|---|---|---|---|---|
| *BV82_1009* | 2.00 | 0.05 | 0.997 | -3.31 | 0.11 |
| *BV82_3318* | 1.95 | 0.01 | 0.999 | -3.46 | 0.04 |
| *BV82_3755* | 2.05 | 0.02 | 0.999 | -3.20 | 0.05 |
| *BV82_4240* | 2.06 | 0.02 | 0.998 | -3.18 | 0.05 |
| *BV82_4243* | 1.97 | 0.05 | 0.991 | -3.40 | 0.13 |
| *BV82_4705* | 1.97 | 0.05 | 0.979 | -3.39 | 0.14 |
| *BV82_4706* | 2.03 | 0.02 | 0.999 | -3.25 | 0.05 |
| *BV82_4709* | 1.95 | 0.02 | 0.998 | -3.45 | 0.06 |
| *BV82_4870* | 1.97 | 0.03 | 0.997 | -3.39 | 0.07 |
| *acpP* | 2.08 | 0.07 | 0.973 | -3.13 | 0.15 |
| *algD* | 2.20 | 0.09 | 0.995 | -2.92 | 0.15 |
| *gyrB* | 1.96 | 0.08 | 0.981 | -3.41 | 0.21 |
| *lexA* | 2.10 | 0.10 | 0.982 | -3.10 | 0.20 |
| *mrdA* | 2.11 | 0.05 | 0.994 | -3.07 | 0.10 |
| *proC* | 2.06 | 0.05 | 0.993 | -3.17 | 0.11 |
| *recA* | 2.00 | 0.05 | 0.996 | -3.33 | 0.12 |
| *rpoB* | 1.90 | 0.04 | 0.993 | -3.60 | 0.13 |
| *rpoD* | 1.96 | 0.02 | 0.999 | -3.42 | 0.05 |
| *tuf* | 2.11 | 0.09 | 0.990 | -3.06 | 0.18 |

*E – primer pair efficiency calculated as in $E = 10^{-1/slope}$ (Rasmussen, 2001)
**E(SE) - efficiency standard error

## 13.2. Supplementary figures

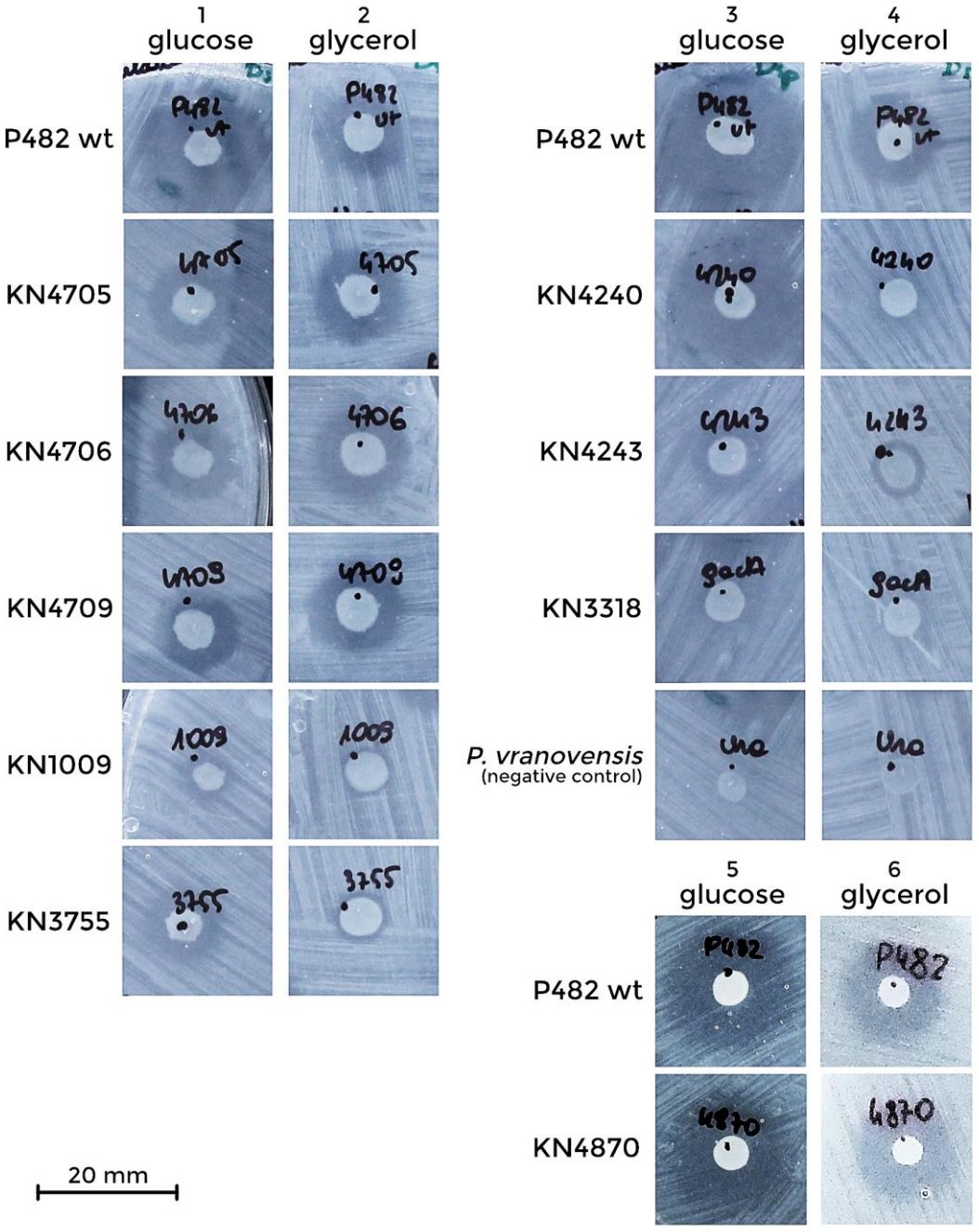


**SUPPLEMENTARY FIGURE 1. Representative *Dickeya solani* IFB0102 growth inhibition zones caused by the colonies of P482 wt and its mutants on M9-agar minimal medium with either 0,4% glucose or 0,4% glycerol.** The squares in each of the columns (numbered 1-6) are the zones observed on a single plate (one biological replicate), where the zone obtained for the wild type P482 is always a reference to which the test zones diameters have been compared.

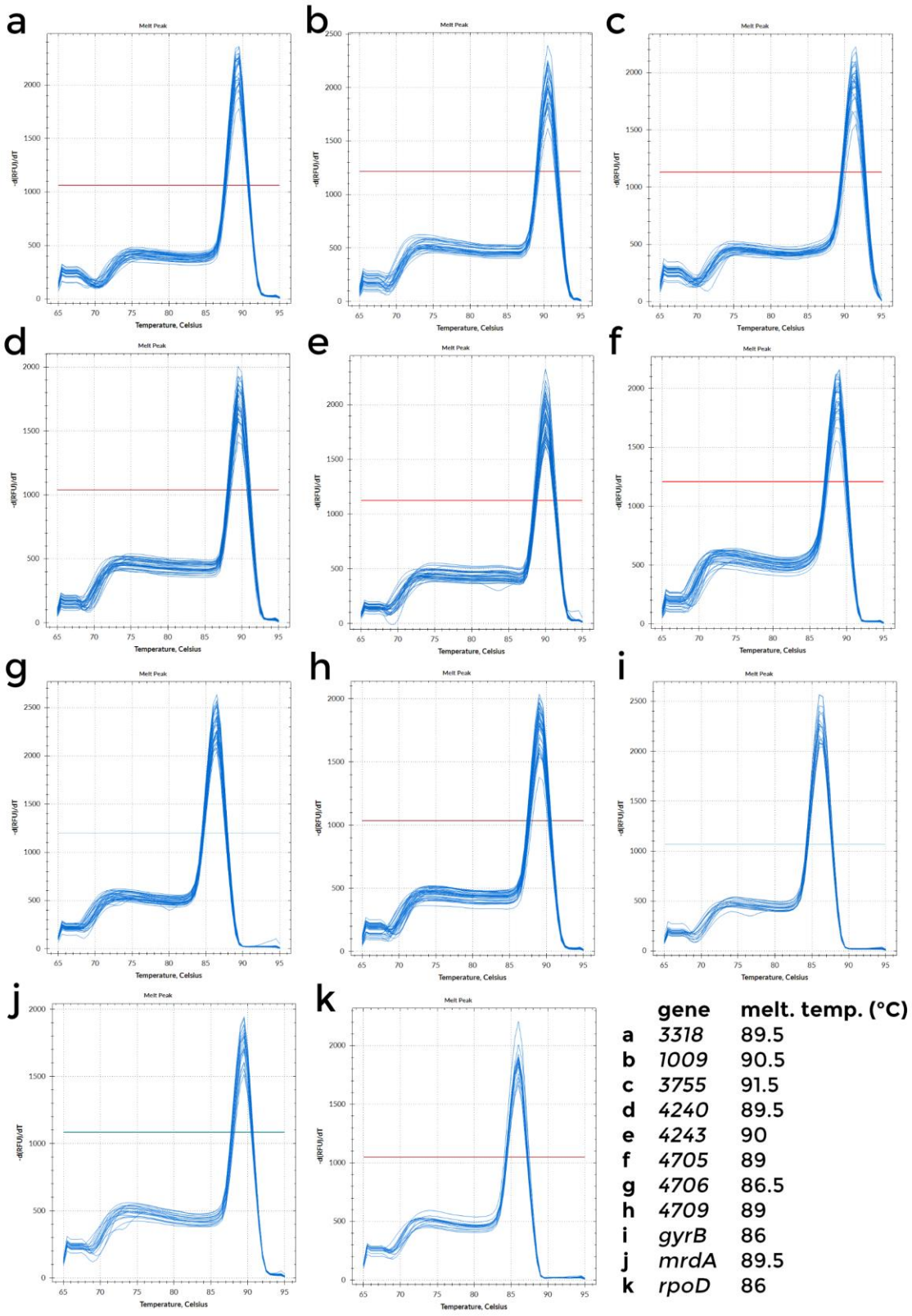


| | gene | melt. temp. (°C) |
|---|---|---|
| a | *3318* | 89.5 |
| b | *1009* | 90.5 |
| c | *3755* | 91.5 |
| d | *4240* | 89.5 |
| e | *4243* | 90 |
| f | *4705* | 89 |
| g | *4706* | 86.5 |
| h | *4709* | 89 |
| i | *gyrB* | 86 |
| j | *mrdA* | 89.5 |
| k | *rpoD* | 86 |

**SUPPLEMENTARY FIGURE 2. The melting curve assay results for the reference and target genes primer pairs.** The curves were generated in the Maestro software (Bio-Rad, USA). Each graph is an overlay of at least 10 melting curves of the products obtained after the qPCR reactions using the given primer pairs and P482 cDNA samples as the template.

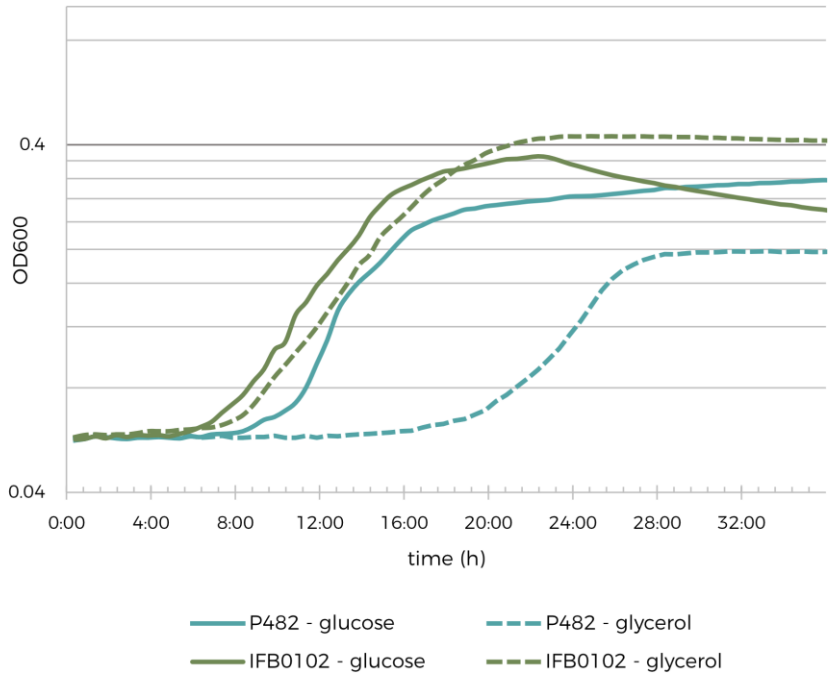


**SUPPLEMENTARY FIGURE 3. Growth curves of *P. donghuensis* P482 and *D. solani* IFB0102 on glucose and glycerol.** The strains were cultured in M9 with 0.4% glucose or 0.4% glycerol as a carbon source. The $OD_{600}$ values at each time point are the mean values of four biological replicates. The curves obtained are presented in a logarithmic scale.

# 14. Acknowledgements

Phew, what a ride.

This study would not have been possible without the relentless support I got from my advisors, peers, colleagues, partner, family and friends.

First and foremost, I would like to express my deepest appreciation to my supervisor, dr hab. **Sylwia Jafra,** prof. UG. Thank you for the years of valuable advice, guidance, patience and belief in my abilities.

I would like to thank my assistant supervisor, dr **Magdalena Rajewska**. Magda, I'm extremely grateful for all your practical suggestions and helpful contributions.

I'm deeply indebted to all of my IFB colleagues with whom I worked over these years. My special thanks go to **Angie, Aldona**, **Tomek, Madzia, Dorotka, Emilia, Maja, and Adam,** thank you for all the support, your passionate work and all the coffee room chats about literally everything.

I'd like to extend my sincere gratitude all the way to Naples, Italy; to prof. **Francesco Vinale** and all the members of his laboratory at IPSP-CNR, who hosted me during my internship and provided me with invaluable guidance. I need to mention the best moral support team, **Alessia, Angela and Mauro** – thank you for making it all fun.

Huge thanks go to my friends, who never let me down and were always patient enough to listen about my problems, give their advice, never hesitated to constructively criticise, and were always there for me. **Daria, Angie** (again), **Anna, Mikołaj, Kinga, Francesco**, you're awesome, I'm so grateful for your support.

To my lovely **family**, for supporting my ideas, pushing me to do my best and believing that obtaining a PhD is not even close to my best. Dziękuję!

Finally, but the most importantly, I would like to thank you, **Kim**. You liqui-dated into my life during this difficult time and somehow, you made it so much lighter. Thank you for your quantum love, perfect consciousness, and infinite amounts of unconditional support. I really wouldn't have done it without you.

# 15. Author information

## MARTA MATUSZEWSKA, MSc

I was born in Ciechanów, Poland on a hot August day in 1992. In 2011 I finished the "*Krasiniak*" High School in Ciechanów (*I Liceum Ogólnokształcące im. Zygmunta Krasińskiego w Ciechanowie*), passed the *matura* exams and moved to Gdańsk to study biotechnology at the Intercollegiate Faculty of Biotechnology of University of Gdańsk and Medical University of Gdańsk. My first steps in science were made possible by the Students' Scientific Association BIO-MED, which introduced me to the molecular biology laboratory. I went on to be a vice-chair of the SSA BIO-MED during years 2 and 3 of my undergraduate degree studies. I finished these studies with a bachelor's degree and an excellent mark in 2014. By this time, I had already fallen in love with microbiology and thus decided to continue my studies at IFB UG & MUG to obtain the master's degree. During this 2-year period I co-authored of my first scientific paper which was a result of a summer internship under the supervision of Rafał Banasiuk, MScEng, and prof. Aleksandra Królicka (IFB UG & MUG). My master's project was done under the supervision of prof. Sylwia Jafra (IFB UG & MUG). I obtained excellent marks with my MSc degree.

Following the graduation in 2016, I decided to pursue a PhD degree to continue and develop the project I realised during my master's studies. This thesis is the final result of hard work and passion that were implied in this decision. During the PhD studies, my greatest joy was teaching the future biotechnologists – overall, I conducted more than 350 hours of classes and training. The PhD studies also brought me the wonderful opportunity which was a 3-month internship at the Institute for Sustainable Plant Protection (CNR, Portici, Naples, Italy). My research during the entire PhD period resulted in the co-authorship of two more peer-reviewed papers, one of which includes a great share of findings from this thesis. Two more manuscripts are currently in preparation.

Apart from my scientific career, I enjoy pursuing other passions, the biggest of which is nevertheless science-related – I am an enthusiastic science communicator and organiser of scientific events. In years 2016 to 2019 I was on the Biotechnology Summer School organising committee; I also locally coordinated the organisation of various science/sci-comm events. I share my knowledge in social media, podcasts and science festivals. My non-scientific hobbies include knitting, social media content creation and marketing, graphic design and literature (non-fiction, science-fiction and fantasy).